The plesiosaur: remarkable morphology, histology, and physiology

Dissertation

zur

Erlangung des Doktorgrades (Dr. rer. nat.)

der

Mathematisch-Naturwissenschaftlichen Fakultät

der

Rheinischen Friedrich-Wilhelms-Universität Bonn

Vorgelegt von

Tanja Wintrich

aus

Berlin, Deutschland

Bonn 2018

Anfertigung mit Genehmigung der Mathematisch-Naturwissenschaftlichen Fakultät der Rheinischen Friedrich-Wilhelms-Universität Bonn

1. Gutachter:	Prof. Dr. P. Martin Sander
2. Gutachter:	Prof. Dr. Martin Scaal
3. Gutachter	Ass. Prof. Dr. Valentin Fischer
Fachnahes Mitglied:	Prof. Dr. Gerhard von der Emde
Fachfremdes Mitglied:	Prof. Dr. Andreas Kemna

Tag der Promotion: 06. Juni 2019
Erscheinungsjahr: 2019

Hiermit versichere ich an Eides statt, die vorliegende Arbeit selbstständig verfasst und keine anderen Hilfsmittel als die angegebenen verwendet sowie aus anderen Werken entnommene Inhalte als solche gekennzeichnet zu haben.

Bonn, Dezember 2018 Tanja Wintrich

Ich habe keine besondere Begabung, sondern bin nur leidenschaftlich neugierig.
(Albert Einstein)

Acknowledgments

First of all, I would like to thank my supervisor Martin Sander for his support, his continuous encouragement, and his flexibility in following my research interests. I am glad that I had the opportunity to be a part of his working group, and I am thankful for everything I learned in the last few years. I thank Martin Scaal for kindly agreeing to be my second reviewer, as well as Gerhard von der Emde, and Thomas Martin, who kindly agreed to be part of the dissertation committee.

Good research, in my opinion, is only possible as a joint effort. This dissertation would not have been possible without many researchers, whom I wish to thank for their support over the last years. I thank Alexandra Houssaye, Shoji Hayashi, and Yasuhisa Nakajima for providing histological thin sections of plesiosaur material and discussing the results. Furthermore, I thank Martin Scaal, Felicitas Pröls, Margarethe Draga, and Andreas Peters for anatomical discussion, and for their support on understanding human anatomy, as well as providing lab support and histological thin sections of living animals. I thank Hans-Joachim Wilke and René Jonas for discussion on biomechanics on the axial skeleton. Furthermore I thank Christine Böhmer, Rico Schellhorn, Ilja Kogan, and Aaron van der Reest for providing histological thin sections, the effort, and discussion on my beloved project on the intervertebral disc. I thank Roger Benson, Patrick Druckenmiller, Valentin Fischer, James Neenan, Robin O´Keefe, Laura Soul, and Nikolay Zverkov for discussing my thoughts on plesiosaur morphology, histology, and physiology. It was a great pleasure to work and cooperate with all of you.

However, without help from the technical staff of the Steinmann Institute, I would have had at least a much harder time, and it would probably not be possible to finish this dissertation. I am grateful to Olaf Dülfer (preparator), Peter Göddertz (system administrator), Dagmar Hambach (administrative assistance), Beate Mühlens-Scaramuzza (administrative assistance), and Georg Oleschinski (photography).

My deepest thank goes to my family, especially to my mom. Thank you for your understanding, financial support, encouragement, and all the discussion we had about every single project in this dissertation. Your view from the outside inspired me to solve all of these questions. Without you I would not be the person I am today, I really hope that you now know that plesiosaurs are marine reptiles and not fish. Love you Mom.

Summary

In this dissertation, contributions to understanding the morphology, histology, and physiology of plesiosaurs, a major group of marine reptiles from the Age of Dinosaurs, are presented. By using comparative methods and new investigations on recent and fossil taxa, new insights of general importance for amniotes (true land animals) are developed. Furthermore, the results demonstrate the potential of interdisciplinary research, combining conventional vertebrate paleontological approaches, human anatomy, developmental biology, and medical biomechanics.

Plesiosaurs are one of the first described vertebrate fossils and raised many questions over the last 300 years in vertebrate paleontology. However, from the beginnings of paleontology as a science, it was also believed that plesiosaurs evolved in the Early Jurassic, and only few studies discussed a Triassic radiation. After an extraordinary discovery in a German clay pit near Warburg in North Rhine-Westphalia, the first Triassic plesiosaur was found and described in this thesis. The nearly complete and articulated skeleton of *Rhaeticosaurus mertensi* showed that already in the Triassic the plesiosaur body plan, unique histology, and physiology had evolved. This means that the evolution of plesiosaurs took place in the Triassic and furthermore, that plesiosaurs crossed the Triassic-Jurassic boundary, surviving the end-Triassic extinction event, unlike several other marine and terrestrial tetrapod groups.

In general, plesiosaurs show two major body plans, the plesiosauromorph body plan and the pliosauromorph body plan. The main difference between the two is that plesiosauromorphs have a small head and a long neck (up to 76 cervical vertebrae) and the pliosauromorphs have a huge head and a short neck. However, both body plans evolved convergently in different lineages in Plesiosauria. Nevertheless, the basal condition is a small head and a relative long neck built up by a high number of cervical vertebrae compared to the ancestor.

Plesiosaur cervical vertebrae, independently of taxon, show a special character: two large and symmetrical foramina piercing the ventral surface of the centra. These foramina are here renamed “intersegmental artery foramina” because they do not represent nutrient foramina, as previously believed, but the entry of intersegmental arteries. Retention of these arteries is a strongly paedomorphic character because intersegmental arteries are an embryonic feature that is normally resorbed in a very early ontogenetic stage during the process of resegmentation. µCt investigations and comparison to the development in modern amniotes showed that plesiosaurs did not resorb the arteries during the resegmentation process. The reason is not understood, but it is probably linked to the fact that the plesiosaur count of cervical vertebrae is the highest seen among all amniotes, suggesting that the processes involved in cervical vertebra development must have been faster than in any other amniote group.

However, not only the intervertebral artery foramina raise intriguing questions but also the function and mobility of the long neck of plesiosauromorphs, which had been the subject of many studies. The plesiosaur neck, even in those taxa where it is longest relative to the body length, surprisingly is quite immobile. The neural spine of the cervical vertebrae is high, the zygapophyses are medially inclined, and the distance between the segments is very small. All of these features in the end must have resulted in an only slightly mobile neck. Hence, the mobility of the neck was tested in this thesis using an innovative approach from human anatomy, finite element modeling. The model indicates very limited mobility of only a few degrees in the intervertebral joint, allowing for the calculation of the total mobility of the neck of less than 180º.

Nevertheless, the long, immobile neck must have been useful. Plesiosaurs, especially the plesiosauromorph forms with the small head and the long neck, were hunting in school of fish. Fish in general are very sensitive to hydrodynamic waves. The small head and the long neck caused a hydrodynamic and optical camouflage effect, preventing the fish or school of fish from recognizing the plesiosaur as a large predator. This would have been the case if the plesiosaur would have had a shorter neck but also a small head. The long neck in plesiosaurs thus represent, a special adaptation to prey acquisition in the aquatic environment.

The studies on the plesiosaur neck led to the formulation of the hypothesis that the intervertebral joints in plesiosaurs and some other fossil reptiles had a proper intervertebral disc (IVD) in the dorsal vertebral column, similar to the IVD of mammals. To test this hypothesis, a comprehensive sample of amniote dorsal vertebrae, fossil and extant, was acquired. Particular emphasis was placed on articulated segments of vertebral columns from black shales. Morphology of the centrum, histology of the articular surface, and preserved soft tissues, such as different kinds of cartilage, confirm that the IVD is not only restricted to mammals.

Ancestral character state reconstruction showed that the IVD evolved convergently at least twice in the phylogeny of amniotes, once in synapsids and once in diapsids, but possibly more often. Furthermore, the reptile synovial joint (of recent snakes and crocodiles) shows also convergent evolution, which had been mentioned briefly in different studies but not shown comprehensively. In general, we see here that the evolution and development of the amniote axial skeleton follows similar rules, independently of whether it is from a mammal or a reptile.

The dissertation concludes with a review of plesiosaur paleobiology and evolution, incorporating both published literature and the research presented here. Plesiosaurs were a unique but highly successful experiment in evolution, making them powerful model organisms for understanding secondary aquatic adaptation in amniotes and the historical contingency of evolution.

Contents

Chapter 1 – Introduction and description of chapters

1.1. The plesiosaur – A remarkable and unique marine reptile

In 1719, 300 years ago, the first partly articulated plesiosaur skeleton was discovered by the "antiquarian" William Stukely in the Jurassic of Nottinghamshire, England. The specimen survives today in the Natural History Museum in London. Stukely's discovery was the subject of the first publication on plesiosaur material in the history of vertebrate paleontology (Stukely 1719). At the time, the skeleton was described as a mixture of a crocodile and porpoise because Stukely recognized the preserved hind limb as a paddle. Three hundred years later, we know that the specimen is a representative of the clade Plesiosauria.

Plesiosaurs belong to the clade Sauropterygia and are one of the most successful and long-lived marine reptile clades, being known from the Late Triassic (Benson et al.; 2012, Wintrich et al., 2017a) up to the end of the Cretaceous (Fischer et al., 2017; Allemande et al., 2018). Plesiosaurs show a unique body plan combined with an extraordinary mode of locomotion and feeding style; furthermore, they show a high diversity and disparity in the fossil record with more than 120 valid genera known today (Fischer et al., 2017). Especially the long-necked plesiosaurs raise many different questions about development, locomotion, and physiology. Although the plesiosaur body plan is not seen in amniotes today, which would have aided in solving questions about the group, morphological, histological, and phylogenetic comparative investigations can help in providing answers to some of these questions and offer new perspectives on recent amniotes, modern ecosystems, and developmental processes.

Interpretations based on fossil bone material alone can be a challenge, especially when it comes to soft tissue reconstructions and biological questions. Today, we can use different techniques, like bone histology and µCt analyses. Paleohistology is the study of fossil bone tissues, and although paleohistology is a destructive method, there are four different signals which can be seen in fossil histological thin sections (Padian & Lamm 2013). First of all, bone histology can answer the question about the ontogenetic stage. Second, bone histology follows a phylogenetic signal and therefore is useful when it comes to a new discovery. Third and fourth, the mechanical loading of bone and therefore also the environment is reflected in the bone histology as well. On the other hand, µCt data is a non-destructive method, which is as useful as histology. Blood vessel systems can be reconstructed, and 3D models generated from µCt datasets can be used for biomechanical analysis. In this dissertation, I used at least one of these methods in each of the chapters to solve questions of the biology behind these unique marine reptiles.

For vertebrate paleontologist, bone material is in general the only resource because soft tissue preservation is rare, only seen in few deposits, and often difficult to interpret. An exception is soft tissues such as cartilage closely associated with bone which may preserve in an altered

state. It is paramount to extract as much information out of the bone as possible. This has increasingly become possible with the advent of new methods such as finite element modeling, going well beyond the pure shape of the bone to be evaluated and captured as characters for use in phylogenetic analyses.

1.2. Aim of dissertation

The aim of the dissertation is to improve understanding of the unique marine reptile clade Plesiosauria. Plesiosaurs were studied for more than two centuries, and the morphology, physiology, as well as the histology raises many different questions. By no means is the research on plesiosaur complete, it is merely a next step to understand one of the longest-lived clade, of marine reptiles. I hope this work gives an overview over why plesiosaurs were so unique in their morphology, histology and physiology and will help stimulate further investigations. The dissertation includes five chapters in addition to this introduction. All chapters are directly associated with each other (Fig. 1), and each chapter focuses on a particular aspect of plesiosaurs, their morphology, histology, or physiology with a focus on the long-necked forms, also functioning as a synthesis of the dissertation, and the last chapter is a complete review about the biology of plesiosaurs.

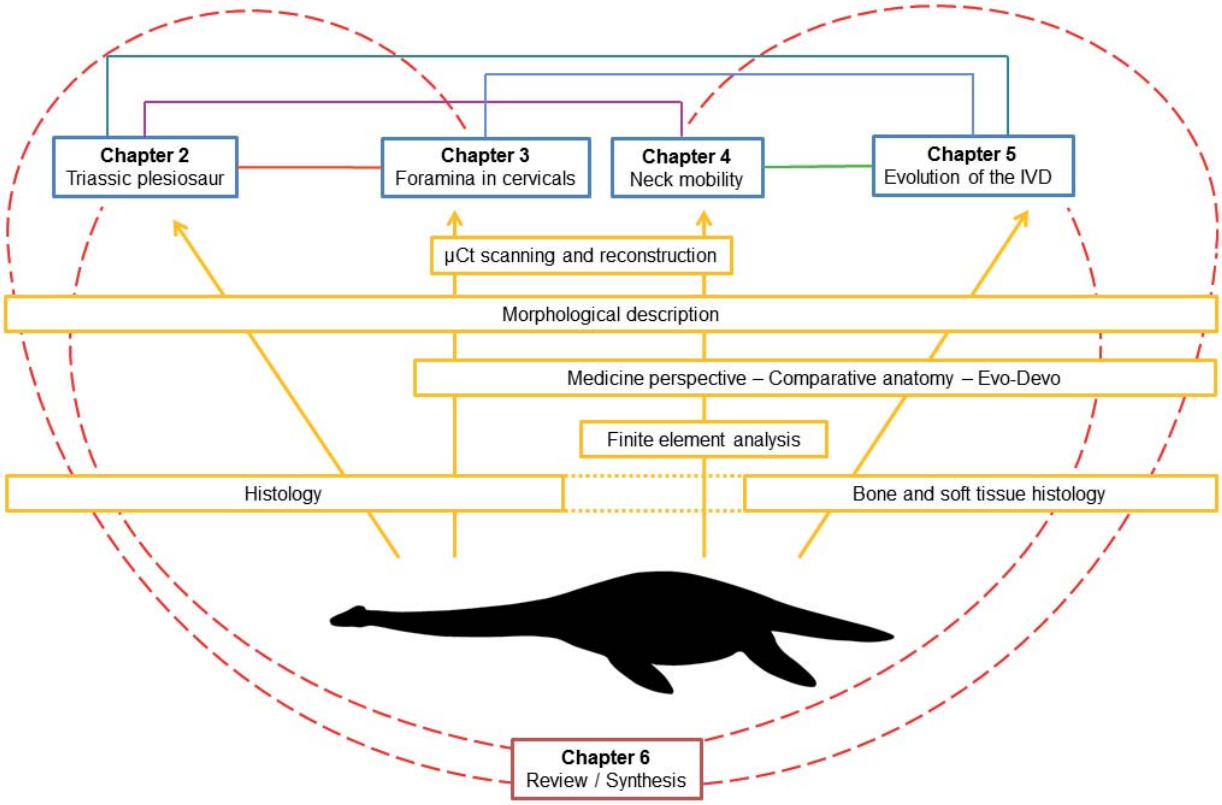

Figure 1: Overview of all dissertation chapters (excluding the introduction, this chapter). Each chapter (blue boxes) shows the connection to the other chapters. Furthermore, the methodology behind the different projects is shown in yellow. In the end, the results from all four chapters (blue boxes) have a great influence on the last chapter (red box) which is a review about plesiosaur evolution and paleobiology in general. Note that the chapter boxes show key words of chapters instead of full chapter titles.

1.3. Description of chapters

Chapter 2 is a description of the first Triassic plesiosaur skeleton, discovered in the Late Triassic (Rhaetian) of Germany (Wintrich et al., 2017a). The new taxon, *Rhaeticosaurus mertensi* Wintrich et al. 2017, was recovered as a basal member of the clade Pliosauridae in a phylogenetic analysis and unequivocally shows that plesiosaurs crossed the Triassic-Jurassic boundary. A Triassic origin of plesiosaurs was suspected for a long time but never corroborated by the find of a skeleton so far. Furthermore, the specific bone histology of plesiosaur is discussed in this chapter, and it is shown that plesiosaurs have truly unique histology which sets them apart from stem sauropterygians. Plesiosaur histology also shows a fast growth, leading to the hypothesis that the histology furthermore indicates a high metabolic rate which was tested recently by Fleischle et al. (2018). During the description of the new taxon *Rhaeticosaurus mertensi*, a special character of the cervical vertebrae aroused attention.

Chapter 3 focusses on this special character, which is only seen in plesiosaur cervical vertebral centra (Wintrich et al., 2017b). The character was previously known as “subcentral foramina”uwhich were believed to contain nutrient arteries entering the vertebral centrum. After µCt scanning and histological investigation of several plesiosaurs cervical vertebrae, it became apparent that the subcentral foramina do not represent nutrient canal entries but the retention of an early ontogenetic structure, the paired intersegmental arteries. These are seen during the early development of the vertebral column in all amniotes and are usually lost after the process of resegmentation. Therefore, the foramina were renamed “intersegmental artery foramina”. The intersegmental arteries develop in the embryo well before ossification and are resorbed during the process of resegmentation. Obviously, this resorption did not take place in plesiosaurs, resulting in a highly paedomorphic character in their vertebral column. The fact, that the intervertebral arteries were not resorbed during the development of the vertebral column could be linked to the extraordinarily high count of the cervical vertebrae in plesiosaurs, suggesting that they had a faster segmentation clock than any other amniote. However, study of the morphology of cervical vertebrae raised the question of neck mobility in plesiosaurs.

Chapter 4 tests hypotheses of the range of motion in intervertebral joints in the neck, and therefore neck mobility, in *Cryptoclidus eurymerus* (Wintrich et al., in revision). *Cryptoclidus* is a derived plesiosaur known from the Middle Jurassic of England and shows the long-necked body plan of plesiosaurs with a count of about 35 cervical vertebrae. To test the hypothesis of a restricted mobility, a morphological description of the cervical vertebrae of this taxon was done followed by a finite element analysis using µCt scans of a single motion segment consisting of two consecutive cervical vertebrae and the joints connecting them. The fact that plesiosaur cervical vertebrae have extremlely narrow intervertebral spaces, as well as medially inclined zygapophyses suggest on morphological grounds that plesiosaurs had greatly restricted neck mobility. This restricted mobility was supported by the finite element analysis of the motion segment as well, indicating a maxim range of motion of the entire neck of less than 180º. For the finite element analysis, a 3D surface model of the motion segment had to be built from CT data of the preserved bones, and a proper intervertebral disc (IVD) was added to the finite element model because any mobility of the vertebral column in plesiosaurs and other fossil reptiles with platycoelous centra would have required an IVD. The IVD of the

model contained a *nucleus pulposus* and an *annulus fibrosus* similar to mammals, with material properties of mammalian IVDs.

The hypothesis about the presence of a proper intervertebral disc in plesiosaurs is tested in **Chapter 5** (Wintrich et al., in review). The test consisted of a histological and morphological description of the articular surfaces of a comprehensive sample of amniotes, covering all major clades, followed by ancestral character state reconstruction (ASR) for the evolution of the intervertebral joints. It is shown that the IVD is not strictly a mammal autapomorphic character but that the IVD evolved convergently at least twice among amniotes, i.e., in synapsids and early in diapsids, but possibly more often. Furthermore, ASR indicates that the synovial joint evolved convergently as well, namely in squamates and crocodilians.

Finally, **Chapter 6** (Wintrich et al., in preparation) provides a review of the unique and enigmatic body plan seen in plesiosaurs and of their paleobiology. The review places particular emphasis on long-necked forms and addresses several open questions about development and the function of different physiological features and offers a reminder of the importance of understanding developmental processes from both, a paleobiological and an evolutionary perspective. Furthermore, all relevant literature and hypotheses were compiled for a complete overview of the remarkable morphology, histology and physiology of plesiosaurs.

I hope that this dissertation will represent a substantial advance in our understanding of plesiosaur evolution, biomechanics, and ecology. Plesiosaurs remind us that we do not completely understand many evolutionary, developmental, and other biological processes and that studying fossil material is important for our understanding of the recent organisms and ecosystem.

References

Allemand, R., Bardet, N., Houssaye, A., & Vincent, P. (2018). New plesiosaurian specimens (Reptilia, Plesiosauria) from the Upper Cretaceous (Turonian) of Goulmima (Southern Morocco). *Cretaceous Research*, *82*, 83-98.

Benson, R. B., Evans, M., & Druckenmiller, P. S. (2012). High diversity, low disparity and small body size in plesiosaurs (Reptilia, Sauropterygia) from the Triassic–Jurassic boundary. *PLoS One*, *7*(3), e31838.

Valentin F., Benson, R. B. J., Zverkov, N., Soul, L., Arkhangelsky, M., Lambert, O., Stenshin, I. M., Uspensky, G. N., Druckenmiller, P. S. (2017). Plasticity and convergence in the evolution of short-necked plesiosaurs. *Current Biology*, *27*(11), 1667-1676.

Fleischle, C., Wintrich, T, & Sander, P. M. (2018). Quantitative histological models suggest endothermy in plesiosaurs. *PeerJ*, *6*, e4955.

Padian, K., & Lamm, E. T. (Eds.). (2013). *Bone Histology of Fossil Tetrapods: Advancing Methods, Analysis, and Interpretation*. University of California Press.

Stukely, W. (1719). III. An account of the impression of the almost entire sceleton of a large animal in a very hard stone, lately presented the Royal Society, from Nottinghamshire. *Philosophical Transactions of the Royal Society*, *30*(360), 963-968.

Wintrich, T., Hayashi, S., Houssaye, A., Nakajima, Y., & Sander, P. M. (2017a). A Triassic plesiosaurian skeleton and bone histology inform on evolution of a unique body plan. *Science Advances*, *3*(12), e1701144.

Wintrich, T., Scaal, M., & Sander, P. M. (2017b). Foramina in plesiosaur cervical centra indicate a specialized vascular system. *Fossil Record*, *20*(2), 279-290.

Wintrich, T., Jonas, R., Wilke, H.-J., & Sander, P. M. (in revision). Neck mobility in the Jurassic plesiosaur *Cryptoclidus eurymerus* – a new approach to understanding the axial skeleton in fossil vertebrates using finite element analysis. *PeerJ*.

Wintrich, T., Scaal, M., Böhmer, C., Schellhorn, R., Kogan, I., van der Reest, A., & Sander, P. M. (in revision). Fossil soft tissues indicate convergent evolution of the intervertebral disc in non-mammalian amniotes. *Nature*.

Wintrich, T., Benson, R. B. J., Böhmer, C., Druckemiller, P., Fischer, V., Neenan, J. M., O´Keefe, R. F., Soul, L., Zverkov, N., & Sander, P. M. (in preparation). Biology and evolution of long-necked Plesiosauria.

Chapter 2

Published as:

Wintrich, T., Hayashi, S., Houssaye, A., Nakajima, Y., & Sander, P. M. (2017). A Triassic plesiosaurian skeleton and bone histology inform on evolution of a unique body plan. *Science Advances*, *3*(12), e1701144.

Author contributions:

Tanja Wintrich designed the research, carried out the research, and wrote the paper.

Tanja Wintrich, Shoji Hayashi, Alexandra Houssaye, Yasuhisa Nakajima and P. Martin Sander provided datasets for the study, contributed to the manuscript preparation, and reviewed drafts of the paper.

Supplementary Material:

A complete description of the unique characters of the new plesiosaur from the Rhaetic bonebeds of Bonenburg in Germany including the analysis runs with PAUP.

SCIENCE ADVANCES | RESEARCH ARTICLE

PALEONTOLOGY

A Triassic plesiosaurian skeleton and bone histology inform on evolution of a unique body plan

Tanja Wintrich,[1] Shoji Hayashi,[2,3]* Alexandra Houssaye,[4] Yasuhisa Nakajima,[5] P. Martin Sander[1,6†]

Secondary marine adaptation is a major pattern in amniote evolution, accompanied by specific bone histological adaptations. In the aftermath of the end-Permian extinction, diverse marine reptiles evolved early in the Triassic. Plesiosauria is the most diverse and one of the longest-lived clades of marine reptiles, but its bone histology is least known among the major marine amniote clades. Plesiosaurians had a unique and puzzling body plan, sporting four evenly shaped pointed flippers and (in most clades) a small head on a long, stiffened neck. The flippers were used as hydrofoils in underwater flight. A wide temporal, morphological, and morphometric gap separates plesiosaurians from their closest relatives (basal pistosaurs, *Bobosaurus*). For nearly two centuries, plesiosaurians were thought to appear suddenly in the earliest Jurassic after the end-Triassic extinctions. We describe the first Triassic plesiosaurian, from the Rhaetian of Germany, and compare its long bone histology to that of later plesiosaurians sampled for this study. The new taxon is recovered as a basal member of the Pliosauridae, revealing that diversification of plesiosaurians was a Triassic event and that several lineages must have crossed into the Jurassic. Plesiosaurian histology is strikingly uniform and different from stem sauropterygians. Histology suggests the concurrent evolution of fast growth and an elevated metabolic rate as an adaptation to cruising and efficient foraging in the open sea. The new specimen corroborates the hypothesis that open ocean life of plesiosaurians facilitated their survival of the end-Triassic extinctions.

INTRODUCTION

Triassic sauropterygians exhibit great morphological and body size disparity and highly varied feeding and locomotor adaptations (*1*) reflected in their bone microstructure (*2*). Nearly all stem sauropterygians are found in coastal or platform deposits of the Tethys Sea. Plesiosaurians, on the other hand, are recorded globally from open-water deposits and have a strikingly uniform bauplan (variation primarily residing in skull size and neck length) (*3*–*6*), with all four limbs modified into hydrofoils used in some kind of underwater flight (*7*). The great similarity between forelimbs and hindlimbs is unique among tetrapods. After nearly 300 years of frequent discoveries of plesiosaurian skeletons from the Early Jurassic to the end of the Cretaceous, we here report the first plesiosaurian skeleton from the Triassic (Figs. 1 and 2 and figs. S1 to S5). The find pertains to a new, small-bodied taxon, *Rhaeticosaurus mertensi* gen. et sp. nov., from the Rhaetian of Germany (Fig. 1). Previously, isolated vertebrae from the Rhaetian bonebeds of England had been assigned to Plesiosauria (*8*), and a partial, poorly preserved, and undiagnostic sauropterygian skeleton from the Russian Arctic (*9*) had hinted at a Triassic origin of the clade, but these finds remain inconclusive (*8*).

RESULTS

Systematic paleontology

Reptilia Linnaeus, 1758
Diapsida Osborn, 1903
Plesiosauria de Blainville, 1835

[1]Bereich Paläontologie, Steinmann-Institut für Geologie, Mineralogie und Paläontologie, Universität Bonn, Nussallee 8, 53115 Bonn, Germany. [2]Osaka Museum of Natural History, Nagai Park 1-23, Higashi-Sumiyoshi-ku, Osaka 546-0034, Japan. [3]Division of Materials and Manufacturing Science, Graduate School of Engineering, Osaka University, 2-1 Yamada-Oka, Suita, Osaka 565-0871, Japan. [4]UMR 7179 CNRS/Muséum National d'Histoire Naturelle, Département Adaptations du Vivant, 57 rue Cuvier CP-55, 75005 Paris, France. [5]Atmosphere and Ocean Research Institute, University of Tokyo, 5-1-5 Kashiwanoha, Kashiwa-shi, Chiba 277-8564, Japan. [6]Dinosaur Institute, Natural History Museum of Los Angeles County, 900 Exposition Boulevard, Los Angeles, CA 90007, USA.
*Present address: Biosphere-Geosphere Science, Okayama University of Science, Ridai-cho 1-1, Kita-ku, Okayama 700-0005, Japan.
†Corresponding author. Email: martin.sander@uni-bonn.de

Phylogenetic definition

We offer the following apomorphy-based definition of Plesiosauria: Sauropterygians with a short, wide trunk–bearing four flippers of even structure and subequal size, the flippers consisting of long, straight propodials combined with very short and dorsoventrally flattened zeugopodials.

Diagnosis

Plesiosauria is diagnosed (see Materials and Methods) by two unique and unambiguous synapomorphies: tooth enamel surface, striations present (character, 106; state, 0; see comment in table S2); orientation of cervical zygapophyses, dorsomedially facing (128, 1). An unambiguous but not unique synapomorphy is as follows: dorsal half of ilium, subequal anterior and posterior expansion (174, 0).

Rhaeticosaurus mertensi gen. et sp. nov.

Etymology

The genus name is based on rhaeticus, latinized adjective meaning "from the Rhaetian stage," and sauros (Greek), meaning lizard or saurian. The specific epithet honors the discoverer of the holotype, Michael Mertens of Schwaney, Westphalia, Germany.

Holotype specimen

LWL-Museum für Naturkunde (Münster, Germany), LWL-MFN P 64047.

Locality and horizon

Clay pit #3 of Lücking brick company, 1 km north of the village of Bonenburg, city of Warburg, North Rhine-Westphalia, Germany (Fig. 1A). The specimen derives from Rhaetian dark marine mudstones of the Exter Formation, 21 m in the section below the Triassic-Jurassic boundary and about 3.5 m below a bonebed containing a vertebrate fauna of Rhaetian age (Fig. 1B and table S1).

Diagnosis

Small-bodied plesiosaurian with an estimated total length of 237 cm (Fig. 2, A and B). The new taxon has two autapomorphies (Fig. 2C): a modified V-shaped neurocentral suture in the anterior and middle

cervical vertebrae. In *Rhaeticosaurus*, the sides of the "V" are ventrally concave, and the tip of the "V" almost reaches the ventral margin of the centrum. In other plesiosaurians with a V-shaped neurocentral suture, the sides of the "V" are straight, and the tip only extends to the middle of the centrum. The second autapomorphy is greatly foreshortened zeugopodials with a humerus/radius ratio of 3.8 and a femur/tibia ratio of 4.3 (Fig. 2, B, D, and E, and table S4). In addition, there are 10 unambiguous but not unique synapomorphies (tables S2 and S3).

Phylogenetic relationships

To assess the systematic position of the Triassic plesiosaurian skeleton, we coded it for a recently published phylogenetic data matrix aimed at clarifying plesiosaurian interrelationships (data file S1) (*4*). *Rhaeticosaurus* was found to be nested within Plesiosauria as a basal member of the Pliosauridae, with *Anningasaura* as the most basal plesiosaurian (Fig. 3A). As a consequence, six nodes in the cladogram are of Triassic age, indicating pre-Jurassic diversification of plesiosaurians into their major clades (Fig. 3A).

Brief anatomical description

The holotype (LWL-MFN P 64047, LWL-Museum für Naturkunde) of *Rhaeticosaurus* is a partial skeleton of a subadult preserving the occiput, lower jaw, vertebral column, pectoral girdle, pelvic girdle, and left limbs (see Fig. 2, figs. S1 to S4, and Supplementary Anatomical Descriptions). Several teeth are preserved in isolation, showing the typical plesiosaurian enamel "striations" (fig. S1, B and C), which consist of sharp ridges of enamel formed on a smooth enamel dentin junction (*10*). We estimate ≥37 neck vertebrae, the 15 anteriormost of which are fully articulated (Fig. 2, A to C). There are large paired subcentral foramina (fig. S2E), as in other early plesiosaurians (*11*). Subcentral foramina are small in basal pistosaurs (*Yunguisaurus*, *Pistosaurus*, and *Augustasaurus*) and lacking in *Bobosaurus* (*12*). The zygapophyseal articular surfaces are medially inclined (Fig. 2C and fig. S2B), as opposed to *Bobosaurus* and all more basal sauropterygians that have horizontal facets (*12*). There are 21 trunk vertebrae of the typical plesiosaurian type (fig. S3), with single round rib articular facets on the end of the prominent transverse processes (fig. S3, B and C). These are entirely formed by the neural arch. The trunk region is short and appears stiff because of the tight articulation of the dorsal centra and the width of the rib cage. There are four sacral vertebrae, and 25 vertebrae are preserved in the tail, with a few more missing (Fig. 2, A and B, and fig. S4). The caudal vertebral centra are disk-shaped (fig. S4B), indicating a short tail compared to non-plesiosaurians. The well-preserved pelvic girdle is represented by both ilia and the left pubis and left ischium (Fig. 2, A and B, and fig. S3A). These bones are similar in shape to those of other early plesiosaurians (*11*) and to *Bobosaurus* (*12*), except for the ilium that is stouter in the latter.

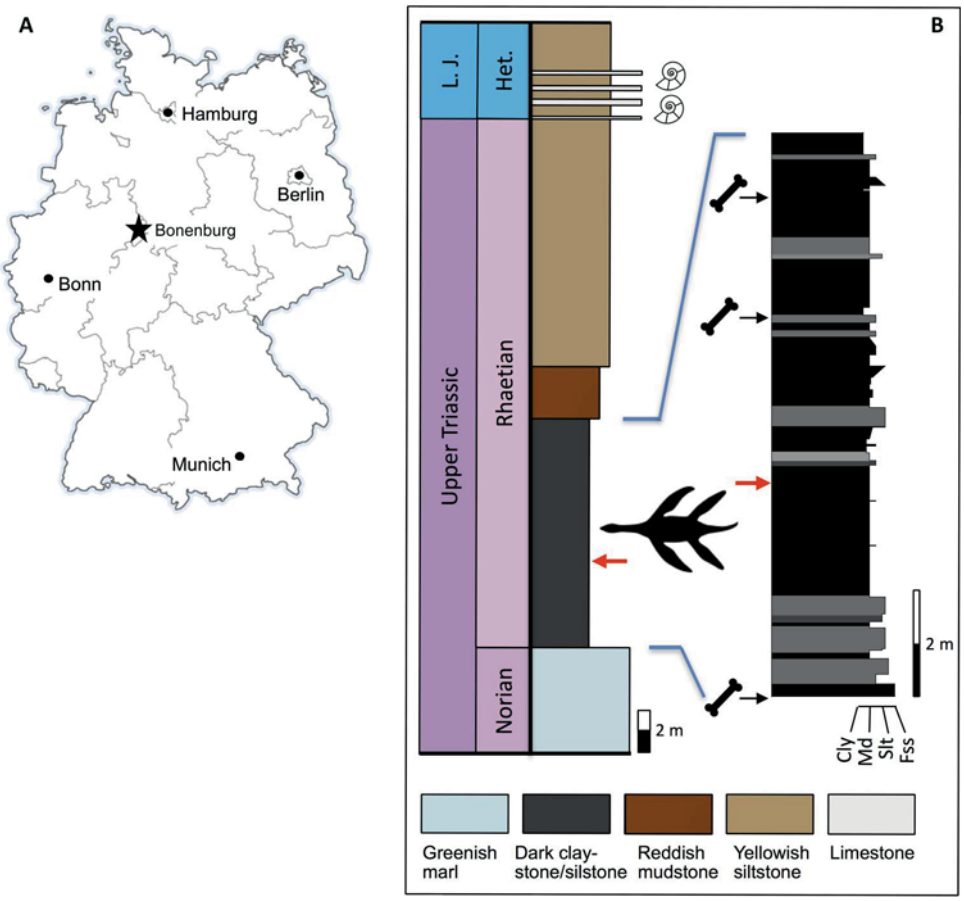

Fig. 1. Locality and horizon of the new species. (**A**) Location of Bonenburg clay pit in eastern North Rhine-Westphalia, Germany. (**B**) Measured section of the Norian to Hettangian deposits with the discovery horizon (indicated by plesiosaurian silhouette and red arrows) of *Rhaeticosaurus mertensi* and the bonebeds with the Triassic vertebrate fauna. Horizons of lowermost Jurassic ammonites indicated by silhouettes. Colors of the rock types in the main stratigraphic column approximate colors in fresh outcrop. Cly, claystone; Fss, fine-grained sandstone; Het., Hettangian; L. J., Lower Jurassic; Md, mudstone; Slt, siltstone.

Despite their distal incompleteness, the forelimb and hindlimb appear to have been rather similar in morphology and length, as in all plesiosaurians (Fig. 2, A and B, and fig. S5). The humerus has a straight shaft, and the distal end is little expanded (fig. S1A). The radius reaches only 26% of the length of the humerus and is dorsoventrally flattened (Fig. 2D, fig. S6C, and table S4). Like the humerus, the femur has nearly straight preaxial and postaxial margins compared to the curved margins in non-plesiosaurian sauropterygians, but it is somewhat more distally expanded than the humerus (Fig. 2E). Tibia and fibula attain less than 25% of femur length and are flattened dorsoventrally (Fig. 2E).

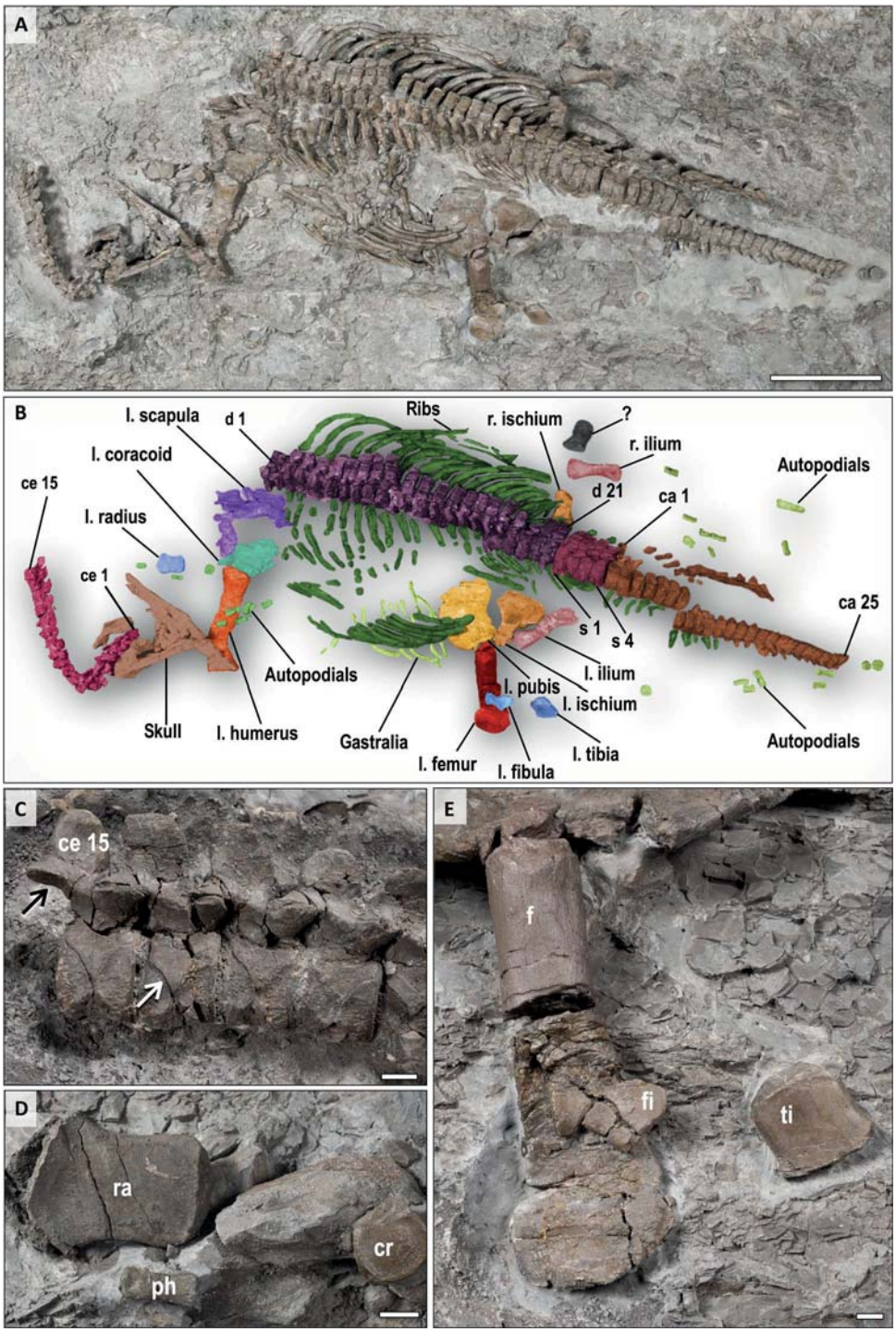

Fig. 2. The holotype of *Rhaeticosaurus mertensi* gen. et sp. nov. (**A**) Photograph. (**B**) Color overlay. (**C**) Cervical vertebrae 10 to 15 in right lateral view showing medially inclined zygapophyses (black arrow) and the autapomorphic ventrally concave V-shaped neurocentral sutures (white arrow). (**D**) Left radius, a phalanx, and a carpal element. (**E**) Left femur, tibia, and fibula. The proximal femur is a cast because the original was sectioned for histology. ca, caudal vertebra; ce, cervical vertebra; cr, carpal bone; d, dorsal vertebra; f, femur; fi, fibula; l., left; ph, phalange; r., right; ra, radius; s, sacral vertebra; ti, tibia; ?, unidentified bone. Scale bars, 20 cm (A) and 1 cm (C to E).

Morphometric analysis

A morphometric analysis (figs. S6 and S7 and table S4) of trunk and limb elements of early plesiosaurians and non-plesiosaurian eosauropterygians results in a clear separation of plesiosaurians from non-plesiosaurians. The analysis reveals that plesiosaurians are characterized by a relatively short trunk and long propodials combined with short zeugopodials (figs. S6 and S7 and table S4). The only ratio in that plesiosaurians overlap with non-plesiosaurians is the humerus/femur ratio. It varies widely in non-plesiosaurians from humeri that are distinctly longer than femora and vice versa, whereas plesiosaurian humeri and femora are generally subequal in

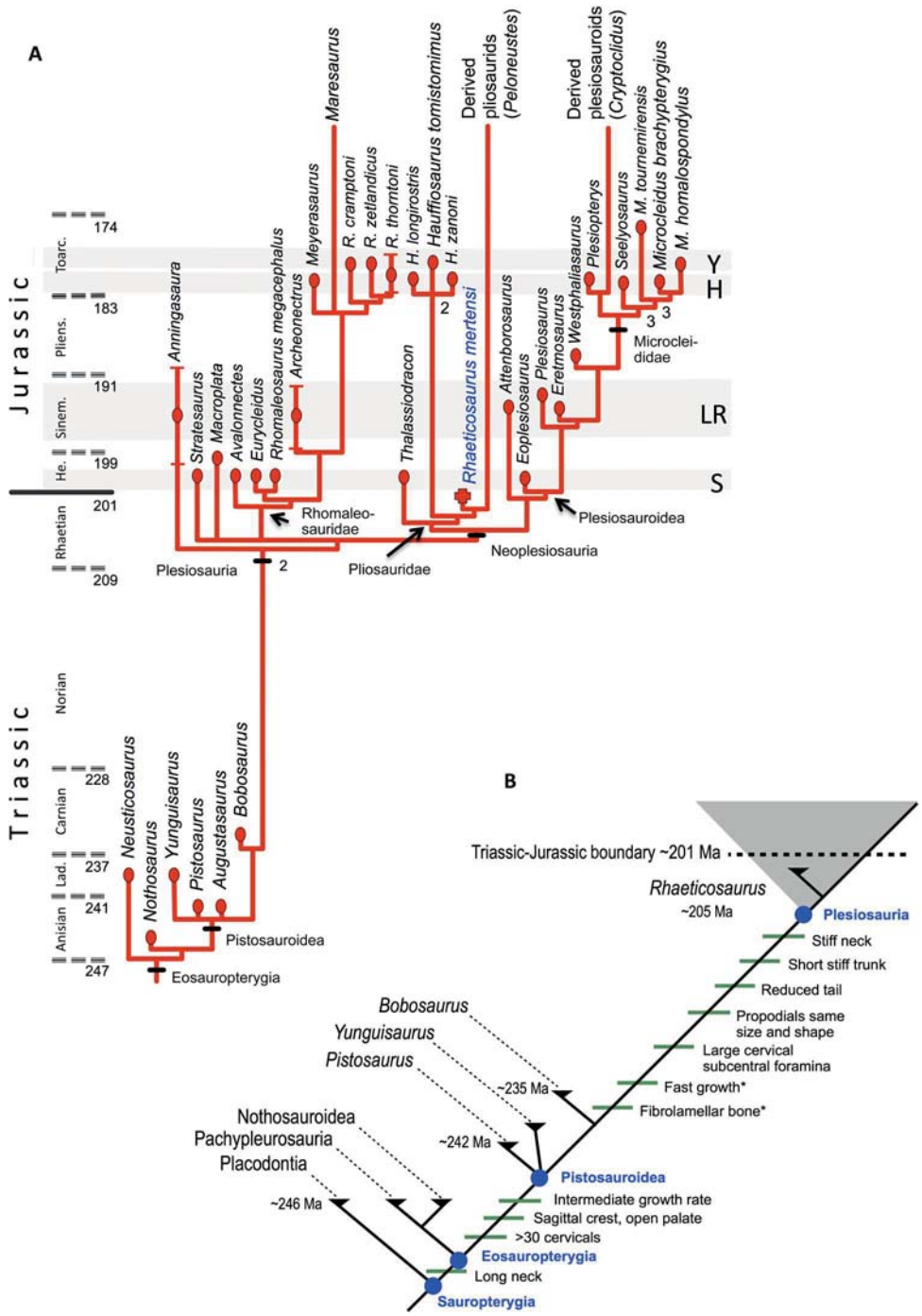

Fig. 3. Calibrated phylogenetic tree of Middle Triassic to Early Jurassic Eosauropterygia and evolution of key features of Plesiosauria. (**A**) Major features of the tree resemble topologies from previous analyses (*4*, *11*) and uses the same clade names. *Rhaeticosaurus mertensi* is a sister to the main radiation of Pliosauridae. (**B**) Evolution of key features of plesiosaurians plotted on the phylogeny of Sauropterygia. Note that these key features were not necessarily recovered as synapomorphies in the phylogenetic analysis and that their arrangement on a specific branch does not imply the order of appearance. Asterisk indicates latest possible appearance of the feature. Lad., Ladinian; He., Hettangian; Pliens., Pliensbachian; Sinem., Sinemurian; Toarc., Toarcian. Geologic time is from Walker *et al.* (*62*). The horizontal gray bands indicate that stratigraphic position of the major plesiosaurian faunas in the Lower Jurassic. LR, Lyme Regis; H, Holzmaden; S, Street; Y, Yorkshire.

length (fig. S6E and table S4). For all five ratios that separate plesiosaurians from non-plesiosaurians, *Rhaeticosaurus* always plotted among plesiosaurians and *Bobosaurus* among non-plesiosaurians. We also computed the humerus/tibia ratio as an additional proxy for relative zeugopodial length because these are the only major limb bones preserved in *Bobosaurus*. *Rhaeticosaurus* again shows a plesiosaurian value, and *Bobosaurus* shows a non-plesiosaurian one (table S4).

In a principal component analysis (PCA) (fig. S7), the two main axes explain 78.1% of the variance (61.0 and 17.1%, respectively). Note that humerus and femur length covary. This is also the case for radius and tibia length and glenoid-acetabular distance that vary antagonistically to distal femur width. All variables contribute to the first axis, although glenoid-acetabular distance, radius length, tibia length, and distal femur width do so to a greater extent. The first axis discriminates plesiosaurians from non-plesiosaurian sauropterygians (fig. S7). In the analysis, plesiosaurians show a proportionally shorter radius and tibia, a shorter glenoid-acetabular distance, and a greater distal width of the femur and, to a lesser extent, the humerus. Conversely, humerus and femur are relatively longer in plesiosaurians than in non-plesiosaurians, as already seen in the ratio histograms (fig. S6). However, there is marked variation in relative humerus and femur length within each group, as shown by the distribution of the taxa along the second axis that is essentially driven by these two variables (and humerus distal width, but to a lesser extent).

Locomotion and feeding

The anatomical features and proportions of *Rhaeticosaurus* have functional implications, particularly for locomotion and feeding. The thin intervertebral cartilages and tall neural spines (Fig. 2C and fig. S2) would have restricted dorsal neck movement, and the thin intervertebral cartilage and medially inclined cervical zygapophyses (as opposed to the horizontally oriented ones of non-plesiosaurians) would have restricted lateral neck movements, suggesting a markedly inflexible neck. The forelimbs and hindlimbs of *Rhaeticosaurus* only differ from later plesiosaurians by having a less expanded distal end of the propodials, but they nevertheless must have functioned as stiff hydrofoils, as in all plesiosaurians (*7*). The extremely short and wide zeugopodium and the straight stylopodial shaft are the major features that set *Rhaeticosaurus* limbs apart from the otherwise similar limbs of some non-plesiosaurians, such as *Yunguisaurus*, in that propulsion by axial undulation still played an important role. The lack of a tight mosaic of zeugopodial and carpal/tarsal bones (*3*) in *Rhaeticosaurus* does not argue against the limbs functioning as hydrofoils because round carpals and tarsals are also seen in many Early Jurassic plesiosaurians with undoubtedly hydrofoil limbs. Only in later plesiosaurians is there a tight mosaic of zeugopodial and carpal/tarsal bones (*3*). The short tail corroborates paraxial locomotion.

Bone histology

Despite a long history of research (*13*–*19*), plesiosaurian bone histology is poorly studied, in marked contrast to basal eosauropterygians. These have been the focus of much recent research (*20*–*23*), resulting in reliable comparative data. We sampled the midshaft of plesiosaurian humeri and femora from most major clades (Fig. 4, figs. S8 to S12, and table S5). Although previous work had offered hints (*13*–*19*), we found that plesiosaurian long bone histology is strikingly uniform (including that of *Rhaeticosaurus*) and that it differs strongly from more basal eosauropterygians. In plesiosaurian propodials, there is no (or only a very small) medullary cavity at midshaft (*13*–*19*), resulting in the preservation of the entire growth record in most specimens we studied (Fig. 4 and figs. S8 to S11). The primary cortex consists of dense, radially oriented primary osteons set in a woven bone matrix (*16*), with dense, large, and plump osteocyte lacunae (*13*) derived from static osteocytes (Fig. 4, D and E, and fig. S12), forming highly vascularized radial fibrolammaller bone tissue (FLB). This tissue suggests very rapid bone apposition (*24*, *25*). In older individuals, even of small species, the primary cortex is completely replaced by dense Haversian bone (fig. S11). The humeri and femora of more basal sauropterygians lack dense Haversian bone (*20*, *22*, *23*), whereas this tissue is characteristic of large endotherms (*24*, *26*) among extant amniotes. Along the evolutionary line to plesiosaurians, an increase in growth rate is first seen in *Pistosaurus* (*20*). This taxon differs from nothosaurs and pachypleurosaurs in having FLB (fig. S9D) (*20*), whereas the former have lamellar zonal bone

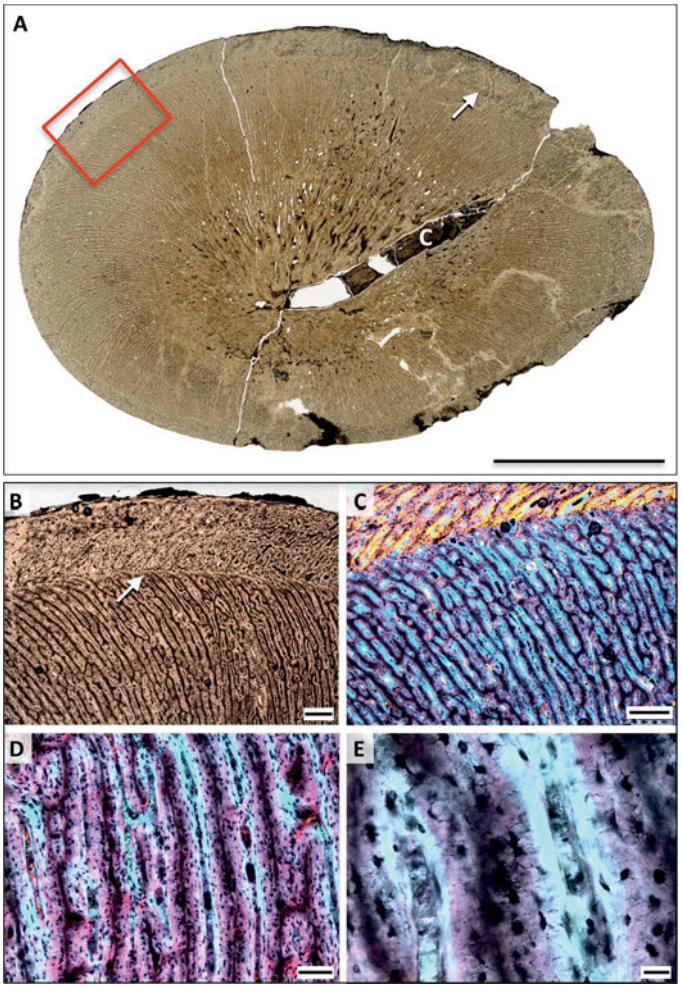

Fig. 4. Bone histology of the holotype of *Rhaeticosaurus mertensi* gen. et sp. nov. (**A**) Midshaft cross section of the femur in normal light. Note the large nutrient canal and the single growth mark (arrow). Box marks enlargement in (B). (**B**) Close-up of outer part of first growth cycle and of second growth cycle. Note the abrupt directional change of the vascular canals at the growth mark (arrow). (**C**) Close-up of (B) in polarized light with lambda filter. (**D**) Radial FLB of the first growth cycle in polarized light with lambda filter. (**E**) Close-up of (D). Note the woven bone scaffold (magenta) surrounded by primary osteons (light blue). In addition, note the plump and densely spaced osteocyte lacunae in the woven bone and the lenticular ones in the primary osteons. c, nutrient canal. Scale bars, 10 mm (A), 500 μm (B and C), 100 μm (D), and 20 μm (E).

tissue (fig. S9, A and B). On the other hand, *Pistosaurus* has more and more densely spaced cyclical growth marks (fig. S9, C and D) at a smaller body size than do plesiosaurians (figs. S9E and S10, A and C), indicating slower cyclical growth marks than in plesiosaurians.

Cyclical growth marks, the first of which appears at >60% of maximum shaft diameter ($n = 4$) (Fig. 4A, figs. S9E and S10, A and C, and table S6), also indicate very fast growth, suggesting that plesiosaurians attained much of their body size within their first year. Local bone apposition rates in the propodial cortex may have been as high as 90 µm/day (see Materials and Methods), comparable with extant mammals and birds and higher than extant reptiles and non-pistosauroid sauropterygians (table S7). Consistent with the qualitative growth rate indicators, *Pistosaurus* shows an intermediate local bone apposition rate. A low number of additional, more densely spaced growth marks in plesiosaurians indicate that final size (several hundred kilograms in the larger taxa) was reached in a few years (fig. S10, A and C). The *Rhaeticosaurus* holotype only shows one growth mark, corroborating its juvenile status.

DISCUSSION

Growth mark development and comparison of growth rates

The observation that the first growth mark in plesiosaurians is found at >60% of maximum shaft diameter (a proxy for final body size) argues against this mark being a neonatal line. However, the observation raises the question whether the first observed mark represents the end of the first year of life or a later growth mark, potentially leading to underestimated ages. This concern arises from the observation for sauropod dinosaurs that in the same individual, only indistinct and irregular growth marks are expressed in the large long bones, but more numerous and well-developed ones are observed in the ribs (*27*). In the case of the propodial cortex of plesiosaurians, several lines of evidence suggest that the first observed growth mark does mark the end of the first year of life. (i) The ribs of some specimens, for example, *Cryptoclidus* STIPB R 324, show the same low growth mark count as the long bones. Low growth mark counts are also seen in another rib and one gastral rib that we have sampled but that lack associated long bones. (ii) The first and later growth marks in the plesiosaurian propodial cortex are distinct when present and of a rather different and unique nature, not consisting of an annulus or a line of arrested growth as in most other amniotes, but of a sudden change in vascular canal orientation, reflecting the reorganization of the vascular network on the bone surface when growth was cyclically interrupted (Fig. 4, B and C, fig. S10, B and D). (iii) The closest similarity to the radial organization of the vascular network of plesiosaurians was recently described for the Triassic species of the Permian-Triassic boundary–crossing therapsid genus *Moschorhinus* (*28*, *29*). In these species, the number of growth marks is evolutionarily reduced to zero to two because of an increased growth rate after the Permian extinction event. (iv) Similar growth rates to what we hypothesize for plesiosaurians are seen in extant mammals (table S7). Although plesiosaurian body mass is difficult to constrain, body mass in the sampled plesiosaurians must have been comparable to that of small to large ungulate species and some small cetaceans, which also reach full size within a few years (*30*–*32*), whereas other cetaceans grow more slowly (*33*).

Growth rate and metabolic rate

On theoretical grounds, there is a link between growth rate and metabolic rate, fast growth needing a fast metabolism to provide the growing organism with the needed materials and energy (*24*, *34*). Growth rate can be inferred from bone histology primarily in two ways: by bone tissue type, such as FLB versus lamellar zonal bone (*35*, *36*), and by a cyclical growth mark record (*36*, *37*). FLB is only found in mammals and birds among extant amniotes, leading to the most basic inference from bone tissue type, that is, that FLB is an indicator of mammalian or avian growth rates (*25*, *35*, *37*, *38*). This inference was questioned in a study by Tumarkin-Deratzian (*39*) who described FLB in wild alligators but did not conclusively document the existence of this tissue type because the study did not include polarized light images. The hypothesis that true FLB exists in alligators (wild and captive) has been falsified by more recent work (*40*). The ability to lay down limited amounts of woven bone in early ontogenetic stages (fetus and neonate) cannot be equated with FLB and thus cannot serve as evidence against the hypothesis that under natural conditions, FLB requires a high basal metabolic rates (*35*, *38*) for its formation. Captive alligators have been reported to lay down FLB when kept under optimal conditions and provided with unlimited food, but this observation does not falsify the above hypothesis. Finally, crocodilians have secondarily reduced bone growth rates and lost FLB in their stem line (*35*, *38*). They also have secondarily reduced metabolic rates (*38*), an evolutionary trend unknown in any other amniote clade. This suggests that the ability of crocodilians to produce FLB in captivity is a plesiomorphy that does not provide evidence against the link between FLB and a high basal metabolic rate.

The dominance of static osteogenesis (*25*, *41*) in plesiosaurian cortical bone is striking (fig. S12) and suggests very high local bone apposition rates, consistent with the low growth mark count observed in the long bones. Taking a quantitative approach based on the bone tissue type criteria of previous studies (*24*, *34*, *35*), it is also clear that plesiosaurians had very high local bone apposition rates. Local bone apposition rates translate into overall growth rates, and high growth rates seen in plesiosaurians suggest basal metabolic rates at the level of extant endotherms (*37*). Virtually all extant endotherms show parental care, which has previously been inferred from a gravid plesiosaurian (*42*). The fast growth of juvenile plesiosaurians appears only possible through parental care, resulting in energy transfer from parent to offspring through feeding and protection.

The link between metabolic rate and maximum rate of growth in mass in extant vertebrates (*24*, *34*, *43*, *44*) could potentially be used to infer plesiosaurian metabolic rates. However, determining maximum rates of growth in mass from the annual growth mark record in plesiosaurian propodials is hampered by the current lack of reliable body mass estimates.

In conclusion, strong bone histological evidence consisting of radial FLB, dominance of static osteocytes, very fast growth, and dense Haversian tissue in the propodial bones of plesiosaurians suggests a basal metabolic rate well elevated over that of typical reptiles at the level of endotherms. Endothermy is consistent with isotopic evidence for homeothermy (*45*) in plesiosaurians.

Plesiosaurian evolution across the Triassic-Jurassic boundary

On the basis of a quantitative analysis of the Mesozoic marine reptile record, open-marine adaptation had been hypothesized to facilitate plesiosaurian and parvipelvian ichthyosaur survival into the Jurassic (*46*). However, for plesiosaurians, evidence for open-marine adaptation was lacking because of the lack of informative Triassic plesiosaur fossils, in contrast to parvipelvian ichthyosaurs that are known from the Norian (*46*). The very diverse plesiosaurian fauna from the earliest Jurassic of the United Kingdom (*11*) and tantalizing Triassic fossils (*8*, *9*, *46*) were consistent with a Triassic origin and diversification of plesiosaurians.

On the other hand, because of the lack of unequivocal Triassic plesiosaurian finds, it was hypothesized that plesiosaurians rapidly colonized open marine habitats only in the aftermath of the Late Triassic extinctions (*11*). The Triassic age and phylogenetic relationships of *Rhaeticosaurus* now shed light on these issues. Under our best-supported phylogenetic hypothesis (see Materials and Methods), at least six plesiosaurian lineages crossed the Triassic-Jurassic boundary (Fig. 3A). Late Triassic and end-Triassic extinction events (*5*, *47*, *48*) were thus survived by diverse lineages of plesiosaurians in addition to parvipelvian ichthyosaurs (*1*, *6*). Most groups that went extinct during these events inhabited coastal waters and shallow carbonate platforms (Placodontia, Nothosauroidea, non-plesiosaurian Pistosauroidea, and Tanystropheidae) (*1*, *5*, *6*) but not the open sea. Although there are two other groups recorded from open-marine sediments that went extinct (thalattosaurs and non-plesiosaurian Pistosauroidea), these were less specialized for a pelagic lifestyle. Plesiosaurians seemingly adapted to life in the open sea (*20*, *46*) during the Late Triassic and not only in the Early Jurassic (*11*) by evolving long-distance cruising capabilities facilitated by a high metabolic rate (evidenced by fast growth and FLB) and underwater flight (evidenced by skeletal morphology and proportions) over a time period of 30 million years (Ma) (Fig. 3B). Open-marine adaptation of plesiosaurians may have facilitated their survival into the Jurassic (*46*) because pelagic prey (fish and soft-bodied cephalopods) (*47*) were less affected by the end-Triassic extinction events than benthic invertebrates and reef organisms (*47*, *48*). These suffered from a calcification crisis (*49*) but formed the food base for the Late Triassic marine reptile groups that went extinct. The scenario of a pre-Jurassic radiation of plesiosaurians begs the question of why the evidence is coming to light only now. The Rhaetian bonebed vertebrae previously assigned to plesiosaurians represent different taxa (*8*) that now appear consistent with a Late Triassic radiation. This radiation may have gone unrecognized for so long because of the extreme paucity of marine reptile localities representing the last 30 Ma of the Triassic (*6*).

MATERIALS AND METHODS

Phylogenetic analysis

To test the phylogenetic relationships of *Rhaeticosaurus*, we added the holotype to a recently published data matrix of 270 characters and 80 operational taxonomic units (OTUs). This matrix was designed to clarify the interrelationships of plesiosaurians and their survival across the Jurassic-Cretaceous boundary (*4*). However, because most of the taxa in the matrix were unquestionably more derived than the Triassic plesiosaurian, we used the taxon sampling of another matrix specifically designed to clarify the relationships of Early Jurassic plesiosaurians (*11*). Three modifications to this taxon sampling were made. For one, following the studies of Fabbri *et al.* (*12*) and Neenan *et al.* (*50*), we combined the *Pistosaurus* skull and postcranial OTUs into a single OTU because there was little doubt that the *Pistosaurus* skull belongs with the *Pistosaurus* postcranium (*51*–*53*). We also added two additional outgroup taxa to the single original outgroup (*Yunguisaurus liae*), the Ladinian pachypleurosaur *Neusticosaurus pusillus* and the Anisian nothosaur *Nothosaurus marchicus* to clarify the relationships of Triassic sauropterygians on the line leading to Plesiosauria. No characters were modified, and no new characters were added. The analysis thus used a matrix of 35 taxa (6 Triassic non-plesiosaurian taxa, *Rhaeticosaurus*, and 28 Early and Middle Jurassic plesiosaurian taxa) and 270 characters (data file S1).

We ran the analysis using the software PAUP v. 4.0b10 (*54*), utilizing the same settings as in the study (*11*) of the Early Jurassic plesiosaurians (500 random addition replicates with TBR branch swapping). Of the 270 characters, only 207 were parsimony-informative because we used a reduced taxon sampling compared to that of Benson and Druckenmiller (*4*), resulting in 30 characters being constant and 33 being parsimony-uninformative. The reduced taxon sampling also meant that we did not have to use the parsimony ratchet because the search in PAUP was sufficiently fast. We initially ran the analysis with only *Neusticosaurus* as the outgroup to minimize assumptions about interrelationships and then added *Nothosaurus* and *Yunguisaurus* to the outgroup. In each case (one, two, and three outgroup taxa), our analyses recovered the same 21 most parsimonious trees that are 764 steps long, with a consistency index of 0.415 and a retention index of 0.554. We then computed a strict consensus tree in which *Rhaeticosaurus* is found to be a basal member of the Pliosauridae (Fig. 3A and table S3). This is a somewhat surprising result, given that the lower jaw of *Rhaeticosaurus* shows features rare or unknown in pliosaurids such as lack of participation of the splenial in the jaw symphysis, the short angular, and the dorsoventral and mediolateral orientation of the retroarticular process (*4*, *11*). In addition, the pliosaurs lack the sharp ridge on the anterior margin of the humerus (*4*, *11*).

Focusing on our analysis, a comparison with the other Lower Jurassic pliosaurids, *Thalassiodracon hawkinsii* (*11*), and the species of *Hauffiosaurus* (*55*) revealed some support through unequivocal and unique syanpomorphies for the placement of *Rhaeticosaurus* within this clade. There is only one unequivocal and unique synapomorphy of *Rhaeticosaurus* and *Peloneustes* (as a representative of more derived pliosaurids): the wide and short tibia (ratio of tibia length to maximum width, 0.8–1.0 character, 255; state, 2). In addition, there is only one unequivocal but not unique synapomorphy (table S3). The Pliosauridae in our analysis have only one unequivocal and unique synapomorphy, the posterior termination of the premaxilla (character, 16; state, 1; broad, deeply interdigitating suture with the frontal or parietal), which is, however, not preserved in *Rhaeticosaurus*. In addition, there are three unequivocal but not unique synapomorphies (table S3). The sister group relationship of the *Rhaeticosaurus-Peloneustes* clade with *Hauffiosaurus* is also supported by a single unequivocal and unique synapomorphy (character, 34; state, 1; lacrimal present, maxilla excluded from orbit margin), which again is not preserved in *Rhaeticosaurus*. In addition, there are eight unequivocal but not unique synapomorphies (table S3). *Hauffiosaurus* differs from both *Rhaeticosaurus* and *Thalassiodracon* in the autapomorphic contact of the neural arch with the articular facets for the cervical ribs (*55*).

In its major features, the consensus tree resembles the ones by Benson and colleagues (*4*, *11*). However, the interrelationships at the base of Plesiosauria are better resolved (Fig. 3A) in our analysis, and there is greater stratigraphic congruency in the Plesiosauria, the Rhomaleosauridae, and the Plesiosauroidea than in either of the previous analyses (*4*, *11*). On the other hand, the nested position of *Rhaeticosaurus* within Pliosauridae is inconsistent with its great stratigraphic age. At least six nodes within Plesiosauria are situated in the Triassic, predating *Rhaeticosaurus*. *Bobosaurus* was always recovered as the sister taxon to Plesiosauria, but the relationships of the basal Pistosauroidea (*Yunguisaurus*, *Pistosaurus*, and *Augustasaurus*) are not resolved. We computed the Bremer support index for the phylogeny in PAUP. The support index of most nodes is only 1, but Plesiosauria is supported by a value of 2. Table S3 provides the list of synapomorphies derived from the consensus tree. The list was also used to diagnose Plesiosauria and *Rhaeticosaurus* (table S2).

Basal plesiosaurian relationships are notoriously difficult to resolve, and support of the resulting hypotheses generally is weak (*4*, *11*), as in our analysis. To specifically evaluate the influence of the newly added taxa (further outgroups and *Rhaeticosaurus*), we reran our analysis without them and obtained a consensus tree that showed a near-complete

loss of resolution at the base of Plesiosauria, as in the preferred phylogenetic hypothesis by Benson and Druckenmiller (*4*). Thus, even if *Rhaeticosaurus* was the most basal plesiosaurian or would fall out in a different position among basal plesiosaurians, phylogenetic analysis including *Rhaeticosaurus* indicated that at least one lineage of plesiosaurian crossed the Triassic-Jurassic boundary, although the isolated plesiosaurian-type vertebrae in the European Rhaetic bonebeds (table S1) (*8*, *56*) suggested that several did, consistent with our phylogenetic analysis.

Phylogenetic definition of Plesiosauria

Despite Plesiosauria being such an iconic taxon and a plesiosaurian skeleton being instantly recognizable as such, the phylogenetic definition of Plesiosauria has proven remarkably problematic (*3*). One issue was the status of the early Carnian sauropterygian fossil *Bobosaurus forojuliensis* (*12*, *57*). In the first phylogenetic analysis of plesiosaurian interrelationships to include *Bobosaurus*, by Benson *et al.* (*11*), *Bobosaurus* was found to be the sauropterygian most closely related to plesiosaurians, a position that has consistently been found in other analyses since (*4*, *12*). Benson *et al.* (*11*) explicitly excluded *Bobosaurus* from the taxon Plesiosauria in their stem-based phylogenetic definition of the clade in 2012. However, in 2014, Fabbri *et al.* (*12*) advocated *Bobosaurus* as the oldest plesiosaurian, writing the stem-based definition of Plesiosauria (*3*) as "all taxa more closely related to *Plesiosaurus dolichodirus* and *Pliosaurus brachydeirus* than to *Augustasaurus hagdorni*." Whereas this definition would make *Bobosaurus* a plesiosaurian, this assignment is inconsistent with many obvious and acknowledged difference between *Bobosaurus* and the group traditionally recognized as Plesiosauria, that is, all latest Triassic and post-Triassic members of the Pistosauroidea (*3*, *4*, *11*). Because of this problem, we chose an apomorphy-based definition for the clade Plesiosauria. Such a definition was also used in an informal way in the recent literature (*58*): "Plesiosauria… had a highly derived body plan, comprising a stiff trunk, limbs modified to form four large flippers, and highly variable neck lengths."

The case of *Bobosaurus* and the problems of defining Plesiosauria illustrate the inherent limitations of stem-based phylogenetic definitions in the face of incomplete fossils and extreme gaps in the fossil record. No pistosauroids are recorded for a time span of about 30 Ma, from the middle Carnian (235 Ma), the age of *Bobosaurus*, to the middle Rhaetian (205 Ma), the age of *Rhaeticosaurus*. Few, if any, other major tetrapod clade, marine or terrestrial, suffers from such a gap in its record. In addition, whereas taxa in phylogenetic definitions should be well known and complete, among basal pistosauroids, this neither applies to *Augustasaurus* nor to *Bobosaurus* but only to *Yunguisaurus liae* (*59*). However, a stem-based definition of Plesiosauria using *Yunguisaurus* would result in *Augustasaurus*, *Pistosaurus*, and *Bobosaurus* being plesiosaurians under most phylogenetic hypotheses (*4*, *11*, *12*), which is not a satisfactory solution. Finally, a node-based definition of Plesiosauria is no solution because of the poor support shared by all competing phylogenetic hypotheses [(*4*, *11*, *12*), this study] of basal plesiosaurian interrelationships. This poor support means an obvious risk of excluding well-known taxa from Plesiosauria in a node-based definition upon further phylogenetic research. In conclusion, an apomorphy-based definition of Plesiosauria is the most adequate course of nomenclatorial action.

Body size estimate

In a recent study, trunk length was used as a proxy for body size in plesiosaurians (*11*) because of interspecific variability of relative skull and neck length and incompletely preserved necks and tails in many specimens. Trunk length was measured from the first dorsal vertebra to the last sacral in the largest adult individuals of the taxon (*11*). The preserved trunk length of the *Rhaeticosaurus* holotype is 649 mm, which was slightly smaller than the smallest known Hettangian plesiosaurian, *Thalassiodracon* [680 mm (*11*)]. However, because WMNM P 64047 is a juvenile and some pectoral vertebrae may be missing, it probably would have grown somewhat larger than the smallest Hettangian plesiosaurians.

Total length can also be estimated for WMNM P 64047 based on two approaches. On the basis of the parts of the skull and vertebral column preserved in articulation on the slab, we estimated the total body length as 2469 mm [lower jaw, 215 mm; neck (including the length of gap in the cervical and pectoral column), 1028 mm; dorsal column, 553 mm; sacral column, 96 mm; tail (including an estimated eight missing distal caudal vertebrae), 577 mm]. Alternatively, by adding up the anteroposterior length of all preserved vertebra, assuming an intervertebral cartilage thickness of 1.5 mm, and interpolating (in the neck), respectively extrapolating (in the tail), the length of the missing vertebrae, we arrived at a slightly lower estimate of 2270 mm for the total body length. The mean of these two estimates was 2370 mm.

Morphometric analysis

We collected morphometric data of trunk and limb elements for a representative sample of eosauropterygian taxa, including three pachypleurosaurs, three nothosaurs, five non-plesiosaurian pistosauroids, and nine plesiosaurians, including *Rhaeticosaurus* (table S4). The full set of variables was obtainable only for eight non-plesiosaurians and eight plesiosaurians. We chose glenoid-acetabular distance over the length of the dorsal vertebral column as our proxy for trunk length because this distance was easily measured in all taxa and functionally relevant for locomotion. We measured the length, medial width, and distal width of the propodials (humerus and femur) to quantify the shape of these bones. Finally, we measured the length of radius and tibia as proxies for zeugopodial size. Among the non-plesiosaurian pistosauroids, the complete variable set could only be obtained for *Wangosaurus* and *Yunguisaurus*. Because *Pistosaurus*, *Augustasaurus*, and *Bobosaurus* were found as successive sister groups to Plesiosauria in previous analyses (*4*, *11*), we also included these taxa in the morphometric analysis despite their incompleteness. Although lacking the forelimb, *Avalonectes* was included in the data set because of its basal position among plesiosaurians in the previous analyses and its earliest Jurassic age (*11*). We usually collected the measurements from a single monograph describing a specific individual using information in the text, as well as the photographs and specimen drawings in the publications (table S4).

To evaluate changes in proportion of the trunk and limbs during eosauropterygian evolution, we computed ratios of various limb measurements to glenoid-acetabular distance and to each other (table S4). We then produced histograms of six ratios for the 16 taxa for that all measurements could be collected (fig. S6 and table S4).

To further quantify these proportional relationships, we conducted a PCA on the data set of the 16 completely represented taxa to explore the distribution of the different taxa in a morphospace. Measurements were all $\log_{10}$-transformed before analysis to meet assumptions of normality and homoscedasticity required for parametric analyses. A size index was calculated for each specimen as the mean of all values and subtracted from each measurement to remove the size effect. The PCA was performed using the statistical software R (*60*).

Histological analysis

As noted in the main text, it was puzzling that the uniqueness of plesiosaurian bone histology was not recognized before, despite the long history of research. Reasons were insufficiently constrained samples in terms of taxonomy [undiagnostic samples (*13*, *16*, *17*)], insufficient clade coverage (*13*–*17*), anatomy [lack of identification of skeletal element (*13*, *14*)], ontogenetic stage [old individuals, in which the peculiar primary FLB had been replaced by secondary Haversian bone (*13*, *14*, *16*, *17*)], and plane of section [plane of section in long bones offset from nutrient canal (*13*, *14*, *16*–*19*)]. A case in point is the 19th century work by Kiprijanoff (*13*) on Russian marine reptiles that described all manner of histology and microanatomy, correctly figuring ichthyosaur microanatomy and plesiosaurian dental histology in the finest detail, but bypassing plesiosaurian microanatomy, only schematically illustrating propodial cross section of seemingly old individuals.

We obtained samples of plesiosaurian propodials across the tree (table S5), representing the widest taxonomic coverage in plesiosaurian histologic studies so far. All individuals except for the *Rhaeticosaurus* holotype and the Japanese elasmosaur were osteologically mature. The humeri and femora were sectioned by two cuts spaced about 5 mm apart across the mid-diaphysis, with the two cuts preferentially enclosing the inner terminus of the nutrient canal because this indicates the site of earliest bone growth (*61*). The location of the nutrient canal was determined either visually or by computed tomography (CT) scanning of the specimens (fig. S8) using the GE phoenix v|tome|x s240 scanner at the Division of Paleontology of the Steinmann Institute, University of Bonn, Germany. Using the 240-kV tube of the scanner, scan parameters were 200 kV, 200 µA, and a voxel size of 142 µm. CT scanning is important because in same bones, the nutrient canal does not extend radially from the center to the surface but deviates proximally. Thus, a section placed at the nutrient foramen may be located proximal to the center of growth, leading to erroneous interpretations in previous studies (*14*, *17*).

The mid-diaphysial slice of bone was then processed into a standard petrographic thin section 50 to 80 µm in thickness. The sections were observed under a Leica DM2500LP polarizing microscope, and digital photomicrographs were taken with a Leica DFC420 color camera mounted on this microscope and edited using the 2007 Leica IMAGE ACCESS EASYLAB 7 software. Overview images were obtained with an Epson V750 high-resolution scanner. The terminology followed the study of Francillon-Vieillot *et al.* (*24*).

A useful proxy for growth rate is the maximum local bone apposition rate in the femur cortex, reflecting the increase in thickness of this bone (*35*). Maximum local bone apposition rate was expressed in micrometers per day and was determined in extant and extinct species in the midshaft region following established protocols (*35*). Four of the nine plesiosaurian specimens histologically sampled were suitable for this analysis (table S6) because they had a complete growth record and at least one postnatal growth mark preserved. One specimen, the juvenile elasmosaur OMNH MV 85, did not show any growth marks, and the remaining four (table S5) were completely remodeled, obliterating the growth mark record. Note that both humeri and femora were included in this analysis because they are of nearly the same length (fig. S6) and show the same histology in plesiosaurians, unlike in the amniotes previously analyzed (*35*). We slightly modified the protocol by measuring apposition along the nutrient canal that represents a homologous location, at least in plesiosaurians, and is close to the region of the thickest cortex (Fig. 4 and figs. S8 to S10). We measured the cortical thickness from the center of the bone (the inner terminus of the nutrient canal, which is well preserved in plesiosaurians because of the lack of medullary resorption) to the first growth marks in millimeters. We then divided this value by 730, accounting for the 365 days in a year, plus a hypothetical gestation period of equal length [365 days as in many dolphin species (*33*)] to cover the prenatal part of the cortex. This procedure was necessary because a neonatal line could not reliably be detected. Whereas the resulting local bone apposition rates (table S6) are only estimates, the margin of error is insignificant in the comparative context (local bone apposition rates in reptiles versus mammals and birds; table S7). Even if we assume an unrealistically short gestation period of 50 days or an unrealistically long one of 500 days (table S6), local bone apposition rates do not overlap with those of extant reptiles (table S7). We were also aware of the higher number of days per year in the geologic past but felt that the error of a few days introduced this way was negligible. On the basis of Amprino's rule (*35*), we assumed that prenatal and postnatal bone apposition rate were very similar because of the uniformity of the primary bone from the onset of osteogenesis in the embryo to the first postnatal growth mark. For estimating the relative size of the plesiosaurians at the end of their first year, we also used cortical thickness along the nutrient canal.

Note that the maximum local bone apposition rate also depends on body size at the time of fastest growth (*35*). Our plesiosaurian data were difficult to correct for size because of the difficulty of determining plesiosaurian body mass, but the size effect was overridden by the general pattern, with the endotherms (birds, mammals) showing apposition rates much higher, mostly an order of magnitude, than the ectotherms in the sample (lizards, turtles, a crocodile). A case in point is the crocodile data point (*Crocodilus niloticus*). This taxon is in the same body mass range as plesiosaurians but grows at only somewhat more than half the rate of the slowest plesiosaurian and only a 10th of the rate of the fastest plesiosaurian (table S7).

SUPPLEMENTARY MATERIALS

Supplementary material for this article is available at http://advances.sciencemag.org/cgi/content/full/3/12/e1701144/DC1

Supplementary Anatomical Descriptions

fig. S1. The holotype of *R. mertensi* gen. et sp. nov.

fig. S2. The holotype of *R. mertensi* gen. et sp. nov., anterior cervical vertebral column.

fig. S3. The holotype of *R. mertensi* gen. et sp. nov.

fig. S4. The holotype of *R. mertensi* gen. et sp. nov.

fig. S5. Reconstruction of the skeleton of *R. mertensi* gen. et sp. nov. based on the available measurements and proportions.

fig. S6. Selected skeletal proportions in Eosauropterygia.

fig. S7. Principal component analysis of trunk and limb measurements in Eosauropterygia.

fig. S8. Examples of CT scans of plesiosaurian long bones used in locating the nutrient canal before sectioning.

fig. S9. Evolution of long bone histology in Triassic Eosauropterygia.

fig. S10. Long bone histology of Jurassic and Cretaceous Plesiosauria.

fig. S11. Long bone histology of a mature Middle Jurassic plesiosaurian.

fig. S12. Long bone histology of the holotype of *R. mertensi* gen. et sp. nov. in longitudinal section.

table S1. Faunal list of bonebed above plesiosaurian discovery horizon.

table S2. Unambiguous but not unique synapomorphies diagnosing *R. mertensi* gen. et sp. nov. in addition to the two autapomorphies.

table S3. List of synapomorphies from phylogenetic analysis.

table S4. Measurements and proportions in the trunk and limbs of Eosauropterygia.

table S5. List of histological samples.

table S6. Local bone apposition rate to the end of the first year and relative body size at the end of the first year in selected sauropterygians.

table S7. Comparison of local bone apposition rates in the femur of selected amniotes compared to local bone apposition rates in the humeri and femora of plesiosaurians.

data file S1. Character matrix in NEXUS format for phylogenetic analysis described in Materials and Methods.

References (*63*–*75*)

REFERENCES AND NOTES

1. N. P. Kelley, N. D. Pyenson, Evolutionary innovation and ecology in marine tetrapods from the Triassic to the Anthropocene. *Science* **348**, aaa3716 (2015).
2. A. Houssaye, Bone histology of aquatic reptiles: What does it tell us about secondary adaptation to an aquatic life? *Biol. J. Linn. Soc.* **108**, 3–21 (2013).
3. H. F. Ketchum, R. B. J. Benson, Global interrelationships of Plesiosauria (Reptilia, Sauropterygia) and the pivotal role of taxon sampling in determining the outcome of phylogenetic analyses. *Biol. Rev.* **85**, 361–392 (2010).
4. R. B. J. Benson, P. S. Druckenmiller, Faunal turnover of marine tetrapods during the Jurassic–Cretaceous transition. *Biol. Rev.* **89**, 1–23 (2014).
5. N. P. Kelley, R. Motani, D.-y. Jiang, O. Rieppel, L. Schmitz, Selective extinction of Triassic marine reptiles during long-term sea-level changes illuminated by seawater strontium isotopes. *Palaeogeogr. Palaeoclimatol. Palaeoecol.* **400**, 9–16 (2014).
6. N. Bardet, J. Falconnet, V. Fischer, A. Houssaye, S. Jouve, X. Pereda Suberbiola, A. Pérez-García, J.-C. Rage, P. Vincent, Mesozoic marine reptile palaeobiogeography in response to drifting plates. *Gondw. Res.* **26**, 869–887 (2014).
7. S. Liu, A. S. Smith, Y. Gu, J. Tan, C. K. Liu, G. Turk, Computer simulations imply forelimb-dominated underwater flight in plesiosaurs. *PLOS Comput. Biol.* **11**, e1004605 (2015).
8. G. W. Storrs, Fossil vertebrate faunas of the British Rhaetian (latest Triassic). *Zool. J. Linn. Soc.* **112**, 217–259 (1994).
9. A. G. Sennikov, M. S. Arkhangelsky, On a typical Jurassic sauropterygian from the Upper Triassic of Wilczek Land (Franz Josef Land, Arctic Russia). *Paleont. J.* **44**, 567–572 (2010).
10. P. M. Sander, The microstructure of reptilian tooth enamel: Terminology, function, and phylogeny. *Münchner Geowiss. Abh.* **38**, 1–102 (1999).
11. R. B. J. Benson, M. Evans, P. S. Druckenmiller, High diversity, low disparity and small body size in plesiosaurs (Reptilia, Sauropterygia) from the Triassic–Jurassic boundary. *PLOS ONE* **7**, e31838 (2012).
12. M. Fabbri, F. M. Dalla Vecchia, A. Cau, New information on *Bobosaurus forojuliensis* (Reptilia: Sauropterygia): Implications for plesiosaurian evolution. *Hist. Biol.* **26**, 661–669 (2014).
13. A. V. Kiprijanoff, Studien fiber die fossilen Reptilien Russlands. *Mém. Acad. Imp. Sci. St. Petersbourg* **7**, 1–144 (1881–1883).
14. Ł. Fostowicz-Frelik, A. Gaździcki, Anatomy and histology of plesiosaur bones from the Late Cretaceous of Seymour Island, Antarctic Peninsula. *Palaeontol. Pol.* **60**, 7–32 (2001).
15. L. Salgado, M. S. Fernandez, M. Talevi, Observaciones histologicas en reptiles marinos (Elasmosauridae y Mosasauridae) del Cretacico Tardio de Patagonia y Antartida. *Ameghiniana* **44**, 513–523 (2007).
16. J. Wiffen, V. de Buffrénil, A. de Ricqlès, J.-M. Mazin, Ontogenetic evolution of bone structure in Late Cretaceous Plesiosauria from New Zealand. *Geobios* **28**, 625–640 (1995).
17. L. Liebe, J. H. Hurum, Gross internal structure and microstructure of plesiosaur limb bones from the Late Jurassic, central Spitsbergen. *Nor. J. Geol.* **92**, 285–309 (2012).
18. J. P. O'Gorman, M. Talevi, M. S. Fernández, Osteology of a perinatal aristonectine (Plesiosauria; Elasmosauridae). *Antarct. Sci.* **29**, 61–72 (2017).
19. L. Ossa-Fuentes, R. A. Otero, D. Rubilar-Rogers, Microanatomy and osteohistology of a juvenile elasmosaurid plesiosaur from the Upper Maastrichtian of Marambio (Seymour) Island, Antarctica. *Bol. Museo Nacional Hist. Natural Chile* **66**, 149–160 (2017).
20. A. Krahl, N. Klein, P. M. Sander, Evolutionary implications of the divergent long bone histologies of *Nothosaurus* and *Pistosaurus* (Sauropterygia, Triassic). *BMC Evol. Biol.* **13**, 123 (2013).
21. A. Houssaye, P. M. Sander, N. Klein, Adaptive patterns in aquatic amniote bone microanatomy—More complex than previously thought. *Integr. Comp. Biol.* **56**, 1349–1369 (2016).
22. N. Klein, P. M. Sander, A. Krahl, T. M. Scheyer, A. Houssaye, Diverse aquatic adaptations in *Nothosaurus* spp. (Sauropterygia)—Inferences from humeral histology and microanatomy. *PLOS ONE* **11**, e0158448 (2016).
23. N. Klein, E. M. Griebeler, Bone histology, microanatomy, and growth of the nothosauroid *Simosaurus gaillardoti* (Sauropterygia) from the Upper Muschelkalk of southern Germany/Baden-Württemberg. *C. R. Palevol* **15**, 142–162 (2016).
24. H. Francillon-Vieillot, V. de Buffrénil, J. Castanet, J. Géraudie, F. J. Meunier, J. Y. Sire, L. Zylberberg, A. de Ricquès, Microstructure and mineralization of vertebrate skeletal tissues, in *Skeletal Biomineralization: Patterns, Processes and Evolutionary Trends,* J. G. Carter, Ed. (Van Nostrand Reinhold, 1990), vol. 1, pp. 471–530.
25. K. Stein, E. Prondvai, Rethinking the nature of fibrolamellar bone: An integrative biological revision of sauropod plexiform bone formation. *Biol. Rev. Camb. Philos. Soc.* **89**, 24–47 (2014).
26. J. D. Currey, The many adaptations of bone. *J. Biomech.* **36**, 1487–1495 (2003).
27. K. Waskow, P. M. Sander, Growth record and histological variation in the dorsal ribs of *Camarasaurus* sp. (Sauropoda). *J. Vertebr. Paleontol.* **34**, 852–869 (2014).
28. A. K. Huttenlocker, J. Botha-Brink, Body size and growth patterns in the therocephalian *Moschorhinus kitchingi* (Therapsida: Eutheriodontia) before and after the end-Permian extinction in South Africa. *Paleobiology* **39**, 253–277 (2013).
29. J. Botha-Brink, D. Codron, A. K. Huttenlocker, K. D. Angielczyk, M. Ruta, Breeding young as a survival strategy during Earth's greatest mass extinction. *Sci. Rep.* **6**, 24053 (2016).
30. M. Köhler, N. Marín-Moratalla, X. Jordana, R. Aanes, Seasonal bone growth and physiology in endotherms shed light on dinosaur physiology. *Nature* **487**, 358–361 (2012).
31. A. S. Barreto, F. C. W. Rosas, Comparative growth analysis of two populations of *Pontoporia blainvillei* on the Brazilian coast. *Mar. Mamm. Sci.* **22**, 644–653 (2006).
32. S. Murphy, E. Rogan, External morphology of the short-beaked common dolphin, *Delphinus delphis*: Growth, allometric relationships and sexual dimorphism. *Acta Zool.* **87**, 315–329 (2006).
33. A. Berta, *Whales, Dolphins, and Porpoises. A Natural History and Species Guide* (University of Chicago Press, 2015), 288 pp.
34. L. Montes, N. Le Roy, M. Perret, V. de Buffrenil, J. Castanet, J. Cubo, Relationships between bone growth rate, body mass and resting metabolic rate in growing amniotes: A phylogenetic approach. *Biol. J. Linn. Soc.* **92**, 63–76 (2007).
35. J. Cubo, N. Le Roy, C. Martinez-Maza, L. Montes, Paleohistological estimation of bone growth rate in extinct archosaurs. *Paleobiology* **38**, 335–349 (2012).
36. A. H. Lee, K. Huttenlocker, K. Padian, H. N. Woodward, Analysis of growth rates, in *Bone Histology of Fossil Tetrapods: Advancing Methods, Analysis, and Interpretation*, K. Padian, E.-T. Lamm, Eds. (University of California Press, 2013), pp. 217–251.
37. K. Padian, K. Stein, Evolution of growth rates and their implications, in *Bone Histology of Fossil Tetrapods: Advancing Methods, Analysis, and Interpretation*, K. Padian, E.-T. Lamm, Eds. (University of California Press, 2013), pp. 253–264.
38. L. J. Legendre, G. Guénard, J. Botha-Brink, J. Cubo, Palaeohistological evidence for ancestral high metabolic rate in archosaurs. *Syst. Biol.* **65**, 989–996 (2016).
39. A. R. Tumarkin-Deratzian, Fibrolamellar bone in wild adult *Alligator mississippiensis*. *J. Herpetol.* **41**, 341–345 (2007).
40. H. N. Woodward, J. R. Horner, J. O. Farlow, Quantification of intraskeletal histovariability in *Alligator mississippiensis* and implications for vertebrate osteohistology. *PeerJ* **2**, e422 (2014).
41. E. Prondvai, K. H. W. Stein, A. de Ricqlès, J. Cubo, Development-based revision of bone tissue classification: The importance of semantics for science. *Biol. J. Linn. Soc.* **112**, 799–816 (2014).
42. F. R. O'Keefe, L. M. Chiappe, Viviparity and K-selected life history in a Mesozoic marine plesiosaur (Reptilia, Sauropterygia). *Science* **333**, 870–873 (2011).
43. J. Werner, E. M. Griebeler, Allometries of maximum growth rate versus body mass at maximum growth indicate that non-avian dinosaurs had growth rates typical of fast growing ectothermic sauropsids. *PLOS ONE* **9**, e88834 (2014).
44. J. M. Grady, B. J. Enquist, E. Dettweiler-Robinson, N. A. Wright, F. A. Smith, Evidence for mesothermy in dinosaurs. *Science* **344**, 1268–1272 (2014).
45. A. Bernard, C. Lécuyer, P. Vincent, R. Amiot, N. Bardet, E. Buffetaut, G. Cuny, F. Fourel, F. Martineau, J.-M. Mazin, A. Prieur, Regulation of body temperature by some Mesozoic marine reptiles. *Science* **328**, 1379–1382 (2010).
46. R. B. J. Benson, R. J. Butler, J. Lindgren, A. S. Smith, Mesozoic marine tetrapod diversity: Mass extinctions and temporal heterogeneity in geological megabiases affecting vertebrates. *Proc. R. Soc. B* **277**, 829–834 (2010).
47. L. H. Tanner, S. G. Lucas, M. G. Chapman, Assessing the record and causes of Late Triassic extinctions. *Earth Sci. Rev.* **65**, 103–139 (2004).
48. M. S. Hodges, G. D. Stanley Jr., North American coral recovery after the end-Triassic mass extinction, New York Canyon, Nevada, USA. *GSA Today* **25**, 4–7 (2015).
49. M. Hautmann, M. J. Benton, A. Tomasových, Catastrophic ocean acidification at the Triassic-Jurassic boundary. *N. Jb. Geol. Paläont. Abh.* **249**, 119–127 (2008).
50. J. M. Neenan, N. Klein, T. M. Scheyer, European origin of placodont marine reptiles and the evolution of crushing dentition in Placodontia. *Nat. Commun.* **4**, 1621 (2013).
51. H.-D. Sues, Postcranial skeleton of *Pistosaurus* and interrelationships of the Sauropterygia (Diapsida). *Zool. J. Linn. Soc.* **90**, 109–131 (1987).
52. P. M. Sander, O. C. Rieppel, H. Bucher, A new pistosaurid (Reptilia: Sauropterygia) from the Middle Triassic of Nevada and its implications for the origin of plesiosaurs. *J. Vertebr. Paleontol.* **17**, 526–533 (1997).
53. O. Rieppel, P. M. Sander, G. W. Storrs, The skull of the pistosaur *Augustasaurus* from the Middle Triassic of northwestern Nevada. *J. Vertebr. Paleontol.* **22**, 577–592 (2002).
54. D. L. Swofford, PAUP*. Phylogenetic Analysis Using Parsimony (*and Other Methods). Version 4.0b10 (Sinauer Associates, 2002).
55. R. B. J. Benson, H. F. Ketchum, L. F. Noé, M. Gómez-Pérez, New information on *Hauffiosaurus* (Reptilia, Plesiosauria) based on a new species from the Alum Shale Member (Lower Toarcian: Lower Jurassic) of Yorkshire, UK. *Palaeontology* **54**, 547–571 (2011).
56. V. Fischer, H. Cappetta, P. Vincent, G. Garcia, S. Goolaerts, J. E. Martin, D. Roggero, X. Valentin, Ichthyosaurs from the French Rhaetian indicate a severe turnover across the Triassic–Jurassic boundary. *Naturwissenschaften* **101**, 1027–1040 (2014).
57. F. M. Dalla Vecchia, A new sauropterygian reptile with plesiosaurian affinity from the Late Triassic of Italy. *Riv. Ital. Paleontol. Strat.* **112**, 207–225 (2006).

58. R. B. J. Benson, M. Evans, M. A. Taylor, The anatomy of *Stratesaurus* (Reptilia, Plesiosauria) from the lowermost Jurassic of Somerset, United Kingdom. *J. Vertebr. Paleontol.* **35**, e933739 (2015).
59. T. Sato, L.-J. Zhao, X.-C. Wu, C. Li, A new specimen of the Triassic pistosauroid *Yunguisaurus*, with implications for the origin of Plesiosauria (Reptilia, Sauropterygia). *Palaeontology* **57**, 55–76 (2014).
60. R Development Core Team, A language and environment for statistical computing (R Foundation for Statistical Computing, 2014); www.r-project.org/.
61. Y. Nakajima, R. Hirayama, H. Endo, Turtle humeral microanatomy and its relationship to lifestyle. *Biol. J. Linn. Soc.* **112**, 719–734 (2014).
62. J. D. Walker, J. W. Geissman, S. A. Bowring, L. E. Babcock, Compilers, Geologic time scale v. 4.0 (Geological Society of America, 2012).
63. P. M. Sander, T. Wintrich, A. H. Schwermann, R. Kindlimann, Die paläontologische Grabung in der Rhät-Lias-Tongrube der Fa. Lücking bei Warburg-Bonenburg (Kr. Höxter) im Frühjahr 2015. *Geol. Paläont.Westf.* **88**, 11–37 (2016).
64. O. Rieppel, A new pachypleurosaur (Reptilia: Sauropterygia) from the Middle Triassic of Monte San Giorgio, Switzerland. *Philos. Trans. R. Soc. Lond. B Biol. Sci.* **323**, 1–73 (1989).
65. P. M. Sander, The pachypleurosaurids (Reptilia: Nothosauria) from the Middle Triassic of Monte San Giorgio (Switzerland) with the description of a new species. *Philos. Trans. R. Soc. Lond. B Biol. Sci.* **325**, 561–666 (1989).
66. O. Rieppel, R. Wild, A revision of the genus *Nothosaurus* (Reptilia: Sauropterygia) from the Germanic Triassic, with comments on the status of *Chonchiosaurus clavatus*. *Fieldiana Geol. New Ser.* **34**, 1–82 (1996).
67. O. Rieppel, *Handbook of Paleoherpetology/Sauropterygia I.: Placodontia, Pachypleurosauria, Nothosauroidea, Pistosauroidea* (Friedrich Pfeil, 2000), 134 pp.
68. L.-T. Ma, D.-Y. Jiang, O. Rieppel, R. Motani, A. Tintori, A new pistosauroid (Reptilia, Sauropterygia) from the late Ladinian Xingyi marine reptile level, southwestern China. *J. Vert. Paleontol.* **35**, e881832 (2015).
69. G. Geissler, Ueber neue Saurier-Funde aus dem Muschelkalk von Bayreuth. *Z. Dtsch. Geol. Ges.* **47**, 331–355 (1895).
70. W. D. Conybeare, Additional notices on the fossil genera *Ichthyosaurus* and *Plesiosaurus*. *Trans. Geol. Soc. Lond. Ser.* **2**, 103–123 (1822).
71. L. Schwermann, P. M. Sander, Osteologie und Phylogenie von *Westphaliasaurus simonsensii*: Ein neuer Plesiosauride (Sauropterygia) aus dem Unteren Jura (Pliensbachium) von Sommersell (Kreis Höxter), Nordrhein-Westfalen, Deutschland. *Geol. Paläont.Westf.* **79**, 1–56 (2011).
72. F. R. O'Keefe, Preliminary description and phylogenetic position of a new plesiosaur (Reptilia: Sauropterygia) from the Toarcian of Holzmaden, Germany. *J. Paleo.* **78**, 973–988 (2004).
73. A. S. Smith, P. Vincent, A new genus of pliosaur (Reptilia: Sauropterygia) from the Lower Jurassic of Holzmaden, Germany. *Palaeontology* **53**, 1049–1063 (2010).
74. A. S. Smith, R. B. J. Benson, Osteology of *Rhomaleosaurus thorntoni* (Sauropterygia, Rhomaleosauridae) from the Lower Jurassic (Toarcian) of Northamptonshire, England. *Monogr. Palaeontogr. Soc.* **168**, 1–40 (2014).
75. N. Klein, Long bone histology of Sauropterygia from the Lower Muschelkalk of the Germanic Basin provides unexpected implications for phylogeny. *PLOS ONE* **5**, e11613 (2010).

Acknowledgments: Access to the Bonenburg clay pit was granted by J. Thater of Lücking Ziegelwerke. A. Hendricks and D. Grzegorczyk provided access to the specimen. Histological sampling was permitted and facilitated by E. Maxwell and L. Chiappe. We thank the staff at the LWL-Museum für Naturkunde for the preparation of the specimen and O. Dülfer for the histological thin sections. We thank M. Aberhan, R. Bussert, and P. E. Olsen for providing the measured sections for Fig. 1B. We acknowledge R. O'Keefe and T. Sato for the insightful discussion and R. Kindlimann for the help with Rhaetian chondrichthyan fossil identification. We thank the reviewers for their insightful suggestions for the improvement of the manuscript. We also thank T. Oda for contributing fig. S2. **Funding:** Funding was provided by the LWL-Museum für Naturkunde, Münster, Germany, the German Research Foundation (grant no. SA 469/47-1) and the Japan Society for the Promotion of Science (project nos. 27/6594 and 26800270). **Author contributions:** T.W. and P.M.S. designed and performed the morphological work and conducted the phylogenetic analysis. P.M.S. and A.H. conducted the morphometric analysis. All authors designed the histological part of the study, contributed the histological samples, and cooperated in their interpretation. P.M.S. and T.W. wrote the manuscript, with contributions from all other authors. **Competing interests:** The authors declare that they have no competing interests. **Data and materials availability:** All data needed to evaluate the conclusions in the paper are present in the paper and/or the Supplementary Materials. Additional data related to this paper may be requested from the authors.

Submitted 4 April 2017
Accepted 16 November 2017
Published 13 December 2017
10.1126/sciadv.1701144

Citation: T. Wintrich, S. Hayashi, A. Houssaye, Y. Nakajima, P. M. Sander, A Triassic plesiosaurian skeleton and bone histology inform on evolution of a unique body plan. *Sci. Adv.* **3**, e1701144 (2017).

Science Advances

AAAS

advances.sciencemag.org/cgi/content/full/3/12/e1701144/DC1

Supplementary Materials for

A Triassic plesiosaurian skeleton and bone histology inform on evolution of a unique body plan

Tanja Wintrich, Shoji Hayashi, Alexandra Houssaye, Yasuhisa Nakajima, P. Martin Sander

Published 13 December 2017, *Sci. Adv.* **3**, e1701144 (2017)
DOI: 10.1126/sciadv.1701144

The PDF file includes:

- table S6. Local bone apposition rate to the end of the first year and relative body size at the end of the first year in selected sauropterygians.
- table S7. Comparison of local bone apposition rates in the femur of selected amniotes compared to local bone apposition rates in the humeri and femora of plesiosaurians.
- Legend for data file S1
- References (*63–75*)

Other Supplementary Material for this manuscript includes the following:
(available at advances.sciencemag.org/cgi/content/full/3/12/e1701144/DC1)

- data file S1 (.txt format). Character matrix in NEXUS format for phylogenetic analysis described in Materials and Methods.

Supplementary Anatomical Descriptions

Skull Anatomy. The skull is not fully preserved, but the occiput and the entire lower jaw are present (fig. S1A). The lower jaw rami are partially broken and disarticulated, but the total length of the right lower jaw can be reliably reconstructed as 215 mm. The mandibular symphysis is laterally expanded in ventral view (fig. S1A) and forms a distinctive ventral ridge. There is no participation of the splenial in the mandibular symphysis. The angular is short and extends less than half of the mandibular length. Although it is uncertain whether the surangular foramen is visible in lateral view, it is clear that the articular lacks a deep anteroposteriorly oriented notch posterior to the glenoid. Furthermore, the dorsoventral orientation of the long axis of the retroarticular process is subhorizontal, and the mediolateral orientation of the long axis is inflected slightly posteromedially (fig. S1A). There are five isolated teeth preserved in the matrix near the jaws, and these show the typical enamel ridges (fig. S1B and C) of plesiosaurians (*10*, *11*).

Postcranial Axial Skeleton. Because of the damage to the cervical vertebral column caused by quarrying, the number of cervical vertebrae is difficult to determine. The anteriormost 15 cervicals are preserved in perfect articulation on the matrix, including the atlas-axis complex. The 16th cervical (fig. S2C to E) was separated from the preceding ones during preparation and was completely free from the matrix. Based on the length of the gap between the posteriormost preserved cervical and the anteriormost trunk vertebra and on the length increase between these two vertebrae, we estimate that no more than 22 cervical vertebrae are missing. Although the gap could have been increased or decreased by disarticulation, we do not believe this to be the case because of the generally high degree of articulation of the axial skeleton, and in particular the anterior cervicals. The length of cervical centrum number 15 is 21 mm. Cervical vertebral anatomy is illustrated in Fig. 2A and C and fig. S2). The anterior cervical centra are distinctly shorter than tall (Fig. 2C), and their mediolateral width is subequal to height or less. The intervertebral articular surfaces are nearly flat, and there is no semi-oval “lip” (*11*) extending ventrally from the anterior articular surface. The space between adjacent articulated centra is only 2 mm wide, suggesting thin intervertebral cartilage (Fig. 2C). A longitudinal ridge is absent from the lateral surface of the centra. In lateral view, the more anterior preserved cervicals have neural spines that are inflected somewhat anterodorsally, whereas the more posterior cervical spines are curved posterodorsally. The anterior cervical neural spines are taller than their anteroposterior length. The width of the cervical zygapophyses is narrower than that of the centrum. Furthermore, the rib facets of the anterior to middle cervical vertebrae are co-joined. The prezygapophyses face dorsomedially and are planar. The medial contact between the left and right prezygapophyses is absent, and the distance between the left and right zygapophyses is subequal to the width of the neural canal. In ventral view, the cervical centra show paired lateral ridges on the ventral surface. The shape of the neurocentral suture in the anterior to middle cervical vertebrae is very distinctive: this suture is not only V-shaped as in some other early plesiosaurians (*11*), but the apex of the “V” nearly extends to the ventral margin of the centrum

and the sides of the "V" are ventrally concave. The remarkable shape of the neurocentral suture in the anterior to middle cervical vertebrae is autapomorphic for *Rhaeticosaurus*. Other early plesiosaurians with a V-shaped neurocentral sutures have straight sides of the "V", whereas non-plesiosaurian sauropterygians, including basal pistosaurs (*51–53*) and *Bobosaurus* (*12*, *57*), have horizontal neurocentral sutures. The V-shaped neurocentral sutures of *Rhaeticosaurus* (Fig. 2C) and several other basal plesiosaurians (*11*) would have tightly integrated centrum and spine, even in growing animals. By increasing sutural surface area and complexity, the risk of sutural dislocation by forces generated during locomotion and feeding was reduced.

There are 21 trunk vertebrae preserved, all of which have the transverse process formed by the neural arch, indicating that they are dorsal vertebrae. Trunk vertebral anatomy is illustrated in Figs 2A and C and fig. S3). Presumably, there was a low number of transitional, so-called pectoral vertebrae, but these were lost before discovery. The length of the first dorsal centrum is 25 mm. The trunk is short compared to the limbs, the ratio of glenoid-acetabular distance to propodial length being 2.6 (see also the *Morphometric Analysis*). The height of the dorsal neural spines is low, less than the height of the centrum, and the transverse process is low on the neural arch, adjacent to the neural canal. The orientation of the transverse processes in the middle dorsal region is approximately horizontal. Neural spine morphology is constant throughout the dorsal series. The neural spines are laterally flattened and have unfinished tips, a sign of immaturity. A strong anteroposterior constriction at the base of the dorsal neural spines is absent, and in lateral view, all spines are anteroposteriorly symmetrical. The mid-posterior dorsal neural spines are not expanded transversely, but are narrow relative to their anteroposterior width. The orientation of the posteriormost dorsal neural spines is dorsal and not anterodorsally inclined, with the posterior dorsal rib facets having a prominent transverse process located entirely on the neural arch. The dorsal vertebrae are tightly integrated and, together with the wide rib cage and robust ribs, suggest an inflexible trunk. The gastralia are well developed and densely spaced in *Rhaeticosaurus* (fig. S3A and D) suggesting the presence of a well developed gastral basket. The gastralia of *Augustasaurus* (*52*) and *Bobosaurus* (*57*) appear thinner and less prominent, although this could be the result of disarticulation in the case of *Bobosaurus*. Immaturity of the holotype skeleton is also suggested by the unfused neurocentral sutures in the posterior dorsal and caudal column (fig. S3 and S4).

Four sacral vertebrae (fig. S4B and C) are present with the sacral ribs. The sacral ribs are cylindrical and have slightly expanded distal ends. The neural spines of the sacral and anterior caudal vertebrae also have distinctly unfinished neural spines. The length of the preserved dorsal region is about 553 mm, and that of the sacral region is 96 mm (cumulative length of the sacral centra), giving a total of 649 mm for the trunk region. The trunk must have been slightly longer because of the missing pectoral vertebrae.

In the caudal vertebral column (fig. S4), 25 vertebrae are preserved in articulation, and a few more probably were lost to disarticulation, leading to an estimate of <33 caudal vertebrae based on preserved vertebral proportions. However, no disarticulated caudals are preserved with the skeleton. The first caudal centrum is 21 mm long, with this dimension gradually decreasing to 10 mm in the last articulated caudal, the 25th. This relatively rapid decrease in size also makes it unlikely that the tail had the high vertebral count seen in non-plesiosaurian [e.g., about 70 caudals in *Yunguisaurus* (*58*), and at least 38 caudals in *Bobosaurus* (*57*)]. In addition, the caudals become relatively longer posteriorly in these taxa (*57*, *58*), unlike in *Rhaeticosaurus*. All caudal vertebral centra are at least twice as wide as long (fig. S4), with the proportions remaining constant. This gives the caudal centra a disk-shaped appearance, compared to *Bobosaurus* and all more basal eosauropterygians that have caudals that are longer than wide. Both the low number of caudals and the shortening of the individual caudals indicate an evolutionary shortening of the tail which is typical for plesiosaurians. The estimated length of the tail, based on a maximum reconstructed count of 33 caudals, is 577 mm, which is shorter than the trunk region. The rib facets of the proximal middle caudal vertebrae are located rather dorsally and almost connect with the base of the neural arch. The outline of the middle caudal centra is suboval in anterior view. The chevron facets of the middle and distal caudal vertebrae are in a low position and flush with the level of the ventral surface of the centrum. There are well developed gastralia (fig. S3D), forming a gastral basket, but the number of elements per segment cannot be reliably determined.

Girdle skeleton. The pectoral girdle is too damaged and poorly preserved to reveal important characters, but the left coracoid and scapula can be discerned, enclosing a pectoral fenestra between them. The pelvic girdle is well preserved. Both ilia are present, as are the left pubis and ischium which are exposed in dorsal view. The dorsoventral length of the well-preserved right ilium is 95 mm. The shaft of the ilium appears straight in lateral view, and the pelvic articular end is equally expanded anteriorly and posteriorly. In addition, the rotation of the dorsal blade relative to the long axis of the pelvic articular end is approximately 45 degrees. The iliac blade is expanded subequally in anterior and posterior direction, and the expanded portion occupies the dorsal half of the ilium. The anteroposterior width of the dorsal blade is expanded over the width of the shaft. There is no tubercle around the mid-length of the posterior surface of the ilium, and the broad fossa on the medial surface of the dorsal blade is absent as well. The mediolateral width of the well-preserved left pubis is 112 mm, and that of the left ischium is 97 mm. The anterolateral cornu of the pubis is absent, and the ratio of the anteroposterior length to the mediolateral width of the pubis is 1.02. The pubis and ischium are similar in shape to those of other basal plesiosaurians and offer no distinctive features. Ischium length to the width ratio is between 1.0 and 1.3.

Limb Skeleton. In the limbs, the left humerus and femur, the left radius, the left tibia and fibula, a single rounded carpal, three rounded tarsals and some metapodials and phalanges are preserved. The distal half of the dorsal and ventral surfaces of the propodials is flat with robust

pre- and postaxial margins. Both propodials have a straight shaft and only slightly expanded distal ends. The length of the humerus is 183 mm, although this value may have been increased slightly by microfaulting. In addition, microfaulting gave the humerus an unnatural S shape, but its true shape can be discerned upon close inspection of the specimen. We thus conclude that in dorsal or ventral view, the preaxial margin of the distal humerus is straight. There is a sharp longitudinal ridge on the anterior surface of the shaft. The shape of the distal end of the humerus is uniformly convex, and the inclination of the proximal end appears straight in dorsal view. The radius is 48 mm long and thus much shorter than the humerus, reaching only 26% of the length of the latter. Among the taxa in the morphometric analysis, only *Rhomaleosaurus thorntoni* has a relatively shorter radius (table S4). The radius shows a concave preaxial margin with a prominent anterior flange extending from the anteroproximal surface. There is a posterodistal facet for the intermedium. Furthermore, the length to maximum width ratio of the radius is 1.21.

Like the humerus, the femur has a straight shaft, and both bones are very similar in shape, unlike in *Yunguisaurus* (*58*). Femur length (185 mm, also slightly increased by microfaulting) is about the same as humerus length, as in some other early plesiosaurians (table S4). In *Yunguisaurus*, the femur is clearly shorter than the humerus, achieving only 85% the length of the humerus. In *Pistosaurus*, the femur seems to be of the same length as the humerus, which is incompletely preserved in the only known partial skeleton (*50*). The humerus/femur ratio is unknown in *Bobosaurus*, although the authors suggest that the femur and hindlimb were shorter than the forelimb (*12*, *57*). However, the ratio of humerus to tibia length is 1.34 in *Bobosaurus*, the lowest in the data set (table S3), strongly suggesting that *Bobosaurus* lacked the short zeugopodials of plesiosaurians. This inference is also supported by the slender tibia of *Bobosaurus* (*12*, *57*). The straight shaft of the humerus and femur of *Rhaeticosaurus* is important because it is not seen in non-plesiosaurian pistosauroids such as *Bobosaurus* (*12*, *57*) and pistosaurs (*51*, *52*). The distal end of the femur is somewhat flattened and expanded, although these features may have been exaggerated somewhat by microfaulting.

The tibia is similarly short compared to the femur (23%) as the radius is compared to the humerus. Since both zeugopodials are preserved in the hindlimb, it can be seen that there is an epipodial foramen between the tibia and the fibula. The length of the tibia is 43 mm. The length to maximum width ratio of the tibia is lower than 1.0, the bone being somewhat wider (46 mm) than long. The fibula is 49 mm long. It has a concave preaxial side but lacks the dorsoventrally convex posterior margin of other basal plesiosaurians (*12*, *57*). In fact, the postaxial margin of the fibula is concave in dorsoventral view as well, resulting in the bone having a shaft, but this may be preservational. There are three rounded tarsals, suggesting that there was much cartilage between the tarsals as in many Early Jurassic plesiosaurians (*12*, *57*). Because of disarticulation and loss of elements from the distal limbs, we cannot be sure that *Rhaeticosaurus* had the same number of carpals and tarsals as later plesiosaurians. However, the preserved metapodials and phalanges are long and slender, being around two to three times as long proximodistally as broad anteroposteriorly, as in later plesiosaurians. Even if the carpus and tarsus were incompletely

ossified, the proportions of the entire limb, particularly with respect to the zeugopodials, are consistent with a hydrofoil function of the limbs, as in later plesiosaurians.

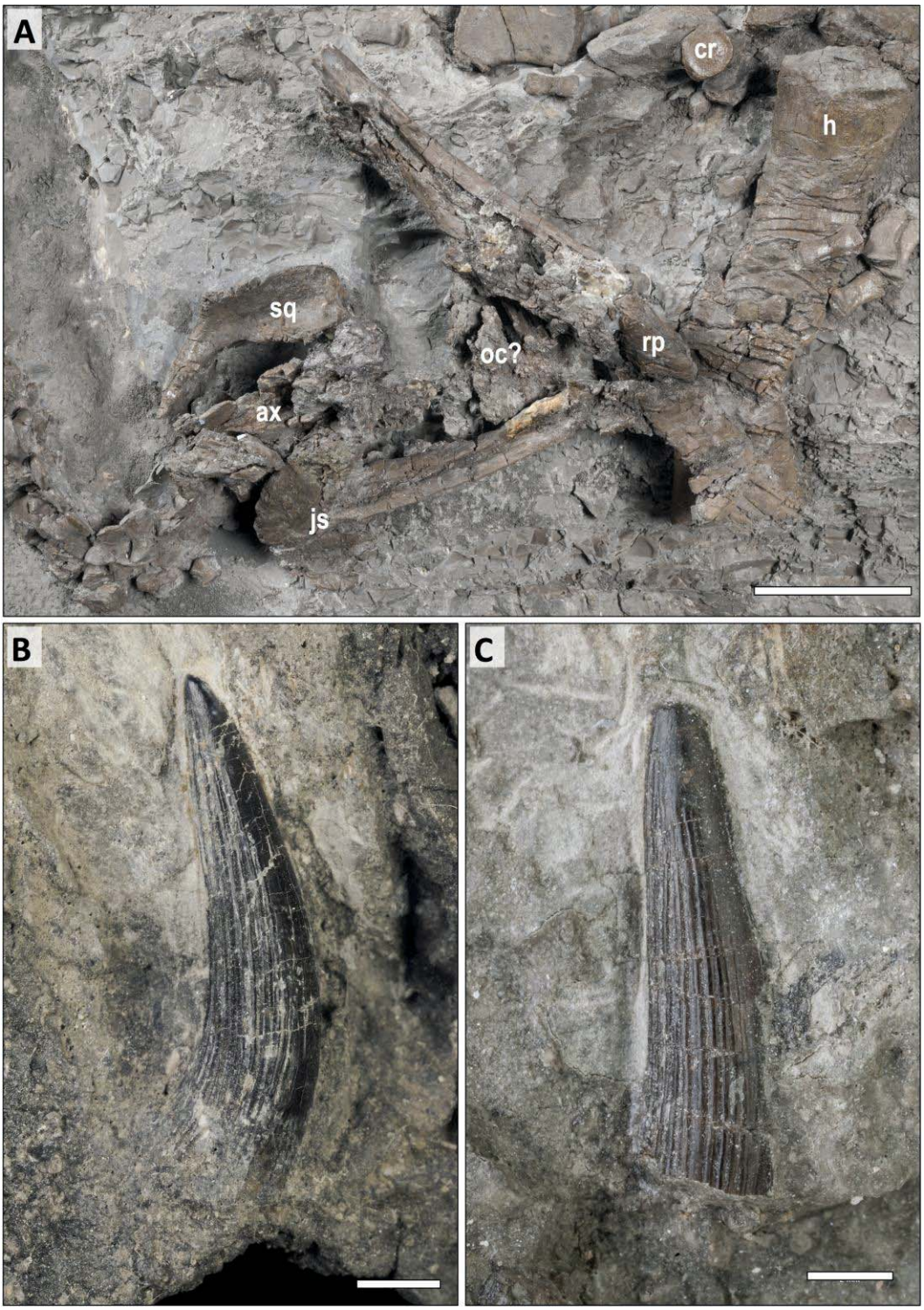

fig. S1. The holotype of *Rhaeticosaurus mertensi* gen. et sp. nov. (**A**) Skull, anterior cervical vertebrae and left humerus. Both lower jaws are seen in ventral view and articulate in the symphysis. The posterior part of the left lower jaw is broken off and rotated away. (**B**, **C**) Two isolated teeth associated with the lower jaws. Note the sharp longitudinal enamel ridges on the surface of the teeth. ax, atlas-axis complex; cr, carpal bone; h, humerus; js, jaw symphysis; oc?, probable occipital region; rp, retroarticular process of left lower jaw in ventral view; sq, squamosal. Scale bars, 5 cm (A), 3 mm (B), 2 mm (C).

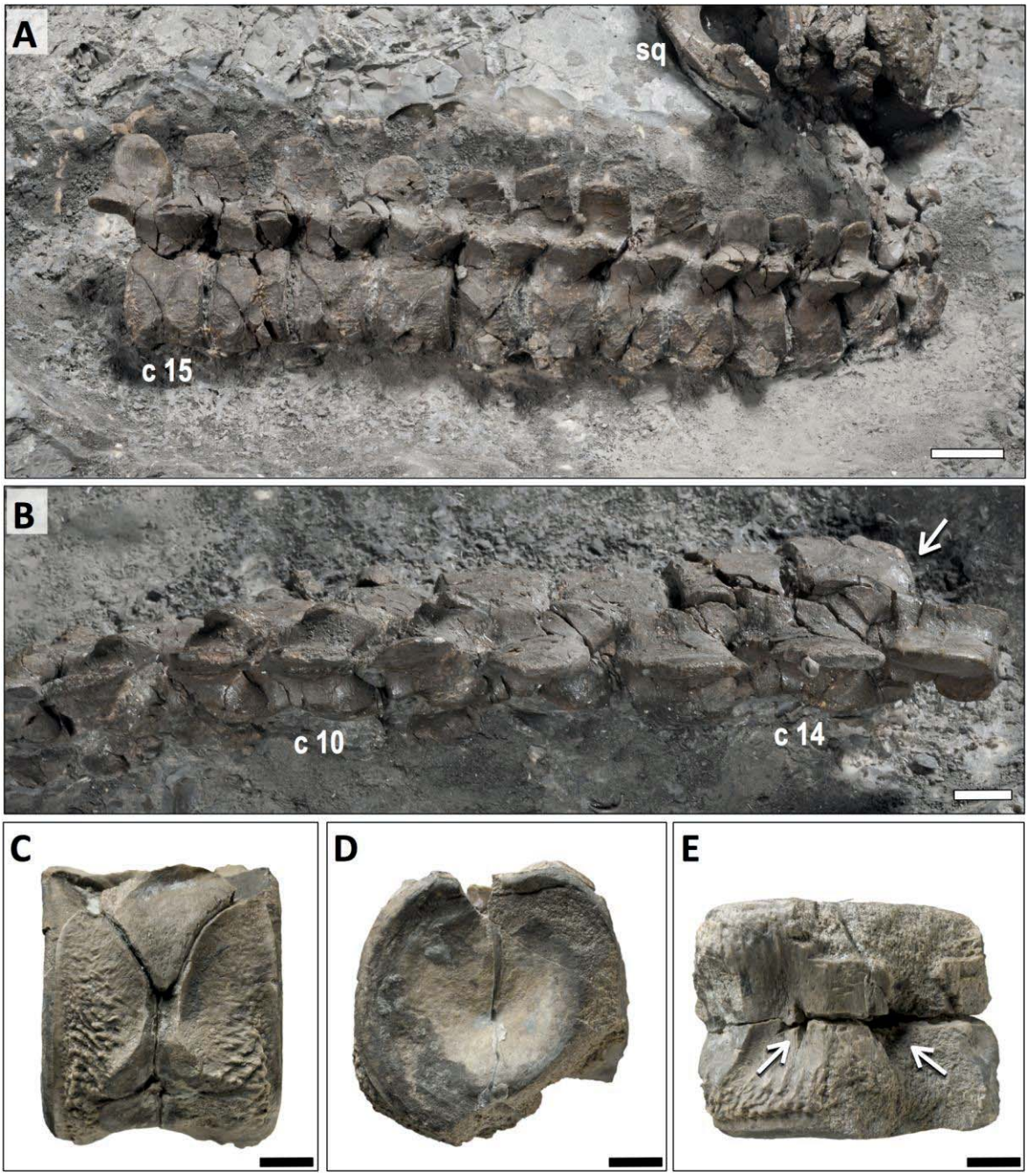

fig. S2. The holotype of *Rhaeticosaurus mertensi* gen. et sp. nov., anterior cervical vertebral column. (**A**) Anterior cervical vertebrae in lateral view and posterior skull region. (**B**) Anterior cervical vertebrae in dorsal view. Note that the width of the cervical zygapophyses (arrow) is narrower than that of the centrum. (**C**) The isolated 16th cervical vertebral centrum in left lateral view. Note the ventrally concave V-shaped neurocentral suture and the co-joined rib facets.(**D**) The same in anterior view, note the flat articular surface with the concave center. (**E**) The same in ventral view. Although the ventral surface is partially damaged, the ventrolateral ridges, the ventral keel, and the deeply sunken large subcentral foramina (arrow) are visible. c 10, cervical vertebra 10; c 14, cervical vertebra 14; c 15, cervical vertebra 15; sq, squamosal. Scale bars, 2 cm (A), 1 cm (B), 5 mm (C-E).

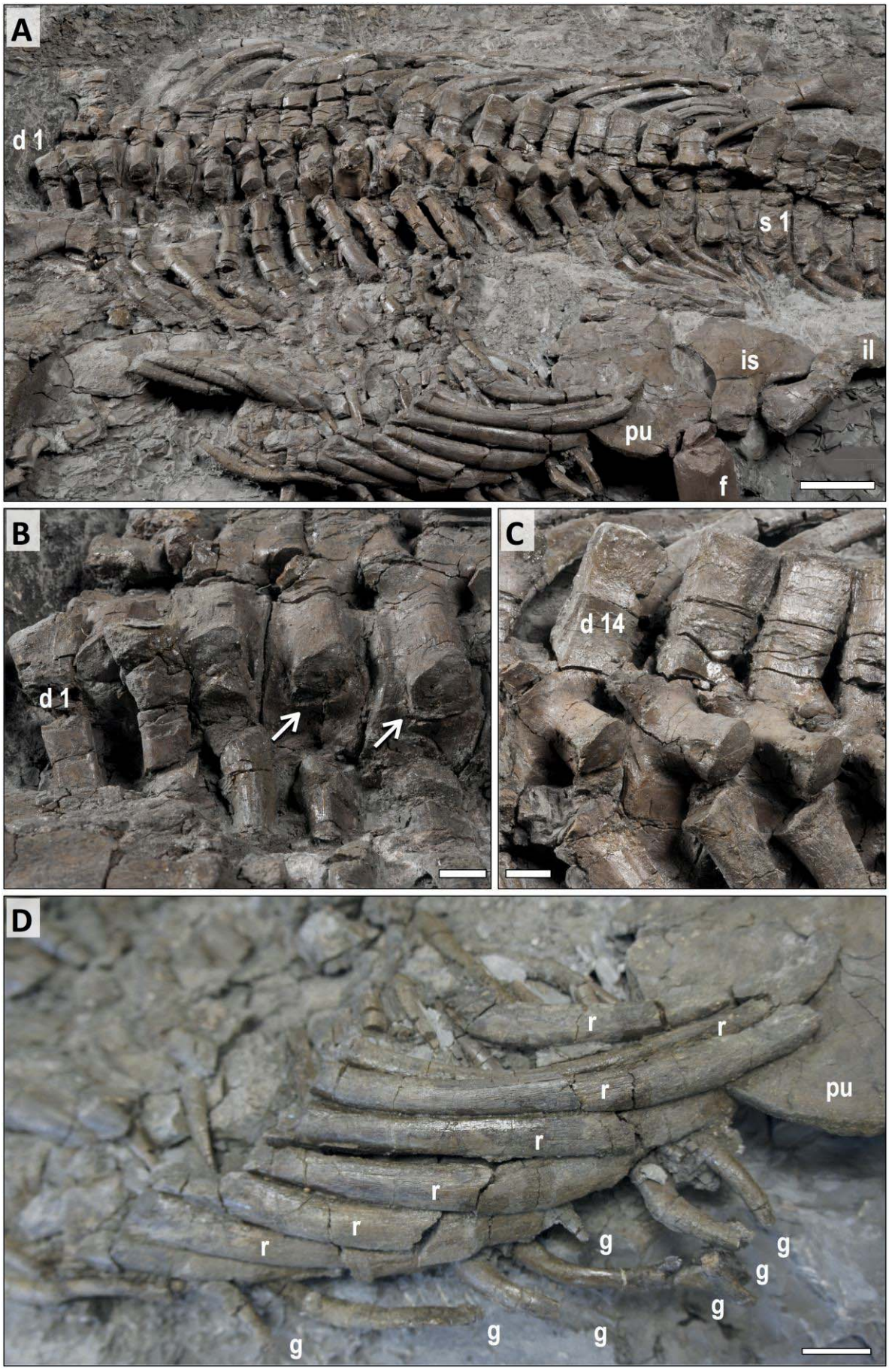
A
d 1
s 1
is
il
pu
f
B
d 1
C
d 14
D
r
r
r
r
r
r
r
pu
g
g
g
g
g
g
g

fig. S3. The holotype of *Rhaeticosaurus mertensi* gen. et sp. nov. (**A**) Overview of trunk region, anterior is to the left. Note the tightly integrated vertebral column and the wide rib cage. (**B**) Dorsal vertebrae 1 to 5. Note the short transverse processes and the neurocentral suture ventral to these (arrows). (**C**) Middle dorsal vertebrae, the 14th to the 17th. Note the well developed transverse processes. (**D**) Distal portion of left trunk ribs and gastralia that underlie these. d 1, dorsal vertebra 1; d 14, dorsal vertebra 14; f, femur; g, gastral element; il, ilium; is, ischium; pu, pubis; r, rib; s 1, sacral vertebra 1. Scale bars, 5 cm (A), 1 cm (B, C), 2 cm (D).

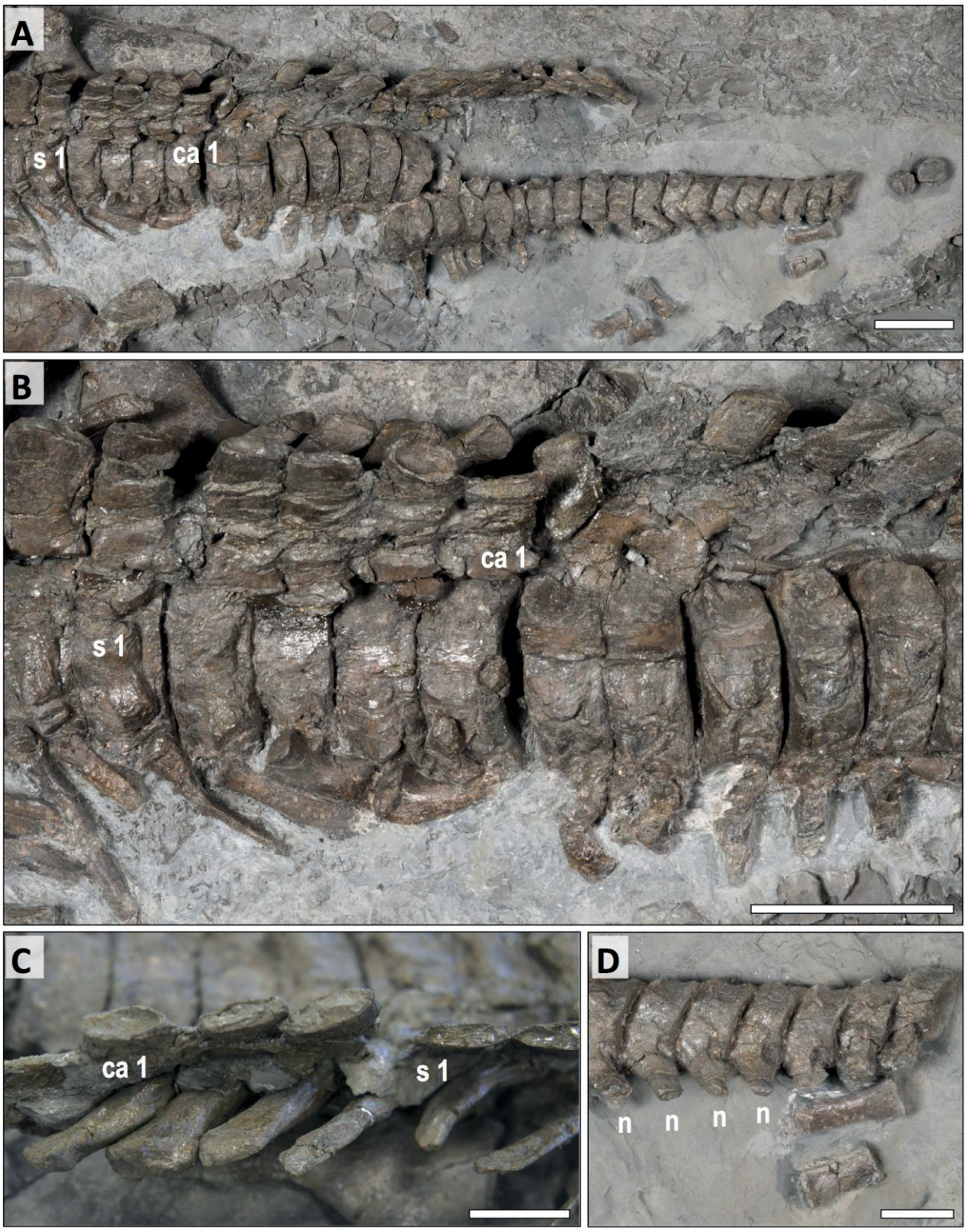

fig. S4. The holotype of *Rhaeticosaurus mertensi* gen. et sp. nov. (**A**) Overview of sacral and caudal vertebral column, anterior is to the left. Note two disarticulated posterior caudals and the isolated phalanges below the posterior tail. (**B**) Sacral and anteriormost caudal vertebral column, enlargement of (A). The first caudal neural arches have separate from the centra, exposing the floor of the neural canal. Note the disk-shaped caudal vertebrae. Note the unfinished ends of the sacral neural spines, suggesting a juvenile ontogenetic stage. (**C**) Sacral vertebrae in dorsal view,

exposing the unfinished ends of the sacral neural spines. Anterior is to the right. (**D**) Articulated part of posterior caudal vertebral column. The vertebrae are exposed in right lateral view, with the neural spines pointing downwards. ca 1, caudal vertebra 1; n, neural arch; s 1, sacral vertebra 1. Scale bars, 5 cm (A, B), 2 cm (C, D)**.**

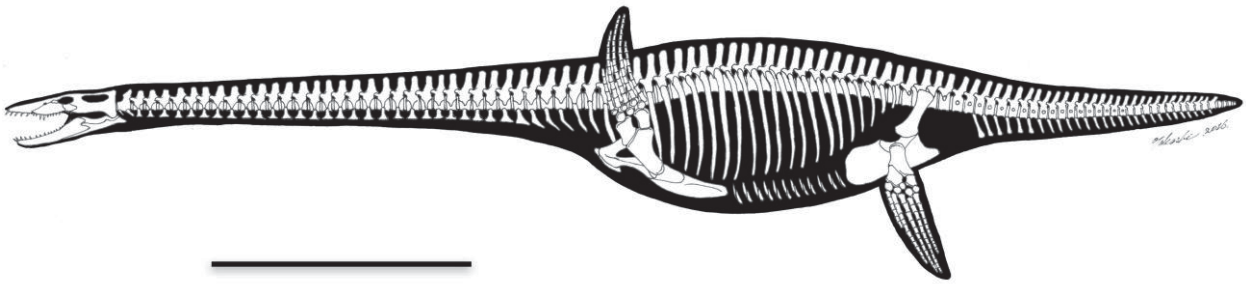

fig. S5. Reconstruction of the skeleton of *Rhaeticosaurus mertensi* gen. et sp. nov. based on the available measurements and proportions. The reconstruction visualizes locomotion by underwater flight with the forelimb at the beginning of the downstroke and the hindlimb at the beginning of the upstroke. Scale bar, 50 cm.

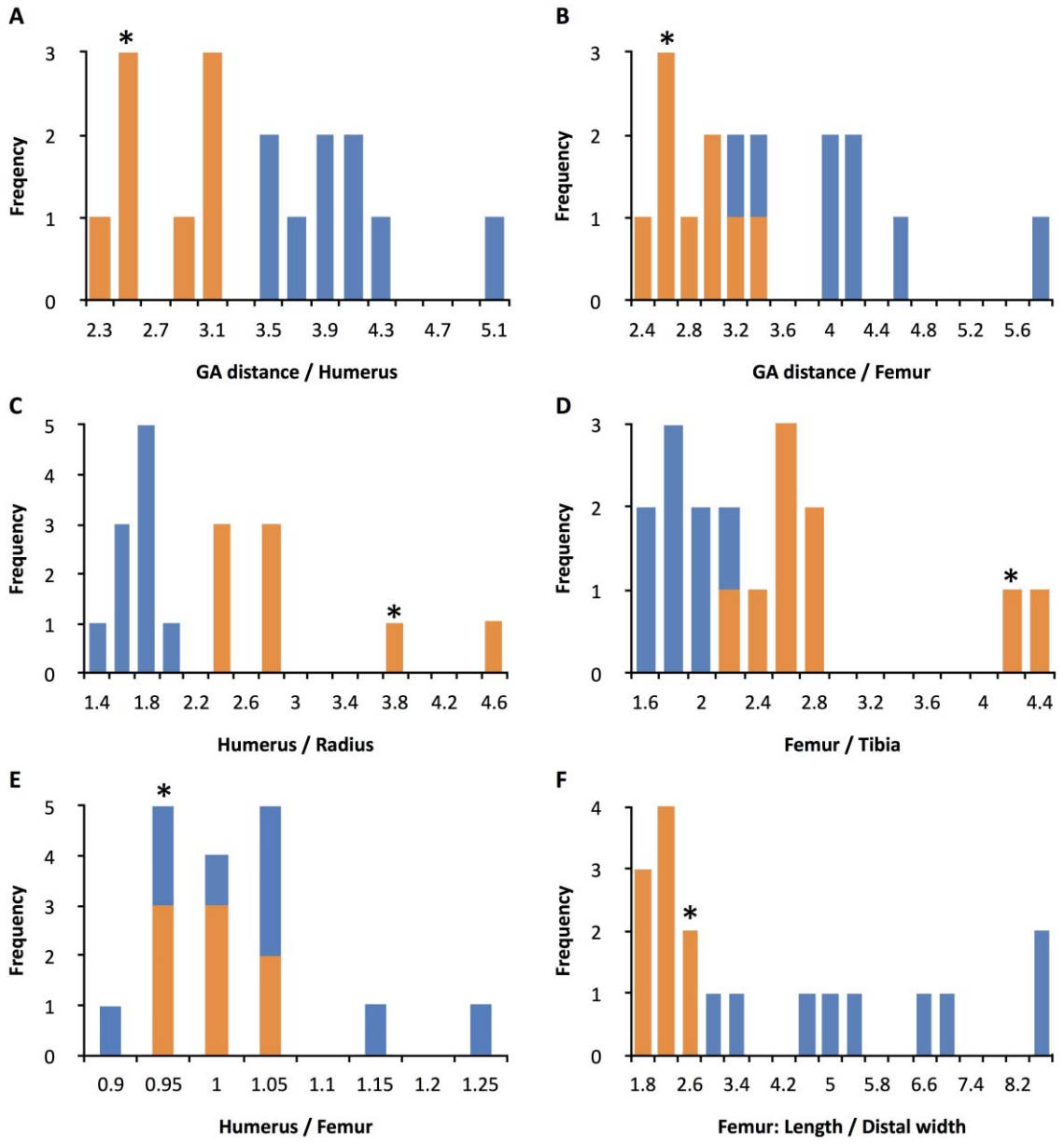

fig. S6. Selected skeletal proportions in Eosauropterygia. The histograms are based on the eight non-plesiosaurians and the eight plesiosaurians for which all variables in table S4 could be measured. Values on the x-axis are the lower value of the classes in the histogram. Orange: plesiosaurians; blue, non-plesiosaurians. Asterisks (*) indicate class of *Rhaeticosaurus mertensi* gen. et sp. nov. (**A**) Glenoid-acetabular distance/humerus ratio. Plesiosaurians do not overlap with non-plesiosaurians. Glenoid-acteabular distance is a proxy for trunk length. (**B**) Glenoid-acteabular distance/femur ratio. Plesiosaurians have a slight overlap with non-plesiosaurians. (**C**) Humerus/radius ratio. Plesiosaurians do not overlap with non-plesiosaurians. (**D**) Femur/tibia ratio. Plesiosaurians have a slight overlap with non-plesiosaurians. (**E**) Humerus/femur ratio. All plesiosaurians have humeri and femora of equal or subequal length whereas humerus/femur ratios vary more widely among non-plesiosaurians. (**F**) Femur length/distal width ratio. Plesiosaurians do not overlap with non-plesiosaurians. Note that *Rhaeticosaurus* ratios always plot with plesiosaurians. GA distance, glenoid-acteabular distance.

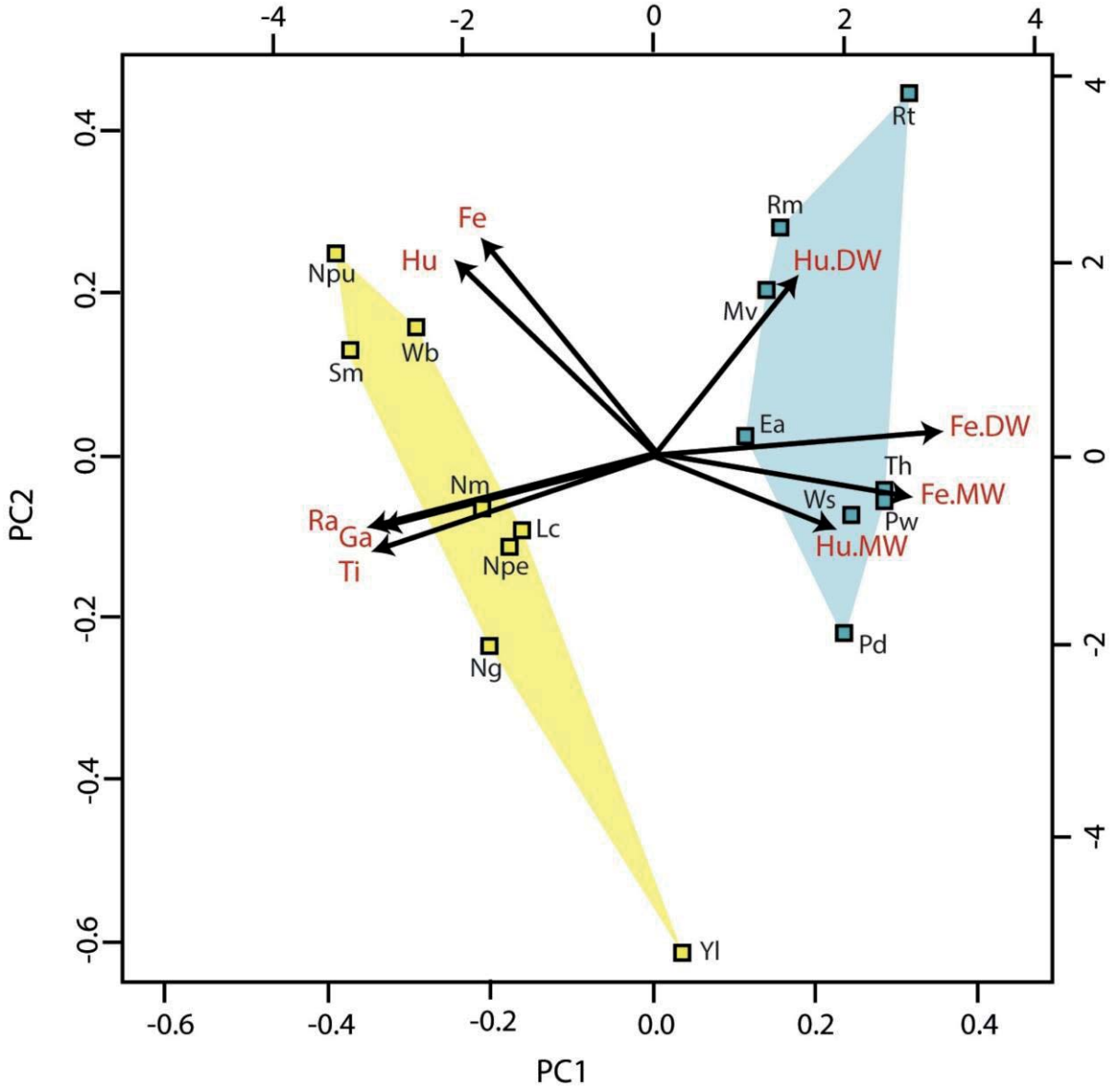

fig. S7. Principal component analysis of trunk and limb measurements in Eosauropterygia. The analysis is based on the eight non-plesiosaurians and the eight plesiosaurians for which all variables in table S4 could be measured. Graph showing the distribution of all taxa examined in the morphospace according to the PCA1 and PCA2 axes. Note the complete separation of plesiosaurians from non-plesiosaurians. Blue: plesiosaurians; Yellow: non-plesiosaurian taxa. Taxon abbreviations: Ep, *Eoplesiosaurus antiquior*; Lc, *Lariosaurus calcagnii*; Mv, *Meyerasaurus victor*; Npu, *Neusticosaurus pusillus*; Npe, *Neusticosaurus peyeri*; Ng, *Nothosaurus giganteus*; Nm, *Nothosaurus marchicus*; Pw, *Plesiopterys wildi*; Pd, *Plesiosaurus dolichodirus*; Rm, *Rhaeticosaurus mertensi* gen. et sp. nov.; Rt, *Rhomaleosaurus thorntoni*; Sm, *Serpianosaurus mirigiolensis*; Th, *Thalassiodracon hawkinsi*; Wb, *Wangosaurus brevirostris*; Ws, *Westphaliasaurus simonsensii*; Yl, *Yunguisaurus liae.* Variable abbreviations: Fe, femur length; Fe.DW, distal width of femur; Fe.MW, minimal shaft width of femur; Ga, glenoid-acetabular distance; Hu, humerus length; Hu.DW, distal width of humerus; Hu.MW, minimal shaft width of humerus; Ra, radius length; Ti, tibia length.

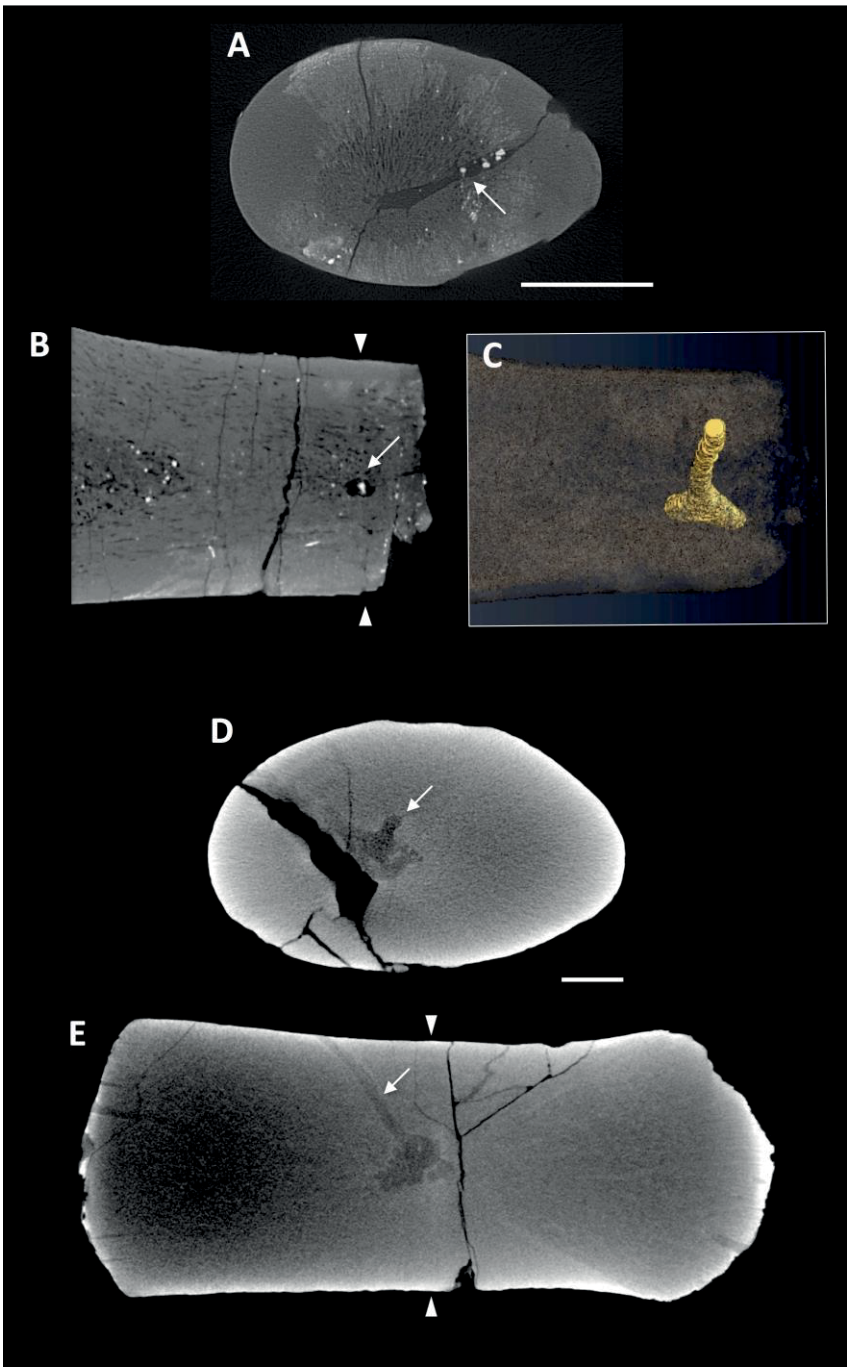

fig. S8. Examples of CT scans of plesiosaurian long bones used in locating the nutrient canal before sectioning. (**A**) Virtual midshaft cross section of the femur of the holotype of *Rhaeticosaurus mertensi* gen. et sp. nov. (**B**) Virtual longitudinal section of same, intersecting the nutrient canal. Proximal is to the left. (**C**) 3D reconstruction of nutrient canal (yellow). Note that the canal deviates only slightly towards proximal. (**D**) Virtual midshaft cross section of the humerus of the indeterminate juvenile elasmosaur OMNH MV 85. (**E**) Virtual longitudinal section of same in plane of nutrient canal. Proximal is to the left. Note that the canal deviates strongly towards proximal. Arrows point to nutrient canal. Arrow heads indicate planes of virtual midshaft sections. Scale bars, 10 mm.

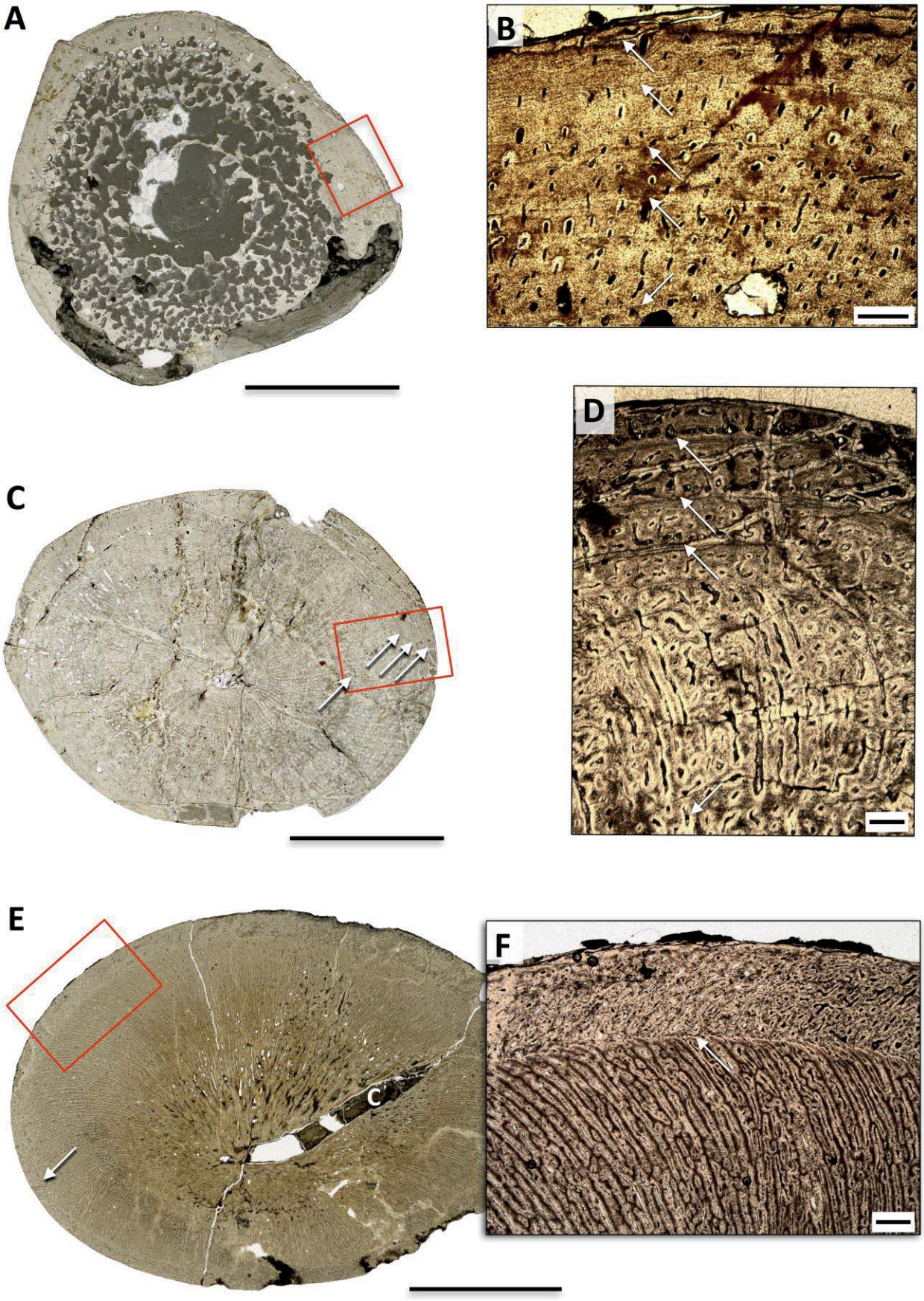
A
B
C
D
E
C
F

fig. S9. Evolution of long bone histology in Triassic Eosauropterygia. (**A**) Midshaft cross section of the femur of *Nothosaurus mirabilis* STIPB R 49 in normal light. Box marks enlargement in (**B**). (B) Close-up of cortex. Note the low vascularity and well developed lines of arrested growth (arrows). (**C**) Midshaft cross section of the humerus of *Pistosaurus longaevus* SMNS 84825 in normal light. Box marks enlargement in (**D**). (D) Close-up of cortex. Note the radial vascularity in the inner cortex and well developed lines of arrested growth (arrows) in the outer cortex. (**E**) Midshaft cross section of the femur of the holotype of *Rhaeticosaurus mertensi* gen. et sp. nov. in normal light. Box marks enlargement in (**F**). (F) Close-up of outer part of first growth cycle and of second growth cycle. Note the abrupt directional change of the vascular canals at the cycle boundary. Arrows point to growth marks. c, nutrient canal. Scale bars, 10 mm (A, C, E) and 500 µm (B, D, F).

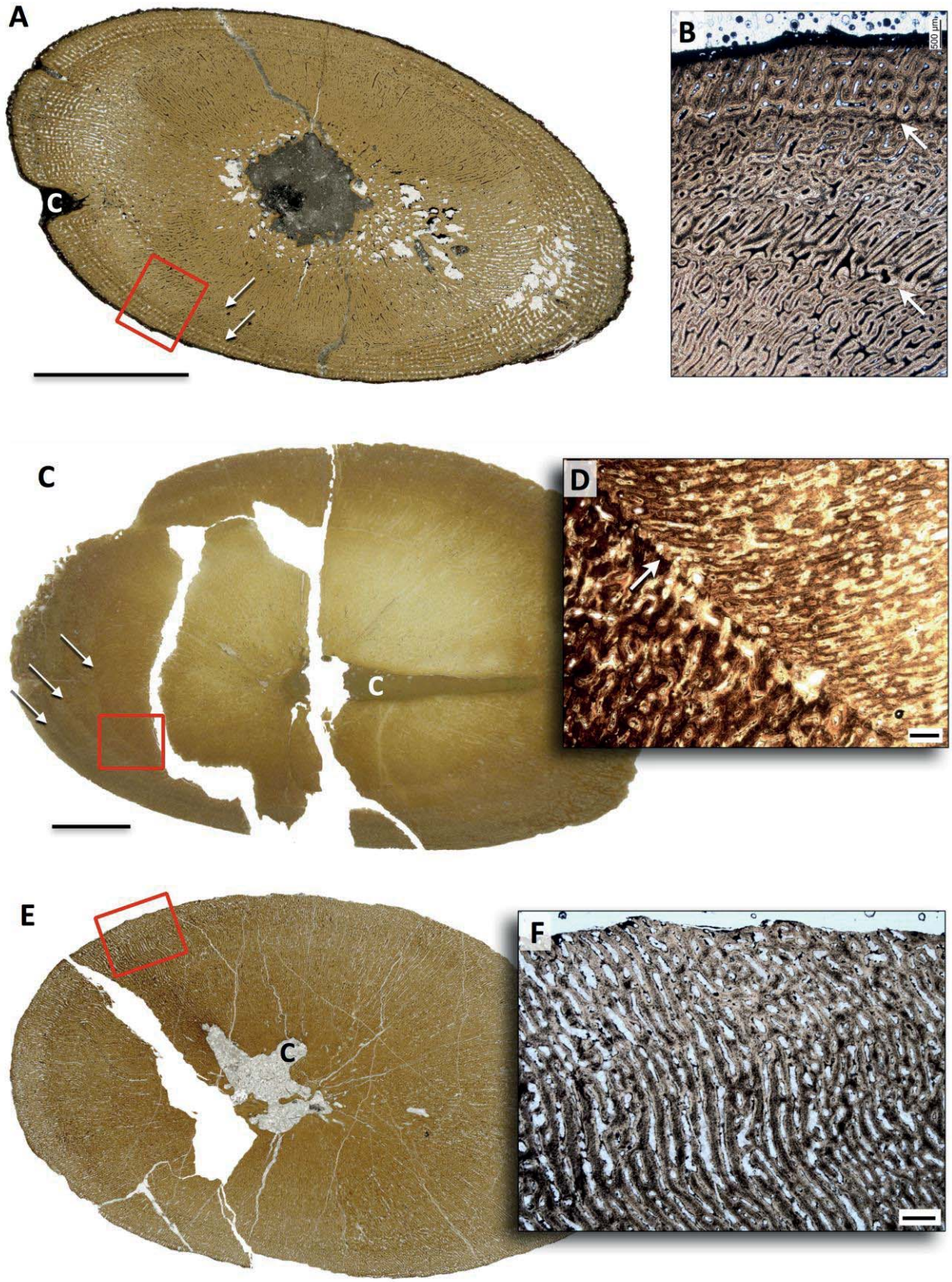

fig. S10. Long bone histology of Jurassic and Cretaceous plesiosaurians. (**A**) Midshaft cross section of the femur of *Plesiosaurus dolichodirus* STIPB R 89 in normal light. Note the small

concavity on the left which marks the entrance of the nutrient canal. Box marks enlargement in (**B**). (B) Close-up of the second and third growth cycles. (**C**) Midshaft cross section of the femur of cryptoclidid plesiosaurian *Crytpoclidus eurymerus* STIPB R 324 in normal light. Note the large nutrient canal on the right. Box marks enlargement in (**D**). (D) Close-up of outer part of first and of second growth cycle, note the abrupt change in direction of the radial vascular canals. (**E**) Midshaft cross section of the humerus of the indeterminate juvenile elasmosaur OMNH MV 85 in normal light. Note the lack of growth marks. Box marks enlargement in (**F**). (F) Close-up of outer cortex. Note the high vascularity and the wavy course of the radial vascular canals. Arrows point to growth marks. c, nutrient canal. Scale bars, 10 mm (A, C, E) and 500 µm (B, D, F).

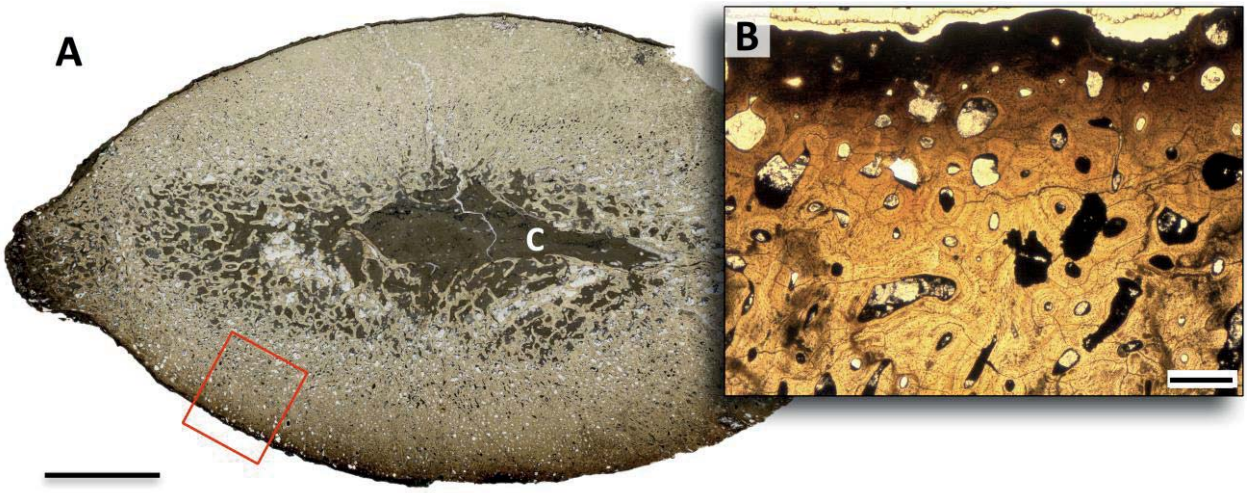

fig. S11. Long bone histology of a mature Middle Jurassic plesiosaurian. (**A**) Midshaft cross section of *Pliosaurus* sp. propodial SMNS 54025 in normal light. The entire cortex consists of dense Haversian tissue. Note the large nutrient canal on the right. Box marks enlargement in (**B**). (B) Close-up of outer cortex. Note the irregular arrangement of the secondary osteons and vascular canals. c, nutrient canal. Scale bars, 10 mm (A) and 500 µm (B).

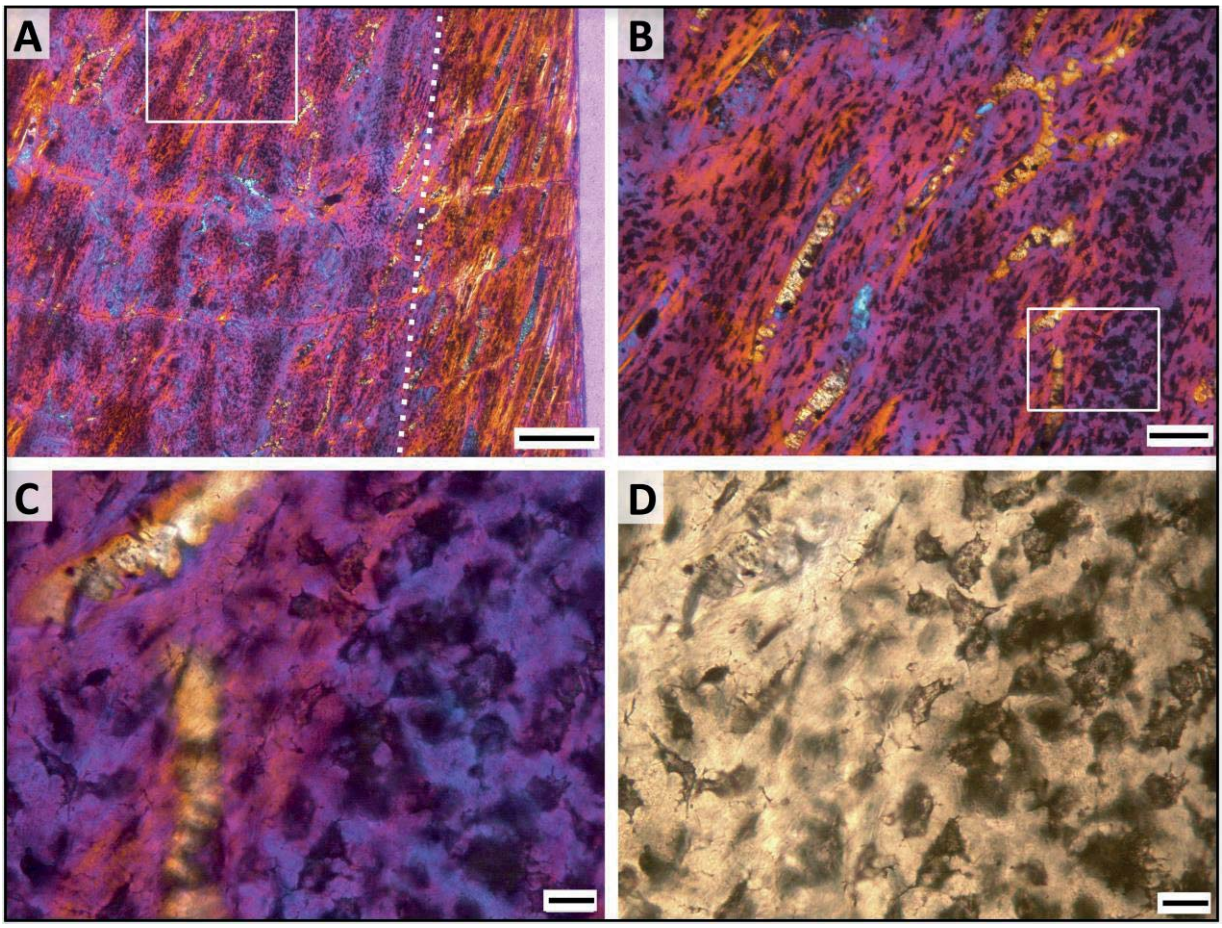

fig. S12. Long bone histology of the holotype of *Rhaeticosaurus mertensi* gen. et sp. nov. in longitudinal section. (**A**) Longitudinal section of the midshaft region of the femur in polarized light with lambda filter. Outer bone surface is to the left. The first growth mark is at the color change from magenta to orange (dotted line). Note the dominance of woven bone (magenta) with a few primary osteons (light blue) in the cortex to the left of the first growth mark. Box marks enlargement in (**B**). (B) Close-up of (A). Note the extreme density of plump, irregular osteocyte lacunae in the woven bone indicating dominance of static osteogenesis consistent with rapid tissue formation. Primary osteons are less distinct than in the cross section. Box marks enlargement in c. (**C**) Close-up of (B). (**D**) Same view as c but in normal light, again showing the plump and densely spaced osteocyte lacunae. Scale bars, 500 µm (A), 100 µm (B) and 20 µm (C and D).

table S1. Faunal list of bonebed above plesiosaurian discovery horizon. The material is accessioned to the collections of LWL-Museum für Naturkunde, Münster, Germany (*63*).

Taxon	Material	Clade	Frequency
Hybodus cloacinus	Teeth	Chondrichthyes	Very common
Lissodus minimus	Teeth	Chondrichthyes	Very common
Rhomphaiodon minor	Teeth	Chondrichthyes	Very common
Nemacanthus monilifer	Fin spines	Chondrichthyes	Very common
Hybodontiformes indet.	Fin spines	Chondrichthyes	Very common
Saurichthys sp.	Teeth	Actinopterygii	Common
Sargodon tomicus	Teeth	Actinopterygii	Common
Ceratodus latissimus	Teeth	Dipnoi	Moderately common
Temnospondyli indet.	Jaw fragments, limb bone	Temnospondyli	Rare
cf. *Shonisaurus*	Vertebrae	Ichthyosauria	Moderately common
Plesiosauria sp. A	Vertebrae	Plesiosauria	Moderately common
Plesiosauria sp. B	Vertebrae	Plesiosauria	Moderately common
Plesiosauria sp. C	Vertebrae	Plesiosauria	Moderately common
Pachystropheus rhaeticus	Vertebrae, limb bones	Choristodera/Thalattosauria	Very common
Lepagia gaumensis	Tooth	Cynodontia	Very rare

table S2. Unambiguous but not unique synapomorphies diagnosing *Rhaeticosuarus mertensi* gen. et sp. nov. in addition to the two autapomorphies. Numbers in parentheses indicate character number and state in the data matrix used in the phylogenetic analysis (Supporting Data). Character state descriptions are from ref. (*4*).

Mandible, retroarticular process, dorsoventral orientation of long axis: posteroventral or subhorizontal (122, 1).

Mandible, retroarticular process, mediolateral orientation of long axis: inflected slightly posteromedially (123, 1).

Splenial participation in mandibular symphysis: does not participate (125, 0).

Angular relative length and participation in mandibular symphysis: short, extends less than half mandibular length (126, 0).

Enamel ‘striations’ (grooves): present (136, 0).
Comment: This character description is poorly worded. The striations referred too are not grooves but thin and sharp ridges formed by the enamel.

Relative neck length: longer than (>1.2 times) trunk length (141, 2).

Cervical zygapophyses, combined width: distinctly narrower than the centrum (164, 2).

Caudal ribs facet location in proximal–middle caudal vertebrae: placed dorsally but neural arch does not form part of facet (188, 1/2).

Sharp longitudinal ridge on anterior margin of humerus: present (246, 1).

Width of epipodials of the hind limb: tibia larger (265, 0).

table S3. List of synapomorphies from phylogenetic analysis. The tree is the strict consensus tree of the phylogenetic analysis described in the “Methods” section and is based on the PAUP log file. This list of synapomorphies was used to diagnose Plesiosauria (node 60 to 59) and *Rhaeticosaurus mertensi* gen. et sp. nov. Abbreviations: H., *Hauffiosaurus*; M., *Microcleidus*; R., *Rhomaleosaurus*.

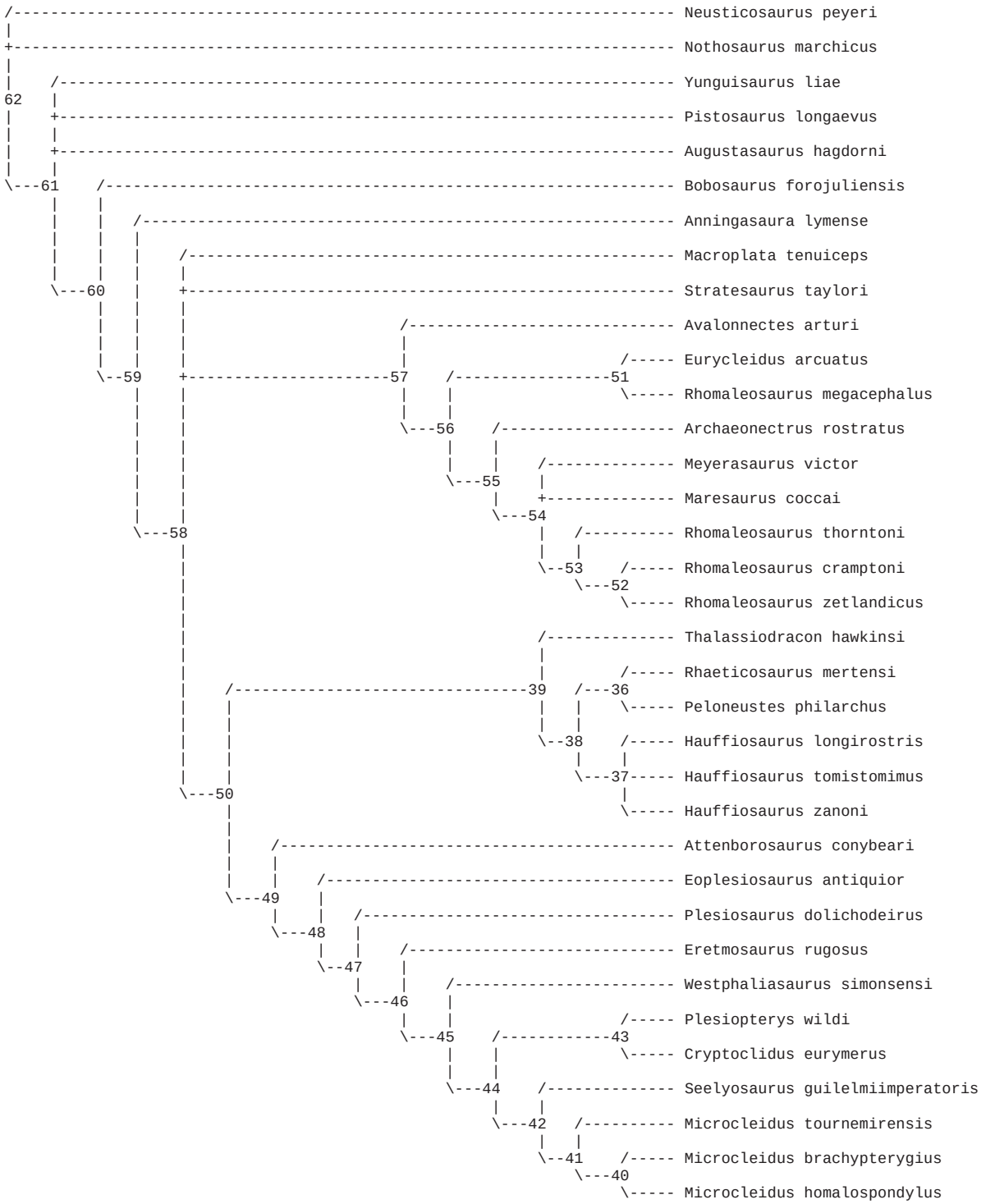

Apomorphy lists:

Branch	Character	Steps	CI	Change
node_62 --> Neusticosaurus	2	1	0.143	1 ==> 0
	10	1	0.286	1 ==> 0
	40	1	0.500	1 ==> 0
	91	1	0.333	1 ==> 0
	111	1	0.333	1 ==> 0
	112	1	0.667	1 ==> 2
	116	1	0.500	1 ==> 0
	131	1	0.375	1 ==> 3
	133	1	0.250	1 ==> 0
	142	1	0.250	0 --> 1
	196	1	0.333	0 ==> 2
	242	1	0.429	1 ==> 2
	245	1	0.250	0 ==> 1
node_62 --> Nothosaurus	1	1	0.200	0 ==> 1
	7	1	0.286	1 ==> 2
	8	1	0.333	0 ==> 1
	9	1	0.500	0 ==> 1
	21	1	0.400	0 ==> 2
	25	1	0.500	0 --> 2
	26	1	1.000	0 ==> 1
	37	1	0.500	0 ==> 1
	41	1	1.000	0 --> 1
	55	1	1.000	0 ==> 1
	62	1	0.250	0 ==> 1
	73	1	0.250	0 --> 1
	78	1	0.333	0 ==> 1
	87	1	0.333	0 ==> 1
	109	1	0.286	0 ==> 1
	113	1	0.250	0 ==> 1
	125	1	0.333	1 ==> 0
	138	1	0.222	0 --> 1
	140	1	0.500	0 ==> 1
	162	1	1.000	0 ==> 1
	176	1	0.200	0 ==> 1
	205	1	0.222	2 ==> 1
node_62 --> node_61	4	1	0.200	0 ==> 1
	22	1	0.500	0 ==> 1
	25	1	0.500	0 --> 1
	29	1	1.000	2 ==> 0
	50	1	0.429	0 ==> 2
	53	1	0.500	0 ==> 1
	57	1	0.333	1 ==> 0
	60	1	0.500	0 --> 1
	63	1	0.500	0 ==> 1
	65	1	0.667	0 ==> 2
	67	1	0.250	0 --> 1
	76	1	1.000	0 --> 1
	120	1	0.400	0 ==> 1
	122	1	0.200	1 ==> 0
	123	1	0.333	0 --> 1
	126	1	0.333	0 ==> 1
	136	1	0.333	1 --> 0
	143	1	0.500	0 --> 1
	149	1	0.500	0 --> 1
	151	1	0.333	0 --> 1
	152	1	0.333	1 --> 4

	156	1	0.333	0 --> 1
	163	1	0.500	1 ==> 0
	178	1	0.500	0 ==> 1
	179	1	0.250	0 ==> 1
	181	1	0.500	1 ==> 0
	189	1	0.333	0 --> 1
	192	1	0.200	0 --> 1
	198	1	0.250	0 --> 1
	203	1	0.286	1 ==> 2
	206	1	0.333	0 ==> 1
	224	1	0.667	0 ==> 2
	226	1	0.500	0 ==> 1
	239	1	0.333	0 ==> 1
	250	1	0.400	2 ==> 0
	260	1	0.333	0 ==> 1
	265	1	0.286	0 ==> 1
node_61 --> Yunguisaurus	2	1	0.143	1 ==> 0
	7	1	0.286	1 ==> 0
	32	1	0.333	0 ==> 1
	35	1	0.333	0 ==> 1
	40	1	0.500	1 ==> 0
	45	1	0.500	0 ==> 1
	103	1	0.286	0 --> 2
	130	1	1.000	0 ==> 1
	131	1	0.375	1 ==> 3
	141	1	0.333	0 ==> 1
	156	1	0.333	1 --> 0
	179	1	0.250	1 --> 2
	205	1	0.222	2 ==> 0
	231	1	0.400	1 ==> 0
node_61 --> Pistosaurus	33	1	0.200	0 ==> 1
	103	1	0.286	0 --> 2
	109	1	0.286	0 ==> 2
	153	1	0.250	1 ==> 2
	157	1	0.333	0 --> 1
	158	1	0.286	0 --> 1
	170	1	0.333	0 ==> 1
	173	1	0.125	0 ==> 1
	176	1	0.200	0 ==> 1
	180	1	0.250	1 ==> 0
	183	1	0.250	0 ==> 1
	191	1	1.000	0 --> 1
	193	1	0.333	0 ==> 1
	201	1	0.200	0 ==> 1
	225	1	0.500	0 ==> 2
	227	1	0.286	1 ==> 0
node_61 --> Augustasaurus	51	1	0.333	0 ==> 1
	70	1	0.250	1 ==> 0
	92	1	0.333	0 ==> 1
	138	1	0.222	0 --> 1
	148	1	0.667	0 ==> 2
	165	1	0.286	0 ==> 2
	177	1	0.250	0 ==> 1
	203	1	0.286	2 ==> 1
	208	1	0.333	0 ==> 2
	256	1	0.500	0 ==> 1
node_61 --> node_60	1	1	0.200	0 --> 1
	4	1	0.200	1 --> 0
	9	1	0.500	0 --> 1
	12	1	1.000	0 --> 1

	15	1	0.667	0 --> 1
	33	1	0.200	0 --> 1
	62	1	0.250	0 --> 1
	86	1	0.500	0 --> 1
	96	1	0.250	0 --> 1
	98	1	1.000	0 --> 1
	100	1	0.500	1 --> 0
	109	1	0.286	0 --> 2
	113	1	0.250	0 --> 1
	123	1	0.333	1 --> 0
	152	1	0.333	4 --> 1
	159	1	0.400	0 --> 1
	160	1	0.750	0 ==> 1
	161	1	0.400	0 ==> 1
	164	1	0.500	0 ==> 1
	165	1	0.286	0 ==> 2
	171	1	1.000	1 ==> 0
	177	1	0.250	0 ==> 1
	181	1	0.500	0 ==> 1
	190	1	0.400	0 --> 1
	196	1	0.333	0 --> 2
	199	1	1.000	0 --> 1
	205	1	0.222	2 --> 1
	214	1	0.667	0 --> 1
	216	1	0.500	1 --> 0
	251	1	0.333	0 --> 1
	254	1	1.000	0 --> 1
	258	1	0.500	0 --> 1
	267	1	1.000	0 --> 1
	268	1	1.000	0 --> 1
node_60 --> Bobosaurus	151	1	0.333	1 --> 2
	153	1	0.250	1 ==> 0
	156	1	0.333	1 --> 0
	178	1	0.500	1 ==> 2
	179	1	0.250	1 --> 2
	185	1	0.333	0 ==> 1
	188	1	0.333	0 ==> 1
	227	1	0.286	1 ==> 0
node_60 --> node_59	17	1	0.200	0 ==> 1
	136	1	0.333	0 --> 1
	137	1	0.400	2 ==> 1
	152	1	0.333	1 --> 2
	167	1	1.000	0 ==> 1
	172	1	0.429	0 ==> 3
	187	1	0.600	3 --> 1
	223	1	0.250	2 --> 0
	244	1	0.500	0 --> 1
	255	1	1.000	0 --> 1
node_59 --> node_58	2	1	0.143	1 ==> 0
	18	1	0.333	0 --> 1
	19	1	0.400	0 --> 1
	31	1	0.500	0 ==> 1
	49	1	0.500	1 --> 0
	50	1	0.429	2 ==> 1
	65	1	0.667	2 ==> 1
	68	1	0.667	0 --> 2
	71	1	0.667	0 ==> 2
	95	1	0.333	0 --> 1
	108	1	0.500	1 --> 0
	114	1	0.250	0 --> 1

	121	1	0.250	0 --> 1
	138	1	0.222	0 --> 1
	148	1	0.667	0 ==> 2
node_58 --> node_50	1	1	0.200	1 --> 0
	19	1	0.400	1 --> 2
	33	1	0.200	1 ==> 0
	43	1	1.000	0 ==> 2
	68	1	0.667	2 --> 0
	70	1	0.250	1 --> 0
	77	1	0.500	0 ==> 1
	84	1	0.667	2 ==> 0
	106	1	0.500	0 --> 1
	109	1	0.286	2 --> 0
	114	1	0.250	1 --> 0
	121	1	0.250	1 --> 0
	127	1	1.000	0 ==> 2
	142	1	0.250	0 --> 1
	152	1	0.333	2 ==> 3
	158	1	0.286	0 --> 1
	180	1	0.250	1 ==> 0
	203	1	0.286	2 ==> 0
	239	1	0.333	1 ==> 0
	252	1	0.500	1 ==> 0
node_50 --> node_39	16	1	1.000	0 ==> 1
	21	1	0.400	0 --> 1
	22	1	0.500	1 --> 0
	29	1	1.000	0 --> 1
	52	1	0.667	0 ==> 1
	62	1	0.250	1 --> 0
	83	1	0.286	2 --> 1
	96	1	0.250	1 --> 0
	101	1	1.000	0 --> 1
	131	1	0.375	1 --> 0
	143	1	0.500	1 --> 0
	172	1	0.429	3 ==> 2
	192	1	0.200	1 --> 0
	201	1	0.200	0 ==> 1
	206	1	0.333	1 --> 0
node_39 --> node_38	4	1	0.200	0 --> 2
	6	1	0.500	0 --> 1
	9	1	0.500	1 ==> 2
	17	1	0.200	1 --> 0
	34	1	1.000	0 ==> 1
	67	1	0.250	1 --> 0
	70	1	0.250	0 --> 1
	71	1	0.667	2 --> 1
	103	1	0.286	0 --> 1
	109	1	0.286	0 --> 2
	112	1	0.667	1 ==> 0
	114	1	0.250	0 --> 1
	115	1	1.000	1 --> 0
	124	1	1.000	0 --> 1
	131	1	0.375	0 --> 2
	138	1	0.222	1 ==> 2
	150	1	1.000	0 --> 1
	157	1	0.333	0 ==> 1
	165	1	0.286	2 --> 0
	205	1	0.222	1 --> 0
	214	1	0.667	1 --> 2
	216	1	0.500	0 ==> 1

	231	1	0.400	1 ==> 0
	232	1	0.333	0 --> 1
	235	1	0.333	2 --> 0
	236	1	0.250	0 --> 1
	242	1	0.429	1 --> 2
	249	1	0.200	0 ==> 1
	250	1	0.400	0 ==> 2
	263	1	0.200	0 --> 1
	264	1	0.250	0 --> 1
node_38 --> node_36	1	1	0.200	0 --> 1
	7	1	0.286	1 --> 2
	11	1	1.000	0 --> 1
	15	1	0.667	1 --> 2
	50	1	0.429	1 --> 3
	51	1	0.333	0 --> 1
	52	1	0.667	1 --> 2
	54	1	1.000	0 --> 1
	83	1	0.286	1 --> 2
	84	1	0.667	0 --> 2
	87	1	0.333	0 --> 1
	90	1	1.000	0 --> 1
	99	1	0.333	0 --> 2
	100	1	0.500	0 --> 1
	103	1	0.286	1 --> 2
	110	1	1.000	0 --> 1
	117	1	0.500	0 --> 1
	120	1	0.400	1 --> 0
	127	1	1.000	2 --> 1
	132	1	0.333	0 --> 1
	137	1	0.400	1 --> 0
	159	1	0.400	1 --> 2
	161	1	0.400	1 --> 2
	165	1	0.286	0 --> 1
	172	1	0.429	2 --> 0
	177	1	0.250	1 --> 0
	187	1	0.600	1 --> 0
	189	1	0.333	1 ==> 0
	194	1	0.500	0 --> 1
	196	1	0.333	2 --> 0
	207	1	0.500	0 --> 1
	220	1	0.250	0 --> 1
	224	1	0.667	2 --> 0
	232	1	0.333	1 --> 2
	244	1	0.500	1 --> 0
	251	1	0.333	1 --> 0
	255	1	1.000	1 ==> 2
	262	1	1.000	0 --> 1
	269	1	0.333	0 --> 1
node_36 --> Rhaeticosaurus	122	1	0.200	0 ==> 1
	123	1	0.333	0 ==> 1
	125	1	0.333	1 ==> 0
	126	1	0.333	1 ==> 0
	136	1	0.333	1 ==> 0
	141	1	0.333	0 ==> 2
	164	1	0.500	1 ==> 2
	172	1	0.429	0 --> 1
	188	1	0.333	0 ==> {12}
	246	1	0.250	0 ==> 1
	264	1	0.250	1 --> 0
	265	1	0.286	1 ==> 0

node_36 --> Peloneustes	152	1	0.333	3 ==> 1
	153	1	0.250	1 ==> 0
	174	1	0.500	0 ==> 1
	175	1	0.333	0 ==> 1
	179	1	0.250	1 ==> 2
	182	1	0.500	0 ==> 1
	186	1	1.000	0 ==> 1
	222	1	0.333	1 ==> 0
	223	1	0.250	0 ==> 2
	224	1	0.667	0 --> 3
	229	1	1.000	0 ==> 1
	231	1	0.400	0 ==> 2
	238	1	1.000	0 ==> 1
	241	1	1.000	1 ==> 0
	242	1	0.429	2 --> 0
	244	1	0.500	0 --> 2
	245	1	0.250	0 ==> 1
	251	1	0.333	0 --> 2
	254	1	1.000	1 ==> 2
	256	1	0.500	0 ==> 1
	259	1	0.333	0 ==> 1
	270	1	0.250	0 ==> 1
node_38 --> node_37	13	1	0.200	0 ==> 1
	14	1	0.500	0 --> 2
	25	1	0.500	1 ==> 0
	28	1	0.500	0 ==> 2
	53	1	0.500	1 ==> 0
	66	1	0.500	0 ==> 1
	73	1	0.250	0 ==> 1
	82	1	0.333	0 ==> 1
	113	1	0.250	1 ==> 0
	121	1	0.250	0 ==> 1
	130	1	1.000	0 ==> 2
	131	1	0.375	2 --> 3
	151	1	0.333	1 --> 2
	183	1	0.250	0 --> 1
	203	1	0.286	0 --> 2
	209	1	0.500	0 --> 2
	227	1	0.286	1 --> 2
	235	1	0.333	0 --> 1
	257	1	0.250	0 ==> 1
node_37 --> H. longirostris	17	1	0.200	0 --> 1
	50	1	0.429	1 ==> 2
	65	1	0.667	1 ==> 0
	99	1	0.333	0 ==> 1
node_37 -> H. tomistomimus	114	1	0.250	1 --> 0
	141	1	0.333	0 ==> 1
	259	1	0.333	0 ==> 1
	265	1	0.286	1 ==> 2
node_37 --> H. zanoni	88	1	0.333	0 ==> 1
	142	1	0.250	1 --> 0
	236	1	0.250	1 --> 0
	242	1	0.429	2 --> 1
	263	1	0.200	1 --> 0
node_39 --> Thalassiodracon	3	1	0.167	0 ==> 1
	7	1	0.286	1 ==> 0
	8	1	0.333	0 ==> 1
	46	1	0.333	1 ==> 0
	61	1	0.333	0 ==> 1
	79	1	0.250	1 ==> 0

	92	1	0.333	0 ==> 1
	141	1	0.333	0 ==> 1
	142	1	0.250	1 --> 0
	158	1	0.286	1 --> 0
	173	1	0.125	0 ==> 1
node_50 --> node_49	4	1	0.200	0 --> 1
	31	1	0.500	1 --> 0
	32	1	0.333	0 --> 1
	35	1	0.333	0 --> 1
	69	1	0.500	0 --> 1
	78	1	0.333	0 --> 1
	111	1	0.333	1 ==> 0
	126	1	0.333	1 --> 0
	128	1	1.000	0 --> 1
	140	1	0.500	0 --> 1
	141	1	0.333	0 ==> 2
	144	1	1.000	0 --> 1
	148	1	0.667	2 --> 1
	182	1	0.500	0 ==> 1
	189	1	0.333	1 --> 0
	194	1	0.500	0 ==> 1
	246	1	0.250	0 --> 1
node_49 --> Attenborosaurus	13	1	0.200	0 ==> 1
	50	1	0.429	1 ==> 2
	61	1	0.333	0 ==> 1
	208	1	0.333	0 ==> 2
	209	1	0.500	0 ==> 2
	219	1	0.500	0 ==> 3
	220	1	0.250	0 ==> 1
	235	1	0.333	2 ==> 1
	270	1	0.250	0 ==> 1
node_49 --> node_48	3	1	0.167	0 --> 1
	7	1	0.286	1 --> 0
	17	1	0.200	1 --> 0
	113	1	0.250	1 --> 0
	133	1	0.250	1 --> 0
	152	1	0.333	3 ==> 4
	161	1	0.400	1 --> 0
	190	1	0.400	1 ==> 0
	197	1	0.333	0 --> 1
	232	1	0.333	0 --> 1
	257	1	0.250	0 --> 1
node_48 --> node_47	159	1	0.400	1 ==> 2
	165	1	0.286	2 --> 0
	227	1	0.286	1 ==> 2
	244	1	0.500	1 ==> 2
	251	1	0.333	1 ==> 2
node_47 --> Plesiosaurus	107	1	0.333	0 ==> 1
	108	1	0.500	0 --> 1
	169	1	0.500	0 ==> 1
	180	1	0.250	0 ==> 1
	201	1	0.200	0 ==> 1
	222	1	0.333	1 ==> 0
	232	1	0.333	1 --> 0
node_47 --> node_46	4	1	0.200	1 --> 0
	48	1	0.200	0 --> 1
	58	1	0.500	1 --> 0
	79	1	0.250	1 --> 0
	84	1	0.667	0 --> 1
	92	1	0.333	0 --> 1

	95	1	0.333	1 --> 0
	97	1	0.333	0 --> 1
	145	1	1.000	0 --> 1
	157	1	0.333	0 ==> 1
	158	1	0.286	1 --> 0
	176	1	0.200	0 --> 1
	185	1	0.333	0 --> 1
	187	1	0.600	1 --> 3
	203	1	0.286	0 --> 2
	216	1	0.500	0 --> 1
	228	1	0.333	1 ==> 0
	235	1	0.333	2 ==> 0
	245	1	0.250	0 --> 1
	246	1	0.250	1 --> 0
	247	1	0.500	0 --> 1
node_46 --> Eretmosaurus	165	1	0.286	0 --> 2
	265	1	0.286	1 ==> 2
node_46 --> node_45	170	1	0.333	0 --> 1
	173	1	0.125	0 ==> 1
	249	1	0.200	0 --> 1
	250	1	0.400	0 ==> 1
	264	1	0.250	0 ==> 1
	270	1	0.250	0 ==> 1
node_45 --> Westphaliasaurus	176	1	0.200	1 --> 0
	217	1	0.500	0 ==> 1
	240	1	0.500	0 ==> 1
	242	1	0.429	1 ==> 0
	247	1	0.500	1 --> 0
	251	1	0.333	2 ==> 1
node_45 --> node_44	158	1	0.286	0 --> 1
	172	1	0.429	3 ==> 0
	192	1	0.200	1 ==> 0
	198	1	0.250	1 --> 0
	207	1	0.500	0 --> 1
	209	1	0.500	0 --> 1
	210	1	1.000	0 --> 2
	212	1	1.000	0 ==> 1
	219	1	0.500	0 ==> 3
	245	1	0.250	1 --> 0
	263	1	0.200	0 ==> 1
node_44 --> node_42	3	1	0.167	1 --> 0
	14	1	0.500	0 ==> 2
	32	1	0.333	1 --> 0
	39	1	1.000	0 ==> 1
	43	1	1.000	2 ==> 1
	57	1	0.333	0 --> 1
	61	1	0.333	0 ==> 1
	66	1	0.500	0 --> 1
	67	1	0.250	1 --> 0
	91	1	0.333	1 --> 0
	96	1	0.250	1 --> 0
	99	1	0.333	0 --> 2
	100	1	0.500	0 --> 1
	103	1	0.286	0 --> 1
	109	1	0.286	0 --> 2
	122	1	0.200	0 --> 1
	138	1	0.222	1 ==> 0
	164	1	0.500	1 --> 2
	166	1	1.000	0 --> 1
	178	1	0.500	1 ==> 2

	179	1	0.250	1 ==> 0
	188	1	0.333	0 ==> 1
	193	1	0.333	0 ==> 1
	210	1	1.000	2 --> 3
	249	1	0.200	1 --> 0
	265	1	0.286	1 ==> 2
node_42 --> Seelyosaurus	152	1	0.333	4 ==> 3
	158	1	0.286	1 ==> 2
	196	1	0.333	2 ==> 1
	209	1	0.500	1 --> 0
	213	1	1.000	0 ==> 1
	236	1	0.250	0 ==> 1
	260	1	0.333	1 ==> 0
node_42 --> node_41	37	1	0.500	0 ==> 1
	38	1	1.000	0 ==> 1
	50	1	0.429	1 ==> 2
	153	1	0.250	1 ==> 2
	154	1	1.000	0 ==> 1
	183	1	0.250	0 ==> 1
	205	1	0.222	1 --> 0
	223	1	0.250	0 ==> 2
	235	1	0.333	0 --> 2
node_41 -> M. tournemirensis	10	1	0.286	1 ==> 2
	48	1	0.200	1 --> 0
	58	1	0.500	0 ==> 1
	82	1	0.333	0 ==> 1
	132	1	0.333	0 ==> 1
	197	1	0.333	1 ==> 0
	198	1	0.250	0 --> 1
	205	1	0.222	0 --> 2
	263	1	0.200	1 ==> 0
node_41 --> node_40	33	1	0.200	0 ==> 1
	151	1	0.333	1 --> 2
	180	1	0.250	0 ==> 1
	200	1	0.500	0 --> 1
	201	1	0.200	0 --> 1
	203	1	0.286	2 --> 0
	207	1	0.500	1 --> 2
	231	1	0.400	1 ==> 0
	245	1	0.250	0 ==> 1
node_40 -> M. brachypterygius	3	1	0.167	0 ==> 1
	4	1	0.200	0 ==> 1
	83	1	0.286	2 ==> 1
	103	1	0.286	1 --> 0
	152	1	0.333	4 ==> 3
	192	1	0.200	0 ==> 1
	220	1	0.250	0 ==> 1
	227	1	0.286	2 ==> 1
	258	1	0.500	1 ==> 0
	265	1	0.286	2 ==> 1
node_40 -> M. homalospondylus	25	1	0.500	1 ==> 2
	251	1	0.333	2 ==> 1
node_44 --> node_43	10	1	0.286	1 --> 0
	27	1	1.000	0 --> 1
	35	1	0.333	1 --> 0
	38	1	1.000	0 --> 2
	45	1	0.500	0 ==> 1
	46	1	0.333	1 --> 0
	60	1	0.500	1 --> 0
	68	1	0.667	0 ==> 1

	83	1	0.286	2 ==> 1
	85	1	1.000	1 --> 0
	89	1	1.000	0 ==> 1
	112	1	0.667	1 ==> 2
	125	1	0.333	1 ==> 0
	131	1	0.375	1 --> 2
	161	1	0.400	0 --> 1
	163	1	0.500	0 ==> 1
	168	1	1.000	0 --> 1
	169	1	0.500	0 --> 1
	170	1	0.333	1 --> 0
	185	1	0.333	1 --> 0
	200	1	0.500	0 --> 1
	206	1	0.333	1 --> 0
	207	1	0.500	1 --> 2
	214	1	0.667	1 --> 2
	220	1	0.250	0 --> 1
	228	1	0.333	0 --> 1
	232	1	0.333	1 --> 2
	234	1	1.000	0 --> 1
	237	1	1.000	0 --> 1
	250	1	0.400	1 --> 2
	252	1	0.500	0 --> 1
	257	1	0.250	1 ==> 0
	269	1	0.333	0 ==> 1
node_43 --> Plesiopterys	48	1	0.200	1 --> 0
	77	1	0.500	1 ==> 0
	78	1	0.333	1 --> 0
	79	1	0.250	0 --> 1
	151	1	0.333	1 ==> 2
	153	1	0.250	1 ==> 2
	196	1	0.333	2 ==> 1
	198	1	0.250	0 --> 1
	270	1	0.250	1 ==> 0
node_43 --> Cryptoclidus	14	1	0.500	0 ==> 1
	51	1	0.333	0 ==> 1
	63	1	0.500	1 ==> 0
	71	1	0.667	2 ==> 1
	72	1	0.500	0 ==> 1
	74	1	0.500	0 ==> 1
	80	1	1.000	0 ==> 1
	82	1	0.333	0 ==> 1
	152	1	0.333	4 ==> 3
	160	1	0.750	1 ==> 3
	161	1	0.400	1 --> 2
	173	1	0.125	1 ==> 0
	176	1	0.200	1 --> 0
	187	1	0.600	3 ==> 0
	190	1	0.400	0 ==> 1
	195	1	1.000	0 ==> 1
	202	1	1.000	1 ==> 0
	203	1	0.286	2 ==> 1
	216	1	0.500	1 ==> 2
	221	1	1.000	0 ==> 1
	222	1	0.333	1 ==> 0
	225	1	0.500	0 ==> 1
	226	1	0.500	1 ==> 0
	227	1	0.286	2 ==> 1
	230	1	1.000	0 ==> 1
	239	1	0.333	0 ==> 1

	240	1	0.500	0 ==> 1
	242	1	0.429	1 ==> 3
	244	1	0.500	2 ==> 3
	245	1	0.250	0 ==> 2
	255	1	1.000	1 ==> 3
	259	1	0.333	0 ==> 1
	260	1	0.333	1 ==> 0
	261	1	1.000	0 ==> {12}
	262	1	1.000	0 ==> 2
	265	1	0.286	1 ==> 0
	268	1	1.000	1 ==> 2
node_48 --> Eoplesiosaurus	193	1	0.333	0 ==> 1
	205	1	0.222	1 --> 2
node_58 --> Macroplata	2	1	0.143	0 ==> 1
	4	1	0.200	0 --> 1
	13	1	0.200	0 ==> 1
	28	1	0.500	0 ==> 1
	62	1	0.250	1 --> 0
	67	1	0.250	1 --> 0
	73	1	0.250	0 ==> 1
	83	1	0.286	2 ==> 0
	120	1	0.400	1 ==> 2
	131	1	0.375	1 ==> 2
	151	1	0.333	1 ==> 2
	153	1	0.250	1 ==> 0
	192	1	0.200	1 --> 0
	217	1	0.500	0 ==> 1
	227	1	0.286	1 ==> 2
	231	1	0.400	1 ==> 2
node_58 --> Stratesaurus	1	1	0.200	1 --> 0
	3	1	0.167	0 ==> 1
	10	1	0.286	1 ==> 0
	17	1	0.200	1 ==> 0
	21	1	0.400	0 ==> 1
	70	1	0.250	1 ==> 0
	79	1	0.250	1 ==> 0
	95	1	0.333	1 --> 0
	99	1	0.333	0 ==> 1
	133	1	0.250	1 ==> 0
	138	1	0.222	1 ==> 0
	149	1	0.500	1 ==> 0
	173	1	0.125	0 ==> 1
	175	1	0.333	0 ==> 1
	225	1	0.500	0 ==> 2
	269	1	0.333	0 ==> 1
node_58 --> node_57	7	1	0.286	1 --> 2
	8	1	0.333	0 --> 1
	9	1	0.500	1 --> 2
	10	1	0.286	1 --> 2
	13	1	0.200	0 --> 1
	21	1	0.400	0 --> 2
	49	1	0.500	0 --> 1
	87	1	0.333	0 --> 1
	99	1	0.333	0 --> 1
	100	1	0.500	0 --> 2
	102	1	1.000	0 --> 1
	111	1	0.333	1 --> 0
	120	1	0.400	1 --> 2
	124	1	1.000	0 --> 2
	159	1	0.400	1 ==> 2

	172	1	0.429	3 ==> 1
	179	1	0.250	1 --> 0
	183	1	0.250	0 ==> 1
	184	1	0.667	0 ==> 2
	208	1	0.333	0 --> 2
	210	1	1.000	0 --> 1
	218	1	1.000	0 --> 1
	228	1	0.333	1 ==> 0
	244	1	0.500	1 --> 2
	257	1	0.250	0 --> 1
node_57 --> Avalonnectes	141	1	0.333	0 ==> {12}
	173	1	0.125	0 ==> 1
node_57 --> node_56	50	1	0.429	1 ==> 2
	57	1	0.333	0 ==> 1
	164	1	0.500	1 ==> 0
	174	1	0.500	0 ==> 1
	205	1	0.222	1 --> 0
	242	1	0.429	1 --> 2
node_56 --> node_51	4	1	0.200	0 --> 1
	6	1	0.500	0 --> 1
	14	1	0.500	0 --> 2
	18	1	0.333	1 --> 0
	19	1	0.400	1 --> 0
	28	1	0.500	0 --> 1
	33	1	0.200	1 --> 0
	83	1	0.286	2 --> 0
	121	1	0.250	1 --> 0
	133	1	0.250	1 --> 0
	179	1	0.250	0 --> 1
	201	1	0.200	0 --> 1
	246	1	0.250	0 ==> 1
	249	1	0.200	0 ==> 1
node_51 --> Eurycleidus	245	1	0.250	0 ==> 1
node_51 --> R. macrocephalus	137	1	0.400	1 ==> 0
	138	1	0.222	1 ==> 2
	153	1	0.250	1 ==> 0
	190	1	0.400	1 ==> 2
	225	1	0.500	0 ==> 2
node_56 --> node_55	15	1	0.667	1 ==> 2
	20	1	0.500	0 --> 1
	52	1	0.667	0 ==> 1
	93	1	1.000	0 --> 1
	99	1	0.333	1 --> 2
	132	1	0.333	0 --> 1
	184	1	0.667	2 --> 1
	196	1	0.333	2 --> 1
	205	1	0.222	0 --> 2
	240	1	0.500	0 --> 1
	250	1	0.400	0 --> 2
	264	1	0.250	0 ==> 1
node_55 --> node_54	2	1	0.143	0 --> 1
	19	1	0.400	1 --> 2
	116	1	0.500	1 ==> 0
	137	1	0.400	1 --> 0
	153	1	0.250	1 ==> 0
	158	1	0.286	0 --> 1
	179	1	0.250	0 --> 2
	187	1	0.600	1 --> 2
	232	1	0.333	0 ==> 1
	236	1	0.250	0 --> 1

node_54 --> Meyerasaurus	2	1	0.143	1 --> 0
	7	1	0.286	2 ==> 0
	10	1	0.286	2 ==> 1
	13	1	0.200	1 ==> 0
	21	1	0.400	2 --> 0
	86	1	0.500	1 ==> 0
	88	1	0.333	0 ==> 1
	97	1	0.333	0 ==> 1
	103	1	0.286	0 ==> 1
	107	1	0.333	0 ==> 1
	109	1	0.286	2 ==> 1
	122	1	0.200	0 ==> 1
	184	1	0.667	1 --> 2
	197	1	0.333	0 ==> 1
node_54 --> Maresaurus	4	1	0.200	0 --> 1
	20	1	0.500	1 --> 0
	46	1	0.333	1 ==> 0
	48	1	0.200	0 ==> 1
	96	1	0.250	1 ==> 0
	137	1	0.400	0 --> 1
	160	1	0.750	1 ==> 2
	172	1	0.429	1 ==> 3
node_54 --> node_53	18	1	0.333	1 ==> 0
	23	1	1.000	0 ==> 1
	59	1	1.000	0 --> 1
	178	1	0.500	1 --> 0
	245	1	0.250	0 ==> 1
	263	1	0.200	0 --> 1
node_53 --> node_52	19	1	0.400	2 --> 0
	138	1	0.222	1 ==> 2
	177	1	0.250	1 --> 0
	190	1	0.400	1 --> 2
	240	1	0.500	1 --> 2
	249	1	0.200	0 ==> 1
node_52 --> R. cramptoni	2	1	0.143	1 --> 0
node_53 --> R. thorntoni	117	1	0.500	0 ==> 1
	120	1	0.400	2 ==> 1
	165	1	0.286	2 ==> 0
	223	1	0.250	0 ==> 2
node_55 --> Archaeonectrus	4	1	0.200	0 --> 2
	135	1	1.000	0 ==> 1
	138	1	0.222	1 ==> 2
	159	1	0.400	2 ==> 1
	173	1	0.125	0 ==> 1
	235	1	0.333	2 ==> 1
node_59 --> Anningasaura	3	1	0.167	0 ==> 1
	10	1	0.286	1 ==> 2
	28	1	0.500	0 ==> 1
	48	1	0.200	0 ==> 1
	69	1	0.500	0 --> 1
	72	1	0.500	0 ==> 1
	73	1	0.250	0 --> 1
	74	1	0.500	0 ==> 1
	83	1	0.286	2 ==> 0
	88	1	0.333	0 ==> 1
	91	1	0.333	1 ==> 0
	97	1	0.333	0 --> 1
	106	1	0.500	0 --> 1
	107	1	0.333	0 --> 1
	122	1	0.200	0 ==> 1

```
131             1  0.375  1 ==> 0
160             1  0.750  1 ==> 3
173             1  0.125  0 ==> 1
175             1  0.333  0 ==> 1
```

table S4. Measurements and proportions in the trunk and limbs of Eosauropterygia. References are to the major publications from which the measurements were taken, either from the text or from the illustrations. Fe, femur length; Fe.DW, distal width of femur; Fe.MW, minimal shaft width of femur; GA, glenoid-acetabular distance; Hu, humerus length; Hu.DW, distal width of humerus; Hu.MW, minimal shaft width of humerus; Ra, radius length; Ti, tibia length. Collections acronyms: FMNH, Field Museum of Natural History, Chicago, USA; GMPKU, Geological Museum of Peking University, Beijing, China; MfN, Museum für Naturkunde, Berlin, Germany; LWL-MFN, LWL-Museum für Naturkunde, Münster, Germany; NHMUK, Natural History Museum, London, UK; PIMUZ, Paläontologisches Institut und Museum Universität Zürich, Zurich, Switzerland; SMF, Senckenberg-Museum, Frankfurt, Germany; SMNS, Staatliches Museum für Naturkunde, Stuttgart, Germany; STIPB, Steinmann Institute Paleontology Collection, University of Bonn, Bonn, Germany; ZMNH, Zhejiang Museum of Natural History, Hangzhou, Zhejiang, China.

Taxon	Spec. #	*Reference*	GA	Hu	Hu.MW	Hu.DW	Fe	Fe.MW	Fe.DW	Ra	Ti	GA/Hu	GA/Fe	Hu/Ra	Fe/Ti	Hu/Ti	Hu/Fe	Fe/Fe DW
Serpianosaurus mirigiolensis	PIMUZ T 3931	Rieppel (1989) (64)	148	36	4	12	34	3	5	21	20	4.11	4.35	1.71	1.70	1.80	1.06	7.08
Neusticosaurus pusillus	PIMUZ T 3934	Sander (1989) (65)	83	21	2.7	7.3	20.0	1.4	2.3	12.0	10.0	3.95	4.15	1.75	2.00	2.10	1.05	8.70
Neusticosaurus peyeri	PIMUZ T 3615	Sander (1989) (65)	45	11	1.8	3.7	10.7	1.5	2.0	6.7	5.6	3.98	4.21	1.69	1.91	2.02	1.06	5.35
Nothosaurus marchicus	MfN I. 007.18	Rieppel & Wild (1996) (66)	227	63	12	18	68	7	13	34	36	3.60	3.34	1.85	1.89	1.75	0.93	5.44
Nothosaurus giganteus	PIMUZ T 4829	Rieppel (2000) (67)	1023	238	40	52	250	35	52	127	132	4.30	4.09	1.87	1.89	1.80	0.95	4.81
Lariosaurus calcagnii	PIMUZ T 3983	Rieppel (2000) (67)	608	162	43	47	128	14	19	74	61	3.75	4.75	2.19	2.10	2.66	1.27	6.74
Wangosaurus brevirostris	GMPKU-P-1529	Ma et al. (2015) (68)	585	163	26	47	166	16	19	86	72	3.59	3.52	1.90	2.31	2.26	0.98	8.74
Yunguisaurus liae	ZMNH M8738	Sato et al. (2014) (59)	1085	210	51	64	183	46	61	113	108	5.17	5.93	1.86	1.69	1.94	1.15	3.00
Pistosaurus longaevus	SMF R4041	Geissler (1895) (69), Sues (1987) (52)	-	178	24	57	178	31	50	114	-	-	-	1.56	-		1.00	3.56
Augustasaurus hagdorni	FMNH PR 1974	Sander et al. (1997) (53)	-	184	24	49	-	-	-	96	-	-	-	1.92	-		-	-
Bobosaurus forojuliensis	MFSN 27285	Dalla Vecchia (2006) (58), Fabbri et al. (2014) (13)	1071	258	42	-	-	-	-	-	193	4.15	-	-	-	1.34	-	-
Rhaeticosaurus mertensi	LWL-MFN P 64047	this study	484	183	32	51	185	37	66	48	43	2.64	2.62	3.81	4.30	4.26	0.99	2.80
Eoplesiosaurus antiquior	TTNCM 8348	Benson et al. (2012) (12)	665	221	54	79	219	32	75	77	81	3.01	3.04	2.87	2.70	2.73	1.01	2.92
Avalonnectes arturi	NHMUK 14550	Benson et al. (2012) (12)	547	-	-	-	207	42	91	-	77	-	2.64	-	2.69		-	2.27
Thalassiodracon hawkinsi	NHMUK 2018	pers. obs. on cast STIPB	355	145	38	70	140	29	64	60	53	2.45	2.54	2.42	2.64	2.74	1.04	2.19
Plesiosaurus dolichodirus	NHMUK 22656	Conybeare (1824) (70)	508	158	42	65	146	31	70	62	62	3.22	3.48	2.55	2.35	2.55	1.08	2.09
Westphaliasaurus simonsensii	LWL-MFN P 58091	Schwermann & Sander (2011) (71)	919	280	65	132	290	58	141	99	112	3.28	3.17	2.83	2.59	2.50	0.97	2.06
Plesiopterys wildi	SMNS 16812	O'Keefe (2004) (72)	505	154	45	87	155	28	70	60	52	3.28	3.26	2.57	2.98	2.96	0.99	2.21
Meyerasaurus victor	SMNS 12478	Smith & Vincent (2010) (73)	1179	442	83	189	411	61	167	151	139	2.67	2.87	2.93	2.96	3.18	1.08	2.46
Rhomaleosaurus thorntoni	NHMUK R4853	Smith & Benson (2014) (74)	1806	710	138	360	681	133	305	152	150	2.54	2.65	4.67	4.54	4.73	1.04	2.23

table S5. List of histological samples. Collections acronyms: LACM, Natural History Museum of Los Angeles County, Los Angeles, USA; LWL-MFN, LWL-Museum für Naturkunde, Münster, Germany; OMNH, Osaka Museum of Natural History, Osaka, Japan; SMNS, Staatliches Museum für Naturkunde, Stuttgart, Germany; STIPB, Steinmann Institute Paleontology Collection, University of Bonn, Bonn, Germany; Histological thin sections are housed in the histology slide collections of the Steinmann Institute, University of Bonn, Germany.

Taxon	Bone	Clade	Spec. Number	Age
Nothosaurus mirabilis[1]	Femur	Nothosauroidea	STIPB R 49	Middle Triassic
Anarosaurus heterodontus[2]	Humerus, femur	Pachypleurosauria	STIPB Wijk08-58	Middle Triassic
Pistosaurus longaevus[1]	Humerus	Pistosauroidea	SMNS 84825	Middle Triassic
Rhaeticosaurus mertensi	Femur	Plesiosauria	LWL-MFN P 64047	Late Triassic
Plesiosaurus dolichodirus	Humerus	Plesiosauria	STIPB R 89	Early Jurassic
Plesiosaurus dolichodirus	Femur	Plesiosauria	STIPB R 90	Early Jurassic
Plesiosauridae indet.	Humerus	Plesiosauria	SMNS 96869	Early Jurassic
Plesiosauridae indet.	Humerus	Plesiosauria	SMNS 96897	Early Jurassic
Cryptoclidus eurymerus	Humerus, femur	Plesiosauria	STIPB R 324	Middle Jurassic
Pliosaurus sp.	Propodial	Plesiosauria	SMNS 54025	Middle Jurassic
Pliosaurus sp.	Femur	Plesiosauria	SMNS 96896	Middle Jurassic
Elasmosauridae indet.	Humerus	Plesiosauria	OMNH MV 85	Late Cretaceous
Polycotylus latipinnis	Femur	Plesiosauria	LACM 129639a	Late Cretaceous

[1] See ref. (20)
[2] See ref. (75)

table S6. Local bone apposition rate to the end of the first year and relative body size at the end of the first year in selected sauropterygians. The holotype individual of *Rhaeticosaurus mertensi* did not live to the end of the second year. The sampled long bones of the non-plesiosaurian sauropterygians were incomplete, but all clearly were smaller too much smaller than the plesiosaurians as evidenced by the total cortical thickness. Cortical thickness was measured from the center of the medullary region and represents the entire thickness of cortical bone deposited by the animal during its lifetime. See text for further explanations.

	Neusticosaurus pusillus PIMUZ T 4211	*Nothosaurus* sp. SMNS 84856	*Pistosaurus grandaevus* SMNS 84825	*Rhaeticosaurus mertensi* LWL-MFN P 64047	*Plesiosaurus dolichodirus* STIPB R89	Plesiosauridae indet. SMNS 96897	*Cryptoclidus eurymerus* STIPB R324
Bone	humerus	femur	humerus	femur	humerus	humerus	femur
Length in mm	?	?	?	185	162	496	315
Number of growth marks	3	5	4	1	2	2	3
Thickness to 1st mark (mm)	1.05	3.2	7.6	16.9	12.1	66	26.5
% total	66	56	54	88	67	75	63
Thickness 1st to 2nd mark (mm)	0.44	1.5	3.3	-	3.8	22	6.5
% total	28	26	24	-	21	25	15
Total cortical thickness (mm)	1.6	5.8	14	19.3	18.1	88	42.2
% total	100	100	100	100	100	100	100
Apposition rate (µm/day) at 365 days gestation	1.4	4.4	10.4	23.2	16.6	90.4	36.3
Apposition rate (µm/day) at 50 days gestation	2.5	7.7	18.3	40.7	29.2	159.0	63.6
Apposition rate (µm/day) at 500 days gestation	1.2	3.7	8.7	19.6	14.0	76.3	30.6

table S7. Comparison of local bone apposition rates in the femur of selected amniotes compared to local bone apposition rates in the humeri and femora of plesiosaurians. All but the sauropterygians are extant taxa for which apposition rate was determined experimentally (*33*). Values for sauropterygians were taken from table S6.

	No. of species	Rate in µm/day
Mammals	3	13.10 - 40.25
Turtles	3	0.24 - 3.55
Lizards	4	1.03 - 7.6
Crocodiles	1	9.45
Birds	5	73.91 - 156.86
Neusticosaurus	1	1.4
Nothosaurus	1	4.4
Pistosaurus	1	10.4
Plesiosaurians	4	16.6 - 90.4

Chapter 3

Published as:

Wintrich, T., Scaal, M., & Sander, P. M. (2017b). Foramina in plesiosaur cervical centra indicate a specialized vascular system. *Fossil Record*, *20*(2), 279-290.

Author contributions:

Tanja Wintrich designed the research, carried out the research, and wrote the paper.

Tanja Wintrich and P. Martin Sander provide datasets to this study

Martin Scaal and P. Martin Sander contributed to the manuscript preparation and reviewed drafts of the paper.

Foss. Rec., 20, 279–290, 2017
https://doi.org/10.5194/fr-20-279-2017

Fossil Record museum für naturkunde
Open Access berlin

Published by Copernicus Publications on behalf of the Museum für Naturkunde Berlin.

Foramina in plesiosaur cervical centra indicate a specialized vascular system

Tanja Wintrich[1], **Martin Scaal**[2], **and P. Martin Sander**[1]

[1]Bereich Paläontologie, Steinmann-Institut für Geologie, Mineralogie und Paläontologie, Universität Bonn, 53115 Bonn, Germany
[2]Institut für Anatomie II, Universität zu Köln, Joseph-Stelzmann-Str. 9, 50937 Cologne, Germany

Correspondence: Tanja Wintrich (tanja.wintrich@uni-bonn.de)

Received: 16 August 2017 – Revised: 13 November 2017 – Accepted: 14 November 2017 – Published: 19 December 2017

Abstract. The sauropterygian clade Plesiosauria arose in the Late Triassic and survived to the very end of the Cretaceous. A long, flexible neck with over 35 cervicals (the highest number of cervicals in any tetrapod clade) is a synapomorphy of Pistosauroidea, the clade that contains Plesiosauria. Basal plesiosaurians retain this very long neck but greatly reduce neck flexibility. In addition, plesiosaurian cervicals have large, paired, and highly symmetrical foramina on the ventral side of the centrum, traditionally termed "subcentral foramina", and on the floor of the neural canal. We found that these dorsal and the ventral foramina are connected by a canal that extends across the center of ossification of the vertebral centrum. We posit that these foramina are not for nutrient transfer to the vertebral centrum but that they are the osteological correlates of a highly paedomorphic vascular system in the neck of plesiosaurs. This is the retention of intersegmental arteries within the vertebral centrum that are usually obliterated during sclerotome re-segmentation in early embryonic development. The foramina and canals are a rare osteological correlate of the non-cranial vascular (arterial) system in fossil reptiles. The adaptive value of the retention of the intersegmental arteries may be improved oxygen transport during deep diving and thermoregulation. These features may have been important in the global dispersal of plesiosaurians.

1 Introduction

1.1 Sauropterygian evolution and plesiosaur origins

Plesiosauria are Mesozoic marine reptiles that had a global distribution almost from their origin in the Late Triassic (Benson et al., 2012) to their extinction at the end of the Cretaceous (Ketchum and Benson, 2010; Fischer et al., 2017). Plesiosauria belong to the clade Sauropterygia and are its most derived and only post-Triassic representatives, being among the most taxonomically diverse of all Mesozoic marine reptiles (Motani, 2009). Sauropterygia originated in the Early Triassic, diversifying into Placodontia and Eosauropterygia. Eosauropterygia include the Pistosauroidea, which in turn include Plesiosauria and non-plesiosaurian pistosauroids (Benson et al., 2012), most notably the genera *Yunguisaurus*, *Pistosaurus*, and *Augustasaurus* (sometimes grouped in the "Pistosauridae") and *Bobosaurus*, the taxon closest to Plesiosauria. All these stem representatives are Middle Triassic and early Late Triassic (Carnian) in age, meaning that a gap of around 30 million years separates them from the plesiosaurs (Benson et al., 2012; Wintrich et al., 2017).

1.2 The plesiosaur bauplan

Plesiosauria have a unique bauplan, with an unique mode of aquatic locomotion: four-winged underwater flight using limbs modified into pointed flippers (Ketchum and Benson, 2010; Wintrich et al., 2017). Morphological disparity within the group is mainly found in the evolution of different neck lengths and skull sizes. Neck length evolution involves a long neck at the base of the clade, with at least 35 cervical verte-

brae, which is unique to "Pistosauridae" and Plesiosauria, all other amniotes having less than 30 cervical vertebrae (Müller et al., 2010). In Pistosauroidea, the increase in neck length evolves by an increase in vertebral number, not by an increase in centrum length as in other well-known long-necked animals, like sauropod dinosaurs (Sander et al., 2011; Taylor and Wedel, 2013). Neck elongation in plesiosaurians culminates in Elasmosauridae with cervical numbers exceeding 70 (O'Keefe, 2001; Zammit et al., 2008; Müller et al., 2010; Noe et al., 2017). The plesiosaurian neck was remarkably stiff (Taylor, 1981; Massare, 1988, 1994; Noe et al., 2017), which appears counterintuitive especially in the long-necked forms.

1.3 Paired foramina in plesiosaurian cervical vertebrae

All plesiosaurian cervical vertebrae show a pair of large foramina on the ventral surface of the vertebral centra (Romer, 1956). These foramina are generally termed "subcentral foramina" (Storrs, 1991; Noe et al., 2017). The large, highly symmetrical subcentral foramina are an autapomorphy of plesiosaurs and are found with great regularity in members of the clade (Wintrich et al., 2017; Benson and Druckenmiller, 2014; Storrs, 1991; O'Keefe, 2001), but smaller and less symmetrical foramina are found in some pistosaurids (non-plesiosaurian Pistosauroidea) such as *Augustasaurus* (Rieppel et al., 2002) and *Pistosaurus longaevus* (Sues, 1987).

The usage of the descriptive term subcentral foramina has a long tradition, and such paired foramina are seen in many taxa of different lineages outside of Sauropterygia. However, the term subcentral foramen is also somewhat of a wastebasket term. In the case of Plesiosauria, foramina subcentralia (subcentral foramina) were defined by Storrs (1991). He described them as a uniquely derived character shared by virtually all plesiosaurs and as being unknown among other Sauropterygia like pachypleurosaurs, placodonts, and nothosaurid-grade Nothosauriformes. Furthermore, he interpreted the foramina subcentralia as vertebral nutritive foramina in cervical vertebrae. Rothschild and Storrs (2003) hypothesized that the foramina indicated a rich blood supply to the interior of the centra (i.e., acting as nutrient foramina), protecting the vertebrae from decompression syndrome. However, they noted that the foramina showed a "large degree of variability" which is not what we observe (see below).

In addition to these ventral, paired foramina, plesiosaurian cervicals show a pair of large, highly symmetrical foramina on the floor of the neural canal. This character has not received much attention in the literature before (but see Martin and Parris, 2007), probably because it is harder to observe due to its location inside the neural canal. Damaged or sectioned vertebral centra as well as CT scans reveal that the two sets of foramina appear to be connected by two canals that pass through the center of the vertebral centrum. This raises the question as to what occupied the canals in the living animal, with vascular tissue coming to mind.

1.4 Osteological correlates of postcranial vascular features

The vascular system in fossil vertebrates is hard to reconstruct because blood vessels such as arteries and veins as well as the heart are not preserved in fossils (see Maldanis et al., 2016, for an exception). In addition, osteological correlates for features of the vascular systems in fossil reptiles remain little studied (Schwarz et al., 2007, p. 181), particularly outside the head. Some basic principles apply, though, that aid in possibly identifying such correlates. In addition, an understanding of the development of the vascular system is important. During development, some arteries in the embryo become remodeled or resorbed, and during growth, bone will grow around arteries but arteries will not lead to bone resorption. This is seen also in the structure of the human skull bone. Note that this is unlike the situation in postcranial skeletal pneumaticity in dinosaurs including birds, where respiratory tissue invades the interior of bone by inducing bone resorption (Wedel, 2009), a process that continues throughout ontogeny.

1.5 Anatomical interpretation of the paired foramina

At face value, subcentral foramen is a descriptive term for any foramen on the ventral side of a vertebral centrum. However, there are different vascular structures that may have occupied a subcentral foramen. First, the foramina could each have housed a normal nutrient blood vessel pair, consisting of an artery which enters the bone, delivering the oxygenated blood to the interior of the bone, and a vein draining the bone interior. This is the classical situation seen in long bones with a single large nutrient canal (e.g., Seymour et al., 2012; Nakajima et al., 2014) through which a terminal artery, known as arteria nutricia, enters and then ends inside the bone. Since osteogenesis of the vertebral centrum follows the same rules as that of a long bone, this is a plausible hypothesis for the ventral foramina, as recognized by Storrs (1991). The pairing would then be due to bilateral symmetry of the centrum. The second hypothesis would be that the foramina are the entries for arteries which traverse the vertebral centrum in a dorsoventral (or vice versa) direction. These could develop in two different fashions. The arteries could either have been initially located laterally to the vertebral anlage and subsequently been incorporated into the centrum by the growth expansion of the centrum, as has been described in the posterior caudal and fluke vertebrae of whales by Slijper (1939). Alternatively, they could represent persisting intersegmental arteries which develop in the early embryo and are primarily located within the paraxial mesoderm, first between adjacent somites and later, after somite re-segmentation, inside the vertebral anlage.

1.6 Development of the vertebral column and associated vessels

Development of intersegmental arteries is seen in all vertebrates at an early ontogenetic stage. At the onset of the development of the axial skeleton in vertebrate embryos, in a process called somitogenesis, primary segments form in craniocaudal sequence within the paraxial mesoderm (Benazeraf and Pourquie, 2013). These segments, which are formed synchronously on either side of the neural tube and the notochord, are called somites. While the newly formed somites are epithelial spheres, they subsequently undergo several steps of differentiation to form their tissue derivatives, which include axial skeleton, skeletal muscle, and connective tissue of the trunk. In amniotes, the ventral somite half becomes a mesenchymal mass of cells, the sclerotome, which gives rise to all elements of the vertebral column, including the ribs. The dorsal half, in contrast, forms the dermomyotomal epithelium, which again differentiates into the myotome giving rise to axial muscle and the dermatome giving rise to the connective tissue of the skin. A sub-compartment of the sclerotome, the syndetome, gives rise to vertebral ligaments (Brent et al., 2003) and another sub-compartment, the arthrotome, gives rise to intervertebral joints (Mittapalli et al., 2005; Christ et al., 2007).

Importantly, the somites do not represent the definitive segments of the vertebral column as seen in the individual vertebral bones. In a process called re-segmentation, the adjacent cranial and caudal halves of neighboring sclerotomes unite to give rise to a single vertebra, whereas intervertebral muscles and ligaments arising from the myotome and syndetome maintain the original somitic segmentation pattern. In other words, the derivative of a single somite is not a single vertebra, but a so-called motion segment, which includes two vertebral halves tethered together in a flexible fashion by muscles and ligaments. Without re-segmentation a mobile vertebral column would not be possible (Hall, 2015, chap. 16; Scaal, 2016).

Prior to re-segmentation, neighboring sclerotomes are separated by a pair of embryonic blood vessels called the intersegmental artery and vein, which are ventrally connected to the dorsal aorta and posterior cardinal vein, respectively. In a process which is not yet well understood, these vessels usually disappear or undergo remodeling during the re-segmentation process. While at trunk level, the segmental array of vessels is still visible in the adult as, e.g., intercostal vessels, the cervical intersegmental vessels are lost and likely form the vertebral artery and vein.

We hypothesize that in plesiosaurians the intersegmental arteries were retained in cervical vertebrae into the postembryonic stage. Thus, in plesiosaurians, the process of the obliteration of the cervical intersegmental arteries did not happen, and the intersegmental arteries stayed in position and remained functional, extending (following the direction of blood flow) through the center of the cervical vertebral centrum from the ventral surface of the centrum to the floor of the neural canal. Accordingly, we here propose a new term for the large, highly symmetrical paired foramina in plesiosaurian cervicals, i.e., intersegmental artery foramen (IAF), to obtain a more precise terminology in relation to its putative embryological origin. We differentiate between the ventral IAF (vIAF), which corresponds to the traditional subcentral foramen, and the dorsal IAF (dIAF) on the floor of the neural canal. The two foramina are connected by a canal running across the center of ossification of the vertebral centrum, the intersegmental artery canal (IAC). Blood flow in the intersegmental artery located in the IAC would have been from ventral to dorsal, the artery entering through the vIAF and exiting through the dorsal dIAF.

2 Materials and methods

2.1 Materials

Our study of the internal structure of plesiosaur cervical centra is based on a small but representative sample set. It includes a latest Triassic fetal specimen and two Jurassic vertebrae from two different locations. The Triassic fetal cervical is of uncertain systematic affinity and derives from the newly discovered Rhaetian (latest Triassic) bone bed of Bonenburg, Germany (Sander et al., 2016). The Bonenburg quarry exposes an unusually thick stratigraphic section of Rhaetic sediments, including 11 m of dark grey mudstones which contain three different bone beds (BB1 to BB3) of the type known from SW England (Storrs, 1994) and southern Germany (Sander et al., 2016). In BB 2, there are several finds of plesiosaur remains, including about 20 isolated plesiosaur vertebrae with and without neural arch in a good state of preservation, including the fetal centrum studied here. The specimen can be assigned to Plesiosauria based on its platycoelous articular surfaces, the ventral keel, and the large paired ventral and dorsal foramina. Similar plesiosaur vertebrae are also known from Rhaetian bone bed localities in France (Fischer et al., 2014) and England (Storrs, 1994). These Triassic vertebrae can be subdivided into different morphotypes that presumably represent different taxa (Sander et al., 2016), but the fetal centrum currently cannot be assigned to any of these. In addition, we included the cervical vertebrae of an articulated skeleton from the Bonenburg locality, the only articulated Triassic plesiosaur skeleton (Wintrich et al., 2017; Sander et al., 2016). The Jurassic vertebrae studied by us include one isolated posterior cervical (SMNS 50845) of an indeterminate plesiosaur from the Posidonienschiefer Formation (Toarcian, Lower Jurassic) of the famous Holzmaden locality, Germany (see also O'Keefe, 2004) and a cervical vertebra that is part of an articulated skeleton of *Cryptoclidus eurymerus* (STIPB R 324) from the Middle Jurassic Oxford Clay Formation, England (see also Andrews, 1910).

Finally, we used morphological data on cervical vertebral morphology from the literature, specifically character descriptions compiled for phylogenetic analysis (Benson and Druckenmiller, 2014). Therefore, we transformed the information in the phylogenetic character matrix, consisting of the character descriptions and character states, into the morphological information.

2.2 Methods

To test competing hypotheses regarding vascular features, i.e., nutrient canals vs. intersegmental artery canals, the internal morphology of the vertebral centra needs to be revealed, which can be done by µCt scan and by a transversal histological (petrographic) thin section. Histological sectioning (Fig. 1) of the vertebrae was possible for only one specimen: the posterior cervical (SMNS 50845) from Holzmaden. Of course, the problem with histological sectioning is that this method is destructive and thus was not allowed for the other plesiosaur vertebrae which were used in this study. For the two complete vertebrae, we used high-resolution µCt scans to obtain virtual sections and reconstruct the IAC (see below).

2.2.1 Histological sectioning of plesiosaur vertebra

In the study of the IAC in plesiosaur vertebra, obviously an accurate plane of the section that will intersect the canal is crucial. This will be the transverse plane of the vertebral centrum (perpendicular to the body axis), passing through the center of ossification of the bone (Fig. 1). The proper plane can be detected easily if the floor of the neural canal and thus the dorsal IAF is visible in addition to the ventral surface of the centrum. Before sectioning, vertebra SMNS 50845 was molded and cast for reconstruction after sectioning. Next, the area of the surface trace of the plane of the section was covered by a removable epoxy putty (Technovit) to ensure a clean cut of the outer bone surface. Then, two cuts spaced about 5 mm apart were placed on either side of the plane of sectioning to obtain a thin slice of bone containing the IAC. After sectioning, the putty was removed from the bone surface and the gap in the bone was filled in with plaster, with the two halves of the bone being held in place by the mold.

The transverse slice of bone was then processed into a petrographic thin section 50 to 80 µm in thickness, following the standard procedure for fossil bone most recently outlined by Lamm (2013). The sections were then observed under a Leica DM2500LP polarizing microscope, and digital photomicrographs were taken with a Leica DFC420 color camera mounted on this microscope and edited using the 2007 Leica Image Access EASYLAB 7 software. Overview images were obtained with an Epson V750 high-resolution scanner. Terminology follows Francillion-Vieillot et al. (1990).

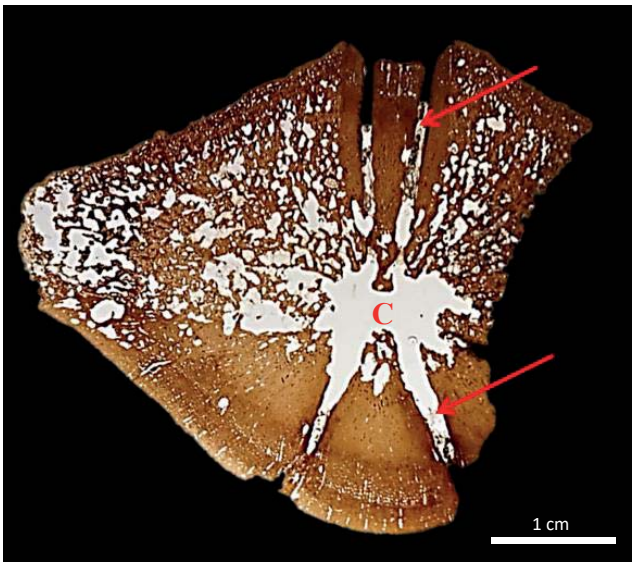

Figure 1. Transversal histological thin section of the posterior cervical vertebra SMNS 50845 from Holzmaden. The left and the right canals appear to meet in the center of ossification (C). However, CT data from other vertebrae suggest that the canals do not meet in the center of ossification, and the apparent connection in this section is probably caused by bone resorption during the formation of the medullary cavity and by damage during grinding of the section.

2.2.2 µCt scanning and 3-D reconstruction of plesiosaur vertebra

The µCt scans for the virtual sections and canal reconstruction were obtained with the vltomelx s CT scanner manufactured by GE Phoenix X-ray at the Division of Paleontology, Steinmann Institute, University of Bonn. On average, each scan was based on 1200 images. Kilovolt and microampere were set to 190 kV and 150 µA, respectively, with a voxel size of 79 µm.

We reconstructed a surface model of the scanned vertebrae with the program Avizo 7.1.1. In order to process the data from the µCt scan, an image stack was created from the dorsoventral plane (Fig. 2). For this, all 1200 µCt recordings were first uploaded into VG Studio Max and then transformed into image stacks in a JPEG format. The images in the stack were then edited and individual structures of interest were marked and color-coded and became visible, a process known as segmentation. The result is a 3-D model of the vertebra with the course of the canals having been traced (Figs. 2, 3). The modeling software Polyworks was used to visualize the course of the intersegmental arteries (Fig. 3).

2.2.3 Morphology information based on the phylogenetic matrix

In order to evaluate the distribution of the ventral vertebral foramina in plesiosaurs, we use published information.

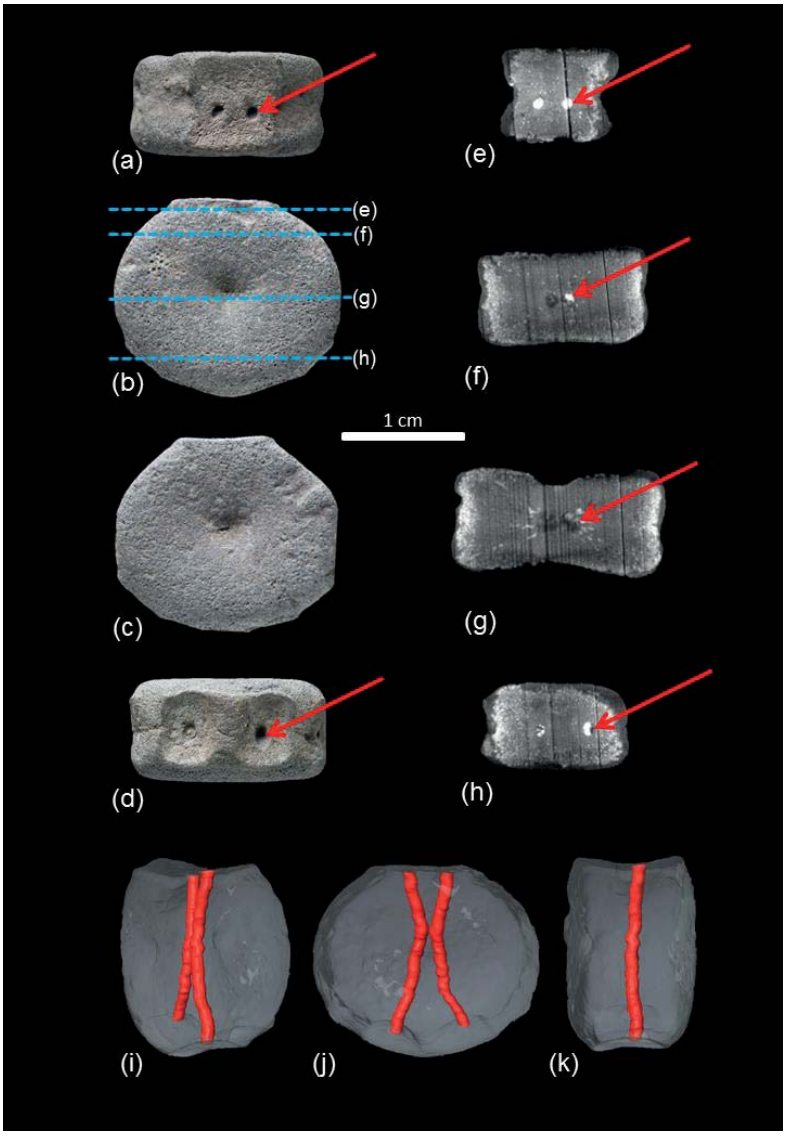

Figure 2. Fetal vertebral centrum of a plesiosaur (LWL-MFN P 64372) from the Rhaetian (latest Triassic) bone bed of Bonenburg (Germany). **(a)** Dorsal view with paired intersegmental artery foramina on the floor of the neural canal (red arrow). **(b)** Posterior view of the fetal vertebral centrum with the locations of the µCt virtual sections **(e)** to **(h)** indicated. **(c)** Anterior view of the centrum. **(d)** View of the ventral surface of the centrum with paired intersegmental artery foramina (red arrow). Note that the foramina are set in a sunken area. **(e–h)** µCt virtual sections through the centrum. The sections also show the orientation of the vascular spaces in the bone, which are arranged radially from the center of ossification. The high-density (white) infillings of these vascular spaces and the intersegmental artery canals are pyrite. The darker fillings are either air or sediment. The red arrows mark the trace of the right canal. **(e)** Section near the dorsal surface of the vertebral centrum. The paired intersegmental artery foramina as the entrance to the intersegmental artery canals are clearly visible. **(f)** This section is ventral to **(e)**; the intersegmental artery canal comes closer together. **(g)** Section through the center of ossification in the middle of the centrum. The canals are close to each other but are still separated. **(h)** Section through the ventral region of the centrum, where the canals are widely separated. **(i–k)** Reconstructed paired intersegmental artery canals connecting the paired dorsal and ventral intersegmental artery foramina, with the fetal centrum rendered semitransparent. Reconstruction was performed with Avizo 7.1.1. **(i)** Oblique anterolateral view. **(j)** Anterior view. The reconstruction shows clearly that the intersegmental artery canals approach each other one third along their course from dorsal to ventral, close to the center of ossification of the centrum. The connection between the canals is limited, but it gives the canals a characteristic X shape. Note the sunken areas of the ventral surface of the centrum. **(k)** Lateral view, showing that the canals are located in the anteroposterior plane of symmetry of the centrum, which is equivalent to the original sclerotome border in the embryo.

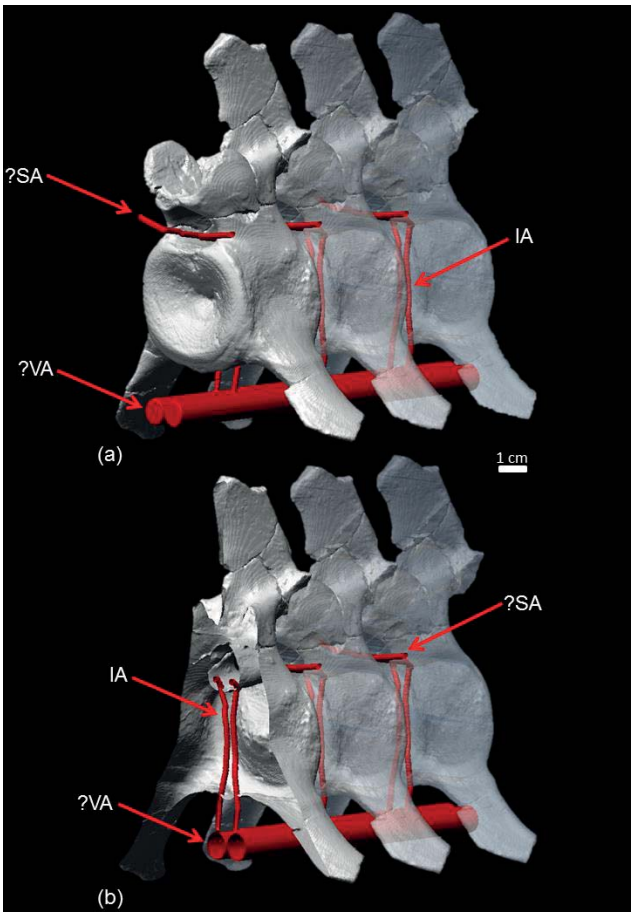

Figure 3. (a) Reconstruction of the arterial system in the plesiosaur neck based on µCT scans, segmentation of the intersegmental artery canals, and modeling of hypothetical vessels in Polyworks. The virtual vertebrae with the intersegmental artery canals are the same cervical (no. 23) of *Cryptoclidus* IPB R 324 repeated three times. Anterior is to the left. **(b)** Cutaway view of the anteriormost cervical vertebra of this row with the intersegmental arteries crossing the centrum in dorsoventral direction. Abbreviations: IA – intersegmental artery passing through the vertebral centrum; VA – hypothetical vertebral artery from which the intersegmental arteries branched off; SA – hypothetical spinal artery receiving blood from intersegmental arteries.

Our analysis was based on the phylogenetic character matrix of Benson and Druckenmiller (2014), with updates for this study. The matrix consists of 80 taxa from the Late Triassic to the Late Cretaceous and of 270 characters: the character description and character state description as well as the coding. Eight characters (141, 152, 156, 166, 177, 179, 187, 191) of the 270 characters deal with special aspects of vertebral morphology such as nutrient foramina, subcentral foramina, and the number of cervical vertebrae that have implications for the reconstruction of the plesiosaurian neck arterial system.

3 Results

3.1 External morphology

Based on the analysis of the phylogenetic character list, the cervical vertebrae of all plesiosaurian terminal taxa in the matrix have large, paired symmetrical foramina on the ventral side of the cervical vertebral centra, conforming to the definition of vIAF. In the dorsal vertebrae there is no evidence of subcentral or nutrient foramina. The absence/presence and possible morphology of ventral foramina is unknown in the transitional pectoral vertebrae, which we consider as part of the trunk because of a lack of sufficiently informative material and a lack of published descriptive information.

Both the ventral and the dorsal IAFs are part of character 156 of Benson and Druckenmiller (2014): "Cervical vertebrae, subcentral foramina and foramina on the dorsal surface of the centrum, within the neural canal". This has three states: "both absent (0); both present (1); dorsal foramina present, but subcentral foramina very small or absent (2)". Character 166 is also relevant for this study in that it captures the presence of a midline keel or rounded ventral ridge on the centrum. Beyond this, the shape of the ventral keel and the size of the pits and foramina differ depending on taxon. We observed that in all cervical vertebrae (with the exception of the atlas–axis complex) from the Rhaetic bone beds of Bonenburg and France and in some of the Early Jurassic plesiosaur cervicals (e.g., Benson et al., 2012), there are paired deep ventral pits. At the bottom of the pits are the vIAFs. The cervical vertebrae of the Triassic articulated skeleton (see Wintrich et al., 2017) and the vertebrae of the indeterminate Jurassic plesiosaur SMNS 50845 and of *Cryptoclidus* IPB 324 have a more even ventral surface without the large keel and deep pits.

All plesiosaur cervical vertebrae in this study show the dIAF on the floor of the neural canal if this is exposed and not covered by sediment. The dIAFs are not coded as separate characters in the Benson and Druckenmiller (2014) matrix but only as part of character 156, as discussed above. dIAFs have rarely been mentioned in morphological descriptions of plesiosaurian cervical centra, as already noted. We observed that the dorsal IAFs are present in all vertebrae personally examined for this study where the neural canal was exposed. State 2 of character 156, "dorsal foramina present, but subcentral foramina very small or absent", is particularly interesting because it correlates with state 0 of character 152, "number of cervical vertebrae", which is "< 15" cervical vertebrae (Benson and Druckenmiller, 2014, appendix S2). This state is seen in the most short-necked pliosaurs *Brachauchenius* and *Stenorhynchosaurus*. This very low number of cervicals is highly derived in plesiosaurians and is less than seen in any stem pistosauroid.

3.2 Internal structure as revealed by µCt data, histology, and fracture surfaces

Both histological sections and segmentation of µCt data reveal that the left and the right vIAFs and the left and the right dIAF are each connected by a canal that passes through the center of ossification of the centrum. This is also seen in fracture surfaces of centra. In the µCt images, the canal is visible well and can be traced easily. It is also clear that these two canals do not end in the center of ossification, as a nutrient canal would do, but pass through it. The general appearance of the two canals in transverse sections is X-shaped because the canals gradually diverge from each other towards both the ventral and dorsal intersegmental foramina. The left and the right canals appear to be connected in the central region in the thin section of SMNS 50845, and it appears that the canals merge in a medullary cavity which resorbed the original center of ossification (Fig. 1). However, in the 3-D reconstructions of the fetal vertebra (WMNM P 64372) (Fig. 2) and the adult vertebra (STIPB R 324) (Fig. 3), the canals do not appear to meet in the center of ossification, only approaching each other closely. These conflicting observations may be explained by the loss of trabeculae in the ossification center during the preparation of the thin section of SMNS 50845 (Fig. 1), resulting in an apparent connection between the canals.

4 Discussion

4.1 Interpretation of the paired canals

Plesiosaur vertebral foramina have been observed and described from so many taxa and have been used as characters in phylogenetic analyses that it is clear that they are a pervasive feature of plesiosaur cervicals (Storrs, 1991; O'Keefe, 2001; Benson and Druckenmiller, 2014; Wintrich et al., 2017), with the possible exception of the pliosaur-type forms (see above). Thus, we feel that our results are representative of all plesiosaur cervicals although we only investigated three specimens in detail. The course of the paired canals through the vertebral centrum would suggest that these structures originally housed continuous arteries traversing the vertebral centrum in ventrodorsal direction, which opens up the possibility that they contained persisting intersegmental arteries, not nutrient ones, which would have ended within the central region of the vertebra. Furthermore, the crossing of the vertebral centrum is a feature which we argue should originate at an early developmental stage. This is because in the case of nutritive canals, the vascular system does spread into bone tissue (as mentioned above), whereas in continuous blood vessels, the bone tissue grows around the vessels instead. It is also known that bone tissue cannot resorb or displace features of the vascular system such as arteries because osteoclasts only resorb mineralized surfaces (Hall, 2015, chap. 15). This suggests that the arteries were already present in the vertebral primordium at the stage in early development when the sclerotomes were re-segmented and, subsequently, the cartilage primordia of the centra of the vertebra were formed. As the primordium of the centrum grew and ossified, the arteries and with them the canals also enlarged in size. The divergence of the canals is explained by the retention of the homologous locations inside the centrum and on its surface as ventral and dorsal intersegmental foramina.

While posterior caudal and fluke vertebrae of extant whales have similar canals piercing the vertebral centra and housing arteries (Slijper, 1939), their morphology and origin is rather different, as described in detail by Slijper (1939) and confirmed by a study of the tail segment of a complete adult skeleton of the bottlenose dolphin *Tursiops truncatus* (LACM 97723; Slijper, 1939). First of all, the paired canals do not pass through the center of ossification of the centra but in an arch around it. This indicates that the vessels were incorporated into vertebrae only in the juvenile, not in the embryo. Second, it can be observed that the canals form by the gradual (from anterior to posterior, not ontogenetically) incorporation of an artery lateral to the centrum. The artery more anteriorly only pierces the transverse process and then more posteriorly becomes incorporated deeply into the centrum. The canals in the whale caudal vertebrae are thus not homologous to those in the plesiosaurian cervical vertebrae. A possible exception to the non-homology of the canals in plesiosaurs and whales may be the vertebra depicted by Houssaye et al. (2015, fig. 14) in which canals are seen passing dorsoventrally through the center of ossification. However, these canals do not show the strong symmetry that is so typical of plesiosaurs. The lack of symmetry in the canals in *Basilosaurus* suggest that they do not represent persisting intersegmental arteries but originated later in ontogeny.

4.2 Developmental retention of the intersegmental arteries in plesiosaurs

An understanding of the arteries crossing the primordium requires some considerations of the embryonic development of the vascular system of the head, neck, and body stem. In terms of the evolutionary patterns in the framework of heterochrony, the retention of intersegmental arteries in plesiosaurians would have to be considered a case of extreme paedomorphosis (Alberch et al., 1979; McNamara, 1997). Also, regionalization of the body is an important aspect to consider because the molecular boundary between the neck and the trunk is distinct (Müller et al., 2010) and highly conserved: the cervical column in the mouse, crocodile, and chicken shows expression of *Hox4* and *Hox5* but lacks expression of *Hox6* genes (Böhmer et al., 2015), and this pattern is also observed in legless tetrapods such as snakes and Gymnophiona (Woltering et al., 2009).

In the embryo, a paired primary dorsal aorta differentiates by vasculogenesis and is located underneath the paraxial mesoderm. The primary dorsal aortae gradually change position from lateral to medial. Eventually, both dorsal aortae fuse in the midline of the embryo ventral to the notochord, which leads to the formation of a single large median aorta (Wiegreffe et al., 2007; Garriock et al., 2010). Initially, the intersegmental arteries branch off in dorsal direction from the paired dorsal aortae, passing in between the sclerotomes before re-segmentation. Their subsequent development is not well studied. In the trunk at thoracic levels, they relocate laterally to form the intercostal arteries. In the neck, they seem to obliterate in their proximal part during re-segmentation, whereas their distal part outside the vertebral centra fuses with neighboring segments to form the vertebral artery (Arey, 1924, p. 212).

Importantly, we found evidence for intersegmental artery retention only in the cervical vertebral centra, not in the dorsal vertebral centra. Thus, if plesiosaurians retained intersegmental arteries, then the question arises as to which vessels these intersegmental arteries were connected to. As mentioned above, in principle the intersegmental arteries in extant embryos arise from the paired aortae. In the neck, however, they form longitudinal anastomoses which give rise to the aorta vertebralis, while the connections to the dorsal aorta become obliterated. In snakes like *Elaphe obsoleta*, the Arteria vertebralis, in turn, emits segmental branches which reach the spinal canal where they anastomose longitudinally to give rise to the A. spinalis and associated vessels (Zippel et al., 1998). As in plesiosaurs the intersegmental vessels lead to the spinal canal. Thus, we postulate that in analogy to the anatomy of snakes, the intersegmental vessels join the longitudinal spinal artery in the spinal canal. As to their origin, we speculate that they branch off a longitudinal vertebral artery which has arisen from the paired dorsal aortae of earlier embryonic stages (Fig. 3). As no fossil correlates are preserved, this scenario remains forcibly speculative, but the vascular anatomy as postulated here would likely not be problematic in an adult plesiosaurian from a functional point of view. The extreme evolutionary neck elongation by an increase in segment number (not segment elongation) in the plesiosaur line (including pistosaurids) may have required or have been facilitated by a developmental retention of strong bilateral arteries derived from the paired aortae and with it the intersegmental arteries arising from them.

We shall now evaluate the hypotheses explaining why plesiosaurians did not resorb the intersegmental arteries, retaining the embryonic vascular system. The first hypothesis involves developmental constraints linked to the uniquely high number of cervicals in plesiosaurs (the low number of pliosaur-type plesiosaurs being secondarily derived). This, like any other hypothesis explaining the persistence of intersegmental arteries, has to be consistent with the lack of IAF in the dorsal and presumably pectoral vertebrae, the numbers of which are not unusually high in plesiosaurians compared to other amniotes (Müller et al., 2010; Coffin and Poole, 1988).

The uniquely high number of cervical vertebrae means that in the plesiosaurian embryo there was also a uniquely high number of cervical somites and sclerotomes. As noted above, no other vertebrate group evolved such an enormously long neck via an increase in the number of segments, i.e., vertebrae (Müller et al., 2010). A model for understanding the development of the very high number of cervical segments in plesiosaurians might be the segmentation process in snakes, that have evolved very high numbers of dorsal segments. There, it has been shown that the molecular mechanisms of somitogenesis are principally the same as in vertebrates with lower segment numbers, but that somitogenesis proceeds much faster leading to initially smaller somites which, however, later on grow to a normal size relative to the size of the snake species concerned (Gomez et al., 2008). In snakes, the extremely high number of dorsal vertebrae ("precloacal" in morphological terminology) correlates with a corresponding extension the expression of thorax-specific *Hox* genes, like *Hox6*, along the body axis (Cohn and Tickle, 1999). It is therefore likely that in long-necked plesiosaurian embryos, cervical *Hox* gene expression was maintained over many segmentation rounds, which probably occurred relatively rapidly when compared to short-necked species (both ancestral to plesiosaurians and derived within plesiosaurians, i.e., in the pliosaur type). A potential link between frequency and speed of somitogenesis on the one hand and the formation of intersegmental vessels on the other hand is yet unknown.

Furthermore, we do not know if plesiosaurians developed paired vertebral arteries arising from the aorta in addition to retaining the intersegmental arteries. These vertebral arteries would have extended along (?) the vertebral centrum, with nutrient arteries branching off and vascularizing the vertebral body through lateral nutrient foramina as seen in mammals (Rothman and Simeone, 1975). Such lateral nutrient foramina are common in marine mammals but differ from the vIAF of plesiosaurians in their smaller size, larger number, and asymmetrical irregular placement.

In the tuatara, *Sphenodon punctatus*, there are also paired foramina in the caudal centra, and classical embryological research (Schauinsland, 1906, fig. 323) clearly shows a paired artery extending dorsoventrally across the cartilage primordium of the caudal centrum in dolphins (Schauinsland, 1906).

4.3 Functional interpretation and adaptive value of intersegmental arteries

The probable persistence of intersegmental arteries and the possible presence of vertebral arteries in the plesiosaurian neck raise the question of the function and adaptive value of these features. Several advantages can be hypothesized, beginning with what is known in the few extant amniotes that

seemingly retain intervertebral arteries. In the tree-climbing rat snake *Elaphe obsoleta*, intersegmental arteries are retained in the neck region. This is interpreted as an adaptation for maintaining cerebral blood flow in spite of gravitational stress, e.g., during climbing (Zippel et al., 1998). This observation offers an exciting parallel to the situation in plesiosaurians, where high hydrostatic pressure during deep diving (> 200 m) might have required segmental transvertebral arterial anastomoses to provide sufficient cerebral blood supply. If intravertebral intersegmental arteries were developed as additional arteries in plesiosaurians, there would be a higher oxygen transport capacity than in a single pair of intersegmental arteries per vertebra. This capacity would enable faster transport of oxygen for storage into muscles during deep diving. A similar hypothesis was presented by Rothschild and Storrs (2003), suggesting that the increased blood flow to the interior of the centra protected them from avascular necrosis. However, this hypothesis is not consistent with the persistence of intersegmental arteries because they would not have supplied the interior of the centrum with extra blood.

Other functional hypotheses explaining the retention of intersegmental arteries related to deep diving involve the protection from compression of the blood vessels by their location in canals in the vertebrae. If there were anastomoses with the vertebral arteries, an increase in the number of segments would mean more anastomoses and again greater transport capacity. Other, as yet less easily hypothesized advantages might be related to the compression of the upper respiratory and digestive tracts. Hypotheses involving a long neck and high cervical vertebral numbers invite future tests based on the comparison with the cervical vertebral column of short-necked plesiosaurian (i.e., pliosaur-type) that evolved several times in the history of plesiosaurians, together with the seeming loss of ventral IAF (see phylogenetic data matrix in Benson and Druckenmiller, 2014).

4.4 Persistent intersegmental arteries: increasing adaptation to a pelagic lifestyle?

As discussed above, IAFs are a unique character of plesiosaurians. However, it is not only plesiosaurs that have paired foramina on the ventral side of their cervical vertebrae. The non-plesiosaurian pistosauroids *Pistosaurus longaevus* and *Augustasaurus hagdorni* also show paired foramina (Sues, 1987; Rieppel et al., 2002), whereas *Yunguisaurus liae* (Sato et al., 2014) and *Bobosaurus forojuliensis* (Dalla Vecchia, 2006) do not share the character. The reason for this could be the degree of adaptation to the pelagic habitat and colder waters in the pistosauroid lineage (Krahl et al., 2013). *Augustasaurus* is the first and only unequivocal non-plesiosaurian pistosauroid which is found outside the Tethys realm on the western coast of North America (Sander et al., 1997). Possible other non-plesiosaurian pistosauroids outside the Tethys are *Corosaurus* from Wyoming (Storrs, 1991) and *Alexeyisaurus* from Arctic Russia (Sennikov and Arkhangelsky, 2010), but the systematic position of the former is unstable, and the latter is too poorly preserved for a reliable systematic assignment.

Since available evidence suggests that sauropterygians originated in the Tethys (Neenan et al., 2013) and all other Triassic pistosauroids are known from this realm (Benson et al., 2012), the ancestors of *Augustasaurus* must have emigrated from the warm equatorial waters of the Tethys and either dispersed around the polar northern or southern coast of Pangaea or across Panthalassa. Either way, an elevated metabolic rate and endothermy appear to be prerequisites for this dispersal (Krahl et al., 2013). The persistence of intersegmental arteries in the neck could have been incipiently present in *Augustasaurus* and would have been useful for improved thermoregulation in the colder pelagic waters of Panthalassa. If pistosauroids dispersed across Panthalassa to reach western North America, several other adaptations would be necessary. These include, for example, cruising adaptations in aquatic locomotion by underwater flight. Also, the ability of deep diving (see above) is an adaptation to the pelagic habitat because prey there is sparser and more evenly distributed across the water column (and not at the sea bottom) than in coastal habitats. Plesiosaurians show all these features of adaptation to a pelagic habitat and not surprisingly are globally distributed at least by the Middle Jurassic (Bardet et al., 2014).

5 Conclusions

Plesiosaurians cervical vertebrae bear a peculiar set of bilaterally paired foramina on their ventral side, matched by paired foramina on the floor of the neural canal. CT scanning, thin sectioning, and the observation of fracture surfaces reveals that the foramina on each side are connected by a canal that passes through the center of ossification of the vertebral centrum. The foramina and canals thus did not house nutritive blood vessels supplying the center of the bone but must have contained blood vessels that entered ventrally and exited dorsally. The location of the canals in the anteroposterior middle of the centra, their high bilateral symmetry, and their course through the center of ossification suggests that the blood vessels contained in the canals represent an embryonic vascular feature, the intersegmental arteries that persisted into the adult. The plesiosaurian intersegmental arteries became incorporated into the primordium of the vertebral centrum during re-segmentation in the embryonic axial skeleton and thus were not resorbed, unlike in almost all other amniotes. The persistence of the intersegmental arteries is correlated to, and presumably linked with, the uniquely high number of cervical vertebrae, stiffening of the neck, and increased pelagic adaptation in plesiosaurs compared to non-plesiosaurian sauropterygians. Possible adaptive advantages

of the persistent intersegmental arteries must be sought in deep diving and in thermoregulation in the neck.

Data availability. All data needed to evaluate the conclusions in the paper are present in the paper. Additional data related to this paper may be requested from the authors.

The specimens and thin sections on which this study is based are reposited in the following institutions, here listed with their abbreviations: LWL-MFN – LWL- Museum für Naturkunde, Muünster, Germany; SMNS – Staatliches Museum für Naturkunde, Stuttgart, Germany; STIPB – Steinmann Institute Paleontology Collection, University of Bonn, Bonn, Germany.

Competing interests. The authors declare that they have no conflict of interest.

Special issue statement. This article is part of the special issue "Secondary adaptation of tetrapods to life in water – Proceedings of the 8th International Meeting, Berlin 2017". It is a result of the 8th International Meeting on the Secondary Adaptation of Tetrapods to Life in Water, Berlin, Germany, 3–8 April 2017.

Acknowledgements. First and foremost we thank Michael Mertens of Schwaney (North Rhine-Westphalia, Germany) for his untiring efforts in collecting marine reptiles from the Rhaetian bone beds of Bonenburg and facilitating their transfer to the LWL-MFN collections. We thank Olaf Dülfer (Bonn) for help with specimen preparation, Georg Oleschinski (Bonn) for photography, and Rico Schellhorn (Bonn) for help with illustrations and discussion. Reviews by Alexandra Houssaye and two anonymous reviewers are gratefully acknowledged. This project was funded by the Deutsche Forschungsgemeinschaft (DFG, grant number SA 469/47-1) and by the LWL-Museum für Naturkunde (Münster, Germany) through the archeological and paleontological heritage mitigation scheme of the State of North Rhine-Westphalia.

Edited by: Florian Witzmann
Reviewed by: Alexandra Houssaye and two anonymous referees

References

Alberch, P., Gould, S. J., Oster, G. F., and Wake, D. B.: Size and shape in ontogeny and phylogeny, Paleobiology, 5, 296–317, 1979.

Andrews, C. W.: A descriptive catalogue of the marine reptiles of the Oxford Clay, The British Museum (Natural History) London, London, 202 pp., 1910.

Arey, L. B.: Developmental Anatomy. W. B. Saunders Company, Philadelphia and London, 1924.

Bardet, N., Falconnet, J., Fischer, V., Houssaye, A., Jouve, S., Pereda Suberbiola, X., Pérez-García, A., Rage, J.-C., and Vincent, P.: Mesozoic marine reptile palaeobiogeography in response to drifting plates, Gondwana Research, 26, 869–887, https://doi.org/10.1016/j.gr.2014.05.005, 2014.

Bénazéraf, B. and Pourquié, O.: Formation and segmentation of the vertebrate body axis, Annu. Rev. Cell Dev. Bi., 29, 1–26, 2013.

Benson, R., Evans, M., and Druckenmiller, P.: High diversity, low disparity and small body size in plesiosaurs (Reptilia, Sauropterygia) from the Triassic – Jurassic boundary, PLoS ONE, 7, e31838, https://doi.org/10.1371/journal.pone.0031838, 2012.

Benson, R. B. J. and Druckenmiller, P. S.: Faunal turnover of marine tetrapods during the Jurassic–Cretaceous transition, Biol. Rev., 89, 1–23, https://doi.org/10.1111/brv.12038, 2014.

Böhmer, C., Rauhut, O., and Wörheide, G.: Correlation between Hox code and vertebral morphology in archosaurs, Proc. Roy. Soc. B, 282, 20150077, https://doi.org/10.1186/s40851-017-0069-4, 2015.

Brent, A. E., Schweitzer, R., and Tabin, C. J.: A somitic compartment of tendon progenitors, Cell, 113, 235–248, 2003.

Christ, B., Huang, R., and Scaal, M.: Amniote somite derivatives, Dev. Dynam., 236, 2382–2396, 2007.

Coffin, J. D. and Poole, T. J.: Embryonic vascular development: immunohistochemical identification of the origin and subsequent morphogenesis of the major vessel primordia in quail embryos, Development, 102, 735–748, 1988.

Cohn, M. J. and Tickle, C.: Developmental basis of limblessness and axial patterning in snakes, Nature, 399, 474–479, 1999.

Dalla Vecchia, F. M.: A new sauropterygian reptile with plesiosaurian affinity from the Late Triassic of Italy, Rivista Italiana di Paleontologia e Stratigrafia, 112, 207–225, 2006.

Fischer, V., Cappetta, H., Vincent, P., Garcia, G. r., Goolaerts, S., Martin, J. E., Roggero, D., and Valentin, X.: Ichthyosaurs from the French Rhaetian indicate a severe turnover across the Triassic-Jurassic boundary, Naturwissenschaften, 101, 1027–1040, https://doi.org/10.1007/s00114-014-1242-7, 2014.

Fischer, V., Benson, R. B. J., Zverkov, N. G., Soul, L. C., Arkhangelsky, M. S., Lambert, O., Stenshin, I. M., Uspensky, G. N., and Druckenmiller, P. S.: Plasticity and convergence in the evolution of short-necked plesiosaurs, Current Biology, 27, 1667–1676.e3, https://doi.org/10.1016/j.cub.2017.04.052, 2017.

Francillon-Vieillot, H., de Buffrénil, V., Castanet, J., Geraudie, J., Meunier, F., Sire, J. Y., Zylberberg, L., and de Ricqles, A.: Microstructure and mineralization of vertebrate skeletal tissues, in: Skeletal Biomineralization: Patterns, Processes and Evolutionary Trends, Vol. 1, edited by: Carter, J. G., Van Nostrand Reinhold, New York, 471–530, 1990.

Garriock, R. J., Czeisler, C., Ishii, Y., Navetta, A. M., and Mikawa, T.: An anteroposterior wave of vascular inhibitor downregulation signals aortae fusion along the embryonic midline axis, Development, 137, 3697–3706, 2010.

Gomez, C., Özbudak, E. M., Wunderlich, J., Baumann, D., Lewis, J., and Pourquié, O.: Control of segment number in vertebrate embryos, Nature, 454, 335, 2008.

Hall, B. K.: Bones and Cartilage. 2nd Edition. Developmental and Evolutionary Skeletal Biology, Academic Press, San Diego, 2015.

Houssaye, A., Tafforeau, P., De Muizon, C., and Gingerich, P. D.: Transition of Eocene whales from land to sea: evidence from bone microstructure, PloS ONE, 10, e0118409, https://doi.org/10.1371/journal.pone.0118409, 2015.

Ketchum, H. F. and Benson, R. B.: Global interrelationships of Plesiosauria (Reptilia, Sauropterygia) and the pivotal role of taxon sampling in determining the outcome of phylogenetic analyses, Biol. Rev., 85, 361–392, https://doi.org/10.1111/j.1469-185X.2009.00107.x, 2010.

Krahl, A., Klein, N., and Sander, P. M.: Evolutionary implications of the divergent long bone histologies of *Nothosaurus* and *Pistosaurus* (Sauropterygia, Triassic), BMC Evolutionary Biology, 13, 1–23, 2013.

Lamm, E.-T.: Chapter 4 – Preparation and sectioning of specimens, in: Bone Histology of Fossil Tetrapods. Advancing Methods, Analysis, and Interpretation, edited by: Padian, K. and Lamm, E.-T., University of California Press, Berkeley, 55–160, 2013.

Lara Maldanis, L., Carvalho, M., Almeida, M. R., Freitas, F. I., de Andrade, J. A. F. G., Nunes, R. S., Rochitte, C. E., Poppi, R. J., Freitas, R. O., Rodrigues F., Siljeström S., Lima, F. A., Galante, D., Carvalho, I. S., Perez, C. A., de Carvalho, M. R., Bettini, J., Fernandez, V. and Xavier-Neto, J.: Heart fossilization is possible and informs the evolution of cardiac outflow tract in vertebrates, Elife, 5, e14698, https://doi.org/10.7554/eLife.14698, 2016.

Martin, J. E. and Parris, D. C. (Eds.).: The Geology and Paleontology of the Late Cretaceous Marine Deposits of the Dakotas, Geological Society of America Special Paper 427, 2007.

Massare, J. A.: Swimming capabilities of Mesozoic marine reptiles, Paleobiology, 14, 187–205, 1988.

Massare, J. A. and Callaway, J. M.: *Cymbospondylus* (Ichthyosauria: Shastasauridae) from the Lower Triassic Thaynes Formation of southeastern Idaho, J. Vertebr. Paleontol., 14, 139–141, 1994.

McNamara, K. J.: Shapes of Time. The Evolution of Growth and Development, Johns Hopkins University Press, Baltimore, 342 pp., 1997.

Mittapalli, V. R., Huang, R., Patel, K., Christ, B., and Scaal, M.: Arthrotome: a specific joint forming compartment in the avian somite, Dev. Dynam., 234, 48–53, 2005

Motani, R.: The evolution of marine reptiles, Evolution: Education and Outreach, 2, 224–235, 2009.

Müller, J., Scheyer, T. M., Head, J. J., Barrett, P. M., Werneburg, I., Ericson, P. G. P., Pol, D., and Sánchez-Villagra, M. R.: Homeotic effects, somitogenesis and the evolution of vertebral numbers in recent and fossil amniotes, P. Natl. Acad. Sci. USA, 107, 2118–2123, 2010.

Nakajima, Y., Hirayama, R., and Endo, H.: Turtle humeral microanatomy and its relationship to lifestyle, Biol. J. Linn. Soc., 112, 719–734, 2014.

Neenan, J. M., Klein, N., and Scheyer, T. M.: European origin of placodont marine reptiles and the evolution of crushing dentition in Placodontia, Nature Communications, 4, 1–7, https://doi.org/10.1038/ncomms2633, 2013.

Noè, L. F., Taylor, M. A., and Gómez-Pérez, M.: An integrated approach to understanding the role of the long neck in plesiosaurs, Acta Palaeontologica Polonica, 62, 137–162, 2017.

O'Keefe, F. R.: Preliminary description and phylogenetic position of a new plesiosaur (Reptilia: Sauropterygia) from the Toarcian of Holzmaden, Germany, J. Paleontol., 78, 973–988, 2004.

Rieppel, O., Sander, P. M., and Storrs, G. W.: The skull of the pistosaur *Augustasaurus* from the Middle Triassic of northwestern Nevada, J. Vertebr. Paleontol., 22, 577–592, 2002.

Romer, A. S.: Osteology of the Reptiles, The University of Chicago Press, Chicago, 772 pp., 1956.

Rothman, R. H. and Simeone, F. A: The spine. Vol. 1. WB Saunders, Philadelphia, 1975.

Rothschild, B. M. and Storrs, G. W.: Decompression syndrome in plesiosaurs (Sauropterygia: Reptilia), J. Vertebr. Paleontol., 23, 324–328, 2003.

Sander, P. M., Christian, A., Clauss, M., Fechner, R., Gee, C., Griebeler, E. M., Gunga, H.-C., Hummel, J., Mallison, H., Perry, S., Preuschoft, H., Rauhut, O., Remes, K., Tütken, T., Wings, O., and Witzel, U.: Biology of the sauropod dinosaurs: the evolution of gigantism, Biol. Rev. of the Cambridge Philosophical Society, 86, 117–155, 2011.

Sander, P. M., Rieppel, O. C., and Bucher, H.: A new pistosaurid (Reptilia: Sauropterygia) from the Middle Triassic of Nevada and its implications for the origin of plesiosaurs, J. Vertebr. Paleontol., 17, 526–533, 1997.

Sander, P. M., Wintrich, T., Schwermann, A. H., and Kindlimann, R.: Die paläontologische Grabung in der Rhät-Lias-Tongrube der Fa. Lücking bei Warburg-Bonenburg (Kr. Höxter) im Frühjahr 2015, Geologie und Paläontologie in Westfalen, 88, 11–37, 2016.

Sato, T., Zhao, L.-J., Wu, X.-C., and Li, C.: A new specimen of the Triassic pistosauroid *Yunguisaurus*, with implications for the origin of Plesiosauria (Reptilia, Sauropterygia), Palaeontology, 57, 55–76, 2014.

Scaal, M.: Early development of the vertebral column, Seminars in Cell and Developmental Biology, 49, 83–91, 2016.

Schauinsland, H. H.: Beiträge zur Entwicklungsgeschichte und Anatomie der Wirbeltiere, E. Nägele, Stuttgart, 168 pp., 1903.

Schauinsland, H. H.: Die Entwicklung der Wirbelsäule nebst Rippen und Brustbein, in: Handbuch der vergleichenden und experimentellen Entwicklungslehre der Wirbeltiere, edited by: Hertwig, O., Gustav Fischer Jena, Bd. 3 Teil 2, 339–562, 1906.

Schwarz, D., Frey, E., and Meyer, C. A.: Pneumaticity and soft-tissue reconstructions in the neck of diplodocid and dicraeosaurid sauropods, Acta Palaeontologica Polonica, 52, 167–188, 2007.

Sennikov, A. G. and Arkhangelsky, M. S.: On a typical Jurassic sauropterygian from the Upper Triassic of Wilczek Land (Franz Josef Land, Arctic Russia), Paleontol. J., 44, 567–572, 2010.

Seymour, R. S., Smith, S. L., White, C. R., Henderson, D. M., and Schwarz-Wings, D.: Blood flow to long bones indicates activity metabolism in mammals, reptiles and dinosaurs, Proc. Roy. Soc. B, 279, 451–456, 2012.

Slijper, E. J.: *Pseudorca crassidens* (Owen), ein Beitrag zur vergleichenden Anatomie der Cetaceen, Zoologische Mededeelingen Rijksmuseum van Natuurlijke Historie Leiden, 21, 241–366, 1939.

Storrs, G. W.: Anatomy and relationships of *Corosaurus alcovensis* (Diapsida: Sauropterygia) and the Triassic Alcova Limestone of Wyoming, Bulletin of the Peabody Museum of Natural History, Yale University, 44, 1–151, 1991.

Storrs, G. W.: Fossil vertebrate faunas of the British Rhaetian (latest Triassic), Zool. J. Linn. Soc., 112, 217–259, https://doi.org/10.1111/j.1096-3642.1994.tb00319.x, 1994.

Sues, H.-D.: Postcranial skeleton of *Pistosaurus* and interrelationships of the Sauropterygia (Diapsida), Zool. J. Linn. Soc., 90, 109–131, 1987.

Taylor, M. A.: Plesiosaurs – rigging and ballasting, Nature, 290, 628–629, 1981.

Taylor, M. P. and Wedel, M. J.: Why sauropods had long necks; and why giraffes have short necks, PeerJ, 1:e36, https://doi.org/10.7717/peerj.36, 2013.

Wedel, M. J.: Evidence for bird-like air sacs in saurischian dinosaurs, J. Exp. Zool. A, 311, 1–18, 2009.

Wiegreffe, C., Christ, B., Huang, R., and Scaal, M.: Sclerotomal origin of smooth muscle cells in the wall of the avian dorsal aorta, Dev. Dynam., 236, 2578–2585, 2007.

Wintrich, T., Hayashi, S., Houssaye, A., Nakajima, Y., and Sander, P. M.: A Triassic plesiosaurian skeleton and bone histology inform on evolution of a unique body plan, Sci. Adv., 3, e1701144, https://doi.org/10.1126/sciadv.1701144, 2017.

Woltering, J. M., Vonk, F. J., Müller, H., Bardine, N., Tuduce, I. L., de Bakker, M. A., Knöchel, W., Sirbu, O., Durston, A. J., and Richardson, M. K.: Axial patterning in snakes and caecilians: evidence for an alternative interpretation of the Hox code, Dev. Biol., 332, 82–89, 2009.

Zammit, M., Daniels, C. B., and Kear, B. P.: Elasmosaur (Reptilia: Sauropterygia) neck flexibility: Implications for feeding strategies, Comp. Biochem. Physiol., Part A, 150, 124–130, 2008.

Zippel, K. C., Lillywhite, H. B., and Mladinich, C. R. J.: Contribution of the vertebral artery to cerebral circulation in the rat snake *Elaphe obsoleta*, J. Morphol., 238, 39–51, 1998.

Chapter 4

In revision (File as submitted to PeerJ is included here):

Wintrich, T., Jonas, R., Wilke, H.-J., Sander, P. M. (in revision, PeerJ). Neck mobility in the Jurassic plesiosaur *Cryptoclidus eurymerus* – a new approach to understanding the axial skeleton in fossil vertebrates using finite element analysis.

Author contributions:

Tanja Wintrich designed the research, carried out the research and wrote the paper.

Tanja Wintrich, René Jonas, Hans-Joachim Wilke and P. Martin Sander provide datasets to the study and contributed to the manuscript preparation, wrote the paper, reviewed drafts of the paper. René Jonas provided the final element analysis; Tanja Wintrich did the interpretation of the results.

Neck mobility in the Jurassic plesiosaur *Cryptoclidus eurymerus* – a new approach to understanding the axial skeleton in fossil vertebrates using finite element analysis

TANJA WINTRICH[1*], RENÉ JONAS[2], HANS-JOACHIM WILKE[2] AND P. MARTIN SANDER[1,3]

[1]Steinmann-Institut für Geologie, Mineralogie und Paläontologie, Rheinische Friedrich-Wilhelms-Universität Bonn, Bonn, Germany

[2]Institut für Unfallchirurgische Forschung und Biomechanik, Universität Ulm, Ulm, Germany.

[3]Dinosaur Institute, Natural History Museum of Los Angeles County, Los Angeles, USA

Abstract

The sauropterygian clade Plesiosauria arose in the Late Triassic and survived to the very end of the Cretaceous. Plesiosauria evolved the greatest species diversity of any marine reptile clade, attaining a global distribution. Plesiosauria consist of two clades, Rhomaleosauridae and Neoplesiosauria. Basal Neoplesiosauria have very long necks with at least 30 cervicals, but show qualitative osteological evidence for a stiff neck. Here we quantify neck mobility in lateral, ventral, and dorsal direction based on finite element modeling of neck vertebrae of the Middle Jurassic plesiosaur *Cryptoclidus eurymerus*. We model the mobility in a single motion segment, consisting of two adjacent vertebrae and the joints connecting them. Based on the model with a maximum intervertebral spacing of 3 mm, we find that in *Cryptoclidus*, the maximum angle of lateral deflection in the motion segment was 2º. The maximum angle of ventral deflection was 5º and of dorsal deflection was 5º. When these values are multiplied by the number of cervical vertebrae, it becomes apparent that neck mobility was rather limited in all directions. The maximum angle of total lateral deflection in the neck was 67º. The maximum angle of total ventral deflection was 148º and of total dorsal deflection was 157º. This raises the question of the function of such a long but immobile neck. We posit that the long neck served in visual and hydrodynamic camouflage, hiding the bulk of the body from the small but abundant prey, such schooling fish and squid. Neck immobility may have been advantageous in withstanding the strong hydrodynamic forces acting on the neck during predatory strikes.

1. Introduction

Plesiosaurians are secondarily aquatic reptiles known from the Late Triassic through the Late Cretaceous (Storrs, 1993; Wintrich et al., 2017), which show a body design adapted extremely well to the aquatic environment. The clade Plesiosauria can be split into two subclades, the Rhomaleosauridae and the Neoplesiosauria, whereas the Neoplesiosauria can be split further into two the Plesiosauroidea and the Pliosauridae (Benson, Evans & Druckenmiller, 2012; Benson & Druckenmiller, 2014). In general, there are three different body plans in plesiosaurs. First, there are forms with an extremely small head and a long neck, second, with a massive and large head on a short neck. The third body plan, mainly seen in the Rhomaleosauridae, is a larger head and shorter neck than the small-headed and long-necked plesiosaurs, but a smaller head and a longer neck a massive, than in the large-headed and short-necked plesiosaurs.

In the evolution of plesiosaurs, there is a remarkable change in the count of the cervical vertebrae (e.g., data compiled by Müller et al., 2010; Benson, Evans & Druckenmiller, 2012; Benson & Druckenmiller, 2014). More basal Plesiosauria, like *Rhaeticosaurus mertensi*, *Thalassiodracon hawkinsi*, *Eoplesiosaurus antiquior,* and *Avalonectes arturi* (Benson, Evans & Druckenmiller, 2012; Wintrich et al., 2017) have a relatively short neck with not more than 36 cervical vertebrae, whereas derived Plesiosauroidea of the subclade Elasmosauridae are famous for increasing the count of cervical vertebrae to over 70, like in *Aphrosaurus furlongi* that has up to 73 vertebrae (Zammit, Daniels & Kear, 2008). These are by far the highest number of cervical vertebrae of any vertebrate (Müller et al., 2010; Wintrich et al., 2017). However, the function of such a long neck is sparsely discussed. In the literature, there are some speculations. One thought is that the plesiosaur neck is immobile and was used for ambush hunting (Taylor, 1981; Massare, 1988; Massare, 1994). Furthermore, and contrary to Taylor (1981) and Massare (1988, 1994), several authors (Taylor, 1987; McHenry, Cook & Wroe, 2005; Noé, Taylor & Gòmez-Pèrez, 2017) suggested a grazing-style feeding pattern on the sea bottom in Plesiosauria, especially in Elasmosauridae, requiring a mobile neck. Besides these speculations, Taylor (1981) and Storrs (1993) proposed an upward S-shape curving neck posture for hunting prey from above the water surface while the plesiosaur's body was submerged. This was taken further by Wilkinson & Ruxton (2011) who suggested that plesiosaurs had a hunting style similar to long-necked birds such as cormorants, relying on fast acceleration of the head on a highly mobile neck.

The question of the mobility of the neck is extensively discussed from a biomechanical perspective in the literature on mammals and dinosaurs, including birds (e.g. Putz, 1992; Boszczyk, Boszczyk & Putz, 2001; Buchholtz & Schur, 2004; Dzemski & Christian, 2007; Zammit, Daniels & Kear, 2008; Christian & Dzemski, 2011; Wilkinson & Ruxton, 2011; Cobley, Rayfield & Barrett, 2013; Stevens, 2013; Taylor & Wedel, 2013; Krings et al., 2014; Viglino et al., 2014; Molnar, Pierce & Hutchinson, 2016) but in a very limited way for plesiosaurs.

Vertebral centrum shape, neural arch morphology, especially of the zygapophyses, the space between two centra, the muscles, ligaments, and cartilages all impose limitations on the mobility of the vertebral column (Buchholtz & Schur, 2004; Niemeyer, Wilke & Schmidt, 2012; Stevens, 2013). Functional anatomy allows testing of hypotheses of neck mobility and limitations of neck range of motion (ROM) in plesiosaurs based on the cervical vertebral column and the morphology of the individual cervical vertebrae. Although a previous detailed study (Zammit, Daniels & Kear, 2008) had noted the limited mobility of the plesiosaur neck based on functional morphology, this was done only in a two-dimensional way in an analog model. In a more traditional approach, Noé et al. (2017) reviewed the osteology of the neck of long-necked plesiosaurians and concluded that the neck was most mobile in ventral direction. This view is consistent with a recent case study focussing on the leptoclidid plesiosaur *Nichollssaura* which reconstructed a rather mobile and flexible neck consisting of only 24 vertebrae based on the digital manipulation of 3D surface models of individual cervical vertebrae (Nagesan, Henderson & Anderson, 2018).

The current work expands on these studies by employing an approach from computational biomechanics, sourced from the field of human biomechanics (Yoganandan et al., 1996; Niemeyer, Wilke & Schmidt, 2012). Specifically, we use three-dimensional finite-element models developed for investigations of human spine function that include soft part anatomy to model intersegmental mobility. This approach goes beyond osteological arguments (Noè, Taylor & Gomèz-Perèz, 2017), the manipulation of analog models (Zammit, Daniels & Kear, 2008), and of digital osteological models (Nagesan, Henderson & Anderson, 2018) of the kind first successfully employed in the study of dinosaur neck biomechanics (e.g., Stevens, 2013). Our model organism is the cryptoclidid plesiosaur *Cryptoclidus eurymerus* from the Middle Jurassic of England (Andrews, 1910) which is the very well represented in museum collections.

For a better understanding of the morphological, mechanical, and biological characters to be discussed in our paper, we first review the most important definitions in functional morphology of the vertebral column in general and the neck in particular. We then discuss previous thoughts and our assumptions about the nature of the connection between the vertebral centra, specifically the type of joint. We conclude that in plesiosaurs, the centra were closely spaced at only a few mm apart and connected by an intervertebral disc (IVD) which we then implement in our finite element models.

The aim of our study is to estimate the ROM in the cervical vertebral column of an extinct marine reptile, the plesiosaur *Cryptoclidus eurymerus*, using finite element modeling. Comparison of the material settings is used here to evaluate the ROM and therefore discuss the stiffness and functional implications of the cervical vertebral column which gives insights into the paleobiology of plesiosaurs.

2. Terminology and anatomy

2.1 Degrees of freedom

In a three-dimensional space, six degrees of freedom are possible, three involving rotation and three involving translation. However, translation can be neglected in the function of the vertebral column along its axis. Therefore, only three degrees of freedom affect the vertebral column. These are X_r, Y_r, and Z_r for a centrum with intervertebral discs. Whereas X_r describes dorsoventral movement around a mediolaterally oriented axis, Y_r describes the rotation or twist of a segment around a longitudinal axis, and Z_r describes the lateral movement of a segment by rotation around a vertical axis. Regarding these degrees of freedom, actual movement is limited by different osteological structures. X_r is affected by the centrum morphology, the distance between the centra, the zygapophyses, the neural spine, and the ribs. Y_r is affected only by the zygapophyses, and Z_r is affected by the distance between the centra, the zygapophyses, and the ribs.

2.2 The motion segment

Two adjacent vertebrae that are connected by muscles and ligaments, and their articulations, are called the “motion segment” or “Junghans functional unit”. We here use the term motion segment. The motion segment is the smallest definable biomechanical unit in the vertebral column. Here, we first determine the angle of maximum mobility of the motion segment for *Cryptoclidus* and then derive the mobility in the entire neck.

2.3 Joints in the amniote vertebral column

In order to determine the true mobility of the plesiosaur neck, we need to discuss anatomical features in the vertebral column. In particular, the question of how two vertebrae are connected must be considered because the joints between vertebrae have an important influence on function and therefore on mobility (Currey, 2002).

The tetrapod joint is a mobile connection between two or more bony or cartilaginous skeletal elements. Usually, joints can be divided into three main groups, diarthroses, amphiarthroses, and synarthorses. Diarthroses are ´real joints´ and are also called synovial joints. They are a freely movable system. In the vertebrae, for example, the zygapophyses are a synovial plane joint. Amphiarthroses and synarthroses are connections between bones that are made by fibrous connective tissue or cartilage, allowing limited ROMs. Examples of synarthroses are sutures between bones, and examples of amphiarthroses are intervertebral disks (IVD´s). Among extant amniotes, lepidosauromorph reptiles and crocodiles have synovial joints connecting the vertebral centra. In mammals, there is an IVD in this position. The IVD consists of an *annulus fibrosus* and a *nucleus pulposus*. The nucleus pulposus is a round structure consisting of loose fibers suspended in a mucoprotein gel, whereas the annulus fibrosus consists of fibrocartilage. In the basal lepidosaur *Sphenodon*, there is a continous notochord (Wettstein, 1962), whereas birds have unique type of joint with a saddle-shaped surface and no nucleus pulposus.

2.4 Centrum and intervertebral joint morphologies and tissues

Among amniotes, different shapes of the centrum evolved, some of which are convergent (Romer, 1956). The plesiomorphic condition is the *amphicoelous* centrum with deeply concave, funnel-shaped anterior and posterior faces, sometimes connected by a small foramen for the notochord. If the centrum is anteriorly and posteriorly flat, it is called *platycoelous* (synonym *acoelous*), whereas a centrum with an anteriorly concave and posteriorly convex face is called *procoelous*; the other way around it is called *opisthocoelous*. These different centrum shapes influence the mobility and also limitation of movement of the vertebral column. Plesiosaur centra are typically reported to be platycoelous or weakly amphicoelous, as in the cervicals of *Cryptoclidus* (Benson, Evans & Druckenmiller, 2012; Benson & Druckenmiller, 2014).

Furthermore, for understanding vertebral column mobility and neck mobility in amniotes, the distance between the centra and the question of the presence of different cartilage tissues and intervertebral discs are important. Due to the fact that soft tissue is rarely preserved in the fossil record, it is difficult to determine which kind of tissue was located between the amphicoelous or platycoelous centra of extinct amniote clades. Romer (1956) suggested that in the amphicoelous centra of basal amniotes, there must have been modified notochordal material or fibrous tissue between the vertebrae.

2.5 Zygapophysis (also apophyseal joint, facet joint, or dorsal intervertebral joint)

Not only the centra are relevant for the mobility of the vertebral column, but the zygapophyses are also important. Zygapophyses are processes arising from the neural arch, bearing intervertebral articulation facets that restrict vertebral rotation around the long axis. They are also called apophyseal joints, facet joints, and dorsal intervertebral joints. The anteriorly facing zygapophyses are called prezygapophyses, and those facing posteriorly are called postzygapophyses. The prezygapophyses have their articulation facet oriented dorsally, whereas the facets of the postzygapophyses are ventrally oriented. In reptiles (including birds), the zygapophyseal surfaces are flat or only slightly curved. The mediolateral and anteroposterior angles of the zygapophyses differ between taxa and greatly influence the mobility of the vertebral column. Each of the two bony zygapophyses in the facet joint bears an articular surface that is covered by an usually thin layer of hyaline cartilage. There is a thin joint cavity in between the articular surfaces, forming a synovial joint that allows translational movement only. The thickness of the cartilages and the joint cavity affects intervertebral mobility because the distance between the zygapophyses is not negligible.

The articular surface of the zygapophyses shows variation in relative size. If a vertebra has large and expanded zygapophyseal articular surfaces compared to the articular surfaces of the centrum, it has a higher ROM, if other osteological stops are equal.

2.6 Limitation in ROM by osteological stops and the osteological neutral pose (ONP)

Basically, there are three directions of movement in the vertebral column: lateral, ventral, and dorsal, reflecting two of the three degrees of freedom. Note that in medicine and in some biological publications, ventral movement is termed “flexion” and dorsal movement is termed “extension”, a terminology that we apply to our models as well.

Movement in the motion segment is limited most obviously by the osteological stops, i.e., the point where bones in a joint would collide. These also can be observed well in fossils (Stevens, 2013). However, it has to be kept in mind that joints included cartilage and other soft tissues and that the vertebral column is also supported by muscles and ligaments. This means that the osteological stops constrain the maximal movement in the vertebral column and that the actual movement probably was less. Lateral movement is limited by osteological stops mostly formed by the centrum and the zygapophyses. Dorsal movement is mostly restricted by osteological stops formed by the zygapophyses and the neural spine, whereas ventral movement is restricted by osteological stops formed by the ventral margin of the centrum and also by the zygapophyses. It thus becomes apparent that the zygapophyses play a crucial role in the mobility of the vertebral column.

The habitual posture of the neck in a terrestrial amniote commonly coincides with the osteological neutral pose (ONP) (Stevens, 2013). The ONP is defined as the specific pose of the vertebrae in articulation, where two adjacent vertebrae are held by the animal with 100% overlap of the zygapophyses (Taylor, Wedel & Naish, 2009).

2.7 Inferences from morphology and biomechanics on the plesiosaur intervertebral joint

Prerequisite to finite element model building of a motion segment is the formulation of hypotheses about the nature of the soft tissue intervening between the two vertebral bodies and their spatial arrangement. Two aspects are of primary importance: the spacing of the vertebra and the types of intervertebral joints. Let us first consider the spacing. Plesiosaurs are commonly found as articulated or partially articulated skeletons due to their pelagic habits and preservation in conservation deposits. Citing only a few examples, such as the Hettangian and Sinemurian deposits of southern England (Benson, Evans & Druckenmiller, 2012; Benson, Evans & Taylor, 2015), the Posidonien-Schiefer Formation of Germany (O'Keefe 2004), the Cretaceous dark mudstones and chalks deposited in the Western Interior Seaway of North America (e.g., O'Keefe & Chiappe, 2011; Schumacher & Martin, 2016), and the inland Eromanga Sea of Australia (Zammit, Daniels & Kear, 2008), these provide good evidence of the natural position of the vertebra. Even the oldest and only Triassic plesiosaur skeleton, from the Rhaetian Exter Formation of Germany (Wintrich et al., 2017), preserves such evidence. This skeleton as well as many others cited above preserves necks in tight articulation, showing an intervertebral spacing of 1 to 2 mm (e.g., Wintrich et al., 2017, fig. 2c; Benson, Evans & Taylor, 2015, fig. 13; Andrews, 1910) and very tight articulations of the

zygapophyses. This preservational evidence is consistent with anatomical evidence of zygapophyseal overlap in the ONP discussed above, which also indicates short distances between the centra. An apparent exception is the leptoclidid plesiosaur *Nichollssaura borealis* that preserves considerably wider intervertebral spacing of several millimeters (Nagesan, Henderson & Anderson, 2018) but differs from *Cryptoclidus* and other small-headed plesiosaurs in its reduced number of only 24 cervical vertebrae (Druckenmiller & Russell, 2008).

In the case of plesiosaurs, conventional wisdom such as "all reptiles have a synovial joint between adjacent centra" (hypothesis 1) is pitted against clear evidence for the presence of an IVD (hypothesis 2). Let us first consider hypothesis 1, a synovial joint. The medial inclination of the zygapophyses in plesiosaur vertebrae in connection with a synovial joint between adjacent centra would reduce the mobility to a minimum. As a derived cryptoclidid plesiosaur, *Cryptoclidus eurymerus* reached nearly the maximum of zygapophyseal inclination, which is 82º as measured in IPB R324 (but also illustrated by Andrews, 1910).

A flat synovial joint has indeed three degrees of freedom, but does not allow rotation about the axis, but rather a translation along the axis. Furthermore, the translation along the axis would be restricted by the zygapophyses, which would mean that the plesiosaur neck has no mobility at all. Although crocodiles have a synovial joint between their vertebrae (Wettstein, 1962) they differ in having procoelous centra, and thus the synovial joint functions as a very mobile ball-and-socket joint. This shape allows three degrees of freedom, which increases mobility. Accepting the first hypothesis would give the minimum ROM for plesiosaurs.

Under hypothesis 2, there would be a similar structure to that seen in mammals, an IVD, in between the centra in the plesiosaur neck. This would increase mobility to the point where other features become limiting, such as the zygapophyses. An IVD would provide the maximal ROM. A cartilaginous structure in between the vertebral centra, consisting only of hyaline cartilage and fibrocartilage without a nucleus pulposus, appears implausible because it also would lead to a minimal ROM. We thus conclude that the most likely situation in plesiosaurs is an IVD.

3. Material and methods

3.1 Material

The Middle Jurassic plesiosaur we studied is a rather complete and well preserved skeleton (IPB R324) of the cryptoclidid plesiosaur *Cryptoclidus eurymerus. C. eurymerus* is a derived plesiosaur which exhibits some basal plesiosaur characters which makes the taxon useful for determining mobility in plesiosaur necks. The skeleton is from the Lower Oxford Clay (Callovian) of Peterborough, England, and is on display at the Goldfuß Museum of the Steinmann Institute, University of Bonn, Germany. IPB R324 was purchased from the foremost collector of Oxford Clay fossils, Alfred Leeds, through the Bonn fossil dealer Bernhard Stürz in 1911. Original Leeds collection stickers on the bones suggest that the skeleton is a composite, consisting of three individuals (written comm., Jeff Liston, 2015). The neck, skull and rest of the axial skeleton, however, derive from a single individual (written comm., Jeff Liston, 2015). The cervical vertebral column of IPB R324 consist of 32 vertebrae which are preserved, followed by 3 pectorals. Four of the cervical vertebrae are entirely casts which had been inserted in different places to fill size gaps during mounting. This insertion presumably also was motivated by the report by Andrews (1910) of "about 32 cervical vertebrae for *Cryptocleidus*". Andrews (1910) does not explain the meaning of "about", i.e., whether there is intraspecific variation or uncertainty because of incomplete preservation. However, in this study, we will use the count of 32 cervical vertebrae. It has been suggested that the neck is more mobile in its anterior third (e.g., Nagesan et al., 2018) and less mobile at the base. To take these variations into account, we took a well preserved middle cervical for our model. Cervical vertebrae 21 to 23 were removed from the mount for µCt scanning, and all cervical vertebrae were removed for morphological study. Vertebra number 22 is the best preserved one in this region, showing little deformation and only slight restoration at the tip of the neural spine. CT scanning revealed that cervicals 21 and 23 are too deformed and too restored to serve in the finite element analysis.

3.2 Methods

3.2.1 µCt scanning and 3D reconstruction

Surface models based on µCt-scans are the basis for the quantitative and qualitative description of vertebral morphology in general and features relevant for neck mobility in particular. The scans were recorded with the v|tome|x s scanner manufactured by GE

phoenix|x-ray (Wunstorf, Germany) and operated by the Steinmann Institute. A total of 1000 images with an exposure time of 667 ms and an average of 4 were recorded per scan. Voxel size was 190.97 µm, the voltage was set to 120 mV, and the current was set to 100 µA. The image stack generated by the software VG Studio Max from the rotational X-ray images collected by the scanner was transformed from .jpg files to DICOM files for 3D model building.

A three-dimensional surface model of the cervical vertebra no. 22 was generated from the DICOM files using Avizo 8.0.1 (FEI, Hillsboro, Oregon, USA). The surface model was then duplicated in order to build a single motion segment. Duplication was necessary because a motion segment could not be built from the scans of two adjacent vertebrae because of poor preservation (see above). For an anatomically accurate positioning of the two vertebral models (cervical vertebra no. 22 and its duplicate) relative to each other, the spinal canal as well as the articular surfaces of the zygapophyses were used as references. The anatomical positioning of the two vertebrae was also conducted in Avizo.

3.2.2 Finite element modeling

3.2.2.1 General anatomical assumptions for model

Since we employ models that are from a biomedical background and were developed for mammalian intervertebral joints, we assumed for this study the presence of an IVD in plesiosaurs. As noted above, models were easy to adapt for this study because of the inferred presence of an IVD in plesiosaurs. Therefore, we modeled the plesiosaur motion segment including a very simplistic IVD. The IVD was represented in the model by an annulus ring, a nucleus and two bony endplates. The implemented nucleus was based on the nucleus pulposus of a human cervical IVD. According to a series of studies (e.g. Eckling, 1960; Oda, Tanaka & Tsuzuki, 1988; Töndury & Theiler, 1990; Tonetti et al., 2005), the nucleus pulposus of the human cervical IVD mainly consists of fibrocartilaginous tissue. Therefore we did not implement an incompressible fluid which is most often used for models of the lumbar IVDs of humans.

3.2.2.2 Model dimensions and material properties

There is no data available concerning the exact original disc length in plesiosaur IVDs. However, based on the observed close spacing of the cervical vertebral centra in most plesiosaur fossils and the ONP derived from vertebral morphology (see above), three different

models were built (Fig. 1), only differing in IVD length. The length of the IVD at its dorsal margin in the three different models was approximately 1, 2, and 3 mm to model IVDs of that minimal length. Furthermore, articular cartilage with a thickness of approximately 0.2 mm was modeled within the gaps between the articulated pre- and postzygapophyses of the left and the right side of the vertebrae, simulating the two facet joints (Fig. 1). Although a thickness of 0.2 mm for the articular cartilage might appear unrealistically thin, the virtual articulation of the vertebra in the model that gave the best fit and the overlap of the zygapophyses resulted in such a small gap of 0.2 mm. Wider gaps could only be created with poorer fits of the zygapophyses.

The zygapophyseal articular cartilage also included contact elements, which were needed to simulate the physiological constraints generated by the facet joints. We neglected the presence of a facet joint capsule in order to obtain the widest ROM possible allowed by the morphology of the vertebrae, i.e., by the osteological stops. For this purpose, we also decreased the stiffness value (Young's modulus) of each soft tissue component to the minimum required for a stable finite element simulation (*Table 1*). In contrast to the FE models of the human IVD, we did not include any fiber layers within the annulus ring due to the lack of data for plesiosaurs. Furthermore, we implemented the bone tissue of the vertebrae using rigid material behavior in order to avoid any contribution to the overall ROM by the deformation of the vertebral bodies.

3.2.2.3 Model building, FE analysis, and total ROM calculation

The FE model generation, including all soft tissue components, material settings, and boundary conditions, was performed using custom made Python programs. The final models consisted of 68,212 to 87,220 elements and 323,480 to 427,569 nodes, depending on the setting for the IVD length (Fig. 1). The shorter the distance was the between the vertebrae, the more nodes were required, because a more dense mesh of nodes and elements was required.

The posterior surface of the posterior vertebra was fixed concerning all six degrees of freedom (see Fig. 1). Regarding the FE simulations, we applied pure bending moments to the anterior surface of the anterior vertebral body using a coupling node. The bending moments included flexion, extension, lateral bending and axial rotation. We are aware that this is an oversimplification of the real situation where, in the living animal, muscles inserting on different regions of the neural arch would have exerted these moments which then would have been transmitted to the vertebral centrum via the peduncles of the neural arch.

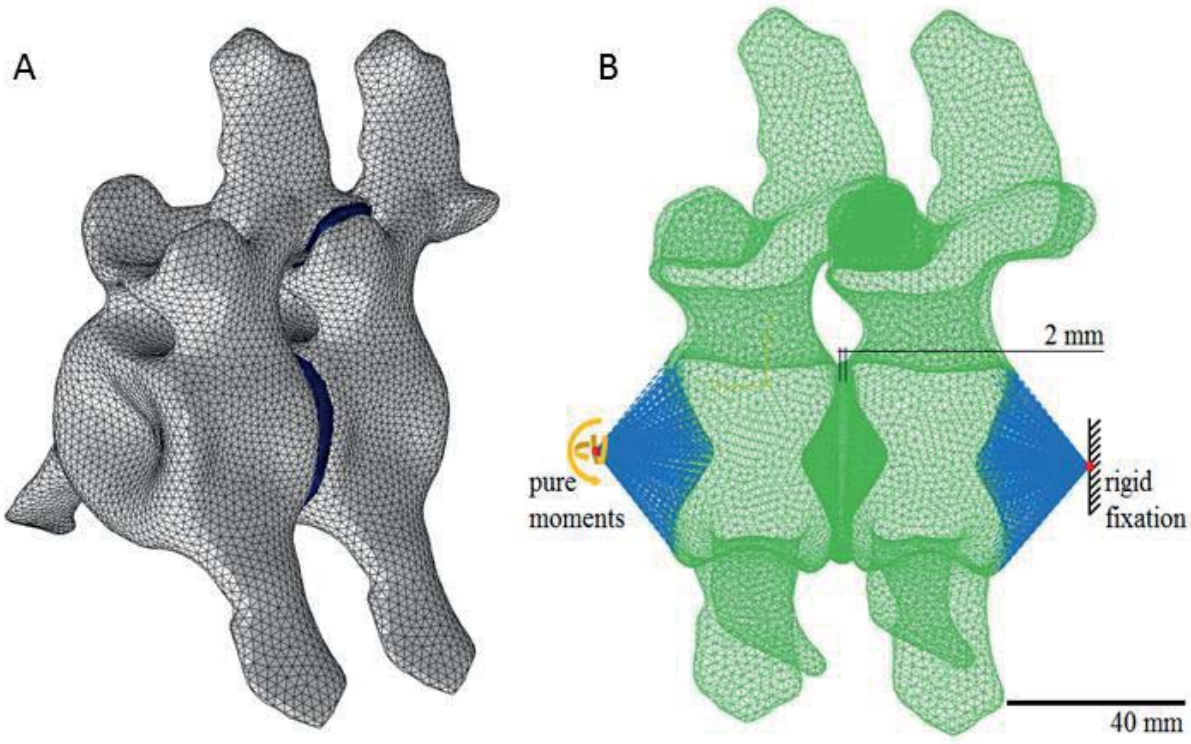

Figure 1: FE model with a dorsal IVD length of 1 mm.

This model consisted of 68,212 nodes and 323,480 elements. **A:** Left anterolateral view of the model. Grey is the bone material. Dark blue is the soft tissues between the two vertebrae. **B:** The model in sagittal section Grey is the bone material, green is the nucelus matrix, red is the zygapophyseal cartilage, light blue is the annulus cartilage. For material properties, see Table 1.

In addition to the material parameters and the intervertebral space, we also had to estimate the value for these moments since obviously no data are available for the plesiosaur. We gradually increased the applied bending moment until the finite element simulation became unstable, which was above 4 Nm. We applied the same bending moment in all load directions, as is customary in finite element simulations of the human spine. Each moment was applied separately. Thus, a total of 6 load cases (positive and negative direction of flexion-extension, lateral bending, and axial rotation) were computed for each of the three models (intervertebral spacing 1, 2, and 3 mm), resulting in a total of 18 simulations.

The final FE simulations were conducted using Abaqus 6.11 (Simulia, Dassault Systèmes, Vélizy-Villacoublay, France). The ROM for each load case was measured at the anterior

coupling node, which was also used for load application (Fig. 1). To compute total neck mobility of the IPB *Cryptoclidus* specimen, we multiplied the ROM obtained for each load case by the number of cervical vertebrae, i.e., 32. We are aware that this is a considerable oversimplification, but we justify this approach in the Discussion section.

Table 1: Material properties used in the FE simulations of the plesiosaur neck motion segment. E = Young's modulus

Tissue	**Material setting**
Anulus matrix	E (MPa): 0.8, υ (Poisson ratio): 0.45
Nucleus matrix	E (MPa): 0.5, υ (Poisson ratio): 0.45
Bone tissue of vertebrae	rigid
Bony endplates	E (MPa): 600.0, υ (Poisson ratio): 0.3
Facet cartilage	E (MPa): 100.0, υ (Poisson ratio): 0.3

4. Results

4.1 ROM in the modeled motion segment

The three different analyses were based on the different intervertebral spacing and the different load cases (Fig. 2). The ROM increased with increased IVD length in all load cases, but it is generally small, ranging from at most 5° to less than one degree. In the load cases with the 3-mm IVD, dorsal and ventral ROM is above 4°, decreasing to about 3° in the 2-mm IVD model. At an IVD thickness of 1 mm, about 1° is obtained. Lateral ROM is about 2° in the 3-mm IVD, and 1 degree in the 2-mm IVD, and 1 degree in the 1-mm IVD (Fig. 2).

Rotational ROM in general is of limited importance for the total ROM and the function of the plesiosaur neck. The difference between load cases is least for an IVD thickness of 1 mm, where ROM never exceeds one degree. With increasing IVD thickness, differences between load cases become more apparent, and the greatest ROM is seen in the dorsal and ventral flexion at 3 mm IVD thickness, while rotational ROM is least (Fig. 2). Interestingly, relative ventral and dorsal ROM is similar in all analysis, with dorsal ROM always being slightly greater than ventral ROM. Left lateral and right lateral ROM as well as left and right rotational ROM are closely similar.

Figure 2: Graph of ROM in the modeled motion segment depending on the length of the IVD.

Obviously, the longer the IVD, the greater the ROM. Abbreviations: Xr +, dorsal flexion; Xr -, ventral flexion; Yr +, left lateral flexion; Yr -, right lateral flexion; Zr, rotation around long axis.

4.2 Total ROM in the *Cryptoclidus* neck

Of course, total ROM of the *Cryptoclidus* neck depends crucially on IVD length. Based on the about 32 cervicals in the Bonn specimen of *Cryptoclidus eurymerus* IPB R324, we obtained three values for each direction (dorsal, ventral, and lateral) of total neck mobility. Assuming an IVD length of 1 mm, we obtain a total ROM of only 49° for dorsal flexion, 46º for ventral flexion, and 37º for lateral flexion (Fig. 3; *Table 2*). Assuming an IVD length of 2 mm, we obtain a total ROM of 103° for dorsal flexion, 97º for ventral flexion, and 56º for lateral flexion. Finally, for the greatest likely IVD length of 3 mm, we obtain a total ROM of only 157° for dorsal flexion, 148º for ventral flexion, and 67º for lateral flexion. Thus, the greatest mobility was clearly present in the dorsal direction, closely followed by the ventral direction. Lateral flexion was most limited in *Cryptoclidus*, never even approaching 90º. At an intermediate IVD length of 2 mm, *Cryptoclidus* would have been able to bend its neck slightly beyond a 90º angle in dorsal and ventral direction, and only with an IVD length significantly greater than 3 mm, the neck could have been bent into a full half circle in dorsal or ventral direction and a quarter circle in lateral direction (Fig. 3). Taking *Cryptoclidus* as a proxy, mobility in the neck of long-necked plesiosaur was rather limited, in strong contrast to the high number of cervical vertebrae intuitively suggesting great, snake-like mobility.

Table 2: Calculated total ROM in degrees for dorsal flexion, ventral flexion, and lateral flexion in the *Cryptoclidus* neck. This was obtained by multiplying the ROM for the modeled motion segment in dorsal, ventral, and lateral direction with the number of 32 cervical vertebrae. Abbreviations: L, left; MS, motion segment; R, right.

IVD length	Dorsal ROM in MS	Total ROM dorsal	Ventral ROM in MS	Total ROM ventral	Lateral ROM in MS	Total ROM lateral (mean of L/R)
1 mm	1	49	1	46	1	37
2 mm	3	103	3	97	2	56
3 mm	5	157	5	148	2	67

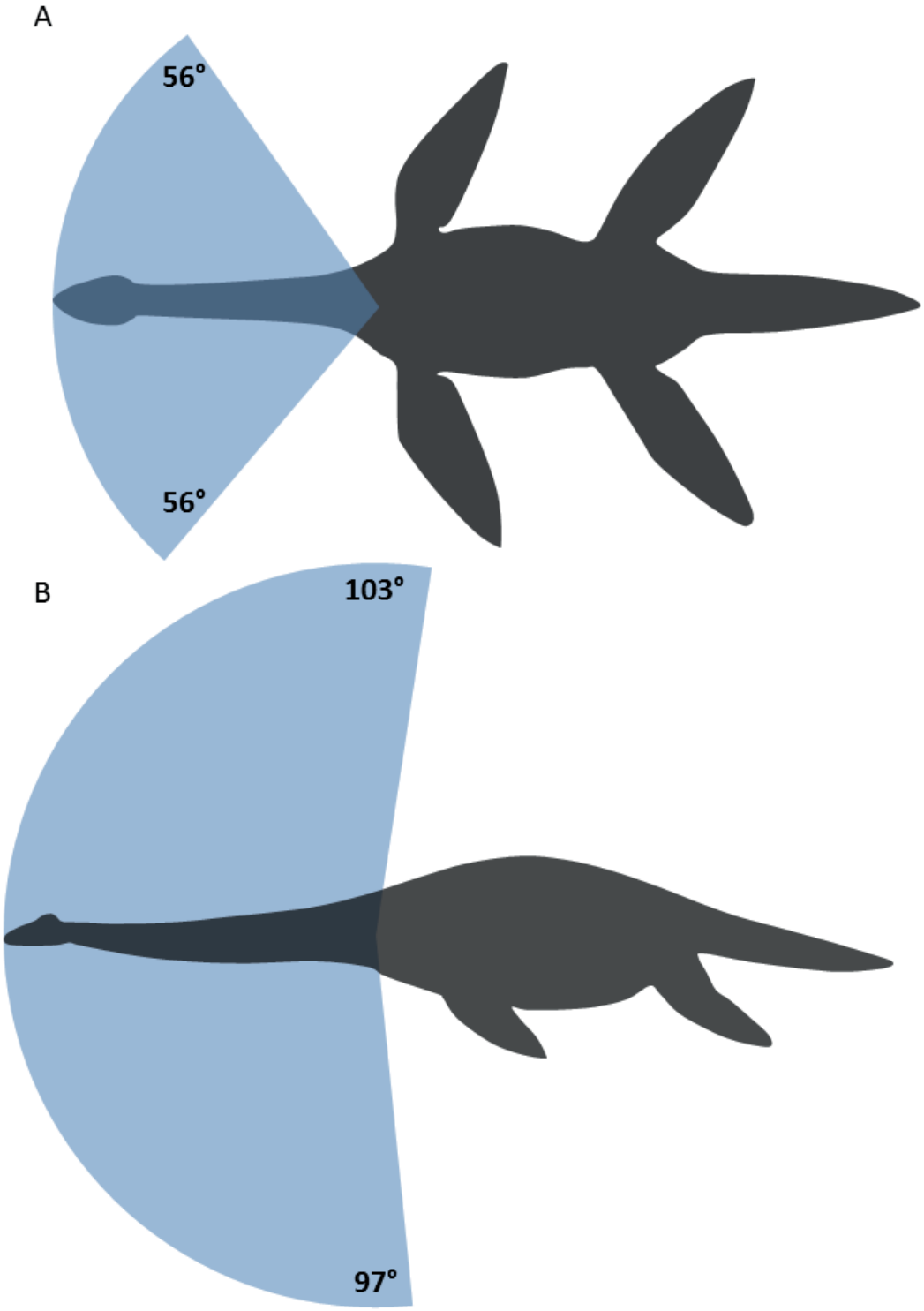

Figure 3: Maximal neck mobility in *Cryptoclidus eurymerus* with an intervertebral disc length of 2 mm. A) lateral and B) dorsoventral direction based on the multiplication of the maximum ROM in the modelled motion segment by the number of 32 cervical vertebrae.

5. Discussion

5.1 Methodological issues

Accurate FE analyses require a sufficient approximation of the reality. Most importantly, this includes the geometry of the object, its material properties, and the prevalent boundary conditions. Modeling and simulating biological tissue using finite element methods has become very popular in research and product development (Yoganandan et al., 1996). However, these studies remain challenging due to the complexity and inhomogeneity of biological materials (Freutel et al., 2014; Viceconti et al., 2005). The material parameters used in this study are not based on experimental data because we are dealing with fossils. Instead, we use well-justified assumptions. Due to the lack of knowledge about the mechanical properties of soft tissues of plesiosaurs in general, and *Cryptoclidus eurymerus* in particular, we reduced the stiffness of the modelled IVD to a minimum, as noted in the Methods section. By using this material setting, we were able to estimate the greatest ROM that can be achieved with the given vertebral anatomy. Another limitation of our analysis concerns the missing data about the true IVD thickness. Therefore we modelled and tested three different IVD lengths based on the range of observed intervertebral spacing. We only worked with one cartilage thickness in the face joints because any significant deviation from this thickness resulted in unrealistically disarticulated joints. However, further investigations concerning the true intervertebral spacing and the thickness of the soft tissue in the facet joints in plesiosaurs are clearly needed in order to obtain more reliable estimations of the total ROM.

As noted in the Methods section, our study is based on the 3D surface model of a single vertebra obtained from µCT data. The vertebra was used to create a single motion segment by simply duplicating it. This approach is justified because of the very gradual morphological change along the cervical vertebral column (e.g., Andrews, 1910, and personal observations on IPB R324) which in turn is related to the very high number of segments. The error caused by duplicating the vertebra is assumed to be relatively small compared to the error resulting from the missing soft tissue data. We note that our surface model is based on actual fossils, not on a model of the vertebrae. This is also the explanation for the slight difference between the left and right lateral bending values, which theoretically should be the same. The difference is probably due to the slight asymmetries in the actual scanned vertebra.

The resolution of the model meshes (node density) was high. Using an even denser mesh would not have offered further improvement in the accuracy of the models since the error

introduced by the lack of knowledge of actual tissue parameters is assumed to be much higher than that introduced by lower mesh density.

Finally, we offer justification of our approach of using a method from human biomechanics for understanding a long extinct marine reptile. The strength of this approach is that it is a mature and well established method from a large and applied field of research and thus will produce reliable and reproducible results. The weakness, of course, lies in the assumption about soft tissue input parameters that cannot be measured in fossils. However, we feel that the advantage of reproducibility and method maturity outweigh this weakness. As similar philosophy underlies the study of Hummel et al. (2008) on dinosaur nutrition which remains highly cited.

5.2 Reconstruction of actual ROM in the *Cryptoclidus* neck

In pistosauroid evolution, three major steps in neck evolution can be recognized, from pistosaurids (non-plesiosaurian pistosauroids) to basal plesiosaurs (outside of Cryptoclidia sensu Benson & Druckenmiller, 2014) to derived plesiosaurs.

In pistosaurids such as *Pistosaurus*, *Augustasaurus*, and *Yunguisaurus*, orientation of the prezygapophyses is nearly horizontal (Rieppel, Sander & Storrs, 2002), as in all other stem sauropterygians, and the articular surface area is large in the comparison to the vertebral centrum. In pistosaurids excluding *Bobosaurus forojuliensis*, the number of the cervical vertebrae is between 37 and 49. In basal plesiosaurs, the numbers of cervical vertebrae decreases slightly in comparison to pistosaurs but increases in the derived plesiosaurs again. The zygapophyses in basal plesiosaurs are medially inclined at 45°, and in derived plesiosaurs they may be inclined at over 80°, which is seen in *Cryptoclidus eurymerus*. It can be hypothesized that this would restrict lateral mobility over dorsoventral mobility, as shown by our results.

To obtain the total neck mobility, we had multiplied the ROM modeled for a specific cervical motion segment by the number of cervical vertebrae. This is only a first approximation since it appears likely that the ROM of the motion segment differs between the anterior and posterior parts of the cervical column, as is seen in elasmosaurs (Zammit, Daniels & Kear, 2008; Otero, Soto-Acuña & O´Keefe, 2018). We are thus aware that the most accurate result for total neck mobility would be obtained if we were to model the entire cervical column and add up the maximum ROM for each motion segment. Clearly, the next step in this research

would be to characterize the distribution of mobility along the neck from anterior to posterior, which would be particularly interesting in the extremely long-necked elasmosaurs. Similar studies have been conducted for sauropod dinosaurs (e.g., Dzemski & Christian, 2007; Christian & Dzemski, 2011), for example.

Our reconstruction based on the medical biomechanical investigation of neck mobility are consistent with the inferences on mobility based on osteological stops and zygapophyseal inclination in the neck vertebral column (discussed above), suggesting that in *Cryptoclidus* dorsoventral mobility was greater than lateral mobility because of the strongly medially inclined zygapophyses. The results are also consistent with inferences based on morphological characters in phylogenetic data matrices (e.g., Benson & Druckenmiller, 2014).

However, our results do not agree with the osteology-based interpretations by Noè, Taylor & Gomèz-Perèz (2017) favoring ventral mobility of the neck. On the other hand, the results obtained by 2D analog modeling by Zammit et al. (2008) are more consistent with ours, giving a similar range of values of ROM per motion segment. Because of the higher number of vertebrae in elasmosaurs, Zammit et al. (2008) obtained considerably greater total neck mobility than we did in *Cryptoclidus*, especially in the 1- and 2-mm IVD models. Zammit et al. (2008) differ in finding roughly equal mobility in all directions (75-177º), unlike the clearly lower lateral mobility we obtained (<67º). Finally, the most recent study by Nagesan et al. (2018) also found high mobility in a relatively long-necked plesiosaurs, the leptoclidid *Nichollssaura*, but this taxon appears to differ from at least other small-headed plesiosaurs in the number of its cervical vertebrae having been reduced to only 24. To compensate for this reduction but maintaining neck length, the lineage may have evolved wider intervertebral spacing, and we doubt whether this taxon is representative for long-necked and short-headed plesiosaurs in general.

Certainly our investigation is an approximation, but it shows clearly which morphological features and morphometric variables determine mobility. Although several characters in addition to IVD length influence neck mobility, the most important of these is zygapophysis morphology. Specifically, anteroposterior length of the articular surface, thickness of the joint cartilages between the pre- and postzygapophysis, and medial inclination are characters that need to be understood and measured to determine motion segment mobility and thus that of the entire neck.

5.3 Influence of reconstruction of IVD

The reconstruction of the IVD obviously also influences the models. As already noted by Romer (1956), the question of what kind of soft tissues intervene between the two bony centra in a motion segment is open. He speculated that the "conjoined hollows may be filled with modified notochordal material or fibrous tissue" (Romer, 1956, p 223). We argue that the intervertebral space in the plesiosaur motion segment was not developed as a synovial joint because a synovial joint would only have allowed translational movement due to the amphicoelous or platycoelous centrum shape. An intervertebral space purely consisting of a disc of fibrocartilage would not been movable either because of the very limited elasticity of this tissue both under tension and compression. Thus, we arrived at the conclusion that plesiosaurs possessed an IVD of some kind (Wintrich et al. in revision). In the IVD, there would have been at least two kinds of tissue, the distribution of which needed to be considered for our model. These are the cartilage of the annulus fibrosus and the notochord-derived cells of the nucleus pulposus. While the material parameters were estimated as discussed above, we also need to consider the anatomical arrangement of the different tissue types. We reconstructed the annulus fibrosus on the convex part of the articular surface outside of the sunken area. The remainder of the intervertebral spaced was filled up by the nucleus pulposus. The question of the exact nature and distribution of the tissues filling the intervertebral space is beyond the scope of this paper.

5.4 Influence of muscles and ligaments

When considering mobility, the influence of muscles and ligaments has to be discussed as well, both from the perspective of functional morphology in living animals (e.g., Dzemski & Christian, 2007; Taylor, Wedel & Naish, 2009; Stevens, 2013; Taylor & Wedel, 2013) and from the perspective of the fossil record, i.e., the posture of the neck in articulated fossils. In taphonomic studies (e.g., Reisdorf & Wuttke, 2012), it has been shown that neck mobility changes in different taphonomic stages: (1) First, in the living animal, mobility is at a minimum. Here, all muscles and ligaments remain connected to the cervical vertebral column and furthermore all nerves are intact, restricting any mobility beyond the osteological stops. (2) Second, mobility is greater when the animal is freshly dead. Despite all muscles and ligament still being intact, in a dead animal, an experimental hyperextension is unproblematic, leading to greater mobility than in the living animal (Dzemski & Christian, 2011). (3) Third, mobility is maximal when all muscles and ligaments are removed from the skeleton by decay

processes. Here, only the osteological stops, basically provided by the zygapophyses, the neural spine, the centrum, and the ribs, determine mobility. This situation applies to articulated skeletons in marine deposits, such as those of plesiosaurs from the Lower Jurassic of Lyme Regis (UK) and the Posidonienschiefer-Formation of Holzmaden (Germany) and the equivalent Toarcian rocks of Whitby (UK). The articulated plesiosaur specimens preserved in situ from these deposits general show a very straight neck (e.g., Beardmore et al., 2012; Benson, Evans & Druckenmiller, 2012), corroborating the limited mobility of the neck in long-necked plesiosaurs.

5.5 Functional and paleobiological implications

We show in our study that the neck of the plesiosaur *Cryptoclidus eurymerus* has a limited ROM in dorsal bending (extension), ventral bending (flexion), and especially lateral bending. The term "limited" refers to a maximal total neck mobility in dorsal and ventral direction of less than 160º and in lateral direction of less than roughly 70º (*Table 2*). Especially given that these values are upper limits of mobility, mobility was also significantly less than what has been found in previous quantitative studies (Zammit, Daniels & Kear, 2008; Noè, Taylor & Gomèz-Perèz, 2017; Nagesan, Henderson & Anderson, 2018). Because of the similar morphology of their cervical vertebrae, it can be assumed that most, if not all plesiosaurs had a limited ROM, inconsistent with the very long necks that intuitively would be associated with great flexibility, as in long-neck birds, for example. The long necks evolved in basal sauropterygians, retaining the ancestral lateral mobility as indicated by the horizontal zygapophyses that are wider than the centra (Rieppel, 2000; Sato et al., 2014). While lateral undulation appears to have become less important in swimming in taxa such as *Yunguisaurus* (Sato et al., 2014), the laterally mobile neck was retained. This raises the question as to why plesiosaurs retained these long necks but reduced mobility, and thus how the long-necked plesiosaur body plan originated.

After the swimming style in the lineage leading to plesiosaurs evolved from axial undulation to paraxial underwater flight at some time in the Late Triassic (Benson, Evans & Druckenmiller, 2012; Sato et al., 2014; Wintrich et al., 2017), the long neck was no longer needed in undulatory locomotion. However, the long neck could have had more functions than use in locomotion. Long necks evolved in several amniote clades for improving food acquisition by extending the reach and maneuverability of the head. Indeed, a considerably variety of functional interpretations have been offered for the long plesiosaur neck, as

reviewed by Noè, Taylor & Gomèz-Perèz (2017). Alternatively to these, there is the hypothesis that in plesiosaurs, the long neck is best understood as an adaptation to camouflage. This idea was first briefly expressed by Massare (1988, 1994) but never given serious consideration since. However, the idea is most consistent with our results on limited neck mobility.

Long-necked plesiosaurs hunting in schools of fish with a small head on a long neck would have increased the chance of catching the fish, i.e., predation success, because fish are sensitive to hydrodynamic waves. With the long neck and the small head, the hydrodynamic disturbance, which could be recognized by the prey, would have been smaller than if the neck would have been shorter. A similar hydrodynamic camouflage has been described for the Triassic slender-bodied fish *Saurichthys* (Kogan et al., 2015). In addition, there would have been a visual camouflage effect in that the long neck and small head would have hidden the true bulk of the predator.

The remaining issue is the evolutionary decrease in neck mobility from the laterally mobile neck in non-plesiosaurian pistosauroids to the limited mobility detected in this study. One hypothesis is that the mobile long neck originally played a role in lateral undulatory swimming, a function that was no longer relevant in plesiosaurs. With elongation of the neck mainly serving in hydrodynamic and visual camouflage, other functional constraints became important. Both during cruising and attack, the long neck needed to remain straight, and the long neck would have made steering difficult, with small deflections having a great effect (Alexander, 1989, p. 137). The straight posture in a mobile neck would require muscle effort to maintain. The evolution of osteological stops and thin intervertebral joints might have been energetically more advantageous than using muscle power to keep the neck straight.

An interesting pattern is observed in the evolution from basal plesiosaurs to more derived long-necked ones, i.e., *Cryptoclidus,* which is in the focus of this study. As noted, zygapophyseal inclination towards medial evolutionarily increased from 45º to over 80º, suggesting a decreased lateral and increased dorsoventral mobility. This is what is born out by our calculation of total neck mobility, with dorsal and ventral flexion distinctly greater than lateral flexion, especially in the simulations with the longer IVDs. This raises the question of the adaptive background of this evolutionary change. We suggest that the pattern is linked to an increase in swimming performance which would increase dorsoventral moments in the body (because of the dorsoventral movement of the flippers) which then would be transmitted

to the neck (see also Alexander, 1989). Increased mobility might have served in dampening of such moments. However, while testable, this hypothesis would require extensive biomechanical modeling of a swimming *Cryptoclidus*, and we only point out the pattern here.

6. Conclusions

One of the most distinctive features of plesiosaurs is their sometimes exceedingly long neck which, however, is convergently reduced in some large-headed forms. In these, the neck does not present a challenge, unlike in the long-necked forms. A classical plesiosaur taxon is *Cryptoclidus* from the late Middle Jurassic Lower Oxford Clay of the UK. Because this taxon is well represented by several skeletons, we investigated the mobility of its neck using a two-fold approach. Using a simple finite element model of a motion segment from the middle cervical region, we simulated the ROM of this segment in dependence of IVD length. We then calculated total neck ROM by multiplying segment ROM by the number of cervical vertebrae (32) and find that the lateral mobility of the neck is less than the dorsal and ventral ones which are of about the same degree. However, total mobility in all directions is low, never exceeding 160º. This is counter-intuitive, given the serpent-like appearance of the neck, but consistent with qualitative anatomical observations of cervical vertebral anatomy. We hypothesize that the reduced mobility of the neck in long-necked plesiosaurs compared to that of their ancestors is due to the function of the neck in hydrodynamic and visual camouflage combined with the high moments exerted on this neck during swimming and attacking. The greater mobility of the neck in dorsoventral direction compared to the lateral direction may also be linked to the change in locomotion from lateral undulation to underwater flight and the subsequent elaboration of this swimming style.

7. Acknowledgments

We thank Olaf Dülfer (Bonn) for help with specimen preparation and Rico Schellhorn (Bonn) for help with illustrations and discussion. Furthermore we thank the reviewers for their insightful suggestions for the improvement of the manuscript.

Funding

Funding was provided by the German Research Foundation (grant no. SA 469/47-1) and the LWL-Museum für Naturkunde, Münster, Germany. The funders had no role in study design, data collection and analysis, decision to publish, or preparation of the manuscript.

8. References

Alexander RM. 1989. *Dynamics of dinosaurs and other extinct giants*. New York: Columbia University Press.

Andrews CW. 1910. *A catalogue of the marine reptiles of the Oxford Clay, Part I*. London: British Museum (Natural History).

Boszczyk BM, Boszczyk AA, Putz R. 2001. Comparative and functional anatomy of the mammalian lumbar spine. *The Anatomical Record* 264(2) 157-168.

Benson RBJ, Evans M, Druckenmiller PS. 2012. High diversity, low disparity and small body size in plesiosaurs (Reptilia, Sauropterygia) from the Triassic–Jurassic boundary. *PLoS One* 7(3) e31838.

Benson RBJ, Druckenmiller PS. 2014. Faunal turnover of marine tetrapods during the Jurassic–Cretaceous transition. *Biological Reviews* 89(1) 1-23.

Benson RBJ, Evans M, Taylor MA. 2015. The anatomy of *Stratesaurus* (Reptilia, Plesiosauria) from the lowermost Jurassic of Somerset, United Kingdom. *Journal of Vertebrate Paleontology* 35:e933739.

Buchholtz EA, Schur SA. 2004. Vertebral osteology in Delphinidae (Cetacea). *Zoological Journal of the Linnean Society* 140(3) 383-401.

Beardmore SR, Orr PJ, Manzocchi T, Furrer H, Johnson C. 2012. Death, decay and disarticulation: modelling the skeletal taphonomy of marine reptiles demonstrated using *Serpianosaurus* (Reptilia; Sauropterygia). *Palaeogeography, Palaeoclimatology, Palaeoecology* 337 1-13.

Christian A, Dzemski G. 2011. Neck posture in sauropods. *Biology of the sauropod dinosaurs: understanding the life of giants.* Bloomington Indiana University Press, 251-260.

Cobley MJ, Rayfield EJ, Barrett PM. 2013. Inter-vertebral flexibility of the ostrich neck: implications for estimating sauropod neck flexibility. *PLoS One* 8(8) e72187.

Currey JD. 2002. *Bones: structure and mechanics*. Princeton: Princeton University Press.

Druckenmiller PS, Russell AP. 2008 Skeletal anatomy of an exceptionally complete specimen of a new genus of plesiosaur from the Early Cretaceous (Early Albian) of northeastern Alberta, Canada. *Palaeontographica Abt. A* 283, 1–33.

Druckenmiller PS, Russell AP. 2009 The new plesiosaurian genus *Nichollssaura* from Alberta, Canada: replacement name for the preoccupied genus *Nichollsia*. *Journal of Vertebrate Paleontology* 29, 276.

Dzemski G, Christian A. 2007. Flexibility along the neck of the ostrich (*Struthio camelus*) and consequences for the reconstruction of dinosaurs with extreme neck length. *Journal of Morphology* 268(8) 701-714.

Ecklin U. 1960. *Die Altersveränderungen der HWS.* Heidelberg: Springer-Verlag.

Freutel M, Schmidt H, Dürselen L, Ignatius A, Galbusera, F. 2014. Finite element modeling of soft tissues: material models, tissue interaction and challenges. *Clinical Biomechanics*, 29(4), 363-372.

Krings M, Nyakatura JA, Fischer MS, Wagner H. 2014. The cervical spine of the American barn owl (*Tyto furcata pratincola*): I. Anatomy of the vertebrae and regionalization in their S-shaped arrangement. *PloS One* 9(3) e91653.

Kogan I, Pacholak S, Licht M, Schneider JW, Brücker C, Brandt S. 2015. The invisible fish: hydrodynamic constraints for predator-prey interaction in fossil fish *Saurichthys* compared to recent actinopterygians. *Biology Open* bio-014720.

Mercder SR, Jull GA. 1996. Morphology of the cervical intervertebral disc: Implications for McKenzie´s model of the disc derangement syndrome. *Manual Therapy* 1(2): 76-81.

Müller J, Scheyer TM, Head JJ, Barrett PM, Werneburg I, Ericson PG, Pol D, Sánchez-Villagra MR. 2010. Homeotic effects, somitogenesis and the evolution of vertebral numbers in recent and fossil amniotes. *Proceedings of the National Academy of Sciences, USA* 107(5) 2118-2123.

Massare JA. 1988. Swimming capabilities of Mesozoic marine reptiles: implications for method of predation. *Paleobiology* 14(2) 187-205.

Massare JA. 1994. Swimming capabilities of Mesozoic marine reptiles: a review. In: Maddock L, Bone Q, and Rayner JMV, eds. *Mechanics and Physiology of Animal Swimming*. Cambridge: Cambridge University Press, 133-149.

McHenry CR, Cook AG, Wroe S. 2005. Bottom-feeding plesiosaurs. *Science* 310(5745) 75-75.

Molnar JL, Pierce SE, Hutchinson JR. 2014. An experimental and morphometric test of the relationship between vertebral morphology and joint stiffness in Nile crocodiles (*Crocodylus niloticus*). *Journal of Experimental Biology* 217(5) 758-768.

Nagesan, RS, Henderson, DM, Anderson, JS. 2018. A method for deducing neck mobility in plesiosaurs, using the exceptionally preserved *Nichollssaura borealis*. *Royal Society Open Science* 5(8) 172307.

Niemeyer F, Wilke HJ, Schmidt, H. 2012. Geometry strongly influences the response of numerical models of the lumbar spine—a probabilistic finite element analysis. *Journal of Biomechanics* 45(8) 1414-1423.

Noè LF, Taylor MA, Gómez-Pérez M. 2017. An integrated approach to understanding the role of the long neck in plesiosaurs. *Acta Palaeontologica Polonica*, 62(1) 137-162.

Oda J, Tanaka H, Tsuzuki N. 1988. Intervertebral disc changes with aging of human cervical vertebra: from the neonate to the eighties. *Spine* 13(11) 1205-1211.

O'Keefe FR. 2004. Preliminary description and phylogenetic position of a new plesiosaur (Reptilia: Sauropterygia) from the Toarcian of Holzmaden, Germany. *Journal of Paleontology* 78 973 – 988.

O'Keefe FR, Chiappe LM. 2011. Viviparity and K-selected life history in a Mesozoic marine plesiosaur (Reptilia, Sauropterygia). *Science* 333 870-873.

Otero RA, Soto-Acuña S, O'Keefe FR. 2018. Osteology of *Aristonectes quiriquinensis* (Elasmosauridae, Aristonectinae) from the upper Maastrichtian of central Chile. *Journal of Vertebrate Paleontology* 38 e1408638.

Putz R. 1992. The detailed functional anatomy of the ligaments of the vertebral column. *Annals of Anatomy-Anatomischer Anzeiger* 174(1) 40-47.

Reisdorf AG, Wuttke M. 2012. Re-evaluating Moodie's opisthotonic-posture hypothesis in fossil vertebrates. Part I: Reptiles—the taphonomy of the bipedal dinosaurs *Compsognathus longipes* and *Juravenator starki* from the Solnhofen Archipelago (Jurassic, Germany). *Palaeobiodiversity and Palaeoenvironments* 92 119-168.

Rieppel O. 2000. *Handbook of paleoherpetology. Part 12A. Sauropterygia I. Placodontia, Pachypleurosauria, Nothosauroidea, Pistosauroidea*. Munich: Friedrich Pfeil.

Rieppel O, Sander PM, Storrs GW. 2002. The skull of the pistosaur *Augustasaurus* from the Middle Triassic of northwestern Nevada. *Journal of Vertebrate Paleontology* 22(3) 577-592.

Romer AS. 1956. *Osteology of the reptiles*. Chicago: University of Chicago Press.

Sato T, Zhao L-J, Wu X-C, Li C. 2014. A new specimen of the Triassic pistosauroid *Yunguisaurus*, with implications for the origin of Plesiosauria (Reptilia, Sauropterygia). *Palaeontology* 57 55-76.

Schumacher BA, Martin JE. 2016. *Polycotylus latipinnis* Cope (Plesiosauria, Polycotylidae), a nearly complete skeleton from the Niobrara Formation (early Campanian) of southwestern South Dakota. *Journal of Vertebrate Paleontology* 36: e1031341.

Stevens KA. 2013. The articulation of sauropod necks: methodology and mythology. *PLoS One* 8(10) e78572.

Storrs GW. 1993. Function and phylogeny in sauropterygian (Diapsida) evolution. *American Journal of Science* 293(A) 63-90.

Taylor MA. 1981. Plesiosaurs-rigging and ballasting. *Nature* 290 628-629.

Taylor MA, Wedel MJ. 2013. Why sauropods had long necks; and why giraffes have short necks. *PeerJ* 1 e36.

Taylor MA. 1987. How tetrapods feed in water: a functional analysis by paradigm. *Zoological Journal of the Linnean Society* 91(2) 171-195.

Taylor MP, Wedel MJ, Naish D. 2009. Head and neck posture in sauropod dinosaurs inferred from extant animals. *Acta Palaeontologica Polonica* 54(2) 213-220.

Töndury G, Theiler K. 1990. *Entwicklungsgeschichte und Fehlbildung der Wirbelsäule*. Stuttgart: Hippokrates Verlag Bd. 98(2) 74-83.

Tonetti J, Potton L, Ribound R, Peoch M, Passagia JG, Chirossel JP. 2005. Morphological cervical disc analysis applied to traumatic and degenerative lesions. *Surgical and Radiologic Anatomy* 27(3) 192-200.

Viceconti M, Olsen S, Nolte LP, Burton K. 2005. Extracting clinically relevant data from finite element simulations. *Clinical Biomechanics*, 20(5) 451-454.

Viglino M, Flores DA, Ercoli MD, Alvarez A. 2014. Patterns of morphological variation of the vertebral column in dolphins. *Journal of Zoology* 294(4) 267-277.

Wettstein Ov. 1962. Crocodilia. In: Kükenthal W, Krumbach T, ed. *Handbuch der Zoologie*. Bd. 7(1) Berlin: Walter de Gruyter & Co.

Wilkinson DM, and Ruxton GD. 2011. Understanding selection for long necks in different taxa. *Biological Reviews* 87:616-630.

Wintrich T, Hayashi S, Houssaye A, Nakajima Y, Sander PM. 2017. A Triassic plesiosaurian skeleton and bone histology inform on evolution of a unique body plan. *Science Advances* 3(12) e1701144.

Wintrich T, Scaal M, Böhmer C, Schellhorn R, Kogan I, van der Reest A, Sander PM. In revision. Fossil soft tissues indicate convergent evolution of the intervertebral disc in non-mammalian amniotes. *Nature*.

Yoganandan N, Kumaresan S, Voo L, Pintar FA. 1996. Finite element applications in human cervical spine modeling. *Spine* 21(15) 1824-1834.

Zammit M, Daniels CB, Kear BP. 2008. Elasmosaur (Reptilia: Sauropterygia) neck flexibility: Implications for feeding strategies. *Comparative Biochemistry and Physiology Part A: Molecular & Integrative Physiology* 150(2) 124-130.

Chapter 5

In revision (File as submitted to Nature is included here):

Wintrich, T., Scaal, M., Böhmer, C., Schellhorn, R., Kogan, I., van der Reest, A., Sander, P. M. (in revision Nature). Fossil soft tissues indicate convergent evolution of the intervertebral disc in non-mammalian amniotes.

Author contributions:

Tanja Wintrich designed the research and carried out the research and wrote the paper.

Tanja Wintrich, Christine Böhmer, Rico Schellhorn, Ilja Kogan, Aaron van der Reest, and P. Martin Sander provide datasets to the study and contributed to the manuscript preparation, wrote the paper, reviewed drafts of the paper.

Supplementary Material:

Main Introduction, complete histological description, and discussion of all taxa, including the results of the soft tissue material.

Fossil soft tissues indicate convergent evolution of the intervertebral disc in non-mammalian amniotes

TANJA WINTRICH[1*], MARTIN SCAAL[2], CHRISTINE BÖHMER[3], RICO SCHELLHORN[1], ILJA KOGAN[4], AARON VAN DER REEST[5] AND P. MARTIN SANDER, P. M.[1,6]

[1]Steinmann Institute for Geology, Mineralogie and Paleontology, University of Bonn, Nussallee 8, 53115 Bonn, Germany *tanja.wintrich@uni-bonn.de

[2]Institute of Anatomy II, University of Cologne, Joseph-Stelzmann-Str. 9, 50937 Cologne, Germany.

[3]UMR 7179 CNRS, Muséum national d'Histoire naturelle, Département Adaptations du Vivant, case postale 55, 57 rue Cuvier, F-75231 Paris cedex 05, France

[4]Institut für Mineralogie, Technische Universität Bergakademie Freiberg, Brennhausgasse 14, 09596 Freiberg, Germany.

[5]Department of Biological Sciences, University of Alberta, Edmonton, Alberta, Canada, T6G 2E9, Canada.

[6]Dinosaur Institute, Natural History Museum of Los Angeles County, 900 Exposition Boulevard, Los Angeles, CA 90007, USA

Abstract

Morphology of the vertebral column has been used as a key anatomical character in defining and diagnosing groups of amniotes[1], such as the intervertebral disc (IVD), which has been considered to be unique to mammals[2]. However, although the importance of soft tissue analysis in fossils is clearly recognized today[3,4,5], investigations on soft tissue in the vertebral column, namely of joints and intervertebral spaces, have not been done yet[3]. Here we show that the anatomy of intervertebral joints in extinct amniotes can be reconstructed from the fossil remains of different types of joint-forming tissues preserved on the articular surfaces and in the intervertebral space of the dorsal vertebrae. Sampling of 17 different extinct amniote clades revealed intervertebral tissue types seen in extant reptiles and, surprisingly, a proper IVD in some taxa other than mammals, including non-avian dinosaurs, ichthyosaurs, plesiosaurs, and marine crocodiles. Using polarised light microscopy, we found fossil soft tissues such as different types of cartilage and probable notochordal material in ground palaeohistological sections. These identifications are based on comparison with microtome sections of extant animals. The distribution of the fossil tissues allowed us to infer the soft part anatomy of the intervertebral space[2]. Ancestral character state reconstruction[6] indicates that the IVD evolved at least twice, in mammals and in diapsid reptiles. The reptilian IVD dissappeared at the end of the Cretaceous because the only surviving dinosaurs, birds, had evolved a different type of intervertebral joint. Likewise, extant reptile groups (squamates, crocodiles, turtles) independently evolved a synovial ball-and-socket joint in the dorsal vertebral column. The tuatara and some geckos reverted to the ancestral condition of a persisting notochord.

Maintext

The intervertebral disc (IVD) is of eminent functional and clinical importance in the human vertebral column and has been studied from multiple perspectives in biological, medical and veterinary science. The crucial function of the IVD is to withstand biomechanical forces acting on the axial skeletons and gradual failure of IVD function from degenerative processes often leads to pathological symptoms[7]. Due to the lack of soft tissue preservation in fossil amniotes, however, evolutionary origins of the IVD have been poorly understood. As increasing numbers of fossil amniote specimens with preserved intervertebral tissues are discovered, analyses of these soft tissues have the potential of modifying our view of the evolution of the IVD. In comparative anatomy, the assumption prevails that reptiles lack an IVD because of their procoelous and opisthocoelous vertebral centrum morphology[1,8] forming a synovial ball-and-socket joint. This is true in extant reptiles, except for the tuatara *Sphenodon punctatus*[9,10] and some gekkonid lizards[11]. In the fossil record, we see that generalised centrum morphology does not indicate ball-and-socket joints[1] with hyaline cartilage. Instead, amphicoelous and platycoelous vertebral centra prevailed independent of major clade affinity. Romer[1] describes a general evolutionary progression from amphicoelous notochordal via amphicoelous non-notochordal to platycoelous during the transition from aquatic to terrestrial environments. The colonisation of diverse terrestrial environments, including the conquest of the arboreal and aerial habitats, were accompanied by substantial changes in the morphology of the vertebrae, but also in the articulations between the segments where motion occurs[1].

In mammals, the IVD is composed of two distinct parts, one of which is embryologically derived from the notochord. This is the nucleus pulposus (NP), the central hydrophilic proteoglycan-rich gelatinous core of the IVD. The NP is surrounded by a lamellate collagenous ring of fibrocartilage tissue, the annulus fibrosus (AF). The NP is formed at an early ontogenetic stage and is derived from embryonic notochord cells, whereas the fibrocartilaginous AF is derived from sclerotomes[12,13,14,15]. The NP has no direct contact with the bony surface of the centra, being separated by a layer of hyaline cartilage (endplate). In contrast, the AF is anchored to the peripheral part of the centra via fibrocartilage and direct insertion of fibers into the bone[16]. Since a joint is an integrated system of bone and other connective tissues, the bone histology of the amniote centrum is importan as well. The higher- level phylogeny of the amniotes reveals that the basal condition of the vertebral morphology is an amphicoelous vertebral centrum with a notochordal canal, as already seen in the amniote sistergroup, Diadectomorpha[1] (Fig. 1).

Romer[1] hypothesised that the "conjoined hollows created by amphicoelous vertebral centra were filled by modified notochordal material or fibrous tissue" without raising the issue of the IVD. Except for the IVD, an inconsistency in terminology describing intervertebral tissues (intervertebral cartilage, intervertebral tissue, and intervertebral pad) has caused some confusion when referring to tissues and joint anatomy. However, regardless of vertebral centrum shape of extinct Amniota, there must have been tissues which allowed three-dimensional movement of the vertebral column. Here, we identify the different tissue types present in the intervertebral space of fossil amniotes based on histological investigations of bone and preserved soft tissues.

Histological investigations of fossil tissues have become a powerful tool in palaeontology[17], but in general they are limited to bone tissue. It is known that different soft tissue elements, like osteonal linings, bone collagen fibers, osteoclasts, and even blood vessels may preserve in deep time[18,19]. Apart from the bone, integumentary soft tissues may be preserved[20,3] as well as, very rarely, internal organs[21,22]. Based on the rationale that soft tissues associated with the skeleton might also be preservable, especially in articulated specimens, we histologically sampled diverse fossil taxa across the amniote tree for preserved intervertebral soft tissues (Supplementary Table 1). If possible, we sampled one or several dorsal vertebrae in articulation. We restricted the analysis to the dorsal vertebral column because it shows the least morphological and functional variation, thus improving comparability across taxa.

We observed cartilage formed in the endochondral domain in the joints of all vertebral samples but in various altered states, of different kinds, and different distributions (Figs. 1 and 2). We also observed the fibrous insertion into the periosteal bone of the connective tissue of the joint capsule (of synovial joints) and the insertions of intervertebral ligaments. The distribution and arrangement of bone tissue and preserved hypertrophied cartilage, hyaline cartilage and fibrocartilage allows to constrain the type of intervertebral joint and, in the case of the IVD, the size and location of the AF and NP. These were inferred from the distribution of outward inclined files of hypertrophied cartilage cells (Figs. 1a-c and 2c-e).

Especially in marine reptiles from black shales, we found soft tissue preservation across the intervertebral space, allowing further inferences about the nature of the joint connecting adjacent centra (Fig. 2c). We also sampled extant taxa, in particular *Sphenodon*, for comparison with fossil soft tissues and to clarify contradictory statements in the literature. Turtles were excluded from the analysis because of their uncertain systematic

affinities, the highly modified dorsals in the extant turtles and the lack of histological sample from stem turtles. We then performed ancestral character state reconstructions (ASR) of intercentral joint type for a consensus amniote phylogeny, allowing us to trace the evolution of the amniote intervertebral joint (Fig. 3). Both parsimony and maximum likelihood-based ASR agree (Fig. S29).

The basal amniote joint, as exemplified by the iconic sail-backed synapsid *Dimetrodon*, is a notochord constricted by the vertebral centrum and expanded in the space between the centra (Fig. 3). The expanded portion was surrounded by fibrocartilage forming an AF, as seen in modern geckos[11]. Next, the notochord became interrupted by the closure of the notochordal canal. Notochordal tissue then must have formed an incipient NP that became separated from the bony surface by a layer of hyaline cartilage, the endplate (Fig. 2c-e). This happened convergently twice, once in therapsids and once in the reptile lineage, in early diapsids such as ichthyosaurs (Fig. 3). We found a probable altered NP preserved in ichthyosaur fossils from the Middle Triassic and Early Jurassic (Fig. 2c). From this evolved a platycoelous or slightly amphicoelous centrum with an IVD at least twice, in therian mammals and in higher diapsids (Fig. 3). Alternatively, the platycoelous centrum with an IVD evolved independently in eosauropterygians (a clade of marine reptiles to which plesiosaurs belong), and in archosauromorphs (Fig. 3). The platycoelous centrum with an IVD was then retained in most archosauromorphs, including basal crocodiliforms and most dinosaurs. Modern crocodiles evolved a synovial ball-and-socket joint convergently with lepidosaurs (Fig. 3). The dinosaurs included in our study also retained the platycoelous centrum with the IVD except for the most derived non-avian dinosaur, i.e., the dromaeosaur. In the dromaeosaur, cartilage is greatly reduced, suggesting that the dorsal vertebral centra of these dinosaurs had the same fibrous connection as in extant birds. Based on the ASR, lepidosaurs also evolved a synovial ball-and-socket joint from an equivocal ancestral state (Fig. 3), and *Sphenodon* and certain geckos seemingly reverted to the basal amniote condition, possibly by neoteny.

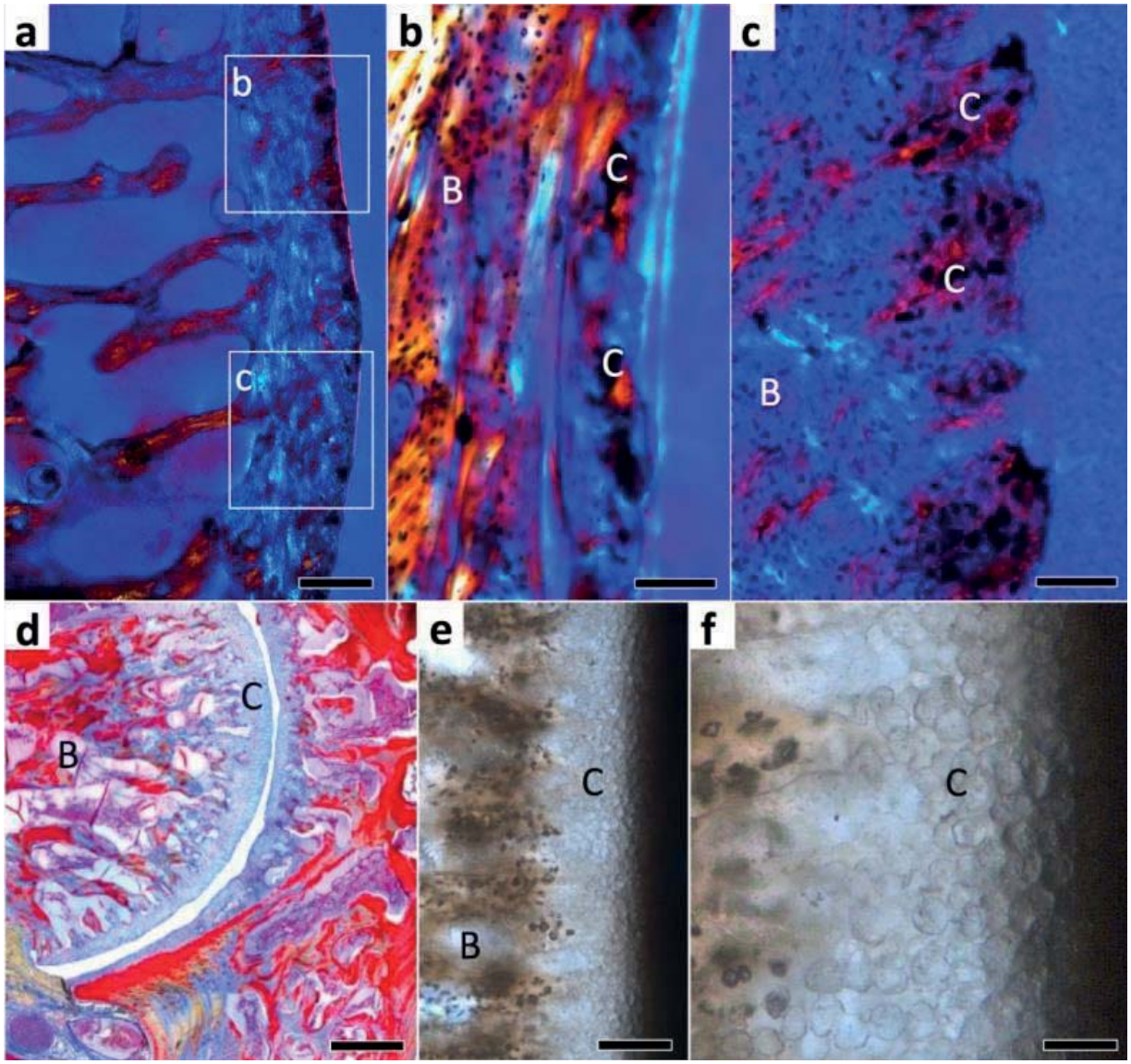

Figure 1 | Histology of mammalian and squamate intervertebral spaces. a, *Phoca vitulina* STIPB M 60, sagittal section of dorsal vertebral centrum showing part of the bony endplate in cross polarised light. b, Enlargement of area b in figure a showing a thin layer of cartilage. Note the irregular arrangement of the chondrocyte lacunae. This tissue is overlain by the nucleus pulposus (NP) of the IVD in life. c, Enlargement of area c in figure a showing cartilage cells (chondrocytes) in inclined files embedded in fibrous bony tissue. This represents the insertion of the annulus fibrosus (AF) of the IVD. d, *Python* sp. STIPB R 662, transverse section of the synovial joint connecting the dorsal vertebral centra. The joint is formed by hyaline cartilage and a thin intervertebral space filled with synovial fluid in life. e, *Mosasaurus missouriensis* STIPB Goldfuß 1230, close up of the joint surface in sagittal section of a dorsal vertebral centrum. Note the globular structures arranged in files representing fossilised hyaline cartilage. f, Enlargement of e. Scale bars in a and d represent 500 µm, scale bars in b, c, and e represent 100 µm, and scale bar in f represents 20 µm. B, bone tissue; C, cartilage.

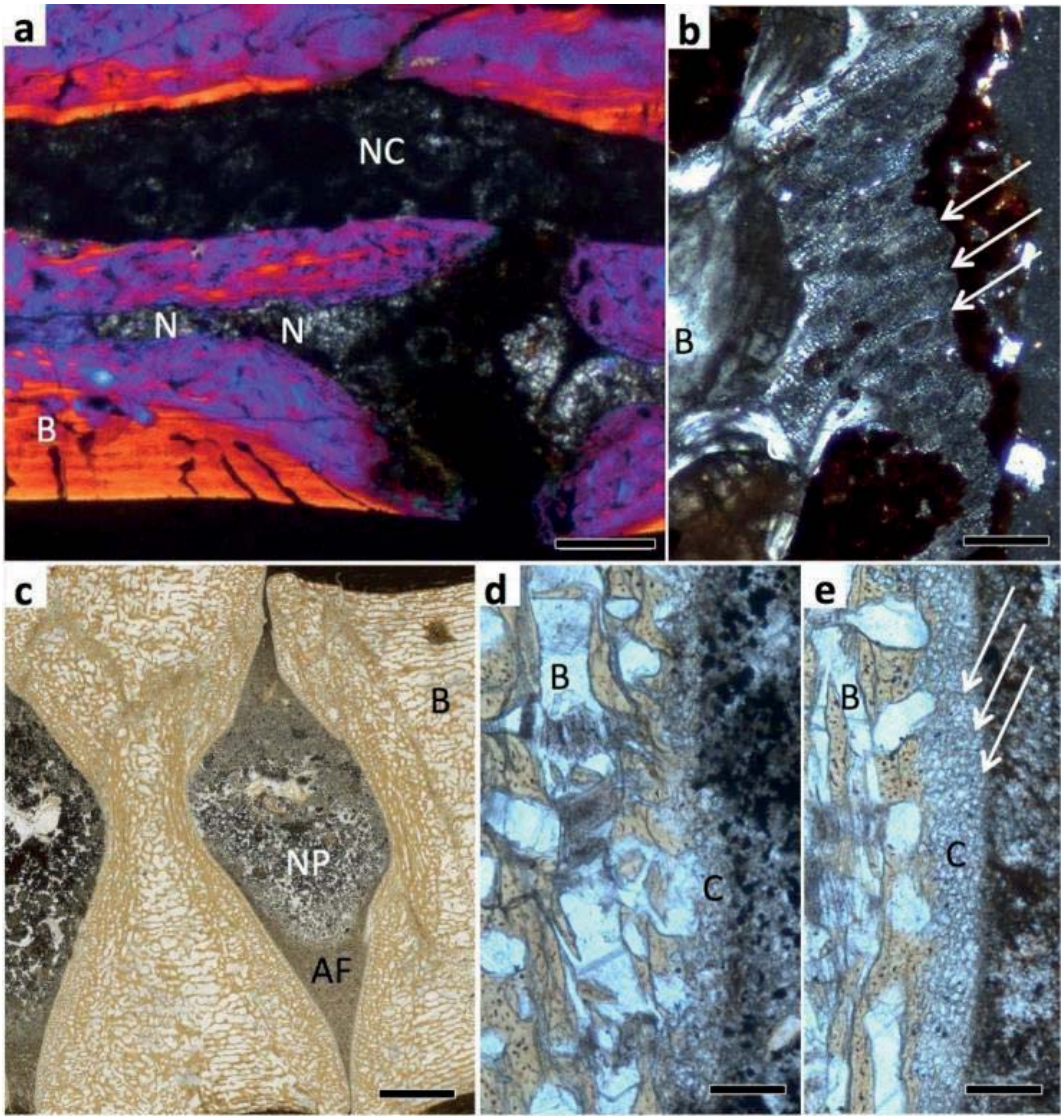

Figure 2 | Histology of mesosaur, ichthyosaur and dinosaur intervertebral spaces. a, *Stereosternum tumidum* STIPB R 622, sagittal section of two articulated dorsal vertebral centra with intervertebral space, showing the notochordal amphicoelous shape and the persisting notochord. b, Hadrosauridae indet. UACVP 59650. Close up of the articular surface showing obliquely arranged mineralized fibers in between poorly defined files of chondrocyte lacunae (arrows). c, *Stenopterygius* sp. STIPB R 661. Sagittal section of two articulated centra showing the amphicoelous shape. Note the differentiation of the content of the intervertebral space into a coarse and a fine fraction, probably representing the nucleus pulposus (NP) and the annulus fibrosus (AF). d, Enlargement of the concave part of the articular surface, showing a thin layer of irregularly arranged chondrocyte lacunae, underlying the nucleus pulposus (NP). e, Enlargement of the convex part of the articular surface, showing obliquely arranged files of chondrocyte lacunae, representing the insertion of the annulus fibrosus (AF) (arrows). Scale bars in a represents 500 µm, scale bar in b represents 10 µm, scale bars in c represents 2 mm, scale bars in d and e represent 20 µm. AF, annulus fibrosus; B, bone tissue; C, cartilage; N, notochord; NC, neural canal; NP, nucleus pulposus.

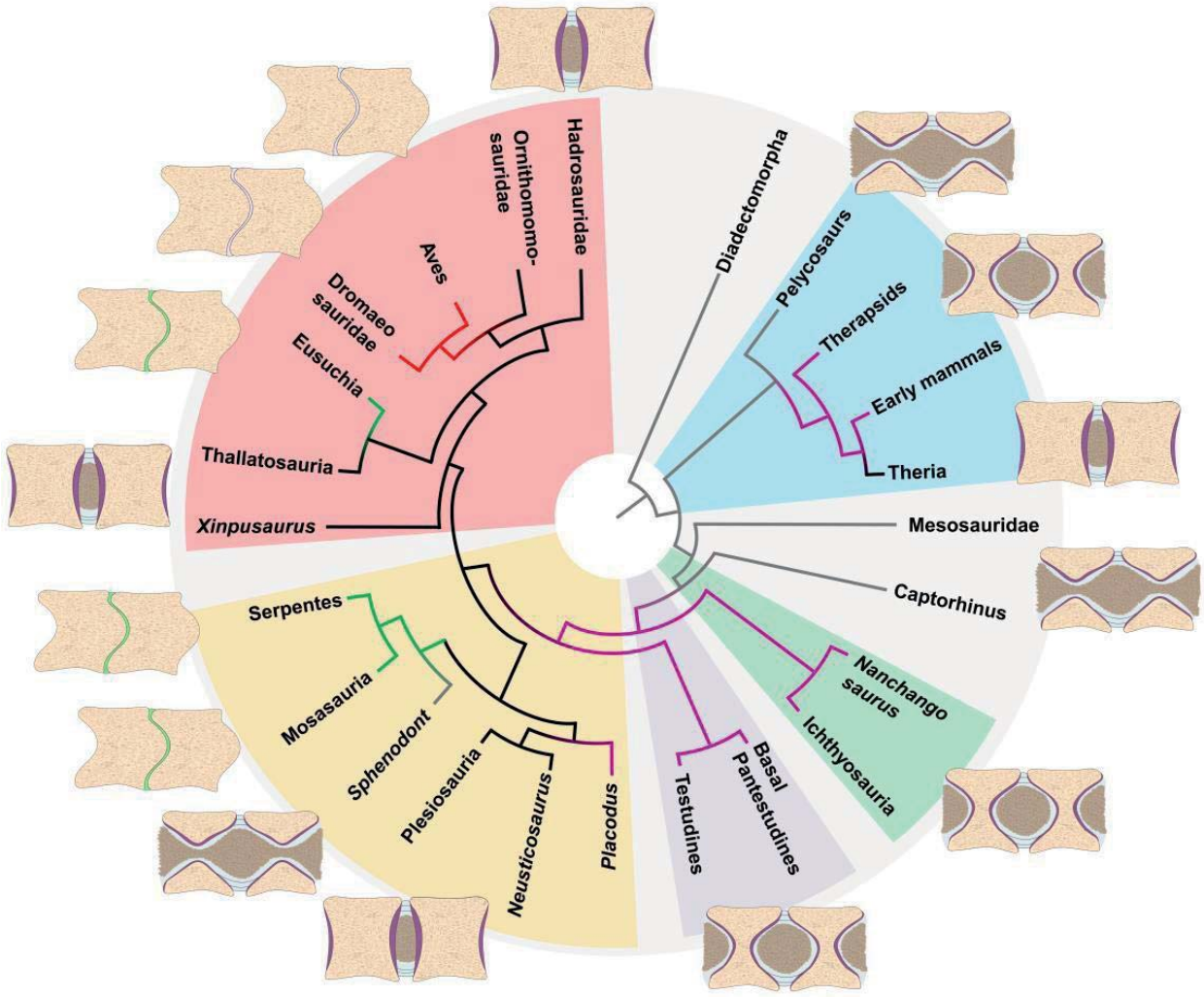

Figure 3 | Ancestral state reconstruction using parsimony of the different types of intervertebral joints in the phylogeny of the higher clades of amniotes. The schematic drawings of the intervertebral joints are explained in the text. Grey branches indicate persisting notochord. Purple branches indicate an intervertebral disc between amphicoelous centra. Black branches indicate an intervertebral disc between platycoelous centra. Green branches indicate a synovial joint with hyaline cartilage in between procoelous or opisthocoelous centra. Red branches indicate a fibrous cartilage joint. Key to clade colours: light blue, Synapsida; light green, Ichthyosauria; light purple, Testudines; light yellow, Lepidosauromorpha; light red, Archosauromorpha.

We suggest an evolutionary and developmental pathway (Fig. 3) of amniote vertebral joint evolution. In the plesiomorphic condition, the vertebral centrum is a ring of bone of periosteal origin surrounding the notochord. This ring of bone is connected to the adjacent vertebrae by a ring of fibrocartilage inserting in the endochondral domain and a ligamentous joint capsule inserting into the periosteal bone. Next, the ring of bone closes up in its centre by ossifying earlier in ontogeny (as observed in ichthyosaurs[23)], and the notochord is interrupted, forming a round aggregation of notochordal cells, the incipient

NP. At this stage, there still is little growth in the cartilaginous endplate. In the next step, cartilage cell proliferation and subsequent ossification increases greatly, resulting in a platycoelous centrum. The rims of the articular surface remain connected by fibrocartilage forming the AF, with the NP being fully developed. The transition to a ball-and-socket joint of reptiles involved the reduction of the

NP and the AF, i.e., the cartilage and notochordal components of the joint. This transition also involved a dramatic increase in anteroposterior asymmetry, with the formation of endochondral bone suppressed in the socket part of the joint and hypertrophied in the ball part. This asymmetry may be facilitated by the dual embryonic origin of the vertebral centrum from two somites caused by resegmentation[15]. This pathway presented her results in hypotheses that are testable using developmental genetics, and a promising model organism are geckos which form both amphicoelous and procoelous joints in individuals from the same clutch[24].

The convergent evolution of the IVD in synapsids and reptiles had remained unrecognised for two reasons: First, the general belief was that amphicoelous vertebrae did not house an IVD based on the only extant amphicoelous amniotes, *Sphenodon* and some geckos. We now recognise the presence of an IVD in extinct amphicoelous reptiles, e.g., in ichthyosaurs.

Second, reptile clades that had independently evolved an IVD went extinct at the end of the Cretaceous, after giving rise to synovial ball-and-socket joints and bird-type intervertebral joints. However, we consider it unlikely that these types of joints were the decisive factor in survival. Synovial ball-and-socket joints also evolved in Jurassic sauropodomorph dinosaurs[25] and in some non-avian theropod dinosaurs[26]. While the biomechanical advantages of ball-and-socket joints appear obvious, among mammals, only the long-necked ungulates approach this condition, raising the question of the evolutionary constraints on the transition from an IVD to a synovial joint. Given the distribution of these features on the amniote tree, further studies on well-preserved fossils may inform on this issue.

Methods Summary

Histological sampling, analysis, and inference

Our sample base comprises 29 vertebral centra of fossil and extant representatives of all major amniote clades, including mammals, non-mammalian synapsids, and reptiles

(including stemdiapsids, lepidosauromorphs, stem archosauromorphs, non-avian dinosaurs and birds) (Tab. 1). For the fossil in our sample, we employed petrographic thin sectioning following standard sampling techniques (e.g., core drilling[27]) and palaeohistological sectioning techniques[28].

Within the limits of availability, we focused on segments of the vertebral column from conservation deposits containing at least two vertebrae in articulation. Extant taxa were either studied from isolated vertebrae using ground sections or from standard soft tissue histology, including staining after decalcification, of segments of the spine and surrounding tissues. Information for extant taxa was complemented by a literature survey.

The histological sections of fossils allow different levels of inference about the nature of the tissues occupying the space between the bony end plates of successive vertebrae. This includes cartilage preserved in different states of alteration and histological correlates of such tissues in the bone and cartilage of the end plate. The direction and presence/absence of files of cartilage and anchoring fibers in the bone allow mapping of the AF and NP (Figs. 1a-c and 2c-e). In some black shale specimens, there is evidence of altered or templated tissues other than hyaline cartilage, i.e., the fibrocartilage of the AF and the cells of the NP. See SI for details of histological methods.

Ancestral character state reconstruction

For the reconstruction of the evolution of the intervertebral articulation in amniotes, we used ancestral character state reconstruction functions[6] in Mesquite[29]. We built a consensus tree of the sampled amniotes based on the literature. Because the phylogenetic position of turtles remains uncertain beyond their diapsid affinities, we placed them in the least nested position on the diapsid stem, but more derived than Ichthyosauria. We recognized five character states describing the different types of intervertebral joints.

References

1 Romer, A. S. *Osteology of the Reptiles*. (The University of Chicago Press 772pp., 1956.)

2 Hall, B. K. *Bones and Cartilage. 2nd Edition. Developmental and Evolutionary Skeletal Biology*. (Academic Press, 2015).

3 Schweitzer, M. H. Soft tissue preservation in terrestrial Mesozoic vertebrates. *Annual Reviews in Earth Planetary Science* **39**, 187–216. (2011).

4 Briggs, D. E. G., Summons, R. E. Ancient biomolecules: Their origins, fossilization, and role in revealing the history of life. *BioEssays* **36**, 482–490. (2014).

5 Service, R. F. Researchers close in on ancient dinosaur proteins. "Milestone" paper opens door to molecular approach. *Science* **355**, 441-442. (2017).

6 Pontarotti P., Hue, I. Road map to study convergent evolution: A proposition for evolutionary systems biology approaches. In: Pontarotti P, ed. *Evolutionary Biology. Convergent Evolution, Evolution of Complex Traits, Concepts and Methods*, 3-21. (Springer Nature, 2016).

7 Chan, W. C., Au, T. Y., Tam, V., Cheah, K. S., Chan, D. Coming together is a beginning: the making of an intervertebral disc. *Birth Defects Research Part C Embryo Today* **102**(1), 83-100. (2014).

8 Zug, G. R., Vitt, L., J., Caldwell, J. P. *Herpetology - An Introductory Biology of Amphibians and Reptiles*. (Academic Press, 2001).

9 Gadow, H. F. *The Evolution of the Vertebral Column. A Contribution to the Study of Vertebrate Phylogeny.* (Cambridge University Press; 356 p., 1933).

10 Gadow H. F. On the evolution of the vertebral column of Amphibia and Amniota. *Philosophical Transactions of the Royal Society London B, Containing Papers of a Biological Character* **187**, 1-57. (1896).

11 Holder, L. A. The comparative morphology of the axial skeleton in the Australian Gekkonidae. *Zoological Journal of the Linnean Society* **44**(297), 300-335. (1960).

12 Scaal, M., Christ, B. Formation and differentiation of the avian dermomyotome. *Anatomy and Embryology* **208**(6), 411-424. (2004).

13 Christ, B., Huang, R., Scaal, M. Amniote somite derivatives. *Developmental Dynamics* **236**, 2382–2396. (2007).

14 Cox, M., Serra, R. Development of the intervertebral disc. In *The Intervertebral Disc: Molecular and Structural Studies of the Disc in Health and Disease*. (eds. I. M. Shapiro & M. V. Risbud). (Springer ,2014).

15 Scaal, M. Early development of the vertebral column. *Seminars in Cell and Developmental Biology* **49**, 83–91. (2016).

16 Nosikova, Y. S., Santerre, J. P., Grynpas, M., Gibson, G., Kandel, R. A. Characterization of the annulus fibrosus-vertebral body interface: identification of new structural features. *Journal of Anatomy* **221**(6), 577-589. (2012).

17 Padian, K., Lamm, E. T. (Eds.). *Bone Histology of Fossil Tetrapods: Advancing Methods, Analysis, and Interpretation*. (University of California Press, 2013).

18 Schweitzer, M. H., Wittmeyer, J. L., Horner, J. R., Toporski, J. K. Soft-tissue vessels and cellular preservation in *Tyrannosaurus rex*. *Science* **307**, 1952-1955. (2005).

19 Wiemann, J. *et al.* Fossilization transforms vertebrate hard tissue proteins into N- heterocyclic polymers. *Nature Communications* **9**, 4741. (2018).

20 McNamara, M. E. *et al.* Reconstructing carotenoid-based and structural coloration in fossil skin. *Current Biology* **26**, 1075–1082. (2016).

21 Maldanis, L. *et al.* Heart fossilization is possible and informs the evolution of cardiac outflow tract in vertebrates. *eLife* **5**, e14698, 14691-14612. (2016).

22 Wang, X. *et al. Archaeorhynchus* preserving significant soft tissue including probable fossilized lungs. *PNAS* **115**, 11555-11560. (2018).

23 Houssaye, A., Nakajima, Y., Sander, P. M. Structural, functional, and physiological signals in ichthyosaur vertebral centrum microanatomy and histology. *Geodiversitas* **40**, 161-170. (2018).

24 Werner, Y. L. The ontogenic development of the vertebrae in some gekkonoid lizards. *Journal of Morphology* **133**(1), 41-91. (1971).

25 Fronimos, J. A., Wilson, J. A. Concavo-convex intervertebral joints stabilize the vertebral column in sauropod dinosaurs and crocodylians. *Ameghiniana* **54**, 151–176. (2017).

26 Holtz, T. R., Brett-Surman, M. K., Farlow, J. O. *The Complete Dinosaur. Second Edition*. (Indiana University Press, 2012).

27 Stein, K., Sander, P. M. in *Methods in Fossil Prepraration: Proceedings of the First Annual Fossil Preparation and Collections Symposium.* Lithodendron: The Occasional Papers of Petrified Forest National Park 1 (eds. M.A Brown, J.F. Kane, & W.G. Parker) 69-80. (2009).

28 Lamm, E.-T. *Bone Histology of Fossil Tetrapods. Advancing Methods, Analysis, and Interpretation* (eds. K. Padian & E.-T. Lamm) 55-160. (University of California Press, 2013).

29 Maddison, W. P., Maddison, D. R. Mesquite: a modular system for evolutionary analysis. Version 3.02 http://www.mesquiteproject.org. (2015).

Acknowledgements: Samples were provided by Liu Jun (Hefei University of Technology, Hefei, China); Thorsten Wappler (Hessisches Landesmuseum Darmstadt, Germany); Silke Schweiger (Naturhistorisches Museum Wien, Vienna, Austria); Heinz Furrer (Paläontologisches Institut und Museum Universität Zürich, Switzerland); Xaver Donhauser, Stuttgart, Germany; Georg Heumann (Steinmann Institute Paleontology Collection, University of Bonn, Germany); Phil Currie (University of Alberta Collection of Vertebrate Paleontology). Olaf Dülfer, Pia Schucht, and Andreas Peters provided technical support. This work received support from the Deutsche Forschungsgemeinschaft (DFG, German Research Foundation) und grant numbers SA 469/47-1 and SA 469/53-1 to PMS and grant number SCHE 1882/1-1 to RS. This is contribution number x of the DFG research unit 2685
”Fossilization”.

Author Contributions: T.W., P.M.S. and M.S. conceived the study, designed analytical protocols, and analyzed the data. T.W. and P.M.S. wrote the manuscript. All authors collected and processed data and provided input to the manuscript.

Author Information Reprints and permissions information is available at www.nature.com/reprints. The authors declare no competing financial interests. Readers are welcome to comment on the online version of the paper. Correspondence and requests for materials should be addressed to T.W. (tanja.wintrich@uni-bonn.de) or P.M.S. (martin.sander@uni-bonn.de).

Reviewer Information Nature thanks XX and the other anonymous reviewer(s) for their contribution to the peer review of this work.

Supplementary Information

Fossil soft tissues indicate convergent evolution of the intervertebral disc in non-mammalian amniotes

Wintrich *et al.*

This Supplementary Information includes:

Supplementary Notes 1-5

1. Supplementary Note 1: Background information on amniote intervertebral joints
2. Supplementary Note 2: Background information on cartilage fossilization
3. Supplementary Note 3: Detailed methods
4. Supplementary Note 4: Specimen descriptions

Supplementary Figures 1-29

Supplementary Tables 1-2

1. Supplementary Table 1: Specimens and taxa used in the study
2. Supplementary Table 2: Summary of results

Supplementary Notes 1-5

1. Supplementary Note 1: Background information on amniote intervertebral joints

1.1 Disparity of vertebral centrum shape and connecting joints

The vertebral column is one of the synapomorphies of vertebrates. During the evolution of the vertebral column from basal vertebrates to amniotes, the structure and morphology changed in different directions and under different selection pressures in different environments. In amniotes, we traditionally distinguish four principal designs of the vertebral bodies or centra (Romer 1956). First, the amphicoelous notochordal vertebral centrum which can be seen, for example, in basal synapsids such as the iconic sail-backed *Dimetrodon*. This vertebral centrum has an hourglass cross section, with a funnel-shaped indentation at the cranial and caudal ends which are connected by a small foramen or canal for the notochord. Second, the non-notochordal amphicoelous centrum in which bone replaced the notochord in the middle of the centrum, such as in ichthyosaurs (Houssaye et al. 2018). Third, the platycoelous vertebral centrum which has a flat surface at the cranial and caudal ends. This structure is seen in mammals and in extinct reptiles, e.g., in most non-avian dinosaurs and in most sauropterygians. In mammals, platycoelous vertebrae are connected by an intervertebral disc (IVD). The fourth vertebral body shape includes procoelous and opisthocoelous. This shape resembles a ball and socket shape, with a bulging surface in the one vertebral centrum and a matching excavation in the following vertebral centrum. In procoelous vertebrae, the socket is anterior and the ball is posterior, whereas in opisthocoelous vertebrae, the ball is anterior and the socket is posterior. However, in both cases they are part of a synovial ball-and-socket joint. An intervertebral ball-and-socket joint is seen in extant reptiles such as most lizards, all snakes, all crocodiles, and the neck vertebrae of turtles. Birds also have ball-and-socket joints that articulate via fibrocartilage. The shape of the vertebral centrum and the nature of the joint is important for the extent and the mode of flexibility of the vertebral column. It has long been recognized that ball-and-socket joints evolved convergently in the different reptile groups, but the IVD has been considered to be unique to mammals.

1.2 Centrum morphology and development in non-tetrapods

Fishes exhibit a wide variety of vertebral designs. The notochord persists throughout life in cyclostomes, ostracoderms, placoderms, acanthodians, most chondrichthyans and several osteichthyans. While there is no evidence for centra formation in jawless vertebrates and acanthodians, ossified vertebral centra occur in a few placoderms (Arratia et al., 2001 and references therein), several fossil sarcopterygians, numerous fossil and most extant actinopterygians. Within chondrichthyans, holocephalians exhibit a persistent notochord with cartilaginous arcualia and no centra, whereas in most neoselachians, cartilage cells from the arcualia invade the fibrous sheath of the notochord, giving rise to cartilaginous chordacentra that expand to form hourglass-shaped vertebrae. Accurate age estimates are often possible due to calcified growth zones that mark annual growth stages, at least unless the growth lines converge and become difficult to discern in very old individuals (e.g., Goldman et al., 2012). The notochord becomes constricted and sometimes incised intravertebrally, but occupies the large intervertebral space between the amphcoelous centra (Ridewood, 1921).

In contrast to extant coelacanth and lungfishes that do not possess vertebral centra, amphicoelous or slightly opisthocoelous centra with a small perforation for the notochord were present in some Palaeozoic dipnoans (Arratia et al., 2001). Among extinct sarcopterygian groups, vertebral centra are known in certain porolepiforms, osteolepiforms and elpistostegalians. Despite the diversity of vertebral morphologies within these groups, the general patterns are the most widespread aspidospondylous (arcocentral) vertebrae consisting of paired basidorsals (neural arches), paired interdorsals (pleurocentra) and paired ventral arches (intercentra), and holospondylous (ring-like) vertebrae known in *Megalichthys*, *Ectosteorhachis* and a few other genera (Laerm, 1979; Arratia et al., 2001). Centrum morphology can vary along the body (Arratia et al., 2001). In any case, the notochord retains its general shape and stabilizing function in most non-tetrapod sarcopterygians.

In fossils of early actinopterygians, vertebral structures of are often covered by scales. Most non-neopterygians exhibit a notochord with cartilaginous or ossified arcualia, and there are only few taxa with chorda- or arcocentral vertebrae in the shape of half-rings or rings. Notable exceptions are the enigmatic Carboniferous fish *Tarrasius*, which shows amphicoelous vertebrae in a tetrapod-like pattern of axial regionalization (Sallan, 2012),

and polypteriforms that possess hourglass-shaped centra with an ontogenetically increasing notochord constriction in the middle (Bartsch, 1988).

A variety of vertebral morphologies is also observed in neopterygians. Pycnodonts, for instance, had a persistent notochord with expanded arcualia but no centra. Vertebrae of many fossil halecomorphs are of arcocentral type, i.e., centrum ossification starts from the dorsal and ventral arcualia. In the recent bowfin *Amia calva*, the notochord is completely excluded from the centra and reduced to intervertebral spaces, leading Bartsch (1988) to use the term *discus intervertebralis* for this structure.

1.3 The intervertebral disc (IVD) in mammals: structure and development

The IVD is a fibrocartilaginous synarthrotic joint connecting the vertebral centra of mammals. It provids intervertebral flexibility allowing for a wide range of movements and is involved in shock absorbance and transmission of mechanical forces (Pattappa et al. 2012; Cox and Serra 2014). The IVD is composed of two distinct parts, a central hydrophilic proteoglycan-rich gelatinous core, the *nucleus pulposus* (NP), and a surrounding ring, the *annulus fibrosus* (AF), which consists of a combination of spirally arranged layers of collagen I and fibrocartilage. The joint formed by the IVD is further stabilized by intervertebral ligaments that insert in the periosteal cortex of the vertebral centrum.

During embryonic development, the NP is formed at an early ontogenetic stage and is derived from the notochord cells, whereas the fibrocartilaginous AF is derived from cells of the sclerotome (Paavola et al. 1980; Theiler 1988; Rufei et al. 1995; Christ et al. 2004, 2007; Cox and Serra 2014; Scaal 2016). Sclerotomes are the ventral compartments of the somites, the primary mesodermal segments of the vertebrate embryo. The sclerotomes are formed by mesenchymal cells which are proliferative and which migrate as expansive cell populations to their destination in the embryo.
Within the sclerotome, at least four subcompartments can be distinguished according to their location in the somite: ventral, central, lateral, and dorsal sclerotome. The ventral sclerotome gives rise to the vertebral centrum and the fibrocartilaginous AF (Cox and Serra 2014, Scaal 2016), the central sclerotome gives rise to the pedicles of the vertebral arches and the heads of the ribs, whereas the dorsal sclerotome forms the lamina of the neural arch and the lateral sclerotome forms the more distal parts of the ribs (Christ et al.

2007; Cox and Serra 2014; Scaal 2016).

During sclerotome development, the process of resegmentation takes place, in which the primary segmentation pattern of the somites is replaced by the secondary segmentation pattern of the vertebrae, which are offset by one segment half. The border between prospective vertebrae, and thus the location of the prospective IVD, is visible already in the intact sclerotome as a fine cleft, which is known as von Ebner's fissure. The AF of the IVD forms from the sclerotomal cells close to von Ebner's fissure, which are derived from the somitocoel of the early somites which has been shown to give rise to vertebral joints and is therefore called arthrotome (Huang et al. 1994; Mittapalli et al. 2005). Furthermore, during development, the NP is derived from the notochord, a rod-shape embryonic structure in amniotes (Stemple 2005; Cox and Serra 2014).

1.3.1 The endplate in mammals

Mammals differ from most other amniotes in the fact that their loing bones have secondary centers of ossification, resulting in bony epiphyses that fuse to the metaphysis upon skeletal maturity. Some mammals also have such secondary centers of ossification in the vertebral centra. In more recent publications dealing with ossification timing in mammals, the pattern is observed that neural arches start to ossify earlier than vertebral centra (Hautier et al. 2013; Hautier et al. 2010), but no statement is given about the presence of epiphyses in vertebrae. There are only few publications describing the presence of bony vertebral centrum epiphyses. Some publications depict rugose vertebral centra surfaces pointing to the presence of bony epiphyses, for example in the kangaroo or the dolphin (Boszczyk et al. 2001: figs. 5b and 11b).

In the albino rat, all vertebral centra have epiphyses at both ends, except atlas and axis, and the last fourteen caudal vertebrae (Strong 1925). Dawson (1927) draws a different picture with bony epiphyses on both ends only in caudal lumbar vertebrae, and all of the caudal vertebrae. Cervical and cranial thoracic vertebrae lack bony epiphyses, while caudal thoracic vertebrae and cranial lumbar vertebrae possess epiphyses only on the caudal ends of the vertebral centra (Dawson 1927). Dawson (1927) furthermore suggests "that Strong (1925) in his account must have mistaken calcified cartilage for bone". The clarification of the discrepancy between these two authors awaits further investigation.

Bony epiphyses are also present for instance in the centra of the European mole (*Talpa europaea*, STIPB M7003), the European water vole (*Arvicola terrestris*, STIPB M1047), and the European hedgehog (*Erinaceus europaeus*, STIPB M7611).

In the reindeer (*Rangifer tarandus*, STIPB M47), the vertebral column shows bony epiphyses at the centra from the posterior end of the axis to the anterior end of the sacrum. The cervical and the lumbar vertebral epiphyses close the sutures with the centra earlier than the thoracal vertebrae. The cervical centra are opisthocoelous, while all other centra are platycoelous. As depicted by Danowitz and Solounias (2015: fig. 4), extant giraffes (*Giraffa camelopardalis* and *Okapia johnston*i) also show opisthocoelous cervicals and (at least) posterior epiphyses. Opisthocoelous neck vertebrae can also be found in rhinos (e.g., the fossil *Stephanorhinus etruscus*, STIPB M2828). The degree of concavity of the posterior neck vertebra surface is comparable in giraffes and rhinos, and less concave in the reindeer. The distribution of bony vertebral centra epiphyses in the wild boar (*Sus scrofa*, STIPB M56) is as in the reindeer from the posterior end of the axis to the sacrum. Contrary to reindeer, giraffes, and rhinos, the wild boar cervical vertebrae show platycoelous centra, as do small mammals like hedgehog, vole, and mole. Kemp (2006) lists this character of the platycoelous vertebral centrum for Therapsida. For Neotherapsida, he furthermore lists the character "epiphyses on atlas vertebra" (Kemp 2006) which suggest the presence of bony vertebral centra epiphyses in Neotherapsida or even more primitive synapsids.

In humans the situation is slightly more complex. As Dar et al. (2011; see references therein) summarize, there is a cartilaginous apophysis (incorrecty called an 'epiphyseal ring'), which ossifies itself, but is not a true epiphysis, because it does not contribute to vertebral centrum growth. The lack of true bony vertebral centrum epiphyses in humans might be a result of our bipedal locomotion.

1.4 Cartilaginous tissues in intervertebral joints and their relationship to bone

The background information provided in this section is textbook knowledge that is necessary, however, for understanding our inferences on soft part anatomy in the fossils. Recommended references are Francillio-Vieillot et al. (1990) and Hall (2015).

1.4.1 Differentiation of cartilaginous cells

Cartilaginous tissue can be differentiated into three types which all contain chondrocytes and which vary with respect to the composition of the extracellular matrix (ECM). The first is the hyaline cartilage (HC), second the elastic cartilage (EC), and third the fibrocartilage (FC). Cartilaginous cells are derivatives of mesenchymal cells, which differentiate into chondroblasts and finally chondrocytes. Here we discuss only the HC and the FC because the EC, which is characterized by the presence of elastic fibers, is not relevant for IVDs and other intervertebral joints.

1.4.2 Hyaline cartilage

Hyaline cartilage is seen, e.g., in joint articular surfaces, in the rib cartilage and in the tracheal cartilage. In diarthroses, which represent true articulations of bone with an intra-articular space, the articular facet is covered by HC. For HC, synovial fluid is essential because of the avascularity of HC. HC extracellular matrix contains collagen type II, proteoglycans, and water. The interactions of different components can be described by the Benninghoff-Arkaden module, which explains the architecture of the HC as an elastic spring and therefore makes the HC pressure elastic, which means that the HC is reversibly compressible. This fact is important for a diarthrosis joint. Except for the diarthrosis joint, HC is also the product of the perichondrium which surrounds all areas of cartilage except for joint surfaces. The perichondrium may be differentiated into two different layers, first the *stratum fibrosum* which is a collagen- fiber connective tissue providing resistance of the cartilage against shear stress, and second a layer called the *stratum chondrogenicum* which contains mesenchymal cells which can differentiate into chondroblasts. The perichondrium is the source of appositional growth in length of skeletal elements.

1.4.3 Fibrocartilage

In humans, the fibrocartilaginous tissue is seen in the annulus fibrosus (AF) of the IVD, the pubic symphysis, in articulation discs and in the meniscus of the knee joint. The difference between HC and FC is that fibrous cartilage contains collagen I fibers in addition to cartilage-specific collagens like collagen II, whereas hyaline cartilage does not. In the IVD we see that the fibers of the AF extend in spiral torsion from one vertebra to the next vertebra. Between the subchondral lamella of a vertebra and the AF, there is a

layer of HC. The joint between two vertebrae in mammals is a synarthrosis as it is lacking an articular cavity.

1.4.4 Bone tissues of the vertebral centrum

Ossification of the vertebral centrum starts by replacement of embryonic cartilage by bone. Specifically, cartilage is resorbed and bone-forming cells (osteoblasts) secrete bone tissue in its place (endochondral bone formation). However, at the anterior and posterior end of the embryonic centrum, new cartilage continues to be formed by cartilage-forming cells (chondroblasts), producing a growth front (growth plate) that underlies the joint between adjacent centra. The part of the centrum that results from this process is the endochondral domain. The process of endochondral bone formation continues until growth of the centrum stops. In some mammals, the process of endochondral ossificaton also takes place towards the joint, resulting in a secondary center of ossification or bony epiphysis (see section 1.3.1). When growth ceases, the secondary center of ossification fuses with the rest of the centrum. The surface of the endochondral bone, forming the articular surface in vertebral centra and long bones, is typically rough or pitted, reflecting the cartilage cover of the bone. Endochondral bone surfaces are commonly called “unfinished” in palaeontology (e.g., Romer 1956).

The cartilage growth front consists of a differentiation part, a proliferation part, and a hypertrophication part. Chondroblasts differentiate from more generalized cells in the differentiation part and divide in the proliferation part, forming characteristic files of cartilage cells (chondrocytes) that are oriented roughly in the direction of growth. Older chondrocytes increase in size and mineralize gradually a hydroxyapatite ECM, providing a local source of for the components of the bone matrix that will replace them. This tissue of enlarged chondrocytes in the hypertrophication zone commonly is called “calcified cartilage”. This has led to confusion in the past with cartilaginous tissues that are more highly and regularly mineralized and are never replaced by bone, such as in the endoskeleton of chondrichthyans (see above). True calcified cartilage is rare in amniotes and was not observed in our study. The cartilage differentiation zone is also the source of the hyaline cartilage of the amniote joint (but not the NP). The fibrocartilage of the joint inserts in the endochondral domain. The tissue showing files of chondrocytes is also called “serial cartilage”.

Returning to the early growth of the vertebral centrum, soon after the onset of endochondral ossification, the embryonic cartilage core will be surrounded by a bone-producing connective tissue containing osteoprogenitor cells and osteoblast, the periost. Bone produced by the periost does not have a cartilage precursor but is deposited layer by layer, producing the growth in girth of the vertebral centrum. The ligaments of the joint capsule and intervertebral ligaments exclusively insert in the periosteal bone. The insertion sites remain visible in the bone tissues as Sharpey's fibers. The different mechanisms of tissue formation between the endochondral bone and the periosteal bone result in a sharp border between the two domains that is preserved until it is obliterated by secondary remodeling. Morphogenesis of the vertebral centrum thus consists of the interplay between growth in the endochondral domain and the periosteal domain. Long bones of amniotes show the same growth mechanism and domains. The surface of the periosteal bone is typically smooth and only pierced by vascular foramina. Periosteal bone surfaces are commonly called "finished" in palaeontology (e.g., Romer 1956).

1.5 Previous discussions on the intervertebral disc in fossil amniotes

In the fossil record, soft tissues are rare because they do not preserve well. This also applies to fossil preservation of the IVD, making it difficult to determine the type of articulation between vertebral centra in extinct animals. One has to rely on the structure of the bones. On comparative grounds, the most common view is that fossil reptiles do not have an IVD because extant reptiles do not show this feature but have ball-and-socket joints instead (except for *Sphenodon punctatus* and some geckoes). A true IVD connects the centra of adjoining vertebrae, precluding the presence of an articular cavity (Frey & Salisbury 2001). However, we see in the fossil record that the centrum morphology is definitively not always a "ball and socket" shape (e.g., Romer 1956). Romer (1956) generally describes the progression from amphicoelous notochordal to amphicoelous non-notochordal to platycoelous types of vertebrae.
Furthermore, if we turn to developmental biology, mammals and birds (or archosauromorphs) are in focus of the research. But the evolutionary aspect of the intervertebral disc and its first occurrence in the fossil record is not clarified yet. In paleontology, there are few mentions about IVDs in fossils at all such as the study by Witzmann et al. (2008) and Hopley (2001). The latter describes a spinal pathology in a plesiosaur vertebra suggesting a disc prolapse and consisting of a Schmorl´s

node, which is a pathologic intrusion of the NP into the bony centrum. Rothschild & Berman (1991) describe th preservation of the intervertebral space in the caudal vertebrae of a sauropod dinosaur.

2. Supplementary Note 2: Background information on cartilage fossilization

2.1 Preservation of non-mineralized skeletal and connective tissues

It has long been understood that the anoxic conditions leading to the deposition of black shales permit the preservation of soft parts, primarily of the integument, meaning that the potential exists that non-mineralized connective tissues will preserve. Hence, ideally, the articulated segments of vertebral column that we studied were still at least partially embedded in the matrix. This is important to be able to compare potentially preserved soft parts in the intervertebral spaces with the host sediment.

Cartilage fossilizes well if it is mineralized, i.e., if the chondrocytes mineralize in a spherulitic arrangement of apatite crystallites, as in the case in calcified cartilage of chondrichthyans. However, fossilization of cartilage has been little studied, and any evidence of cartilage in a fossil traditionally has been subsumed by paleontologist unter the term "calcified cartilage", even if the tissue in question was not mineralized in life (e.g., LeBlanc et al. 2018 Fig. 1e). There is true calcified cartilage in extinct amniotes, i.e., serial cartilage that was not replaced by bone but was fully mineralized in the living animal. An example is provided by some pachypleurosaurs, small Triassic sauropterygians, in which these tissues served to increase skeletal mass (Ricqlès 2001, Houssaye et al. 2013). The term calcified cartilage, however, is also used for the zone of hypertrophy of chondrocytes in the growth plate of amniote long bones (Francillon-Vieillot et al. 1990). This cartilage is replaced completely by endochondral bone during the growth phase of the animal and its presence suggests immaturity. Whereas the hypertrophy zone may show increased mineralization (Francillon-Vieillot et al. 1990), favoring fossilization, the chondrocytes do not show the characteristic spherulitic radial crystallite arrangement of true calcified cartilage. We note that true calcified cartilage was not encountered in this study.

3. Supplementary Note 3: Detailed methods

3.1. Acquisition of histological and morphological data

For this study, we histologically sampled 22 specimens representing 19 taxa of different amniote clades which includes mammalians, non-mammalian synapsids, and reptiles (including non-avian dinosaurs and birds) (see Supplementary Table 1). We used histological ground sections (mostly for fossil taxa), histological demineralized sections (for extant taxa) and morphological data, i.e., the shape of the bony articular surface of the vertebral centra (see Supplementary Table 1). For the stem reptile *Captorhinus*, we used the histological images in LeBlanc et al. (2018). For the morphological part, we checked the general applicability of our observations with information from the rich literature on amniote vertebral centrum morphology, including another three taxa for which morphological (non-mammalian therapsids, basal mammals) and also histological information (*Alligator*) is available. Extant turtles are a special case because they lack intervertebral joints between the dorsal vertebrae which are integrated into the carapace. The stem turtles *Pappochelys*, *Odontochelys*, and *Eorhynchochelys* lack a carapace and have non-notochordal amphicoelous vertebrae (Li et al. 2008, 2018, Schoch & Sues 2015). No histological data are available for these taxa, but we included the published morphological information in some analyses.

3.2. Sampling and histology of fossil and extant non-decalcified material

Two types of fossil material were sampled for this study. First, this is segments of the dorsal vertebral column of articulated skeletons as well as isolated but articulated segments of at least two centra. In the latter, we focused on specimens in which the vertebrae are preserved in close articulation. These specimens originally also pertained to articulated skeletons that were collected in an incomplete state, however. The incomplete state presumably is due to loss to weathering before discovery. The second type is isolated vertebral central that were sampled if articulated column segments were not available.

Articulated column segments are primarily found in conservation deposits such as black shales (e.g., the Posidonienschiefer Formation of southern Germany), but isolated vertebrae derive from a host of different sediment types. The segments of vertebral column

and isolated vertebrae were sectioned as exactly in the sagittal plane as possible. In the case of longer segments (e.g., *Mesosaurus*, *Stenopterygius*, *Neusticosaurus*, etc.), there was some degree of curvature of the vertebral column, but we attempted to intersect at least two adjacent centra in the exact sagittal plane. The half of the segment that represented the closest approximation to the sagittal plane was then processed into a petrographic thin section following standard methods (e.g., Lamm 2013). Thin sections were ground to a thickness of 50 to 80 µm, depending on the degree of dark staining. Thin sections were then examined with a standard polarizing microscope, either a Leica DLMP or a Zeiss Axio Imager und normal and cross-polarized light with and without a lambda filter. Images were taken with a Leica digital camera and processed with ImageAccess EasyLab 7 software.

Dental tissues and bone fossilizes very well at the histological level, and observations using light microscopy are directly transferrable from fossil to extant comparative material (Francillon-Vieillot et al. 1990, Padian & Lamm 2013). Histological descriptions of fossil hard tissues accordingly use the same terminology as for extant amniotes, and this terminology is discussed in detail by Francillon-Vieillot et al. (1990). In normal light, all types of bone tissue (periosteal, endochondral, secondary) show a brownish stain of the matrix developed during fossilization (Wiemann et al. 2018). Osteocyte lacunae are generally visible in this bone matrix. Remains of cartilaginous tissues, on the other hand, generally lack the brownish stain, and are whitish or light grayish translucent. In polarized light, bone is easily distinguished from any kind of cartilage as well because of the birefringence of the bone apatite crystallites. Cartilage and other soft tissue remains lack birefringence or show the birefringence of the templating mineral, e.g., calcite. Preservation of intervertebral ligaments was not observed in this study, but the insertion of these ligaments can reliably be inferred from Sharpey's fibers inserting in the periost.

Although extant material is typically studied in decalcified microtome sections, ground sections (petrographic thin sectioning) of fresh bone can be studied as well. The advantage is a better identification of the bone tissue types because decalcification destroys the birefringence of the bone tissue. In addition, the observational relationship between bone, cartilage, and connective tissue is the same as in fossils,

offering an intermediate in the comparison between fossil ground sections and microtome sections. We studied some extant material using this technique (Supplementary Table 1).

3.3. Microtome histology of extant material

Two taxa (*Sphenodon* and *Python*) were successfully sampled by decalcified microtome section in the sagittal plane of the dorsal and caudal region of the vertebral column from consecutive vertebrae (Tab. 1).

The *Sphenodon* specimen used for sectioning is from the original collection of Reischek made in 1890 for the NHMW. Because it has been stored in ethanol for more than a century, the material was extremely desiccated and tough and therefore difficult to section with the microtome. After several washes in ethanol, rehydration and refixation with 4% paraformaldehyde (PFA), the samples were demineralized for 50 days in 8% EDTA at pH 8. After re-transfer into ethanol, the samples were embedded in paraffin following standard procedures. For sectioning on a standard microtome at 10 µm, special blades for hard tissue were used (N35HR microblades, pfm medical). After mounting on silane-coated glass slides, the sections were treated by HE staining and Heidenhain Azan staining according to standard procedures.

The *Python* samples were generated from fresh frozen material. The muscular tissue was partially removed from the vertebral column without damaging the vertebral ligaments. After fixation for 7 days in 4% PFA, the samples were washed and demineralized for 33 days in 8% EDTA at pH 8. Whole-mount preparations were cut with a razor blade in the median plane. Samples for histological sections were embedded in paraffin, sectioned at 10 µm with a standard microtome and treated by HE staining and Heidenhain Azan staining according to standard procedures.

3.4. Inferences on intervertebral tissues in fossils

Our ground histological sections of fossils allow different inferences, depending on the quality of preservation, about the nature of the tissues occupying the space between the bony end plates of successive vertebrae, These inferences are based on the principles of vertebral centrum and joint differentiation and growth discussed above. Isolated centra in all cases preserve histological evidence for the nature of the cartilage covering the bony end plate. This includes cartilage preserved in different states of alteration and histological correlates of such tissues in the bone and cartilage of the end plate. Based on the numerous descriptions and illustrations of human IVDs (e.g., Hall 2015) and of our own observations on histology of extant mammals (e.g., *Phoca vitulina*, see below), the direction and presence/absence of files of cartilage cells (chondrocytes) and anchoring fibers in the bone allow mapping of the AF and NP. Articulated segments of vertebral column from black shale settings, in addition, appear to preserve altered or templated tissues other than hyaline cartilage, i.e., the fibrocartilage of the AF and the cells of the NP. For details, see the description of the individual specimens.

3.5. Optimization of intervertebral articulation on the amniote tree

For the reconstruction of the evolution of the intervertebral articulation in amniotes, we used ancestral character state reconstruction (ASR, see Pontarotti 2016). We built a consensus tree of the amniotes sampled based on the literature, including 24 tip taxa. Because the phylogenetic position of turtles remains uncertain beyond their diapsid affinities and because no histological data are available for stem turtle vertebral centra, we ran the the ASR both with and without turtles to test whether their inclusion nevertheless might have an effect on the outcome of the ASR. In the analysis including turtles, we placed them in the least nested position on the diapsid stem, but more derived than Ichthyosauria, and we coded their vertebrae as non-notochordal amphicoelous (Li et al. 2008, 2018, Schoch & Sues 2015). We recognized five character states describing the different types of intervertebral joints based on our morphological and histological observations and inferences. These character states are as follows (Supplementary Table 1): 0, amphicoelous centrum with notochordal canal, continuous notochord; 1, non-notochordal amphicoelous centrum with IVD; 2, platycoelous centrum with IVD; 3, synovial ball-and-socket joint; 4, fibrous ball-and- socket joint. Data for non-mammalian

Therapsida, early mammals, and Eusuchia were taken from the literature (Supplementary Table 1). We then entered the consensus phylogeny and the states for the tip taxa into a NEXUS file and analyzed it in Mesquite v. 3.02 (Maddison & Maddison 2015) using both maximum parsimony (MP) and maximum likelihood (ML). For the ML reconstruction, we used the one-parameter Markov k-state probability model. The inclusion of turtles had not effect on the analysis, and we excluded them from further consideration.

4. Supplementary Note 4: Specimen descriptions

4.1. Diadectomorpha

4.1.1. *Diadectes sideropelicus*, STIPB A 169, Lower Permian, Texas, USA (Figure S1, S2,)

4.1.1.1 Morphological observations

The stem amniote *Diadectes* has deeply amphicoelous vertebral centra with a distinctive foramen connecting the anterior and posterior articular facets of the centra. The foramen is generally interpreted as allowing the notochord to pass through. The vertebral centrum is roughly isometric, whith a diameter to length ratio of about 1. The articular surface consists of a concave, funnel-shaped central part and a convex outer rim that is sharply set off from the outer, smooth surface of the centrum.

4.1.1.2 Histological observations

The sagittal section of the adult dorsal vertebra confirms the deeply amphicoelus nature of the centrum. Howver, the section failed to intersect the open notochordal canal because of imprecise processing. The thickness of the endochondral bone underlying the articular surface increases gradually from the center to the periphery of the articular surface, seen as four wedges of endochondral bone radiating outward from the growth center of the vertebra. Thus, throughout growth, the relative thickness of each domain of endochondral bone remains constant. The deeply amphicoelous shape of the centra thus is maintained from the onset of ossification until the termination of growth. The amphicoelous shape thus does not result from the limited production of endochondral bone in the articular area, unlike in all but the most basal ichthyosaurs (Houssaye et

al. 2018). While the boundary between the periosteal and endochondral domain forms a straight line, the outer part of the anterior and the posterio surface is convex, forming a rim around the articular surface.

The concave, "funnel" region of the articular surface lacks any indication of chondrocyte lacunae but is covered by a smooth layer of lamellar bone tissue instead. On the convex outer rim of the articular surface, chondrocyte lacunae are arranged in short, loose files, and there are bone spicules with fibers in between the files. Both ventrally and dorsally, the region of the periosteal bone adjacent to the boundary with the endochondral domain is rich in Sharpey's fibers. These are directed roughly parallel with the domain boundary, intersecting the surface of periosteal bone at a high angle.

4.1.1.3 Interpretation

The amphicoelous shape indicates that there was no synovial joint in *Diadectes* because in this type of joint there is a close morphological match of the two articular surfaces that form the joint. The distinct notochordal canal (not bisected by the sample but seen in the specimen) also is inconsistent with a NP, as is the smooth bone surface of the "funnel". There must have been some other kind of fill, presumably derived from the notochord. We interpret the remains of cartilage and bony spicules on the convex ring of the articular surface as the anchoring site for fibrocartilage, forming an AF. The direction of the fibers in the periosteal bone is consistent with them forming the insertion of a ligamentous connection between the vertebral centra.

4.1.1.3 Discussion

Based on the phylogenetic position of *Diadectes* as a stem amniote, we infer that it is the intervertebral joint of this taxon from which evolved the other kinds of intervertebral joints in amniotes. The vertebrae were connected by an AF on the outer part of the articular suface and by intervertebral ligaments inserting in the periosteal surface. The notochord persisted throughout ontogeny and continued to increase in girth in the intervertebral space in postembryonic and post-hatching ontogeny.

4.2. Synapsida

4.2.1. *Dimetrodon natalis* STIPB R 652a, 653a, 658, Lower Permian, Texas, USA (Figure S3, S4)

4.2.1.1 Morphological observations

As described in detail by Romer & Price (1940), *Dimetrodon* has deeply amphicoelous vertebral centra with a small foramen connecting the anterior and posterior articular facets of the centra. The foramen is generally interpreted as related to the notochord.

4.2.1.2 Histological observations

Sagittal sections of juvenile and adult dorsal vertebrae (STIPB R 653a and STIPB R 652a) and of two fused sacral vertebrae (STIPB R 658) confirm the deeply amphicoelus nature of the centra and the open notochordal canal. The thickness of the endochondral bone underlying the articular surface increases gradually from the center to the periphery of the articular surface, seen as four wedges of endochondral bone radiating outward from the notochordal foramen. Thus, throughout growth, the relative thickness of each domain of endochondral bone remains constant, making up about one eighth of the length of the centrum. The deeply amphicoelous shape of the centra thus is maintained from the onset of ossification until the termination of growth. While the boundary between the periosteal and endochondral domain forms a straight line, the outer part of the anterior and the posterior surfaces are convex, forming a rim around the articular surface.

Even in the juvenile, there is little retention of the original chondrocyte lacunae in the endochondral bone. However, the articular face is covered by a thin layer of chondrocyte lacunae that are arranged in an irregular fashion. These represent the hyaline cartilage cover of the articular surface, i.e., the active chondroblast differentiation zone of the growing vertebra. In the adults, there are no chondrocyte lacunae left except in the notochordal canal and the convex outer rim of the articular surface. There, the lacunae are arranged in short, loose files, and there are bone spicules with fibers in between the files. In the region forming the concave, “funnel” part, the articular surface of the adult actually is covered by a smooth layer of lamellar bone tissue. Both ventrally and dorsally, the region of the periosteal bone adjacent to the boundary with the endochondral domain is rich in Sharpey’s fibers.

These are directed roughly parallel with the domain boundary, intersecting the surface of periosteal bone at a high angle.

4.2.1.3 Interpretation

The amphicoelous shape indicates that there was no synovial joint in *Dimetrodon* because in this type of joint there is a close morphological match of the two articular surface that form the joint. The layer with the irregularly arranged chondroblast lacunae represent the hyaline cartilage cover of the articular surface, i.e., the active chondroblast differentiation zone in the juvenile. In the adults, the lack of a layer of cartilage and the smooth bony surface of the concave part of the articular surface suggest that there was no NP yet but some other kind of fill, presumably derived from the notochord. The lamellar bone layer in the "funnel" is particularly striking because it is not observed in any of the other samples. We interpret the convex ring of the articular surface as the anchoring site for fibrocartilage, forming an AF. The direction of the fibers in the periosteal bone is consistent with them forming the insertion of a ligamentous connection between the vertebral centra, possibly forming some kind of joint capsule.

4.2.1.4 Discussion

It has been consensus that basal synapsids such as *Dimetrodon* did not posses synovial vertebral joints (Romer & Price 1940). This is confirmed by our observations, in particular the persisting notochord. The intervertebral space of *Dimetrodon* must have looked very similar to that of amphicoelous geckos which was described in detail by Holder (1960). In these, the notochord is also continuous, increasing in diameter in the intervertebral spaces and decreasing as it passes through the growth center of the centrum. From an ontogenetic perspective, this means that the embryonic notochord has retained its diameter there but continued to grow in girth in the intervertebral space.

4.2.2. *Phoca vitulina* STIPB M 60, recent (Figure S5)

4.2.2.1 Morphological observations

Phoca vitulina, the common European seal, is represented in our sample by a thoracal vertebra that is part of a complete skeleton. Although the specimen is an adult, there is still a distinctive suture at either end of the vertebral centrum between the secondary centers of ossification (bony end plates, epiphyses) and the body of the centrum. The specimen is extant, and maceration has removed any soft parts. The open epiphyseal suture would indicate immaturity in a terrestrial mammal but is a paedomorphic feature seen in adults of marine mammals.

4.2.2.2 Histological observations

In the sagittal section, the sutures between the epiphysis and the body of the centrum are also distinctive and there is an open slit, not containing any soft parts. The surface facing the suture shows hyaline cartilage of the proliferation zone that then is transformed into bony trabeculae. The same situation is observed on the vertebral centrum facing the suture. The articular surface of the epiphysis is covered by a thin layer of cartilage cells partially embedded in bone matrix. The layer is at most three cells thick over most of the epiphysis.
Only towards the perimeter, the layer becomes thicker, and the cartilage cells are arranged in files with collagen fibres in between. The direction of the files and fibres in this region is obliquely outward from the center of the articular surface. The cartilage cells are distinctly irregular in size. The perimetral region extends right up to the epiphyseal suture.

4.2.2.3 Interpretation

As for all therian mammals, it can be assumed that the specimen possessed an intervertebral disc. However, the macerated specimen offers no direct histological evidence for the AF and NP but was included to aid in interpretation of the fossil samples. The thin layer of cartilage cells on the epiphysis is the remainder of the cartilaginous endplate, and the structures seen along the perimeter are the attachment of the fibrocartilage of the AF of the IVD. The direction of the fibers and files is the same as those in the AF, in a circumferential arrangement around the NP, as seen in soft tissue histological sections of mammals. The geometry of the NP

with a radius that is significantly smaller than that of the endplate and the geometry of the AF means that the angle of insertion of the fibers of the AF and the inclination of the associated cartilage cell files changes towards the periphery of the end plate. The central area of the cartilaginous endplate that lacks fiber insertions maps out the extent of the NP.

4.2.2.4 Discussion

A histological ground section of a macerated specimen of an extant mammal offers indications of some of the soft parts originally present (i.e., cartilaginous endplate, AF, NP) and their spatial arrangement. We then used this information to infer the types and distributions of intervertebral tissues in fossils.

4.2.3 cf. *Eurohippus* HLMD-ME 103, 106, 7835, middle Eocene, Messel, Germany (Figure S6)

4.2.3.1 Morphological observations

Three articulated specimens of ungulates from the famous Eocene lake deposits of Messel (Germany) were sampled in the hope of finding preserved soft parts, for which the locality is famous for, in the intervertebral space. Two of the three specimens are embedded in an artificial matrix and showed evidence of soft part preservation.

4.2.3.2 Histological observations

Two (HLMD-ME 103, 7835) of the three Messel specimen were extremely crushed, showing a near-complete collapse of the trabecular architecture and complete compaction of the internal vascular spaces. Nevertheless, fragments of the bony endplates were sufficiently preserved to show the same features as the *Phoca* vertebra, in particular the distinction between the inner region with very little cartilage and the perimeter with thicker cartilage, cells arranged in files and fibers parallel to these files. The outward direction of these features is the same as in *Phoca*. However, none of the three Messel mammals show an epiphyseal suture zone. Also, none of the Messel mammal specimens showed any indication of the preservation of soft parts of the intervertebral space such as the AF and the NP.

4.2.3.3 Interpretation

The observed histological features are the same as in the extant mammal, *Phoca*, and suggest that the Messel mammals possessed a mammalian-type IVD. The lack of epiphyseal sutures in the Messel mammals indicates that the sampled individuals were adults.

4.2.3.4 Discussion

Apart from the extreme crushing, the preservation of the Messel mammal samples is similar to the macerated extant mammal in our sample. This is somewhat surprising because the articulated bones of two (HLMD-ME 103, 7835) of the three Messel specimens are partially covered by a black carbonaceous film, typically interpreted as soft part preservation. However, the film may mainly represent integumentary tissue, which is what the soft parts typically reported from Messel (fur, feathers, patagia, ears) consist of. Possibly, internal maceration of the carcass on the lake floor destroyed all intervertebral soft tissues.

4.3. Mesosauria

4.3.1.1 *Stereosternum tumidum* STIPB R 622, Irati Formation, Early Permian, Brazil (Figure S7)

4.3.1.2 Morphological observations

Stereosternum tumidum is one of three species of the Mesosauridae that differ in patterns of pachyostosis of the postcranial axial skeleton, i.e., vertebrae and ribs. The centra, neural arches, and ribs of *Stereosternum tumidum* are pachyostotic, as seen in specimen STIPB R 622. Although Romer (1956) described the centra as “notochordal”, the morphology of the articular surfaces of the centra has not been described in detail before. In *Stereosternum tumidum* STIPB R 622 we observed dorsoventrally flattened vertebral centra that are about as long as wide with amphicoelous articular ends.

4.3.1.3 Histological observations

The sagittal section of an articulated set of four anterior dorsal vertebrae, including three intervertebral spaces, reveals elongate centra with a length to height ratio of 4:1. The sections show that the centra are clearly amphicoelous but that the two “funnels” do not approach each other, unlike in all of the other amphicoelous vertebrae in this study. Instead, the “funnels” are connected by a long notochordal canal that reaches 3/4 of the length of the centra. Interestingly, the canal is wider at the center of growth than towards the articular surfaces. The canal is surrounded by endochondral bone with a high density of osteocyte lacunae. The endochondral bone shows a complex, seemingly whorled arrangement of vascular canals. The dorsal part of the centra appears to lack periosteal bone entirely while this domain is well expressed in the ventral part.

There is little persistence of the original chondroblast lacunae in the endochondral bone, with only a few cartilage islands remaining. However, the articular face is covered by a layer of chondrocyte lacunae that are arranged in an irregular fashion and sometimes connect. In the outer part the articular surface, there are bony spicules with fiber insertions that are directed longitudinally. The notochordal canal and its exit region into the articular facet contains large, translucent, crystalline matter. However, most of the intervertebral spaces are filled up by opaque matter. In polarized light, this matter is distinctive from both, the fill of the neural canal (which consist of globular bodies resembling fecal pellets) and the sediment matrix. In polarized light, the opaque matter has a brownish rim. The periosteal bone of the centra shows no indication of intercentral connective tissue, neither dorsally nor ventrally.

4.3.1.4 Interpretation

The long and distinctive notochordal canal of the vertebrae of *Stereosternum tumidum* must have housed the notochord, preserved as translucent, crystalline matter that also fills the central region of the articular facet. The opaque matter may represent the AF, the attachment of which to the centrum is represented by the fiber insertions in the outer part of the articular surface.

4.3.1.5 Discussion

The centra of *Mesosaurus* thus show an unusual combination of amphicoelous articular surfaces and elongate centra with a long notochordal canal. The lack of dorsal periosteal bone is also unusual. The pattern of the notochord persisting in mesosaurs thus is the same as in *Dimetrodon.*

4.4. Hupehsuchia

4.4.1 *Nanchangosaurus suni,* HFUT YAN-10-02, Early Triassic, Hubei, China (Figure S8)

4.4.1.1 Morphological observations

In the specimen it can be observed that the dorsal neural arches of *Nanchangosaurus* are pachyostotic, as are the ribs. This accords with the description of Chen et al. (2014). In this way, the taxon resembles the basal sauropterygian *Neusticosaurus* discussed below. The centrum morphology of *Nanchangosaurus* was not described by Chen et al. (2014), however.

4.4.1.2 Histological observations

In the histological sections, the centra are seen to be deeply amphicoelous but not notochordal. The endochondral domain is thin compared to the periosteal domain. The latter is poorly vascularized by radial canals, and the former consists of thick trabeculae resulting in limited vascular space. The microanatomy thus suggests bone mass increase. The endochondral bone has some interstitial globular bodies representing hypertrophied cartilage. Towards the articular surface, this is followed by a 100 µm thick layer of irregularly arranged globular bodies that lack any evidence of intervening mineralization. The transition to the remaining intervertebral space is very irregular. The intervertebral space is filled up by granular material that consists of round translucent grains with brown matter in between. The grains are distinctly larger than the globular bodies. In one region of contact between the granular material and the globular bodies, there is a brown patch of seemingly organic material. The brown patch is semitranslucent and contains striations and spindle-shaped cells. Under polarized light, it remains brown and is not birefringent and thus is not bone. The anterior and posterior parts of the thick and unresorbed periosteal cortex show thin Sharpey´s fibres SF.

4.4.1.3 Interpretation

The layer of irregularly arranged globular bodies on top of the endochondral bone must represent the proliferation zone of the cartilage, i.e., hyaline cartilage, or possibly fibrocartilage because of the very irregular arrangement and wide spacing of the cells. The granular material could either represent mineral grains of diagenetic origin that replaced the original organic matter or it could represent fibrocartilage. Another option is that it represents altered notochordal material. We prefer this latter option because of the brown patch that is closer in appearance to fibrocartilage than the granular material. In addition, the grains in the granular material are distinctly larger than the chondrocytes of the hyaline cartilage. The coarse granular material thus probably represents an NP, an the brown patch probably represents the remains of an AF. Thus, the evidence suggests that *Nanchangosaurus* possessed an IVD with a large NP.

4.4.1.4 Discussion

The intervertebral articulation anatomy and histology of *Nanchangosaurus* thus differs from all of the previously discussed taxa except for the mammals in that the notochord is no longer continuous but forms a large NP.

4.5. Ichthyosauria

4.5.1 Cymbospondylidae new taxon A, LACM DI 158109, Middle Triassic, Nevada, USA (Figure S9)

4.5.1.1 Morphological observations

We studied a string of anterior dorsal vertebrae that are from an originally complete and only slightly disarticulated skeleton of a new cymbospondylid ichthyosaur from the Middle Triassic Fossil Hill Member of the Favret Formation, Augusta Mountains, Nevada, USA. All ichthyosaurs have deeply amphicoelous centra but the notochordal foramen is vestigial if at all present (Romer 1956; Houssaye et al. 2018). Vertebral shape changes in ichthyosaur evolution from vertebral centra that are longer than high in the most basal taxa (see Moon 2017), the plesiomorphic condition in reptiles, to disc-shaped centra that may be twice as high as long, or

more. The disc-shaped vertebrae are first seen in the cymbospondylids of the Middle Triassic and are present in all Neoichthyosauria.

4.5.1.2 Histological observations

The histology of one of the vertebrae in this string was briefly described and illustrated by Houssaye et al. (2018, Fig. 3G,H). The deeply amphicoelous shape results from the limited of production of endochondral bone in the articular area. This is also seen in some other ichthyosaurs, where there is a negative allometry of the relative amount of endochondral bone contribution (Houssaye et al. 2018). In the new cymbospondylid, the outermost layer of mineralized material surrounds globular spaces that obviously were occupied by chondroblasts in the living animal. The chondroblast spaces are open towards the intervertebral space, suggesting a cover of the articular surface of the vertebra by hyaline cartilage.

The segment of four anterior dorsal vertebrae is of particular interest because of the matter preserved in the intervertebral spaces. There are different types of matter that we interpret as altered intervertebral tissues. The hyaline cartilage described above is overlain by clear sparry calicite that differs from normal calcite in that it appears to have incorporate a fine fibrous matter during crystal emplacement. In the center of this dark matter, there is a round structure consisting of globules of fine-grained material incorporating some irregularly shaped brownish matter. The primary periosteal bone is cancellous but it does contain Sharpey's fibres closest to the articular surface but not in the region in between.

4.5.1.3 Interpretation

We interpret the fibrous matter in the sparry calcite as altered fibrocartilage, representing the AF, and the central, round structure with the globules as the altered NP. The coarse fabric may reflect the much larger cells of notochordal origin that form the NP. The intervertebral spaces in the vertebral column of the new cymbospondylid ichthyosaur were thus occupied by an intervertebral disc attached to the cartilaginous endplates of the vertebral centra. The endplates consisted of a layer of actively proliferating hyaline cartilage. The intervertebral ligaments or the joint capsule appears to have been weakly developed.

4.5.1.4 Discussion

The Fossil Hill Member is a black shale unit characterized by the preservation of complete marine reptile skeletons (e.g., Sander et al. 1997, Fröbisch et al. 2006, 2013) and the preservation of soft parts thus appears possible. The interpretation of the intervertebral matter as altered intervertebral tissue may appear far-fetched at first, and alternative hypotheses need to be examined that would produce the observed pattern. Probably, bacterial activity altered the original intervertebral tissues, but only at the microscopic level, leaving the larger anatomical structures intact. The issue will be examined in more detail in the discussion of the *Stenopterygius* specimen described below.

4.5.2. cf. *Cymbospondylus* sp. STIPB R 660, Lower Triassic, Spitsbergen (Figure S10

4.5.2.1 Morphological observations

The dorsal vertebrae of cf. *Cymbospondylus* are disc-shaped, i.e., shorter than dorsoventrally tall, and deeply amphicoelous with an even slope towards the growth center. They appear to lack a notochordal foramen, however small.

4.5.2.2 Histological observations

The endochondral domain is thin compared to other early ichthyosaurs (Houssaye et al. 2018), and there is only a thin layer of hyaline cartilage facing the intervertebral space. The intervertebral space is filled with matrix not any different from the surrounding matrix. However, an isolated patch of brown material with globular holes can be observed in the matrix in the intervertebral space. The histological section confirms the morphological observation that the vertebrae are not notochordal. The anterior and posterior one tenth of the very thin periosteal cortex of the centrum shows Sharpey's fibers, which are better developed ventrally than dorsally.

4.5.2.3 Interpretation

The globular bodies covering the articular faces are interpreted as hyaline cartilage. The patch of brown material with globular holes is interpreted as altered fibrocartilage.The Sharpey's fibers suggest the presence of an intervertebral ligament.

4.5.2.4 Discussion

The thin layer of hyaline cartilage is the same as in the previous ichthyosaur samples. The patch of fibrocartilage probably derives from the AF, but no evidence of the NP is preserved. The hypothesis of the preservation of altered soft parts in the intervertebral spaces is amenable to testing by examination of modern carcasses from anoxic environments. In addition, ultrastructural and organic geochemical investigations could be very informative.

4.5.3. *Stenopterygius* sp. STIPB R 661, Posidonien-Schiefer Formation, Lower Jurassic, Holzmaden, Germany (Figures S11, S12)

4.5.3.1 Morphological observations

We studied a string of anterior dorsal vertebrae that are from an originally complete and only slightly disarticulated skeleton of *Stenopterygius* sp. from the Early Jurassic Posidonienschiefer Formation of Holzmaden, Germany. This is one of the classical ichthyosaur faunas. As all of the other ichthyosaurs studied here, the *Stenopterygius* vertebrae have deeply amphicoelous, disc-shaped centra.

4.5.3.2 Histological observations

In our specimen of *Stenopterygius*, the layer of endochondral bone underlying the articular face of the vertebrae is thin (less than 1 mm) and did not increase in thickness ontogenetically. The outermost layer of mineralized material surrounds globular bodies that obviously were occupied by chondroblasts in the living animal. The chondroblast spaces are open towards the intervertebral space, suggesting a cover of hyaline cartilage of the articular surfaces of the vertebra. In the center of the articular face, the globular bodies are arranged in poorly defined, surface-parallel layers. Towards the perimeter, the globular bodies become increasingly organized

in to files that diverge increasingly until they are at an angle of 45º to the centrum long axis in the outermost perimeter. The primary periosteal bone is thin but does contain Sharpey's fibers closest to the articular surface but not in the region in between.

The segment of six anterior dorsal vertebrae is of particular interest because of the matter preserved in the intervertebral spaces. The laminated sediment matrix of the specimen did not enter these spaces. Instead, the are different types of matter that we interpret as altered intervertebral tissues. The hyaline cartilage described above is overlain by dark, fine-grained material which takes up the greater part of the intervertebral space. In the center of this dark matter, there is a round structure of translucent matter that shows a coarser fabric.

4.5.3.3 Interpretation

We interpret the dark matter as altered fibrocartilage, representing the AF, inserting into the inclined files of globular bodies, representing chondrocytes. The central, round translucent structure probably represents an altered NP that was separated from the bony part of the centrum by a layer of surface-parallel cartilage. The coarse fabric probably reflects the much larger cells of notochordal origin that form the NP. The intervertebral spaces in the vertebral column of *Stenopterygius* were thus occupied by an IVD attached to the cartilaginous endplates of the vertebral centra. The endplates consisted of a layer of actively proliferating hyaline cartilage. The intervertebral ligaments or the joint capsule appears to have been weakly developed.

4.5.3.4 Discussion

As noted in the description of the Middle Triassic cymbospondylid LACM 158109, we interpret the intervertebral matter as altered intervertebral tissue. Although localized activity of degrading and scavenging organisms could have caused the observed pattern, the activity of most any other organism than bacteria can be excluded for the Posidonienschiefer Formation because of the laminated, anoxic nature of the sediment (Schmidt-Röhl et al., 1999). In fact, the lamination indicates the lack of any metazoan activity. It also appears unlikely that scavenging metazoans would have been able to be active in the intervertebral spaces if the entire surrounding sediment was anoxic. Probably, bacterial activity altered the original intervertebral tissues, but only at the microscopic level, leaving the larger anatomical structures intact.

The comparison with the matter found in the intervertebral spaces of LACM 158109 is important because both specimens show the same pattern, i.e., a ball-shaped structure in the center of the space which is surrounded by different material, setting the "ball" off from the cartilage endplate. This material also completely fills the remaining intervertebral space, close to the margins of the articular surface.

The hypothesis of the preservation of altered soft parts representing an AF and a NP in the intervertebral spaces is amenable to testing by examination of modern carcasses from anoxic environments at the bottom of euxinic lakes and marine basins. In addition, ultrastructural and organic geochemical investigations could be very informative.

4.5.4. *Leptopterygius* sp. STIPB R 235, Lower Jurassic, Lyme Regis, England (Figure S13)

4.5.4.1 Morphological observations

The probable anterior caudal vertebrae are extremely crushed but are similar in size, morphology, and histology to the cf. *Cymbospondylus* ones.

4.5.4.2 Histological observations

The endochondral domain is thin, as in other Jurassic ichthyosaurs (Houssaye et al. 2018), and there is only a thin layer of hyaline cartilage facing the intervertebral space. One of the vertebrae is intersected in its exact growth center and seen to be notochordal, with an interruption in bone tissue. This area in the growth center of the centrum contains several globular spaces with a dark center.

4.5.4.3 Interpretation

The globular spaces with a dark center may be preserved notochordal cells. They are different from the hyaline cartilage of the articular face.

4.5.4.4 Discussion

The thin layer of hyaline cartilage is the same as in the previous ichthyosaur samples. However, the caudal vertebrae differ from the previous three ichthyosaur samples in the presence of the notochord. Retention of notochordal material is surprising for a derived Jurassic ichthyosaur, especially against the background of the non-notochordal cf. *Cymbospondylus* vertebrae. However, the explanation may lie in the caudal position of these vertebrae. At least in non-archosauromorph reptiles, the notochord persists even in the adult tail to facilitate regeneration after autotomy (LeBlanc et al. 2018). This is indicated by the basal reptile *Captorhinus* and extant Lepidosauria. We do not suggest, however, that ichthyosaurs performed caudal autotomy.

4.6. Sphenodonta

4.6.1. *Sphenodon punctatus* NHMW 8108:2, New Zealand, recent (Figure S14)

4.6.1.1 Morphological observations

As noted by Romer (1956), the dorsal vertebrae of *Sphenodon* are amphicoelous and notochordal. A complete skeletal specimen (Collection of the Institute of Anatomy, University of Cologne) confirms these observations which are difficult to make in the partially dissected alcohol specimen (NHMW 8108:2) that we sampled histologicallly. This type of morphology differs from that of more derived lepidosaurs, i.e., squamates, that have evolved a ball-and-socket joint, specifically the opisthocoelous condition (with the exception of some geckos). We observed small ventrally located intercentra in *Sphenodon*, as already stated by Romer (1956).

4.6.1.2 Histological observations

Sagittal microtome histological sections of the dorsal vertebrae show the nature of the intervertebral tissues and the vertebral centrum well. The spongiosa in the center of the vertebral bodies is trabecular, and there is only a thin cortex of periosteal bone. The endochondral bone is covered at its cranial and caudal end by a layer of serial cartilage, i.e., hypertrophied cartilage, but the proliferation zone is not distinct. There is a diffuse boundary with the fibrocartilage of the

intervertebral joint. The fibrocartilage forms a ring connecting the margins of the articular surfaces of the centra in a structure similar to the AF of mammals. The notochord forms a diabolo-shaped core structure within the elongate vertebral bodies. In the middle, the notochord ossifies to form an intravertebral septum. Remarkably, in the intervertebral space, the notochord forms a conspicuous cavity called *vesicula centralis* (vesicle of Romer 1956). We identified a layer of hyaline cartilage between the fibrocartilage and the bony vertebral centrum.

The small intercentra are well visible in the sections and are in functional combination with the fibrocartilage ring.

4.6.1.3 Interpretation and discussion

The *Sphenodon* material is very helpful in interpreting the fossils. The uneven surface of the cartilage cover of the endochondral bone is suggestive of attachment of fibrocartilage which preserves much less frequently in the fossils than the serial and hyaline cartilage. The distribution of soft tissues in the intervertebral space of *Sphenodon* dorsal centra fits the inferences that could have been made for this sample based on hard tissues alone. This supports our inference for fossil vertebrae of similar morphology and histology, e.g., those of *Diadectes*, *Dimetrodon*, and *Captorhinus*. *Sphenodon* thus shows the plesiomorphic amniote condition of the intervertebral joint.

The development of the embryonic vertebral column of *Sphenodon* had already been figured by Howe and Swinnerton (Fig. 116 in Romer 1956), and the adult vertebral histology was described and figured by Wettstein (1931). Our observations largely accord with those of Schauinsland (1902) and Wettstein (1931). However, these authors did not report the layer of hyaline cartilage between the fibrocartilage and the endochondral bone. The layer might have escaped the attention of Wettstein for the lack of Azan staining.

4.7. Squamata

4.7.1 *Mosasaurus missouriensis* STIPB Goldfuß 1230, Late Cretacous, North Dakota, USA (Figure S15)

4.7.1.1 Morphological observations

The vertebrae studied are from the trunk region of a nearly complete, articulated skeleton described by Glodfuß 1841. Like all Mosasauroidea and their possible sister taxon Ophidia, *Mosasaurus* dorsal vertebral centra articulate via well developed ball-and-socket joints, with the socket formed by the anterior articular facet, thus representing the procoelous condition. In other vertebrae of the same skeleton, it can be seen that both the ball and the socket have very smooth and dense surfaces, without any pores or rugosities. This is apparent in other mosasaur vertebrae as well.

4.7.1.2 Histological observations

The vertebral column appears to have been preserved in a hard calcareous concretion, and at the time of the original description by Goldfuß in 1841, the vertebrae could only be freed from the matrix in a crude way, leading to much damage of the bone surface. However, the concretionary development lead to excellent three-dimensional preservation. Accordingly, the thin sections reveal that the vertebrae remain tightly articulated, and the intervertebral space is one mm or less wide. Both articular surfaces, the convex (ball) and concave (socket) one show a continuous, smooth bone layer, as was evident from exposed joint surfaces of other vertebrae. Under the microscope, the smooth surface is seen to consist of compact bone covered by a very thin semi-translucent beige-brown layer with a globular texture. The actual intervertebral space is filled with a dark gray, essentially opaque carbonate matrix, that is interrupted by voids set at irregular distance from each other. At high magnification, the layer is evenly translucent with out any evidence of mineralized matrix and some of the globular bodies contain small brown spots. The periosteal bone of the centra shows SF near the articular region, paralleled by vascular canals and better developed in the ventral region.

4.7.1.3 Interpretation

Because of its similarity to the extant snake intervertebral joint described below, the interpretation of the mosasaur vertebrae is straightforward. Like in the snake, the mosasaur clearly had a synovial joint. The beige-brown layer must be altered hyaline cartilage of the joint surface. The mineral infilling of the thin intervertebral space would have been occupied by synovial fluid in life.

The small brown spots in the chondrocytes may represent cell nuclei fossilized in the process of cell division because they resemble the dark-staining nuclei in the hyaline cartilage of the *Python* vertebrae. Evidence for intervertebral ligaments is stronger in the ventral region.

4.7.1.4 Discussion

While the nature of the intervertebral joint could have been inferred with some confidence from phylogeny and osteological correlates, support from direct observation is important.

The specimen is also important because it again shows that intervertebral unmineralized tissues may survive in an altered state, in this case the layer of hyaline cartilage covering the bony joint surface.

4.7.2 *Python* sp. STIPB R 662, recent (Figure S16)

4.7.2.1 Morphological observations

The procoelous vertebrae of snakes were mentioned already, and the specimen we sampled shows this very well in histological microtome sections. In fact, the procoelous condition could only be observed in the section because the studied vertebrae were not dissected out of the soft tissue.

4.7.2.2 Histological observations

Both the sagittal and the frontal section of the snake vertebrae show the clear procoelous morphology with a tightly fitting ball-and-socket joint. The intervertebral space is only a few hundred μm wide or even, in the median plane, not detectable. However, the width of this space may have been altered during microtome sectioning. Both joint surface can be seen to be made up of hyaline cartilage of the proliferation zone with the cells arranged in columns perpendicular to the joint surface.

There is no even bone surface but irregular bone trabeculae underlying the cartilage, suggesting that the animal was still actively growing. Indeed, endochondral bone trabeculae can be seen, replacing the cartilage. After removal of the cartilage layer, e.g., by soft tissue decay during fossilization, a very uneven joint surface would result.

The margins of the cartilaginous joint surfaces abut the thick joint capsule formed by ligamentous connective tissue. This is clearly visibly by its dark blue color in the Azan staining. The fibers of the joint capsule insert in the periosteal bone of either vertebral centrum.

4.7.2.3 Interpretation

The *Python* intervertebral joint is clearly of the synovial type, with a fluid-filled intervertebral space. This space is surrounded by a joint capsule of connective tissue that contained the synovial fluid.

4.7.2.4 Discussion

Soft tissue histology based on decalcified stained microtome sections is able to image the joint morphology of the intervertebral joint very well.

4.7.3 Ophidia indet. HLMD ME 7624b, middle Eocene, Messel, Germany (Figure S17)

4.7.1.1 Morphological observations

The specimen is a trunk segment of an indeterminate small snake, preserved as several segments consisting of strings of several articulated vertebrae. The intervertebral joints consist of the ball-and-socket joints typical for snakes. The bone is preserved on an artificial resin matrix and surrounded by dark organic remains.

4.7.1.2 Histological observations

The specimen is the least crushed of all the Messel fossils in this study. The bone of the vertebrae consists of compact, nearly avascular lamellar and parallel-fibered bone and limited

areas of cancellous bone, located near the ends of the vertebral centra and in the neural spine. The vertebral centra are opisthocoelous, forming tightly articulating concave/convex joint surfaces. Much like in the extant snake described above, the joint surface is formed by files of hyaline cartilage cells oriented perpendicular to the curved (convex/concave) joint surfaces.
At first, the files appear to be continuous across the joint cleft but upon closer inspection, the joint surface can be seen between the two cartilage layer. A similar phenomenon can be seen in the histological section of the extant snake where the joint surfaces appear to touch in places as a preparation artifact.

4.7.1.3 Interpretation and discussion

The Messel snake agrees in most respects with the extant snake in this study, but because of its smaller size, there are fewer files of cartilage cells. It is clear that the fossil snake possessed the same type of synovial joint consisting of hyaline cartilage and a thin synovial cleft as extant snakes. The complete preservation of the hyaline cartilage suggests that the cells were either already somewhat mineralized in life or that this happened during diagenesis.

4.8. Sauropterygia

4.8.1. *Placodus gigas* STIPB R 86, Muschelkalk, Middle Triassic, Germany (Figure S18)

4.8.1.1 Morphological observations

The vertebrae of *Placodus* and other placodonts are reported to be of the amphicoelous, non- notochordal type (Romer 1956). The centra have articular surfaces with a concave, funnel-shaped center and a weakly concave outer rim.

4.8.1.2 Histological observations

The sample is a transverse thin section section through the center of the vertebral centrum. The section confirms that the notochordal foramen is essentially closed, possibly retaining a lumen of ca. 50 µm. In the inner region of the thin section, the endochondral bone trabeculae shows extensive unmineralized and mineralized cartilage. In a polished section, it can be seen

that endochondral bone formation was limited (resulting in the amphicoelous shape of the centrum) and, as in *Diadectes* and *Dimetrodon*, the outer concave rim is formed by endochondral bone formation. The concave area shows an irregular surface layer of chondrocyte lacunae and the convex area files of chondrocytes with intervening fibrous bone spicules.

4.8.1.3 Interpretation

The distribution of the cartilagineous tissues and bone with fibers, both endochondral and periosteal, is essentially the same as that in hupehsuchians and ichthyosaurs, suggesting the presence of an IVD. The extensive preservation of cartilage in the core of the trabeculae is a paedomorphic feature attributable to aquatic adaptation.

4.8.1.4 Discussion

The inference that placodonts such as *Placodus* had an IVD is supported by the observation that a higly paedomorphic placodont (especially in the vertebrae), *Pararcus diepenbroecki* (Klein & Scheyer 2014), lacks notochordal centra despite lacking fusion between the left and right halfs of the neural arches, the retention of an embryonic state. This suggest that early in placodont ontogeny, the notochord already became discontinuous.

4.8.2. *Neusticosaurus peyeri* PIMUZ T 3768, Meride Limestone, Middle Triassic, Switzerland (Figure S19)

4.8.2.1 Morphological observations

The vertebrae of this small pachypleurosaur are pachyostotic, giving the centra a barrel-shape and the neural arches a swollen appearance (Sander 1989). The dorsal vertebral column is little flexed and appears to have been fairly rigid in life. This is in accordance with the distance between adjacent centra being less than 100 µm. Morphological observations of disarticulated *Neusticosaurus* specimens reveal that the articular surface of the centra is slightly sunken in the center and best called platycoelous with a shallow depression (Sander 1989).

The specimen is a small adult, and its humerus cross section was figured in Sander (1989, Fig. 25k).

4.8.2.2 Histological observations

The ventral side of the specimen is still embedded in the finely laminated sediment. The sediment did not enter the neural canal nor the intervertebral spaces. The neural canal is filled by coarse sparry calcite, with single crystals extending across its lumen. One of the intervertebral spaces is also filled by the same material, but the others contain a grey granular material that interfingers with sparry calcite. The shape of the intervertebral spaces in sagittal section is distinctly lens-shaped.

The articular surfaces of the centra clearly show altered cartilage layers. The superficial layer consist of irregularly arranged globular bodies and is about five globular body diameters thick. This layer is darker beige and less translucent than the underlying layer of serial cartilage, with the globular bodies arranged in files normal to the surface in the center of the articular surface. Towards the margin of the articular surface, the files diverge towards the perimeter and are more highly organized. There are few fibres in between the files in the marginal area and none in the center. The globular space in these files are commonly filled by dark, nearly opaque matter. Deeper into the bone, replacement of the globular bodies by bone tissue and the development of vascular canals is observed. The periosteal bone of the centra shows only a few isolated SF near the articular regions and thus little indication of intercentral connective tissue, neither dorsally nor ventrally.

4.8.2.3 Interpretation and discussion

The layer of darker beige globular bodies clearly represents a layer of actively proliferating, hyaline cartilage, and the globular bodies arranged in files are serial cartilage. The grey granular matter in the intervertebral space is not sufficiently organized to allow inferences as to its original nature. The tight fit of the perimeter of the articular surface combined with the lens-shaped intervertebral space is not consistent with a synovial joint. The proliferating hyaline cartilage is surprising thick for such a small animal. There is no evidence for remains of the notochord. While the cartilage layers are well preserved in the *Neusticosaurus* specimen, the tissue filling up the intervertebral space is not. The pattern of divergence and organization of the

files of sertial cartilage suggests the presence of an IVD with a thin AF in *Neusticosaurus*.

4.8.3. *Plesiosaurus dolichodirus* STIPB R 88, Lower Jurassic, Lyme Regis, England (Figure S20, S21)

4.8.3.1 Morphological observations

The two articulated vertebrae we studied are anterior dorsals, still retaining large intersegmental artery foramina (Wintrich et al 2017a). Like the much smaller *Neusticosaurus*, the *Plesiosaurus* specimen we studied has only a short distance of <1 mm between the articulating vertebrae in the marginal region, and the two centra are nearly touching at their perimeter. This is also seen in other plesiosaur specimens that are preserved in articulation in the matrix, e.g., the geologically oldest plesiosaur *Rhaeticosaurus* (Wintrich et al. 2017b), and also in the stem pistosauroid *Augustasaurus* (Sander et al. 1997, Rieppel et al. 2002). The articular surfaces of plesiosaur centra are essentially flat or slightly bowl-shaped, and generally described as platycoelous (Benson & Druckenmiller 2014). The diameter of the articular surface exceeds that of the main part of centrum, leading to a flared appearance of the former.

4.8.3.2 Histological observations

The sagittal section reveals that the interior of the centrum is largely made up by relatively evenly but widely spaced and longitudinally arranged trabeculae of secondary origin. The primary periosteal cortex is extremely thin, no thicker than the average trabeculae. The articular faces are underlain by an even layer of trabecular bone of endochondral origin that lacks any indication of the retention of notochordal components and of a “notochordal pit”. The flared appearance of the articular surface was caused by the faster growth of the endochondral bone compared to the periosteal bone. The endochondral trabeculae are heavily remodeled and almost completely lack interstitial hypertrophied cartilage (unlike in *Placodus*). The central region of the bony articular face is overlain by a thin layer of poorly organized globular bodies about six to ten bodies thick. In the peripheral region, the globular bodies are arranged in clearly defined files with bony spicules showing fibers in between.
Strong and distinctive Sharpey’s fibres are seen in the one fifth of the periosteal bone adjacent to the articular surface.

The intervertebral space contains a fill of variable appearance, with stringers of lighter and darker colors. The neural canal, on the other hand, is filled by carbonate matrix of even appearance. In one region, the material clearly shows a fibrous structure.

4..8.3.3 Interpretation

The layer of globular bodies represents a layer of hyaline cartilage of the proliferation zone. The uneven surface of this layer is in stark contrast with the smooth layer seen in the mosasaur. The roughness of the hyaline cartilage layer in the peripheral zone is consistent with fibrocartilage forming an AF. The strong Sharpey's fibres in the periosteal bone close to the articular face suggest the presence of strong intervertebral ligaments. The inhomogeneous matrix in the intervertebral space may represent degraded fibrocartilage of the AF and the remains of the NP. In particular, the fibrous material is suggestive of fibrocartilage and does not appear to be of microbial or invertebrate origin.

4.8.3.4 Discussion

In addition to the histological correlates suggesting the presence of an NP, its former presence appears highly likely because of functional requirements. A connection only consisting of fibrocartilage would have restricted intervertebral movement too much.

4.9. Thalattosauria

4.9.1. *Xinpusaurus suni* HFUT GL 17003, 17006, Xiaowa Formation, early Late Triassic, Guanling, Guizhou, China (Figure S22)

4.9.1.1 Morphological observations

Thalattosaur vertebrae are variously described as amphicoelous or platycoelous in the literature (Liu & Rieppel 2005, Rieppel et al. 2006). Vertebral morphology cannot be directly observed in our specimen because of matrix cover, but it can be inferred from the histological sections.

4.9.1.2 Histological observations

In general, bone tissue preservation is poor in both samples. The bone matrix appears opaque and has lost all birefringence in polarized light. In addition, the trabecular fabric is crushed in many places. Nevertheless, the histological sections of the two different-sized *Xinpusaurus* individuals reveal platycoelous vertebral centra with a very shallow depression resulting in a flattened, lens-shaped intervertebral space, that is only one tenth the diameter of the articular faces. This can be estimated in the larger individual, HFUT GL 17006. The articular area is expanded relative to the body of the centrum, and this expansion is more pronounced than in *Plesiosaurus*. The encasing laminated sediment of the Xiaowa Formation does not seem to have entered the intervertebral space.

Both, the periosteal and the endochondral domain consist of cancellous bone. The trabeculae of the endochondral domain are longitudinally oriented. The entire articular face is covered by a layer of dark brown material in which there are files of globular bodies that are eight to ten layers thick. The files of globular bodies are perpendicular to the articular surface in its center but diverge increasingly towards the perimeter until they are at an angle of 45º to centrum long axis. The content of the globular bodies is translucent. This layer shows an abrupt border towards the center of the intervertebral space with another region of globular bodies. These bodies are much more irregularly arranged and lack the intervening dark-brown matrix. They are more irregular in size and commonly larger than the bodies in the brown matrix. This material appears to largely fill the intervertebral space, except for some globular bodies six to eight times as large as the previous ones. These bodies are translucent and have an indistinct border. They mostly have a circular cross section but some are more oval. Because of the poor preservation, SF cannot be detected in the periosteal bone.

4.9.1.3 Interpretation

The layer with the globular bodies in the brown matrix can confidently be interpreted as serial cartilage of the hypertrophy zone. At least the material adjacent to this layer must represent the proliferation zone. However, since the irregularly arranged bodies fill up the entire intervertebral space, some of them must also represent fibrocartilage or even notochordal cells. The diverging orientation of the files, especially well seen in HFUT GL 17006, in the perimeter is the same as observed in the mammalian AF, suggesting the presence of such a structure. The identity of the large globular bodies is enigmatic. They simply could represent gas bubbles that

formed during soft tissue decay and later were filled in by diagenetic minerals. Alternatively, the large globular bodies might represent fecal pellets but this appears unlikely for the reasons discussed in conjunction with the *Stenopterygius* specimen. The intervertebral connection thus appears to have consisted of fibrocartilage in an AF and possible notochordal material, fitting the definition of an IVD.

4.9.1.4 Discussion

The *Xinpusaurus* material offers interesting soft-part preservation despite the poor bone tissue preservation. Taken at face value, *Xinpusaurus* and, by extension, other thalattosaurs possessed an IVD. They clearly did not possesses a synovial joint because the entire intervertebral space is filled by altered cartilaginous material and the layer of hyaline cartilage is very indistinct, especially in comparison with the mosasaur fossil.

4.10. Crocodylia

4.10.1. *Steneosaurus bollensis* STIPB R 663, Posidonienschiefer Formation, Lower Jurassic, Dotternhausen, Germany (Figure S23, S24)

4.10.1.1 Morphological observations

We studied an articulated pair of anterior dorsal vertebrae that are from an originally complete but somewhat disarticulated skeleton of the thalattosuchian crocodile *Stenosaurus bollensis* from the Early Jurassic Posidonienschiefer Formation of Dotternhausen, Germany. Thalattosuchian crocodiles are the second most common marine reptiles in this formation, after ichthyosaurs. Unlike modern crocodiles, thalattosuchians have platycoelous vertebral centra with only slightly concave articular surfaces. Eusuchian crocodiles, on the other hand, have synovial ball-and-socket joints and procoelous vertebrae.

4.10.1.2 Histological observations

The preservation of the vertebrae suffers from some compaction, and the perimeter of the adjacent articular surfaces show some crushing, apparently shortening the distance between the two centra. The interior of the centra consists of loose trabeculae of secondary bone. Directly underlying the articular surfaces is denser bone tissue, forming a bony endplate about 3 mm in thickness. The center of the articular surface is covered by a layer of poorly organized, translucent globular bodies. The layer is about ten diameters of the bodies thick and in same areas is continuous with the bone tissue. Towards the perimeter, the globular bodies become arranged in files that are inclined outwards from the center of the surface. In- between the files, there are sometimes bone spicules containing fibres of the same direction as the files. The intervertebral space is filled by coarse crystal aggregates that seem to have replaced dark organic matter during their growth. The same type of material is also present in the neural canal and adjacent to the vertebrae.

4.10.1.3 Interpretation

The globular bodies are the remains cartilage cells that in the living animal were gradually mineralizing away from the articular surface. The inclined files and bone spicules are the attachment area of the fibrocartilage of the AF. The poorly organized cartilage cells in the central region of the articular surface must have underlain an NP that occupied the intervertebral space.

4.10.1.4 Discussion

Unlike extant eusuchian crocodiles, thalattosuchians with their platycoelous centra apparently had an IVP and not a synovial joint. This is strongly suggested by the distribution of the types of preserved articular cartilage in the specimen studied here.

4.11. Dinosauria

4.11.1. Hadrosauridae indet. UACVP 59650, Dinosaur Park Formation, Late Cretaceous, Alberta, Canada (Figure S25)

4.11.1.1 Morphological observations

In general, hadrosaur dorsal vertebral centra have a simple, cylindrical morphology with platycoelous articular surfaces. The specimen we studied is an isolated hadrosaur dorsal vertebra, and because of constraints on section size, the sagittal histological section only covers the outer part of an anterior or posterior articular surface.

4.11.1.2 Histological observations

The interior of the centrum shows loose, longitudinally arranged trabeculae of secondary bone that become denser and more isotropic below the articular surface. The articular surface itself is covered by seemingly hollow globular structures set in files but with thick layers (wider than the diameter of the globules) of intervening fibrous material that appears to be mineralized in cross-polarized light. The fibers are an order of magnitude smaller than the globules and densely packed. They appear to be oriented mainly perpendicular to the plane of section, i.e., circumferentially oriented, except close to the files, where they are oriented in the direction of the files. In the area covered by the section, all files are inclined towards the perimeter of the articular surface, but inclination increases from <45º to >60º. The globule-and-fiber layer is also preserved in some interstitial spaces of the secondary trabeculae.

4.11.1.3 Interpretation

The arrangement of globular bodies and fibers is unique among the material studied. We interpret this tissue as the mineralized insertion of fibrocartilage into the bony endplate. The increasing inclination of the chondrocyte files towards the margin is consistent with an AF. The observation that secondary bone lamellae replace the globule-and-fiber layer is consistent with its interpretation as mineralized fibrocartilage because secondary replacement explains the lack of a proliferation zone and hyaline cartilage observed in the other samples.

4.11.1.4 Discussion

Since the section does not cover the center of the articular surface, it does not inform on the presence of a NP. However, the orientation of the fibers in the AF is suggestive of it enclosing an NP because otherwise the increasing inclination would be difficult to explain. If there were only

fibrocartilage or a synovial joint between the vertebrae in hadrosaurs, the files would be oriented straight across the intervertebral space, as in our squamate samples. The mineralization and replacement of fibrocartilage by bone may be explained by the large size or an advanced ontogenetic stage of the individual, where chrondrogenesis had long ceased

4.11.2. Ornithomimidae indet. UACVP 56951, Dinosaur Park Formation, Late Cretaceous, Alberta, Canada (Figure S26)

4.11.2.1 Morphological observations

Ornithomimosaur dorsal vertebra are of the platycoelous type with weakly concave articular surfaces (Holtz et al 2012). Our sample only covers part of either the anterior or posterior articular surface, but unfortunately not the peripheral region, nor does it cover the interior of the centrum. The articular surface is still partially covered by sediment.

4.11.2.2 Histological observations

The bony endplate consists of a fairly loose arrangement of bony trabeculae of secondary origin. The articular surface is underlain by a thin layer of bone which is part of this trabecular system. Covering the bone, there is a thin layer of globular structures set in a mineralized matrix. The globular structures are arranged in poorly defined files that are at most eight globules thick and are oriented perpendicular to the surface.

4.11.2.3 Interpretation and discussion

The globular layer in the mineralized matrix represents hypertrophied cartilage, with the proliferation zone not being preserved. Endochondral bone formation had ceased, and a layer of hyaline cartilage must have covered the hypertrophied cartilage in life. The poor definition of the files and their lack of inclination suggest that this was not a region of insertion of fibrocartilage but that a NP was located in the intervertebral space. While the sample only offers incomplete coverage, it is consistent with the interpretation that ornithomimosaurs possessed an IVD.

4.11.3. Dromaeosauridae indet. UACVP 56952, Dinosaur Park Formation, Late Cretaceous, Alberta, Canada (Figure S27)

4.11.3.1 Morphological observations

Dromaeosaur dorsal vertebrae are of the platycoelous type and may have pleurocoels (Holtz et al. 2012).

4.11.3.2 Histological observations

The dromaeosaurid dorsal vertebral centrum we sectioned sagittally is nearly twice as tall dorsoventrally than long and has flat articular surfaces. The interior of the centrum has a large empty space that was pneumatized as indicated by its surrounding trabeculae consisting of pneumosteum. Pneumosteum is a peculiar tissue recently described (Lambertz et al. 2018) in secondary bone trabeculae that formed around pneumatized cavities in the postcranial skeleton of saurischian dinosaurs, including birds. The trabecular architecture of the centrum appears to be controlled by its pneumatization, with the pneumatized space being surrounded by a clear lining of pneumosteum followed by a loose trabecular network. However, the microanatomical architecture of this trabecular network differs in the two articular surfaces, with the direction of anterior being unknown. Towards one articular surface, the trabeculae condense into a poorly defined bony endplate of discontinuous trabeculae. Towards the other, a continuous layer of bone underlies a similar, poorly defined bony endplate. Only very few and isolated globular bodies are seen in the outermost bone matrix.

4.11.3.3 Interpretation

Endochondral ossification had ceased in the specimen, and only a thin and apparently discontinuous layer of hypertrophied cartilage covers the articular surface. The nature of the hyaline cartilage is difficult to infer because it is not preserved. However, the thinness of the preserved hypertrophied cartilage would be consistent with the assumption that the layer of hyaline cartilage was very thin.

4.11.3.4 Discussion

There is no indication of an AF in the dromaeosaur nor of an NP. This dinosaur probably did not have an IVD but already a bird-type intervertebral joint. The meaning of the anteroposterior asymmetry of the trabecular architecture is not clear at present.

4.11.4. Aves indet. HLMD-ME 1022, middle Eocene, Messel, Germany (Figure S28)

4.11.4.1 Morphological observations

The specimen we sampled is a partial skeleton of a medium-sized bird preserving the trunk region. The bones appear crushed and are covered by a dark organic film. The sample covers four dorsal vertebrae and three intervertebral joints.

4.11.4.2 Histological observations

The histologic section reveals that the specimen is heavily crushed, involving both brittle and seemingly also plastic deformation, as seen in the other Messel specimens. The articular surfaces of the centra are affected by this crushing, and their exact morphology is difficult to ascertain, except that there seems to have been a tight fit of curved surfaces. The area between adjacent vertebrae is filled by dark brown amorphous material. The articular surfaces appear to be underlain by dense bone and show only a few globular bodies set in a mineralized matrix. These are scattered near the surface.

4.11.4.3 Interpretation

Despite the heavy crushing, it is clear that the Messel bird did not have much cartilage in its intervertebral joints. The scattered globular bodies represent a thin layer of hypertrophied cartilage. The joint thus appears to have been the same as in other bird dorsal vertebrae.

4.11.4.4 Discussion

Despite the great size difference, there is a distinct similarity between the articular surface histology of the dromaeosaur and the bird. Dromaeosaur dorsals thus appear to have already possessed a bird-type joint.

5. Supplementary Note 5: Synthesis

5.1 Synthesis: Inferences on intervertebral joints from morphology and histology

Based on the detailed descriptions of the histological samples, we are now able to review the relationships between vertebral centrum shape, observed fossilized and fresh tissues, inferred joint tissue types, and inferred joint type (Supplementary Table 2, Figure S29). The observed fossil tissues in the sections are bony tissues, altered cartilaginous tissues, and preserved soft tissues. We review five basic joint types. (1) Amphicoelous, notochordal centra show a concave area with thin cartilage or smooth bone and a convex area with generally short chondrocyte files arranged in longitudinal direction with irregular bone spicules in between. We infer that these vertebral centra had an intervertebral joint consisting of an outer ring of fibrocartilage and an expanded notochord in the central region, as is observed in *Sphenodon*. This appears to be the plesiomorphic condition for amniotes which gave rise to all other joint types. (2) Amphicoelous, non-notochordal centra show a concave area with irregular cartilage (but never bone), an outer area with chondrocyte files arranged in longitudinal direction with irregulary bone spicules in between or long diverging files with an increasing angle of divergence (hupehsuchians, ichthyosaurs). We infer that the taxa that show these features had a proper IVD, supported by the preservation of an altered NP in some ichthyosaurs. This type of morphology and joint is extinct. (3) Platycoelous centra, including those of extant mammals, show a central area with irregular cartilage and an outer area with diverging cartilage files and bone spicules. These two areas demarcate the AF and NP of the mammalian IVD, and we infer that fossil taxa with these features also had an IVD. (4) Procoelous and opisthocoelous vertebral centra that show a distinct layer of hyaline cartilage arranged in files normal to the bony surface suggest the presence of a synovial joint with a narrow joint cavity filled with synovial fluid, as observed in most extant squamates. (5) Procoelous and opisthocoelous vertebral centra of fossil taxa that show only irregular, thin cartilage and bone with fiber insertions suggest the presence of a fibrocartilage joint as in extant birds. We found evidence for intervertebral ligaments in all types of joints.

Supplementary References

Arratia, G., Schultze, H. P., Casciotta, J. Vertebral column and associated elements in dipnoans and comparison with other fishes: development and homology. *Journal of Morphology* **250**(2), 101-172 (2001).

Bartsch, P. Funktionelle Morphologie und Evolution des Axialskelettes und der Caudalis ursprünglicher Knochenfische. *Palaeontographica Abt. A* **204**, 117-236 (1988).

Benson, R. B. J., Druckenmiller, P. S. Faunal turnover of marine tetrapods during the Jurassic–Cretaceous transition. *Biological Reviews* **89**, 1-23 (2014).

Boszczyk, B.M.; Boszczyk, A.A., Putz, R. Comparative and functional anatomy of the mammalian lumbar spine. *The Anatomical Record* **264** (2): 157-168 (2001).

Cox, M. K., Serra, R. Development of the intervertebral disc. In *The Intervertebral Disc* (ed Shapiro**,** I. M., Risbud, M. V.) pp.33-51 (Springer, 2014).

Christ, B., Huang, R., Scaal, M. Formation and differentiation of the avian sclerotome. *Anatomy and Embryology* **208**(5), 333-350 (2004).

Christ, B., Huang, R., Scaal, M. Amniote somite derivatives. *Developmental Dynamics*, **236**(9), 2382-2396 (2007).

Chen, X. H., Motani, R., Cheng, L., Jiang, D. Y., Rieppel, O. The enigmatic marine reptile *Nanchangosaurus* from the Lower Triassic of Hubei, China and the phylogenetic affinities of Hupehsuchia. *PLoS One*, **9**(7), e102361 (2014).

Danowitz, M., Solounias, N. The cervical osteology of *Okapia johnstoni* and *Giraffa camelopardalis*. *PlosOne*, **10**(8): e0136552 (2015).

Dar, G.; Masharawi, Y.; Peleg, S.; Steinberg, N.; May, H.; Medlej, B.; Peled, N., Hershkovitz, I. The epiphyseal ring: a long forgotten anatomical structure with significant physiological function. *Spine*, **36**(11): 850-856 (2011).

Dawson, A.B. Further studies on the epiphyses of the albino rat skeleton, with special reference to the vertebral column, ribs, sternum, and girdles. *The Anatomical Record,* **34**(5): 351-363 (1927).

Francillon-Vieillot, H. *et al.* in *Skeletal biomineralization: Patterns, processes and evolutionary trends. Vol. 1* (ed J.G. Carter) 471-530 (Van Nostrand Reinhold, 1990).

Frey, E. F., Salisbury, S. W. in *Crocodilian Biology and Evolution*. 165-179 (Surrey Beatty & Sons, 2001).

Fröbisch, N., Fröbisch, J., Sander, P. M., Schmitz, L., Rieppel, O. Macropredatory ichthyosaur from the Middle Triassic and the origin of modern trophic networks. *Proceedings of the National Academy of Sciences USA,* **110** 1393–1397 (2013).

Fröbisch, N., Sander, P. M., Rieppel, O. A new species of *Cymbospondylus* (Diapsida, Ichthyosauria) from the Middle Triassic of Nevada and a re-evaluation of the skull osteology of the genus. *Zoological Journal of the Linnean Society of London,* **147**, 515-538 (2006).

Goldman, K.J., Cailliet, G.M., Andrews, A.H., Nathanson, L.J. Assessing the age and growth of chondrichthyan fishes. In *Biology of Sharks and their Relatives* (ed J.Carrier, J. A. Musick, M. R. Heithaus) 423-451 (CRC Press, 2012).

Hall, B. K. *Bones and Cartilage. 2nd Edition. Developmental and Evolutionary Skeletal Biology*. (Academic Press, 2015).

Hautier, L.; Weisbecker, V.; Sánchez-Villagra, M.R.; Goswami, A. Asher, R.J. Skeletal development in sloths and the evolution of mammalian vertebral patterning. *Proceedings of the National Academy of Sciences*, **107**(44): 18903-18908 (2010).

Hautier, L.; Stansfield, F.J.; Allen, W.R.T. Asher, R.J. Skeletal development in the African elephant and ossification timing in placental mammals. *Proceedings of the Royal Society B: Biological Sciences USA*, **279** (1736): 2188-2195 (2013).

Holder, L. A. The comparative morphology of the axial skeleton in the Australian Gekkonidae. *Zoological Journal of the Linnean Society* **44**(297), 300-335 (1960).

Holtz, T. R., Brett-Surman, M. K. Farlow, J. O. *The Complete Dinosaur. Second Edition*. (Indiana University Press, 2012).

Hopley, P. J. Plesiosaur spinal pathology: the first fossil occurrence of Schmorl's nodes. *Journal of Vertebrate Paleontology*, **21**(2), 253-260 (2001).

Houssaye, A. Bone histology of aquatic reptiles: what does it tell us about secondary adaptation to an aquatic life? *Biological Journal of the Linnean Society* **108**, 3–21 (2013).

Houssaye, A., Nakajima, Y., Sander, P. M. Structural, functional, and physiological signals in ichthyosaur vertebral centrum microanatomy and histology. *Geodiversitas* **40**, 161- 170 (2018).

Huang, R., Zhi, Q., Wilting, J., Christ, B. The fate of somitocoele cells in avian embryos. *Anatomy and Embryology (Berlin)* **190**, 243-250 (1994).

Kemp, T.S. The origin and early radiation of therapsid mammal-like reptiles: a palaeobiological hypothesis. *Journal of Evolutionary Biology*, **19**(4): 1231-1247 (2006).

Klein, N., Scheyer, T. M. A new placodont sauropterygian from the Middle Triassic of the Netherlands. *Acta Palaeontologica Polonica* **59**, 887-890 (2014).

Laerm, J. On the origin of rhipidistian vertebrae. *Journal of Paleontology* **53**(1), 175-186 (1979).

Lambertz, M., Bertozzo, F., Sander, P. M. Bone histological correlates for air sacs and their implications for understanding the origin of the dinosaurian respiratory system. *Biology Letters* **14**, 1-5 (2018).

Lamm, E.-T. in *Bone Histology of Fossil Tetrapods. Advancing Methods, Analysis, and Interpretation.* (eds K. Padian, E.-T. Lamm) 55-160 (University of California Press, 2013).

LeBlanc, A. R. H., MacDougall, M. J., Haridy, Y., Scott, D., Reisz, R. R. Caudal autotomy as anti-predatory behaviour in Palaeozoic reptiles. *Scientific Reports*, **8**(1), 3328. (2018).

Liu, J., Rieppel, O. Restudy of *Anshunsaurus hunagguoshuensis* (Reptilia: Thalattosauria) from the Middle Triassic of Guizhou, China. *American Museum Novitates* **3488**, 1-34 (2005).

Maddison, W. P., Maddison, D. R. Mesquite: a modular system for evolutionary analysis. Version 3.02 http://www.mesquiteproject.org. (2015).

Mittapalli, V. R., Huang, R., Patel, K., Christ, B., Scaal, M. Arthrotome: a specific joint forming compartment in the avian somite. *Developmental Dynamics*, **234**(1), 48-53 (2005).

Moon, B. A new phylogeny of ichthyosaurs (Reptilia: Diapsida). *Journal of Systematic Palaeontology* **2017**, 1-27 (2017).

Paavola, L. G., Wilson, D. B., Center, E. M. Histochemistry of the developing notochord, perichordal sheath and vertebrae in Danforth's short-tail (sd) and normal C57BL/6 mice. *Development*, **55**(1), 227-245 (1980).

Padian, K., Lamm, E. T. (Eds.). *Bone Histology of Fossil Tetrapods: Advancing Methods, Analysis, and Interpretation*. (University of California Press, 2013).

Pattappa, G., Li, Z., Peroglio, M., Wismer, N., Alini, M., Grad, S. Diversity of intervertebral disc cells: phenotype and function. *Journal of Anatomy*, **221**(6), 480-496 (2012).

Ricqlès, A. de, Buffrénil, V. de. in *Secondary Adaptation of Tetrapods to Life in Water* (eds J.-M. Mazin, V. de Buffrénil) 289-310 (Verlag Dr. Friedrich Pfeil, 2001).

Ridewood, W.G. On the calcification of the vertebral centra in sharks and rays. *Philosophical Transactions of the Royal Society B* **210**, 311-407 (1921).

Rieppel, O., Liu, J., Bucher, H. The first record of a thalattosaur reptile from the Late Triassic of southern China (Guizhou Province, PR China). *Journal of Vertebrate Paleontology*, **20**(3), 507-514 (2000).

Rieppel, O., Sander, P. M., Storrs, G. W. The skull of the pistosaur *Augustasaurus* from the Middle Triassic of northwestern Nevada. *Journal of Vertebrate Paleontology*, **22**(3), 577-592 (2002).

Rieppel, O., Liu, J. On *Xinpusaurus* (Reptilia: Thalattosauria). *Journal of Vertebrate Paleontology* **26**, 200-204 (2006).

Rufai, A., Benjamin, M., Ralphs, J. R. The development of fibrocartilage in the rat intervertebral disc. *Anatomy and Embryology*, **192**(1), 53-62 (1995).

Romer, A. S. *Osteology of the Reptiles*. (The University of Chicago Press, 1956).

Romer, A. S., Price, L. W. Review of the Pelycosauria. *Special Paper of the Geological Society of America* **28**, 1-538 (1940).

Rothschild, B. M., Berman, D. S. Fusion of caudal vertebrae in Late Jurassic sauropods. *Journal of Vertebrate Paleontology* **11**, 29-36 (1991).

Schmid-Röhl, A., Röhl, J., Oschmann, W., Frimmel, A. Der Posidonienschiefer (Lias-epsilon) Südwestdeutschlands: hochauflösende geochemische, palökologische und sedimmetologische Untersuchungen. *Zentralblatt für Geologie und Paläontologie, Teil I (1997)*, (7-9), 989-1004 (1999).

Sallan, L.C. Tetrapod-like axial regionalization in an early ray-finned fish. *Proceedings of the Royal Society B* **279**, 3264-3271 (2012).

Sander, P. M. The pachypleurosaurids (Reptilia: Nothosauria) from the Middle Triassic of Monte San Giorgio (Switzerland) with the description of a new species. *Philosophical Transactions of the Royal Society of London* **B 325**, 561-670 (1989).

Sander, P. M., Rieppel, O. C., Bucher, H. A new pistosaurid (Reptilia: Sauropterygia) from the Middle Triassic of Nevada and its implications for the origin of plesiosaurs. *Journal of Vertebrate Paleontology* **17**, 526-533 (1997).

Scaal, M. Early development of the vertebral column. *Seminars in Cell and Developmental Biology* **49**, 83–91. (2016).

Schauinsland, H. Die Entwickelung der Eihäute der Reptilien und der Vögel. *Handbuch der Vergleichenden und Experimentellen Entwinklungslehre der Wirbelthiere,* **1** (1902).

Schoch, R. R., Sues, H. D. A Middle Triassic stem-turtle and the evolution of the turtle body plan. *Nature*, **523**(7562), 584 (2015).

Stemple, D. L. Structure and function of the notochord: an essential organ for chordate development. *Development*, **132**(11), 2503-2512 (2005).

Strong, R.M. The order, time, and rate of ossification of the albino rat (*Mus norvegicus albinus*) skeleton. *American Journal of Anatomy*, **36**(2): 313-355 (1925).

Theiler, K. Vertebral malformations. *Advances in Anatomy, Embryology, and Cell Biology*, **112**, 1 (1988).

Wettstein O v. 1. Ordnung der Klasse Reptilia: Rhynchocephalia. In *Handbuch de Zoologie Sauropsida: Allgemeines. Reptilia. Aves* (eds. W. Kükenthal, T. Krumbach, 1–235 (de Gruyter 1931).

Wiemann, J. *et al.* Fossilization transforms vertebrate hard tissue proteins into N-heterocyclic polymers. *Nature Communications*, **9**, 4741 (2018).

Wintrich, T., Hayashi, S., Houssaye, A., Nakajima, Y., Sander, P. M. A Triassic plesiosaurian skeleton and bone histology inform on evolution of a unique body plan. *Sciences Advances* **3**, e1701144, (2017a).

Wintrich, T., Scaal, M., Sander, P. M. Foramina in plesiosaur cervical centra indicate a specialized vascular system. *Fossil Record* **20**, 279-290 (2017b).

Witzmann, F., Asbach, P., Remes, K., Hampe, O., Hilger, A., Paulke, A. Vertebral pathology in an ornithopod dinosaur: a hemivertebra in *Dysalotosaurus lettowvorbecki* from the Jurassic of Tanzania. *The Anatomical Record: Advances in Integrative Anatomy and Evolutionary Biology*, **291**(9), 1149-1155 (2008).

Supplementary Figures 1-29

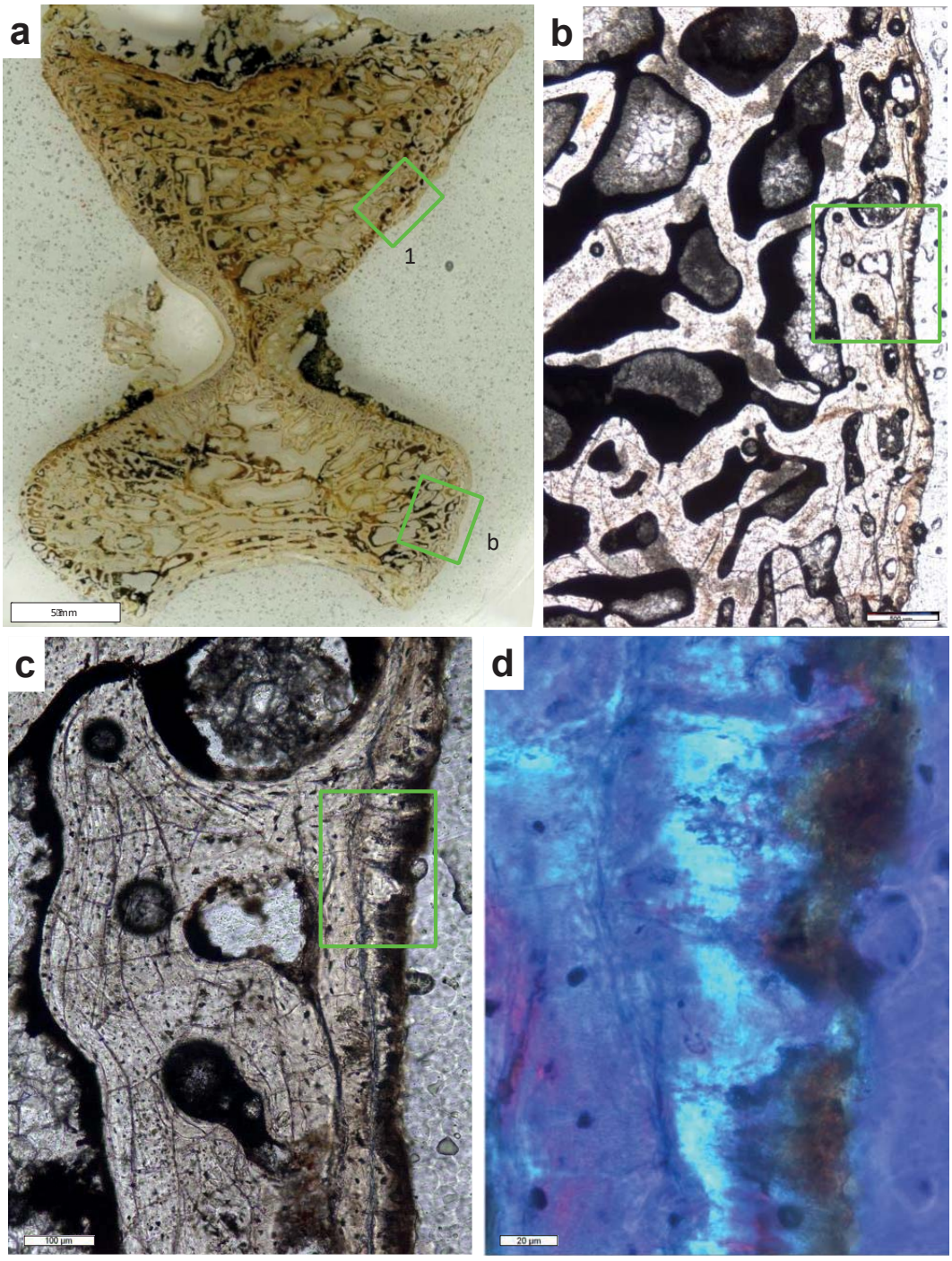

Supplementary Figure S1: Histology of Diadectes sideropelicus STIPB A169, joint with persisting notochord. a Sagittal section of vertebral centrum, neural canal is to the top.1, location of Figure S2a. **b** Enlargement of peripheral part of articular surface in plane polarised light. **c** Closeup of **b**. **d** Close-up of **c** in cross-polarised light and lambda filter. Note the uneven surface and fibre insertions.

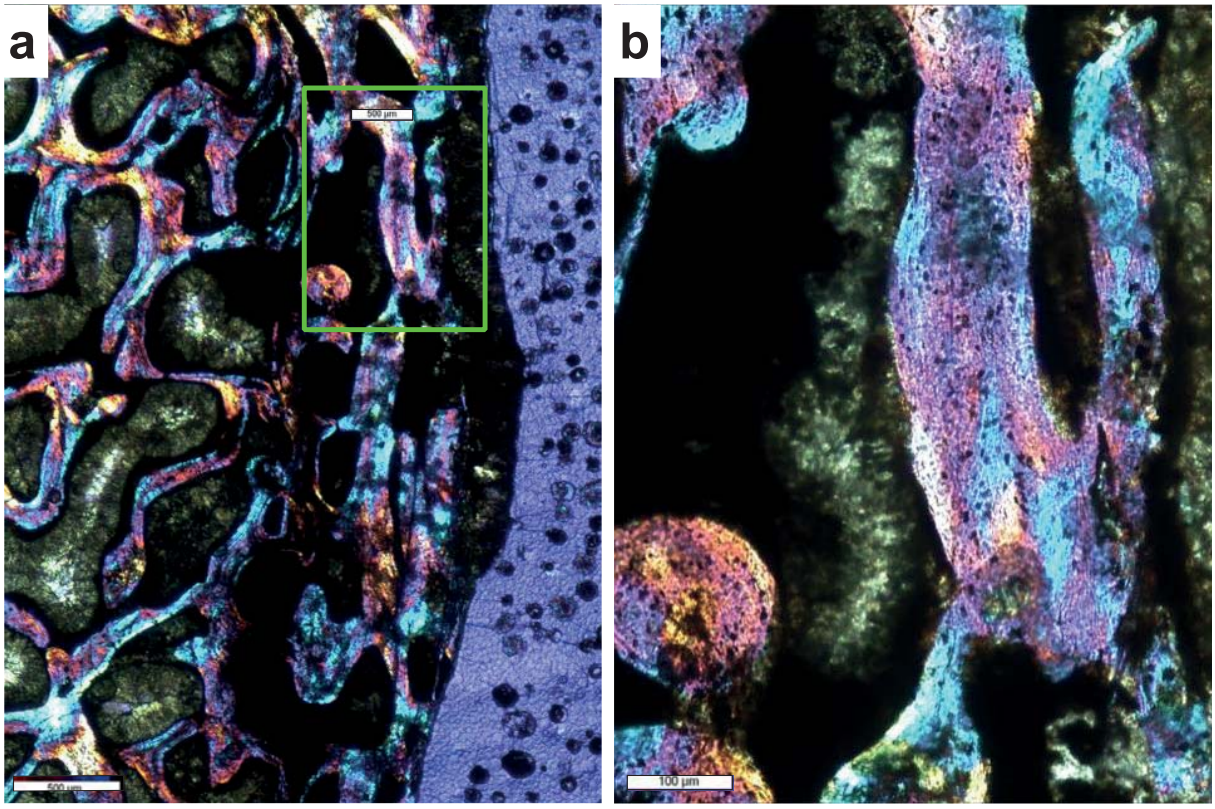

Supplementary Figure S2: Histology of Diadectes sideropelicus STIPB A169 continued. a Inset 1 in Figure S1a, showing the inner part of the articular surface in cross-polarised light and lambda filter. b Closeup, note the smooth trabecular surface facing the intervertebral cavity and the scarcity of chondrocyte lacunae.

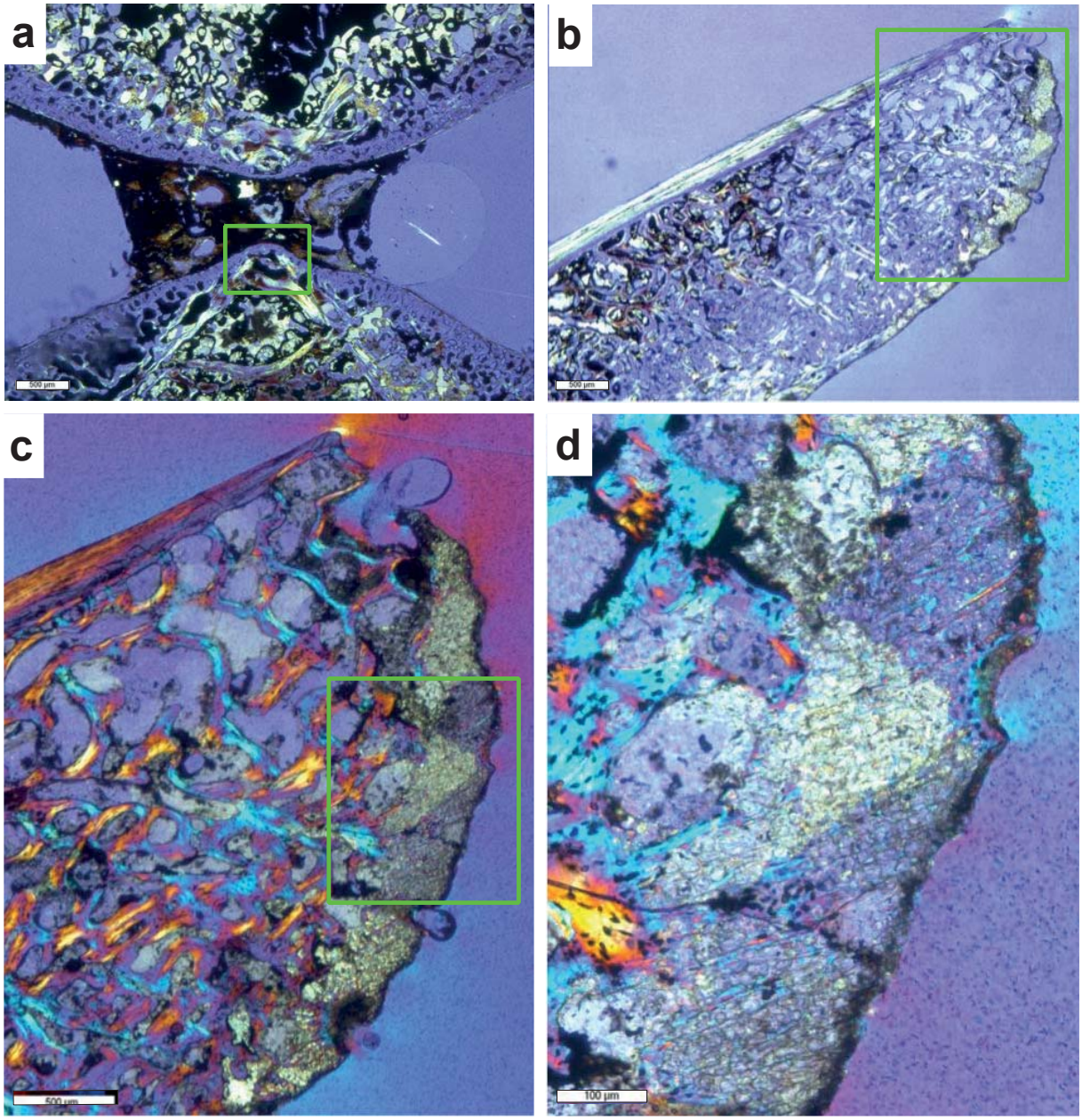

Supplementary Figure S3: Histology of Dimetrodon natalis juvenile STIPB R 652a, joint with persisting notochord. a Sagittal section of the middle of the vertebral centrum, intersecting a large notochordal foramen. Neural canal is to the top. b Sagittal section of the outer part of the vertebral centrum showing a thick layer of fossilised cartilage on top of the endochondral trabeculae. c Closeup of b. d Closeup of c. Note the chondrocyte lacunae arranged in obliquely oriented files and the intervening ossified fibre. All images in cross-polarised light and lambda filter.

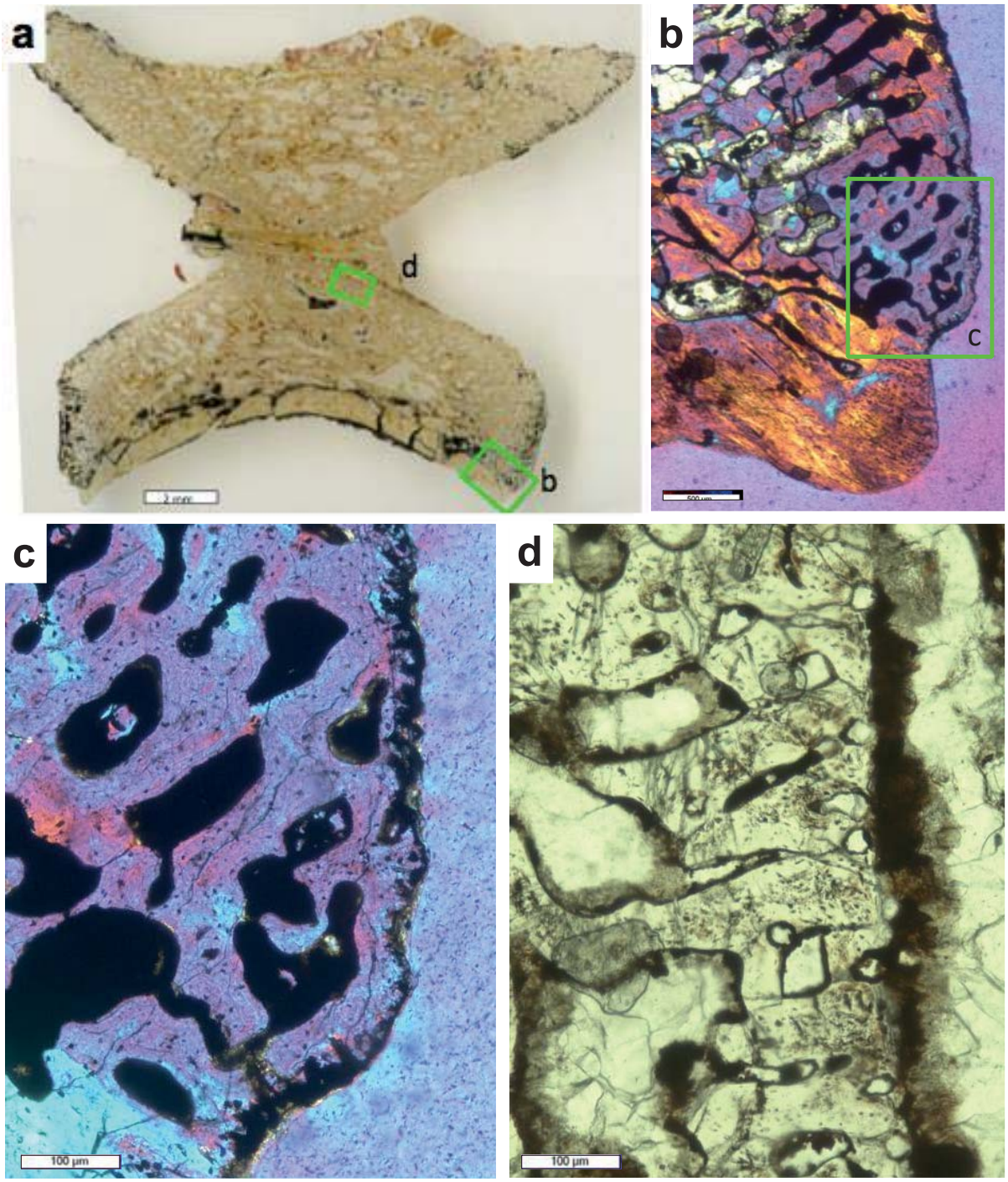

Supplementary Figure S4: Histology of *Dimetrodon natalis* adult STIPB R 653a, joint with persisting notochord. a Sagittal section of vertebral centrum, neural canal is to the top. **b** Enlargement of peripheral part of articular surface (area **b**) in cross polarised light and lambda filter. **c** Closeup of **b**. Note the uneven surface and fibre insertions. **d** Close-up of area **b** in plane-polarised light. Note the smooth surface and lack of chondrocyte lacunae.

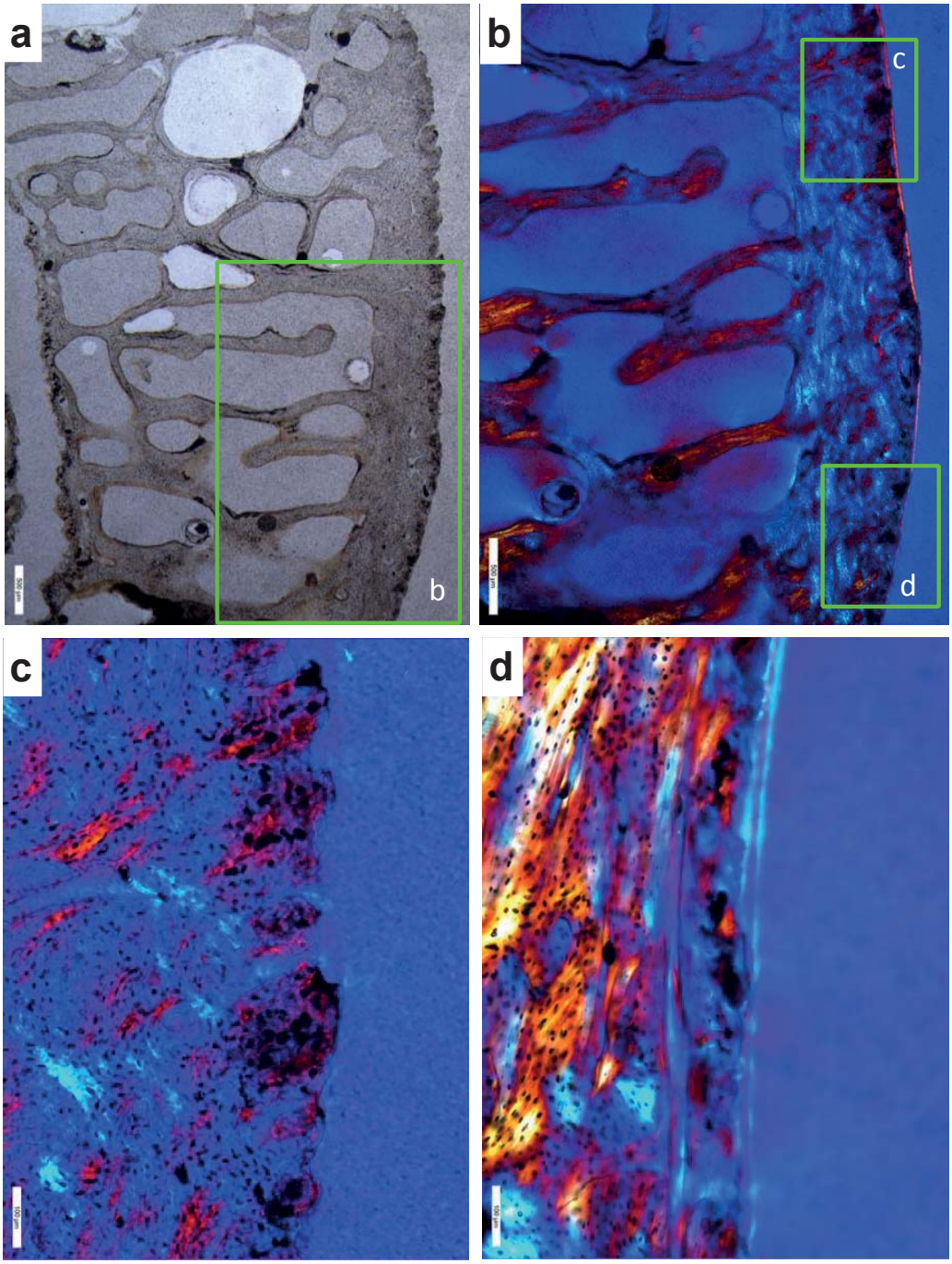

Supplementary Figure S5: Histology of *Phoca vitulina* STIPB M 60, joint with IVD. a Close-up from sagittal section of vertebral centrum, showing part of the bony epiphysis. **b** Enlargement of articular surface (area **b**) showing the transition from the smooth inner part of the articular surface to the peripheral rough surface. **c** Closeup of the rough peripheral surface. Note the oblique orientation of the files of osteocyte lacunae and the fibre insertions. **d** Close-up of the smooth inner surface. Note rarity and poor organisation of the chondrocyte lacunae. Image **a** in plane polarised light, image **b-d** in cross polarised light and lambda filter.

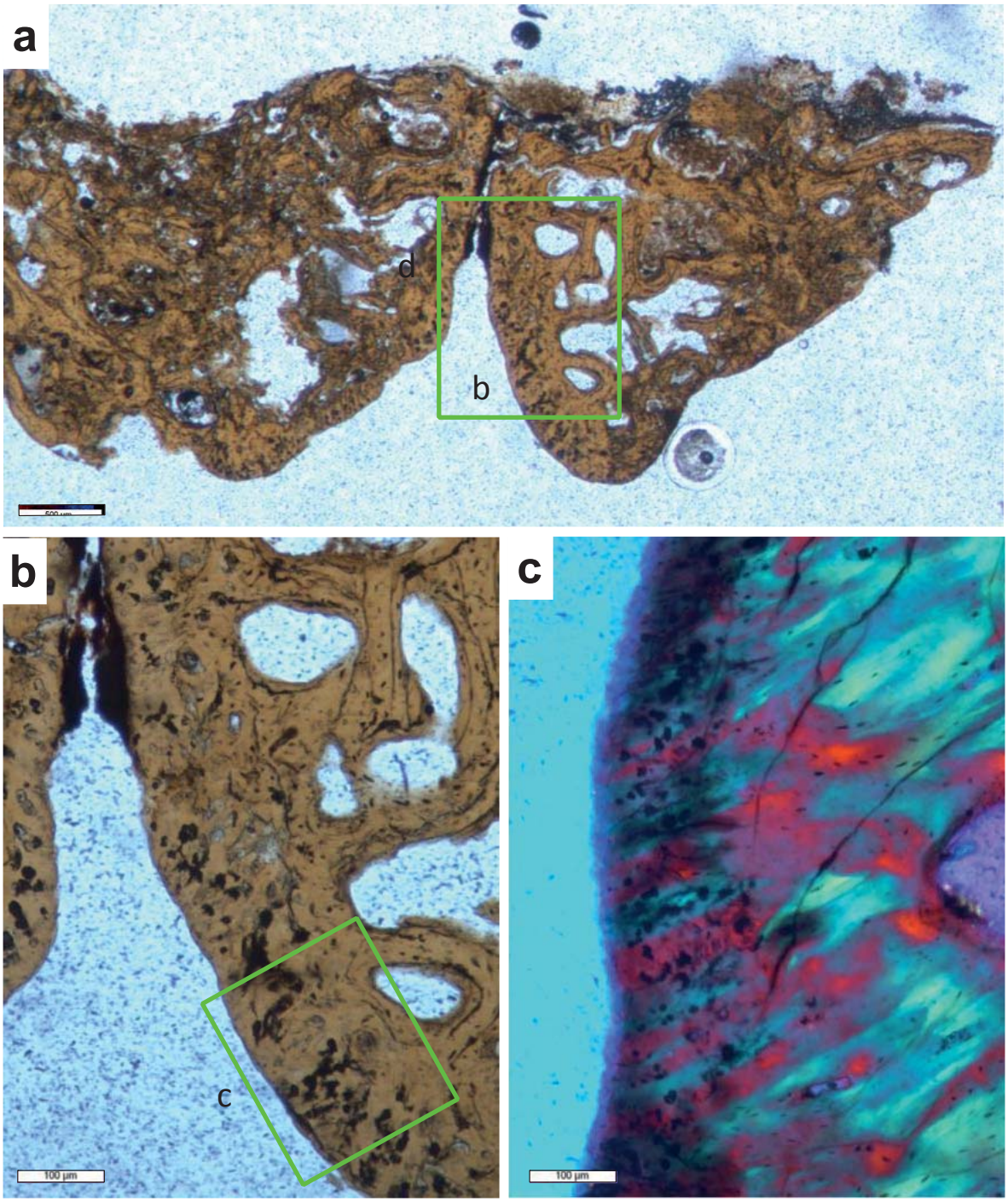

Supplementary Figure S6: Histology of *Eurohippus* sp. HLMD ME 139, joint with IVD. **a** Sagittal section of the outer margin of the articular surface of two articulated vertebral centra in plane polarised light. **b** Enlargement of peripheral part of articular surface in plane polarised light. Note the outwardly directed files of chondrocyte lacunae. **c** Closeup in cross-polarised light and lambda filter. Note the fibre insertions between the chondrocyte files.

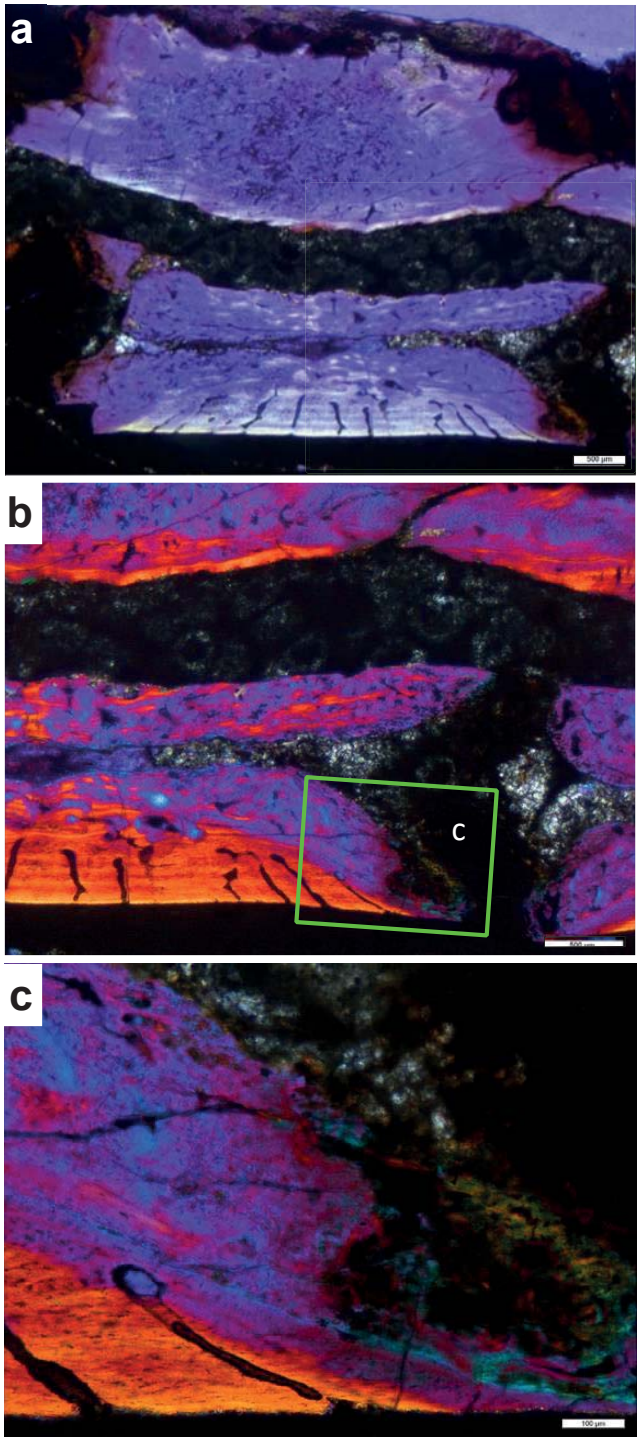

Supplementary Figure S7: Histology of *Stereosternum tumidum* STIPB R622, joint with persisting notochord. a Sagittal section of a segment of vertebral column, neural canal is to the top. Image in plane polarised light. **b** close up of the joint area of two articulated vertebral centra in cross-polarised light and lambda filter. Note the continuous notochordal canal. **c** Closeup of **b**. Note the uneven surface and fibre insertions in the peripheral area.

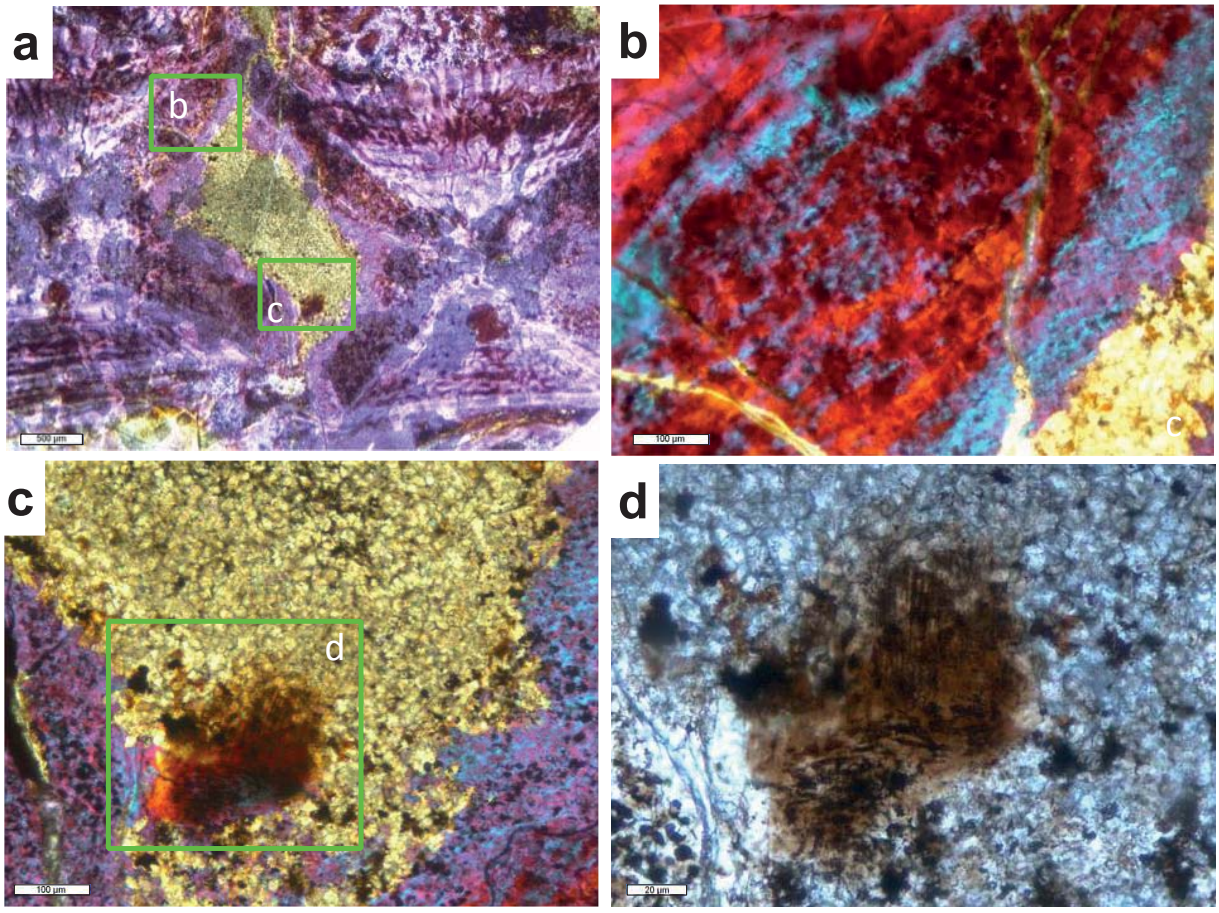

Supplementary Figure S8: Histology of *Nanchangosaurus* HFUT YAN-10-02. a Sagittal section of two articulated vertebral centra in cross-polarised light with lambda filter. **b** Enlargement of "funnel" part of articular surface. Note the outwardly directed files of unmineralised chondrocyte lacunae (blue and pink) followed by a thick layer of endochondral bone with cartilage (mainly red) and periosteal bone (upper left). **c** Closeup of ventral part of articular space in cross-polarised light with lambda filter. Note the patch of brown fibrous tissue and the granular nature of the matrix. **d** Closeup of brown fibrous tissue and the granular matrix in plane polarised light.

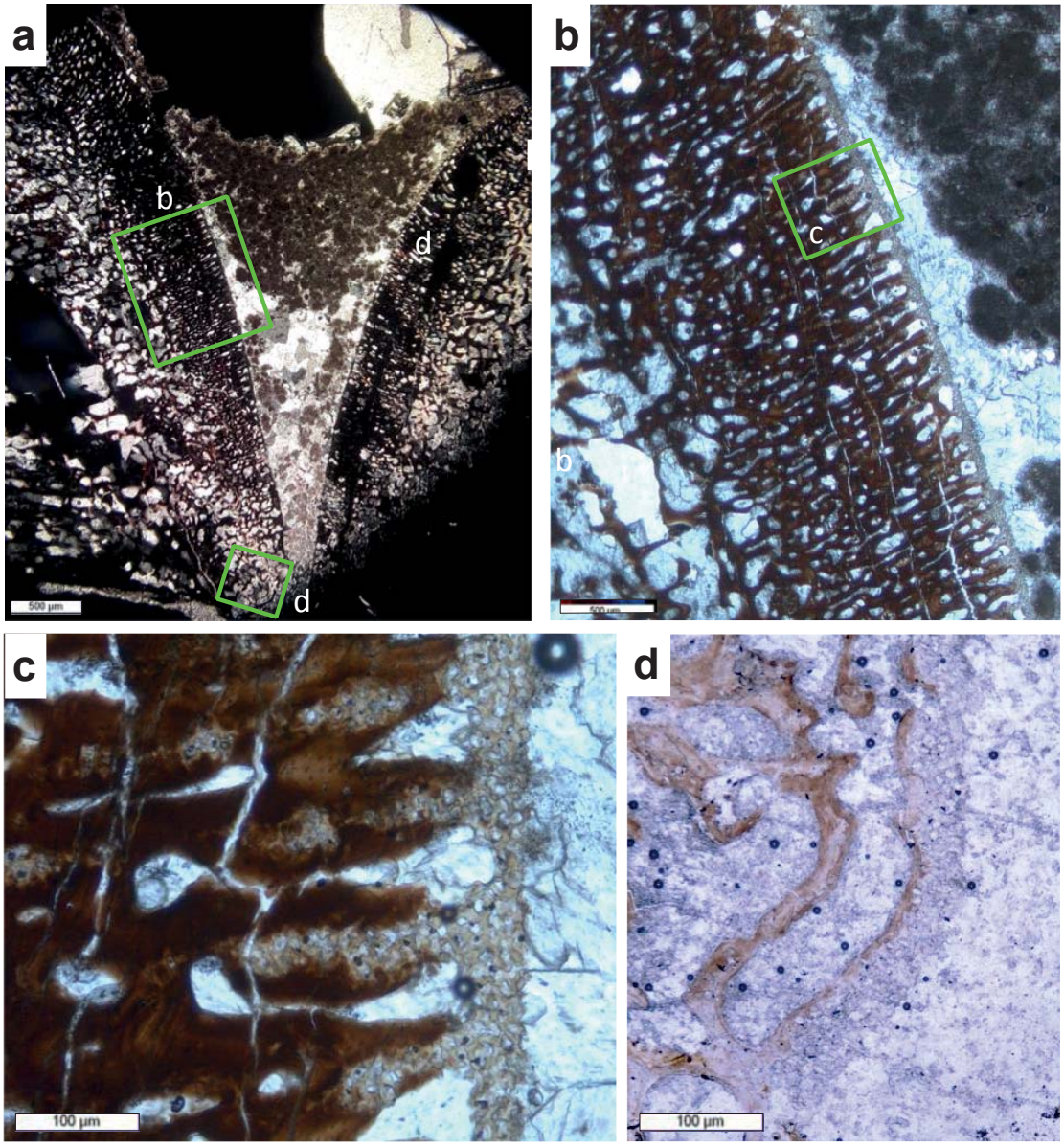

Supplementary Figure S9: Histology of Cymbospondylidae new taxon A LACM DI 158109, joint with IVD. a Sagittal section of the ventral part of two articulated vertebral centra and intervening matter. Neural canal is to the top, image in cross-polarised light. **b** Enlargement of a showing layer of fossilised cartilage on top of the endochondral trabeculae and the globular bodies of the possible NP. Image in plane polarised light. **c** Closeup of **b**. Note the chondrocytes arranged in files (hypertrophy zone) and the replacement of the chondrocytes by endochondral bone. Image in plane polarised light. **d** Closeup of the margin of the articular surface. The arrangement of chondrocyte lacunae into files is indistinct. Image in plane polarised light.

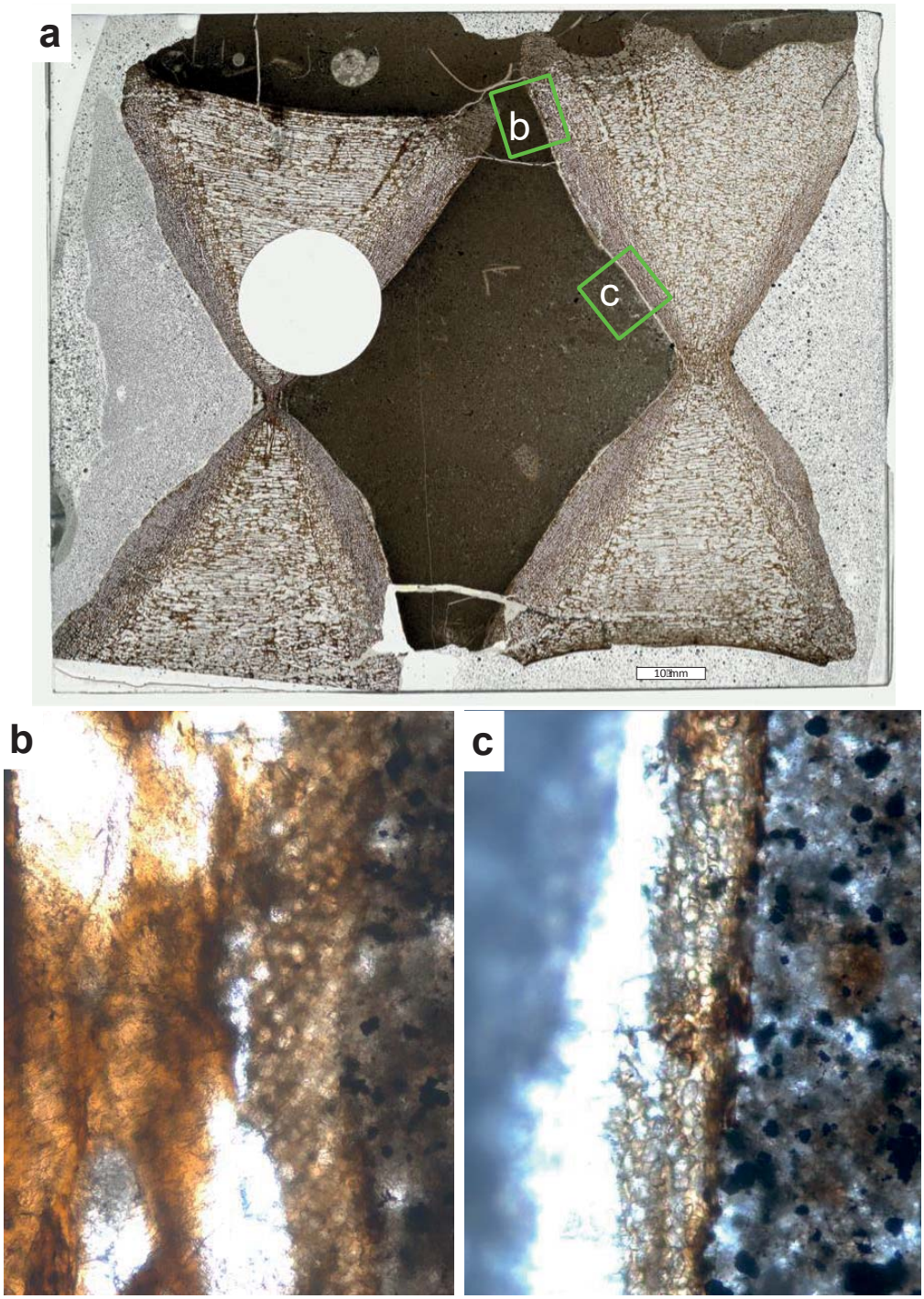

Supplementary Figure S10: Histology of cf. *Cymbospondylus* STIPB R 660, joint with IVD. a Sagittal section of a segment of vertebral column, neural canal is to the top. Image in plane polarised light. Translucent circle resulted from coring of the bone. **b** Enlargement of peripheral part of articular surface (area **b**) in cross polarised light. Note the oblique orientation of the chondrocyte files. **c** Close-up of area **c**. Note the loose and irregular arrangement of the chondrocyte lacunae. Image in cross-polarised light.

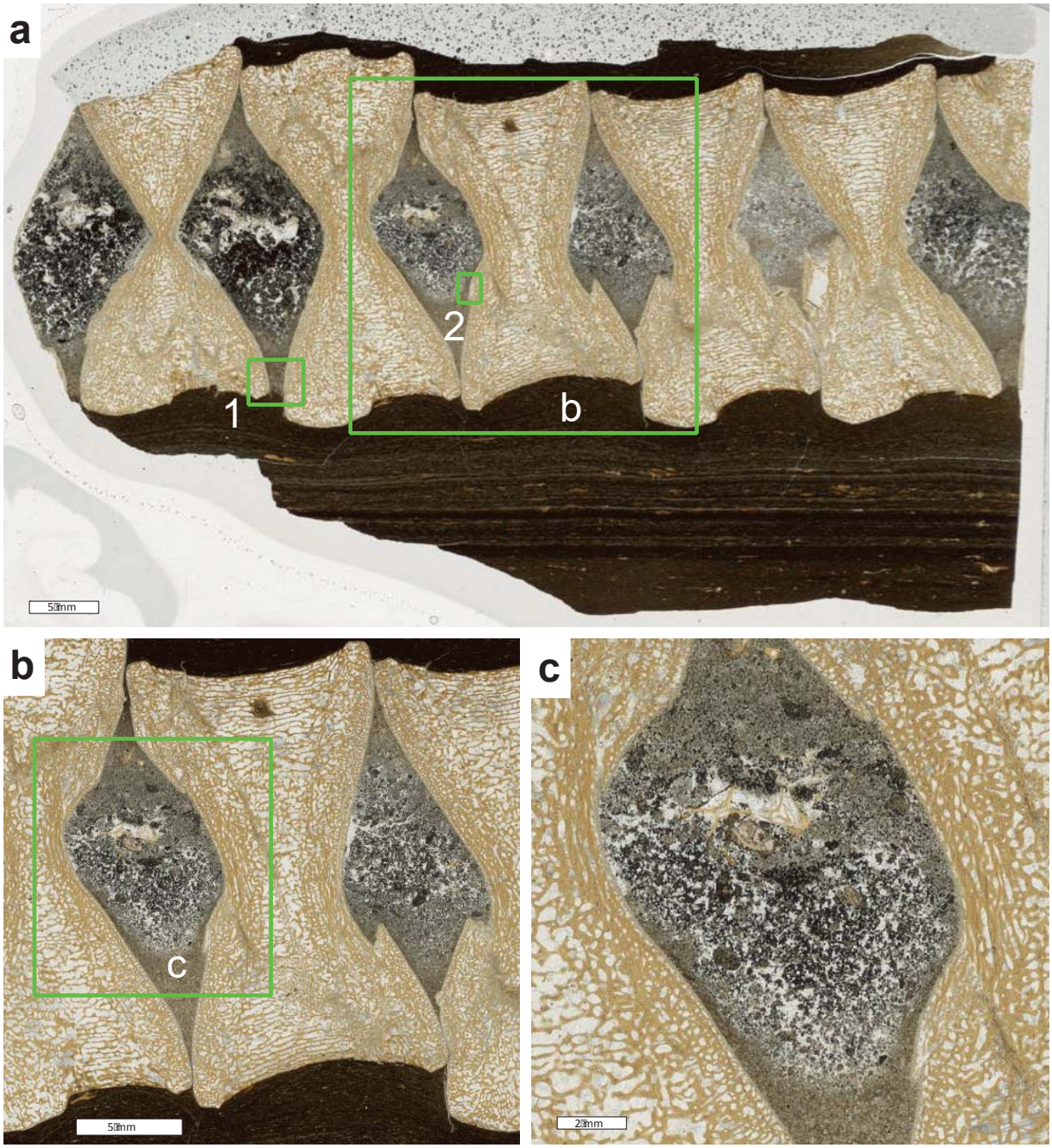

Supplementary Figure S11: Histology of *Stenopterygius* sp. STIPB R 661, joint with IVD. a Sagittal section of a segment of vertebral column, neural canal is to the top. Image in plane polarised light. Note the laminated sediment below the vertebrae and the granular fill of the intervertebral spaces. **b** Enlargement of three articulating vertebrae. Note the apparent preservation of an AF and NP. **c** Close-up of the intervertebral space. All images are in plane-polarised light.

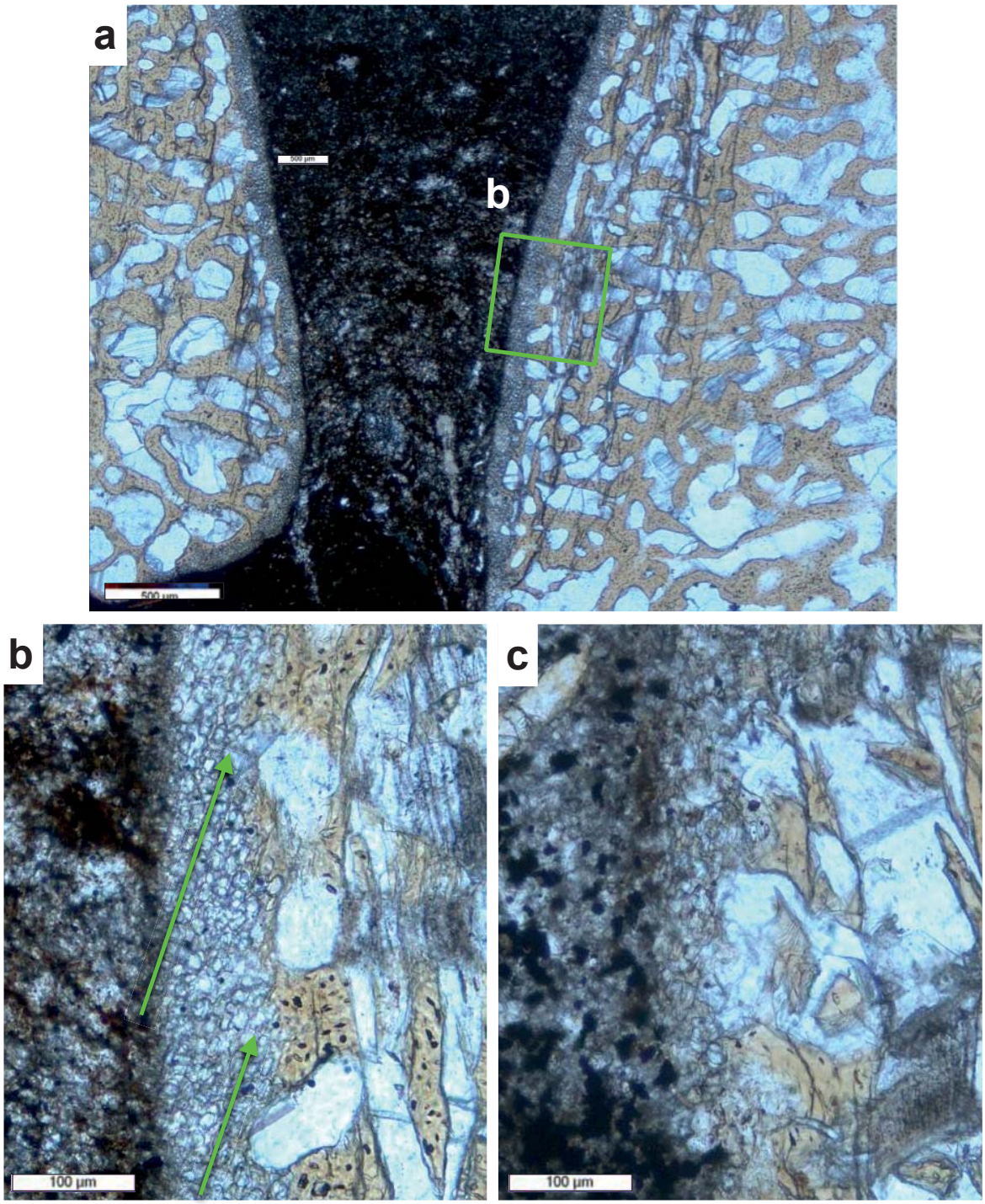

Supplementary Figure S12: Histology of *Stenopterygius* sp. STIPB R 661 continued. a Close-up of the ventral peripheral part of two articulating vertebrae. See previous figure for location (area 1). **b** Enlargement of peripheral part of articular surface. Note the oblique orientation of the chondrocyte files. **c** Close-up of inner articular surface, see previous figure for location (area 1,2). Note the loose and irregular arrangement of the chondrocyte lacunae. All images in cross-polarised light.

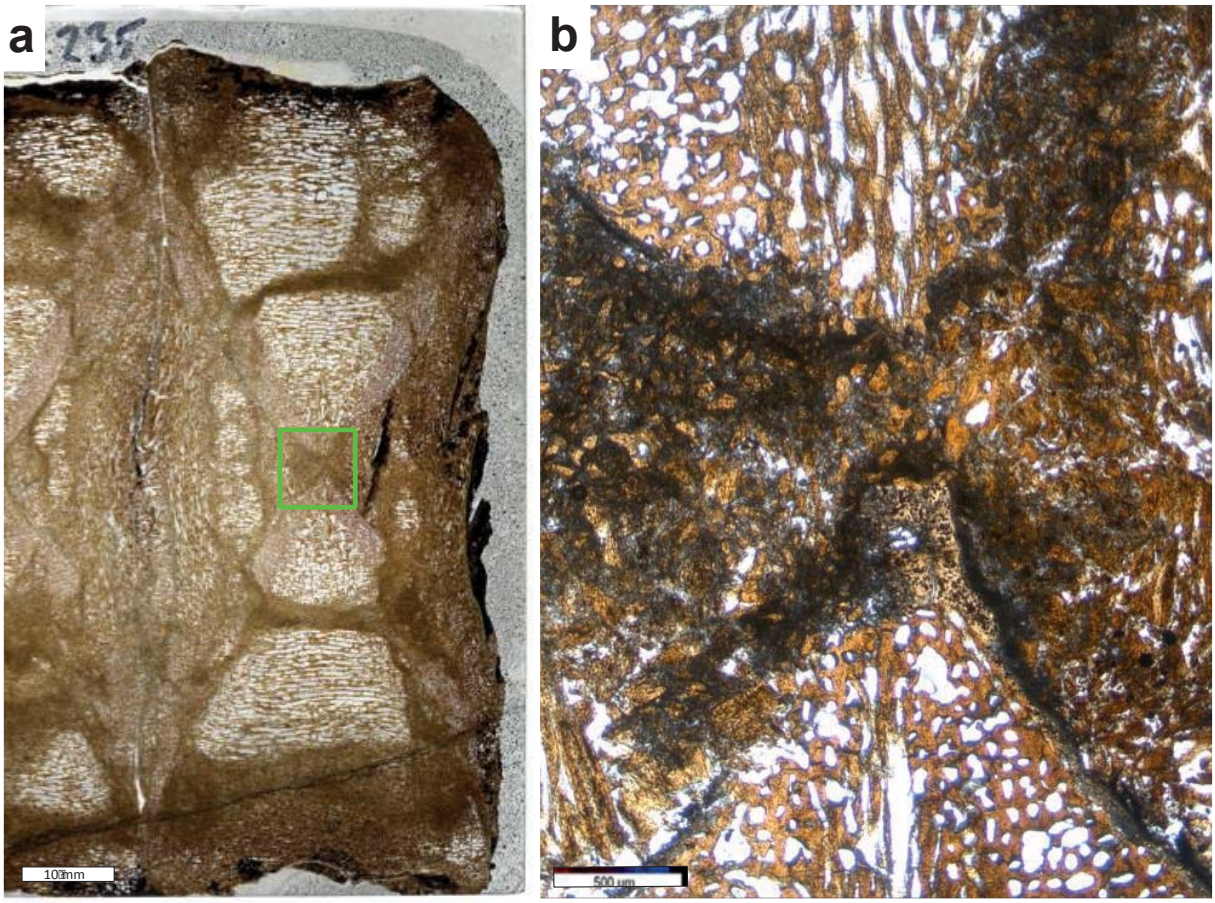

Supplementary Figure S13: Histology of *Leptopterygius* sp. STIPB R235, joint with IVD and vestigial notochord. a Sagittal section of two articulated vertebral centra, neural canal is to the top. **b** Enlargement of middle of the centrum. Note the small notochordal foramen. Images in plane polarised light.

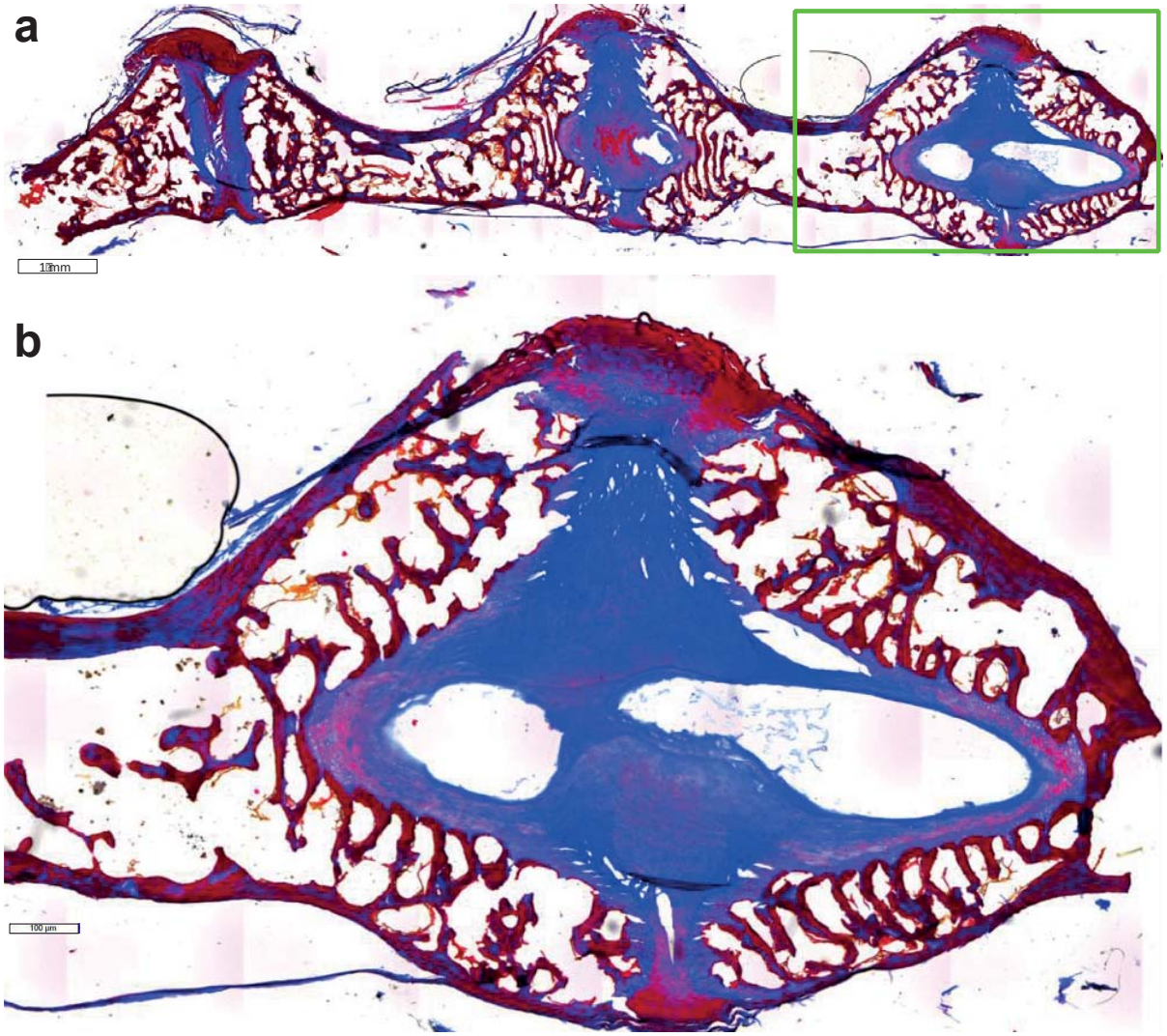

Supplementary Figure S14 Histology of *Sphenodon punctatus* NHMW 8108, joint with persisting notochord. a Oblique sagittal microtome section stained with Azan of three articulated vertebral centra, neural canal is to the top. Red is bone and ligaments, cartilage stains pink and light blue, notochord stains darker blue. **b** Enlargement of the intervertebral joint of the centrum. Note the vesicles in the notochord.

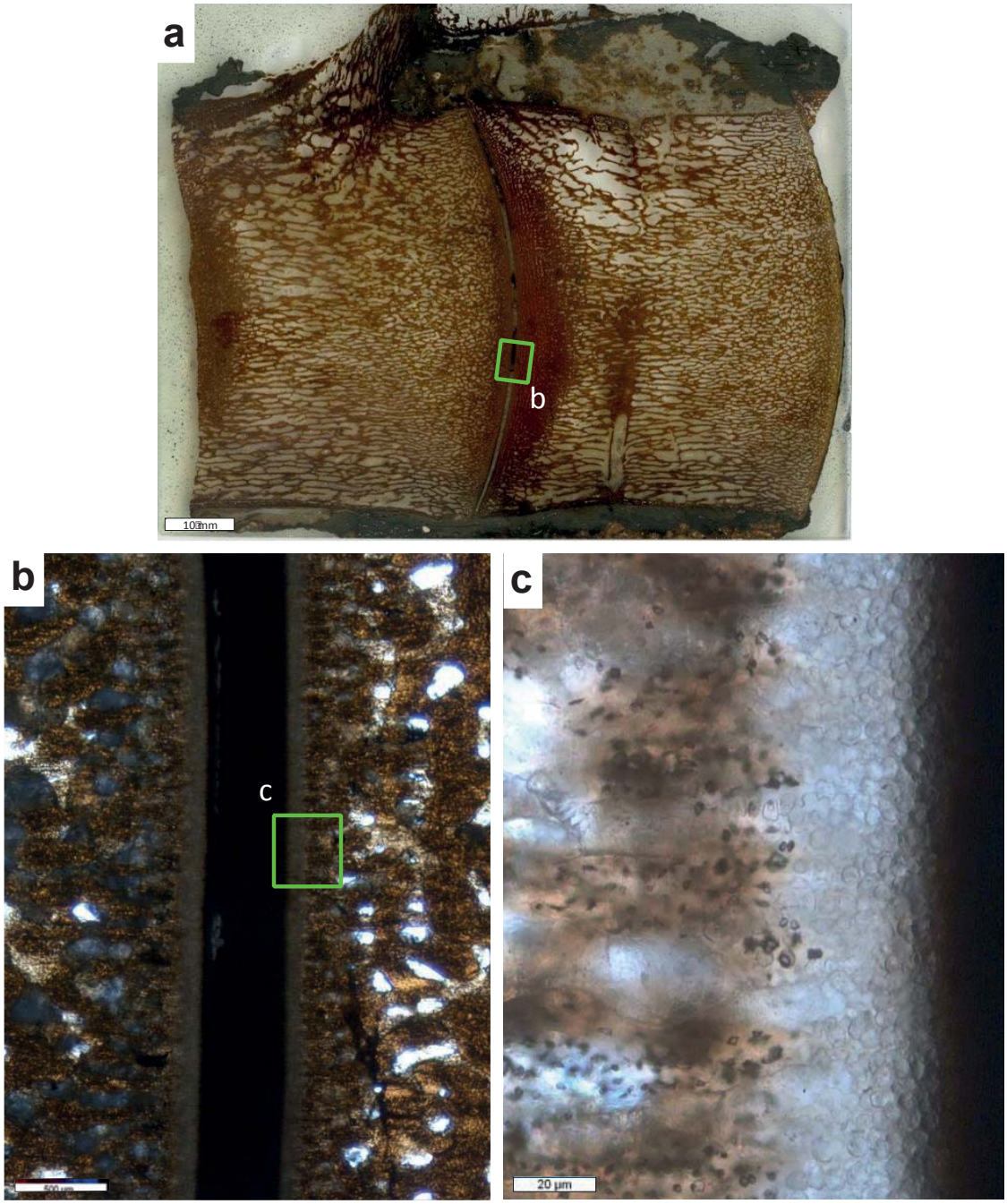

Supplementary Figure S15: Histology of *Mosasaurus missouriensis* STIPB Goldfuß 1230, synovial ball-and-socket joint. a Sagittal section of two articulated vertebra, neural canal is to the top. Image in plane polarised light. **b** Enlargement of peripheral part of articular surface (area **b**) in cross-polarised light. Note the very narrow joint space and the smooth articular surface. **c** Close-up of area **c**. Note the well preserved hyaline cartilage with the chondrocyte lacunae arranged in regular files perpendicular to the surface. Image in cross-polarised light.

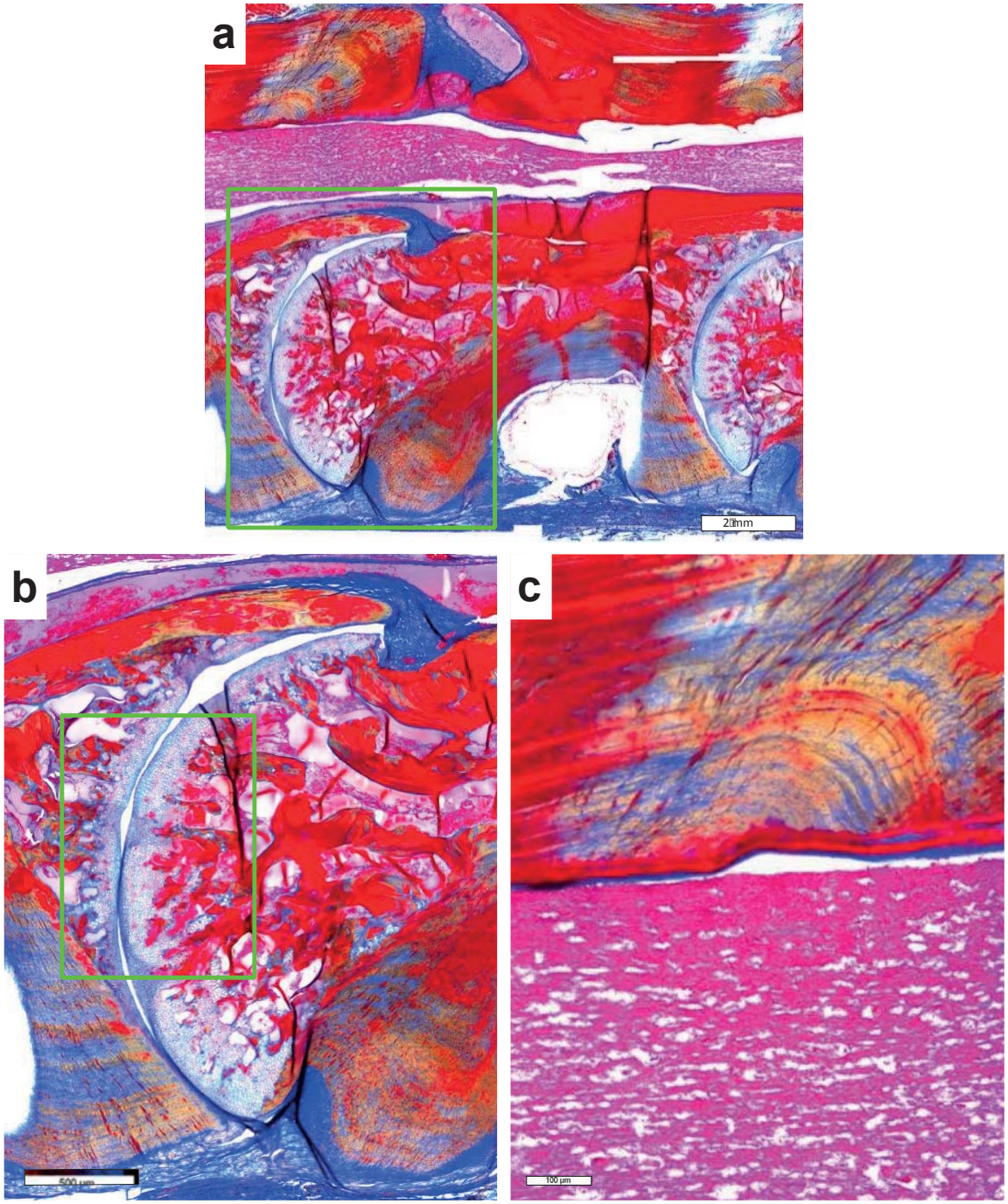

Supplementary Figure S16: Histology of *Python* sp. STIPB R 662, synovial ball-and-socket joint. a Sagittal microtome section stained with Azan of three articulated vertebral centra, neural canal is to the top. Red is bone and ligaments, cartilage stains pink and light blue, ligament stains darker blue. **b** Enlargement of joint. Note the very narrow joint space and the smooth articular surface. **c** Close-up of **b**. Note the hyaline cartilage in which the chondrocyte lacunae are arranged in regular files perpendicular to the surface.

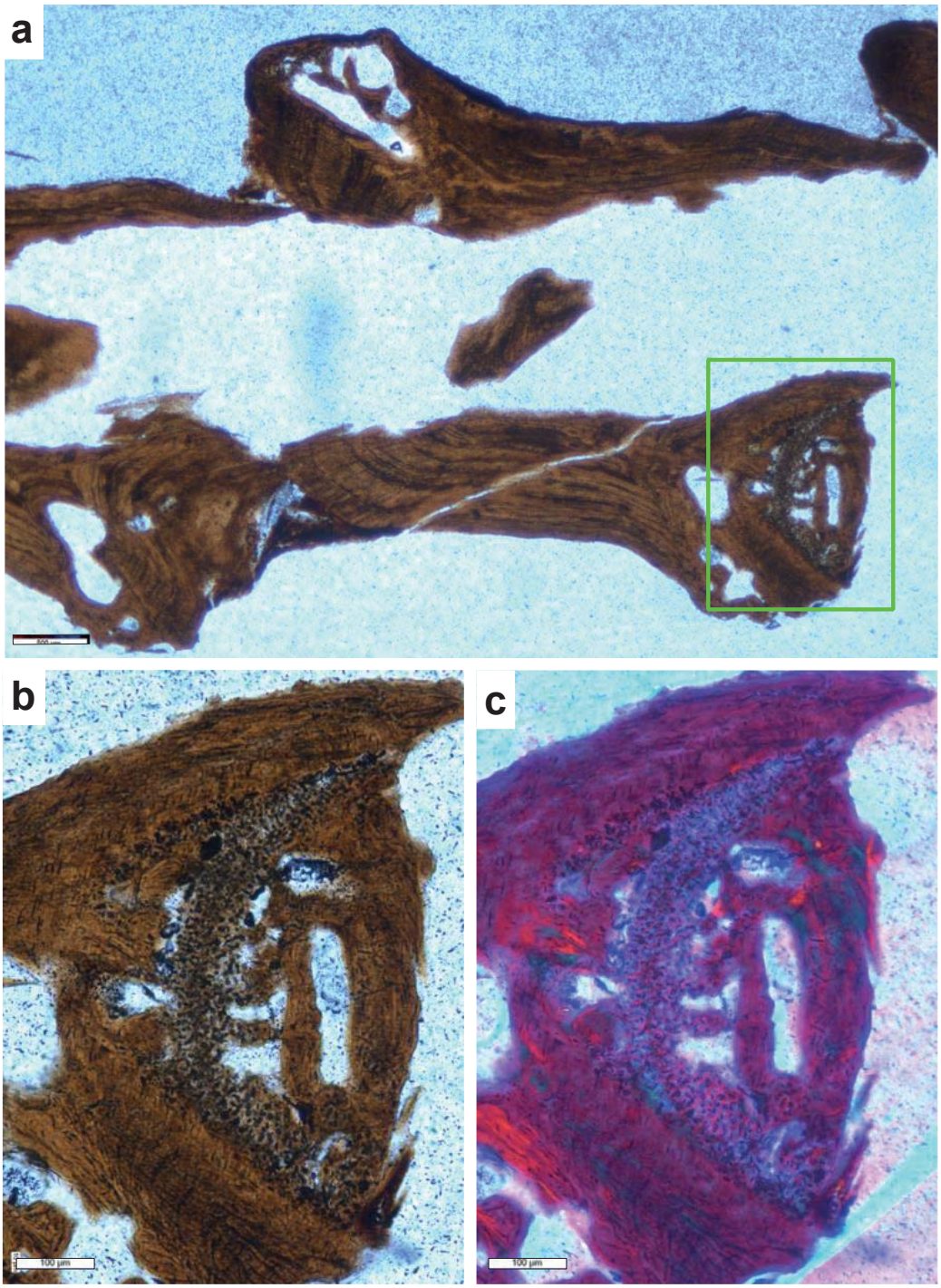

Supplementary Figure S17: Histology of Ophidia indet. HLMD ME 7624b, synovial ball-and-socket joint. a Sagittal section of three articulated vertebra, very large neural canal is to the top. Image in plane polarised light. **b** Enlargement of right joint (green box) in plane polarised light. The joint space is closed over during fossilisation. Note the well preserved hyaline cartilage with the chondrocyte lacunae arranged in regular files perpendicular to the surface. **c** Same as previous but in cross-polarised light and lambda filter.

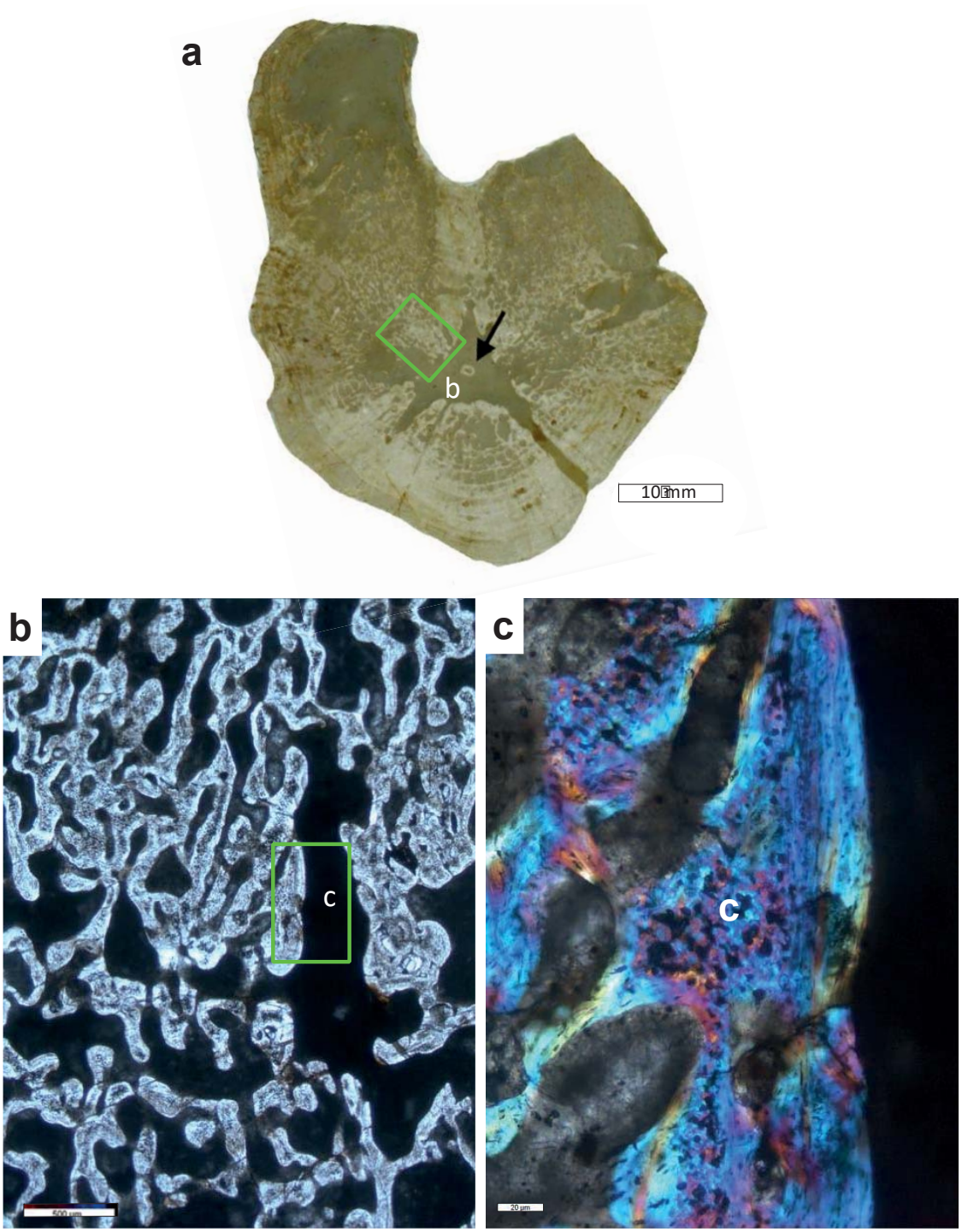

Supplementary Figure S17: Histology of Ophidia indet. HLMD ME 7624b, synovial ball-and-socket joint. a Sagittal section of three articulated vertebra, very large neural canal is to the top. Image in plane polarised light. **b** Enlargement of right joint (green box) in plane polarised light. The joint space is closed over during fossilisation. Note the well preserved hyaline cartilage with the chondrocyte lacunae arranged in regular files perpendicular to the surface. **c** Same as previous but in cross-polarised light and lambda filter.

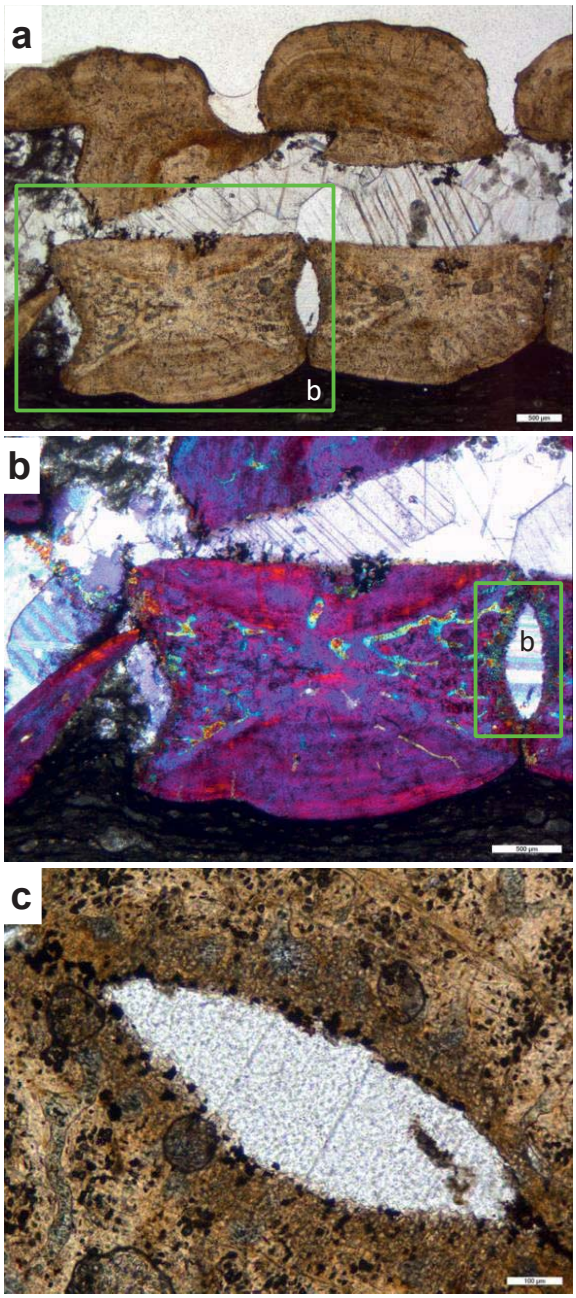

Supplementary Figure S19: Histology of *Neusticosaurus peyeri* PIMUZ T 3768, joint with IVD. a Sagittal section of four articulated vertebrae, neural canal and spine is to the top. Image in plane polarised light. **b** Enlargement of one vertebral centrum articulating with two others in cross-polarised light and lambda filter. Note the platycoelous shape and the clear separation of the periosteal and endochondral domains. **c** Close-up of **b** showing the joint area of two articulated vertebral centra in plane polarised light. Note the cartilage layer on the articular surface of both vertebrae.

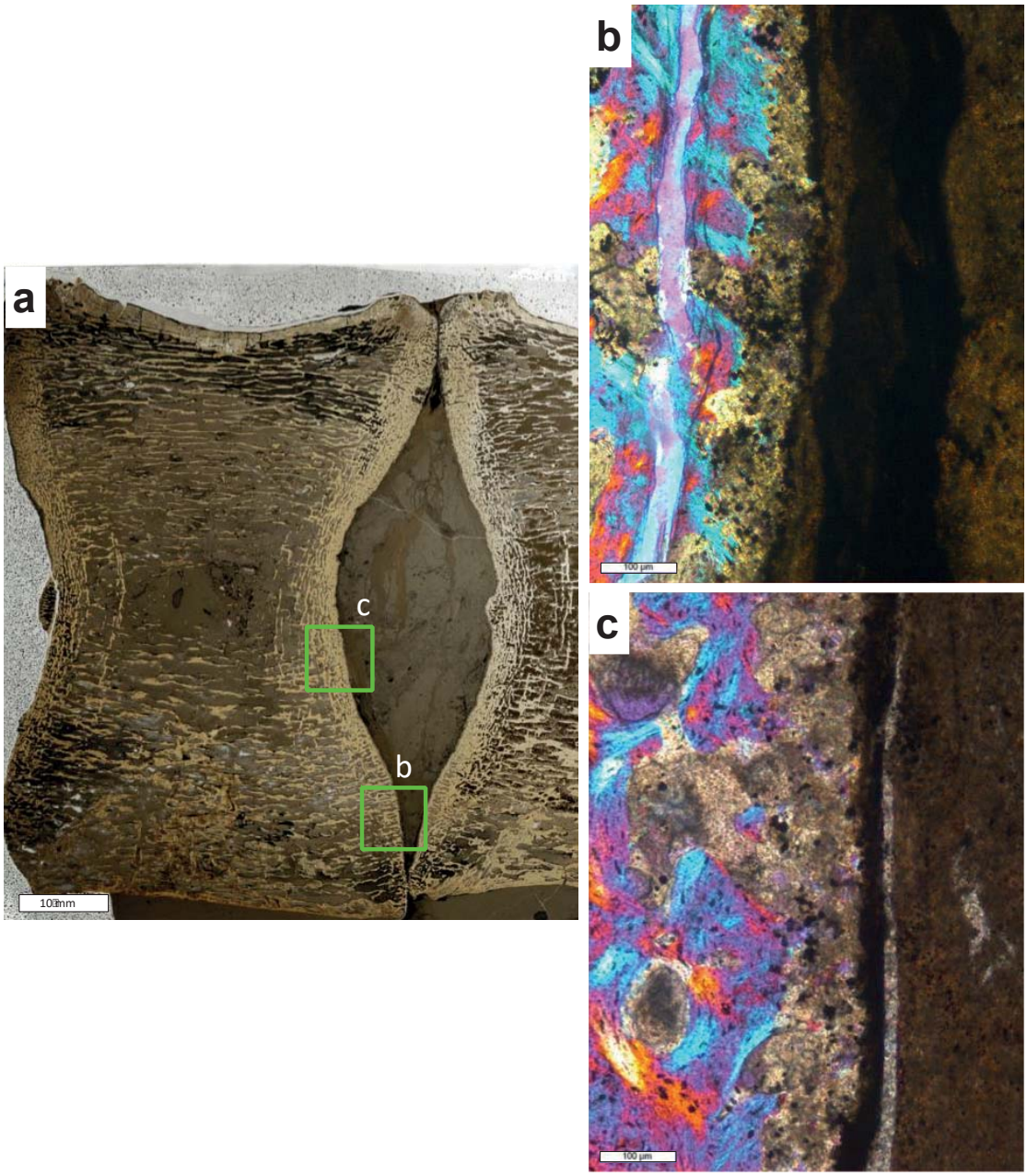

Supplementary Figure S20: Histology of *Plesiosaurus dolichodirus* STIPB R 88, joint with IVD. a Sagittal section of a two articulated vertebral centra, neural canal is to the top. Image in plane polarised light. **b** Enlargement of peripheral part of articular surface (area **b**) in cross polarised light and lambda filter. Note the clear separation of bone and cartilage revealing the peripherally inclined chondrocyte files and the insertion of fibres into the bony areas in between. **c** Enlargement of middle part of articular surface (area **c**). Note the loose and irregular arrangement of the chondrocyte lacunae and the lack of fibre insertions. Image in cross-polarised light.

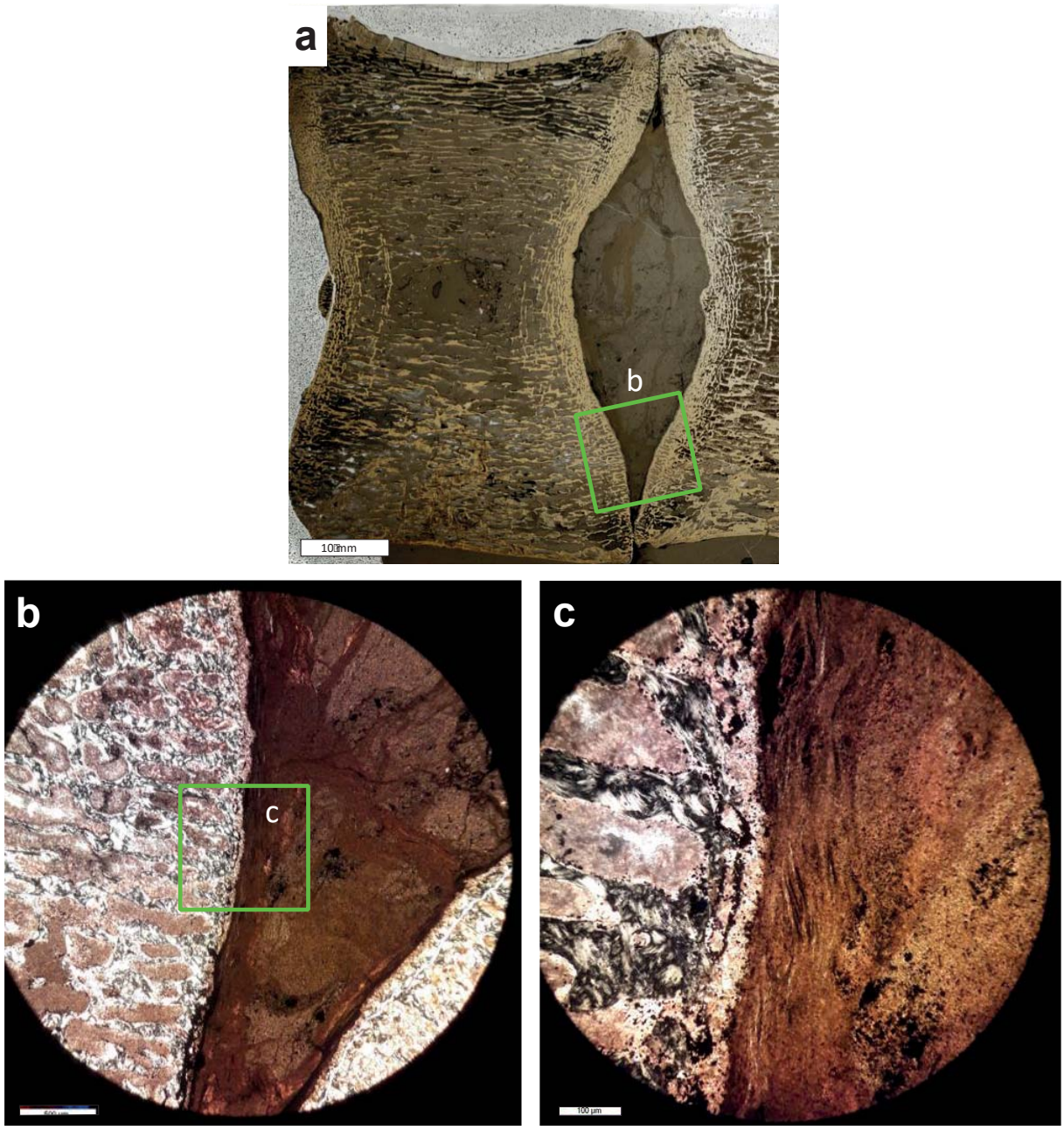

Supplementary Figure S21: Histology of *Plesiosaurus dolichodirus* STIPB R 88 continued. a Sagittal section of a two articulated vertebral centra, neural canal is to the top. Image in plane polarised light. **b** Ventral part of the intervertebral space showing probable altered non-mineralized tissues of the IVD. **c** Enlargement of area c. Note the fibrous layer overlying the cartilage on the articular surface. The fibrous layer probably represent the AF of the IVD. Images in **b** and **c** in cross-polarised light.

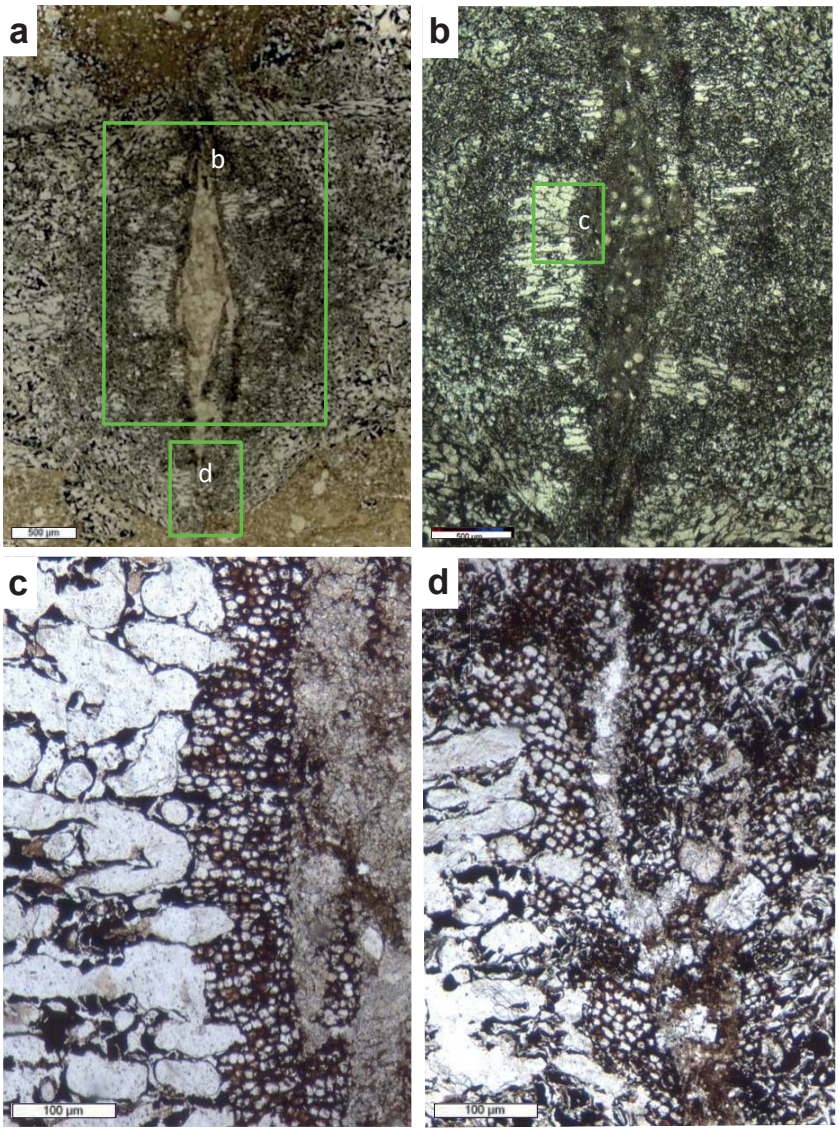

Supplementary Figure S22: Histology of *Xinpusaurus* HFUT GL 17006, joint with IVD. **a** Sagittal section of a two articulated vertebral centra, neural canal is to the top. **b** Enlargement of central part of intervertebral joint. Note the poor preservation of the bone tissue histology, separation of bone and cartilage revealing the peripherally inclined chondrocyte files and the insertion of fibres into the bony areas in between. **c** Enlargement of area **c**. Note the partially mineralized files of chondrocyte lacunae oriented perpendicular to the articular surface.These are overlain by unmineralised and less well organised chondrocytes. **d** Enlargement of peripheral part of articular surface (area **d**). Note the peripherally inclined chondrocyte files. All images in plane polarised light.

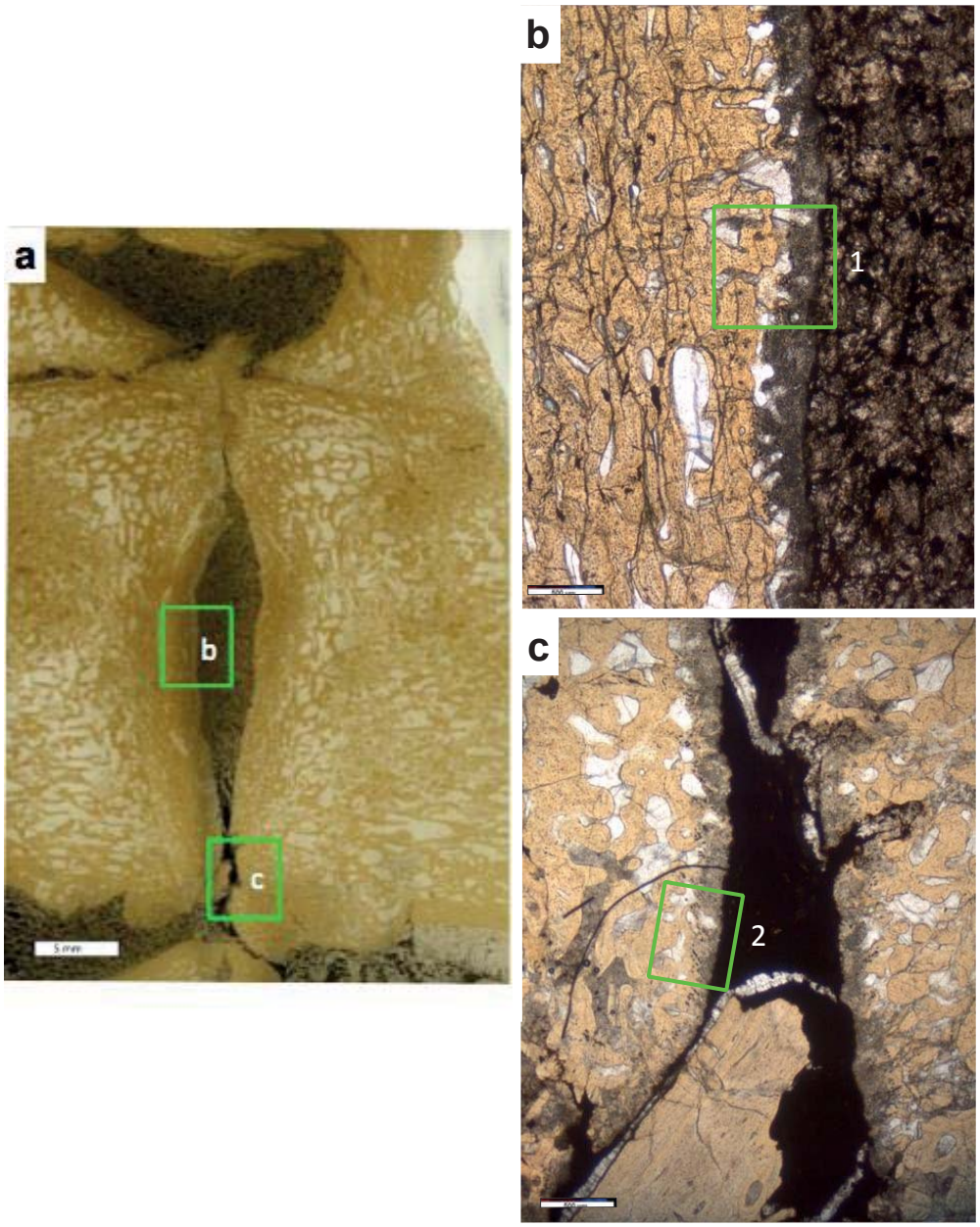

Supplementary Figure S23: Histology of *Steneosaurus* STIPB R 663, joint with IVD. a Sagittal section of two articulated vertebral centra, neural canal is to the top. Image in plane polarised light. **b** Enlargement of middle part of articular surface (area **c**). Note the clear separation of bone and cartilage and the loose and irregular arrangement of the chondrocyte lacunae and the lack of fibre insertions. Image in cross-polarised light. c Enlargement of peripheral part of articular surfaces (area **b**) in cross polarised light. Note the clear separation of bone and cartilage revealing the peripherally inclined chondrocyte files and the insertion of fibres into the bony areas in between. See following figure for close-ups.

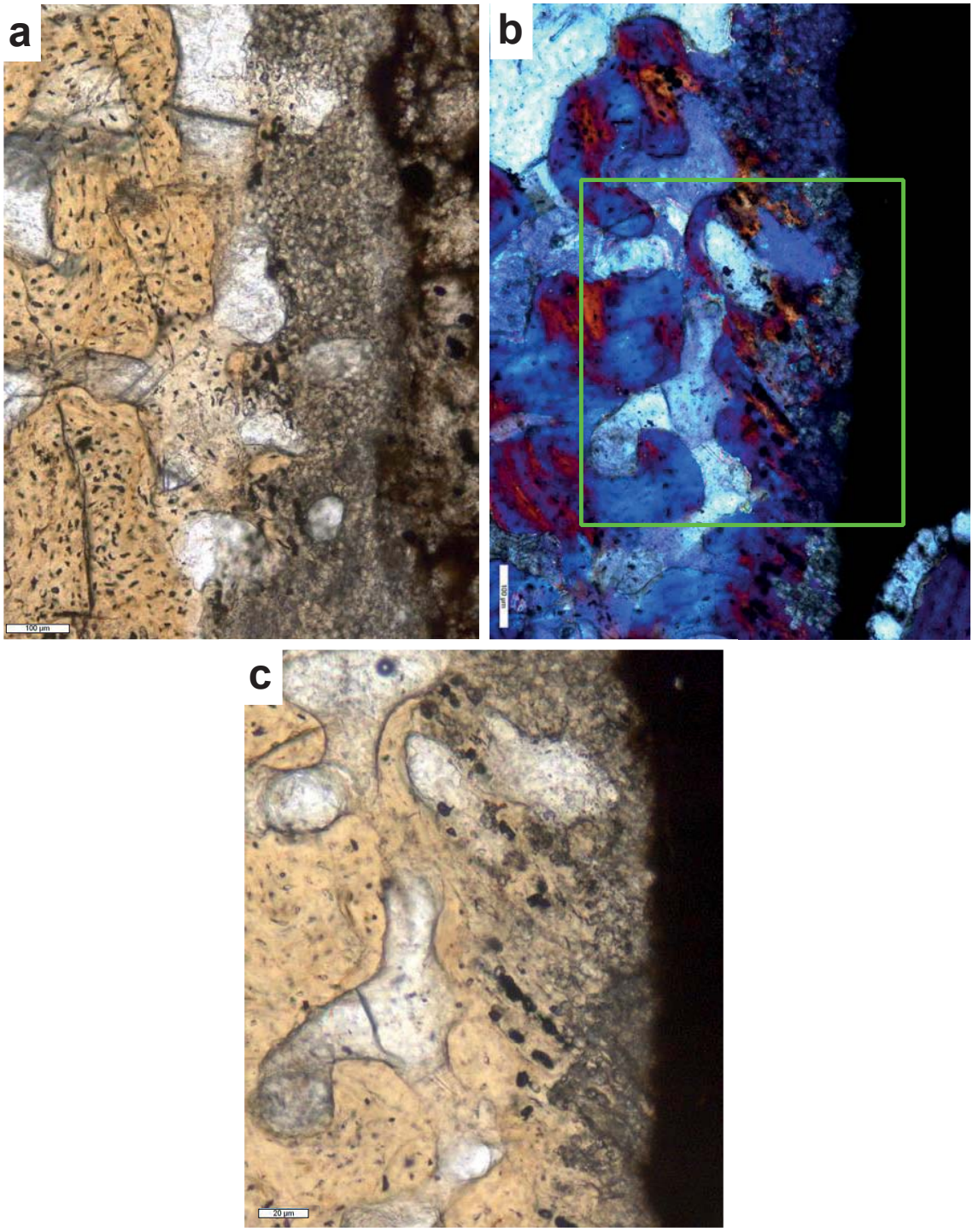

Supplementary Figure S24: Histology of *Steneosaurus* STIPB R 663 continued. a Close-up of area 1 in previous figure, cross-polarised light. **b** Close-up of area 2 in cross-polarised light and lambda filter. Note the oblique orientation of the chondrocyte files. **c** Close-up of **b** in plane polarised light. Note the distinctive chondrocyte lacunae.

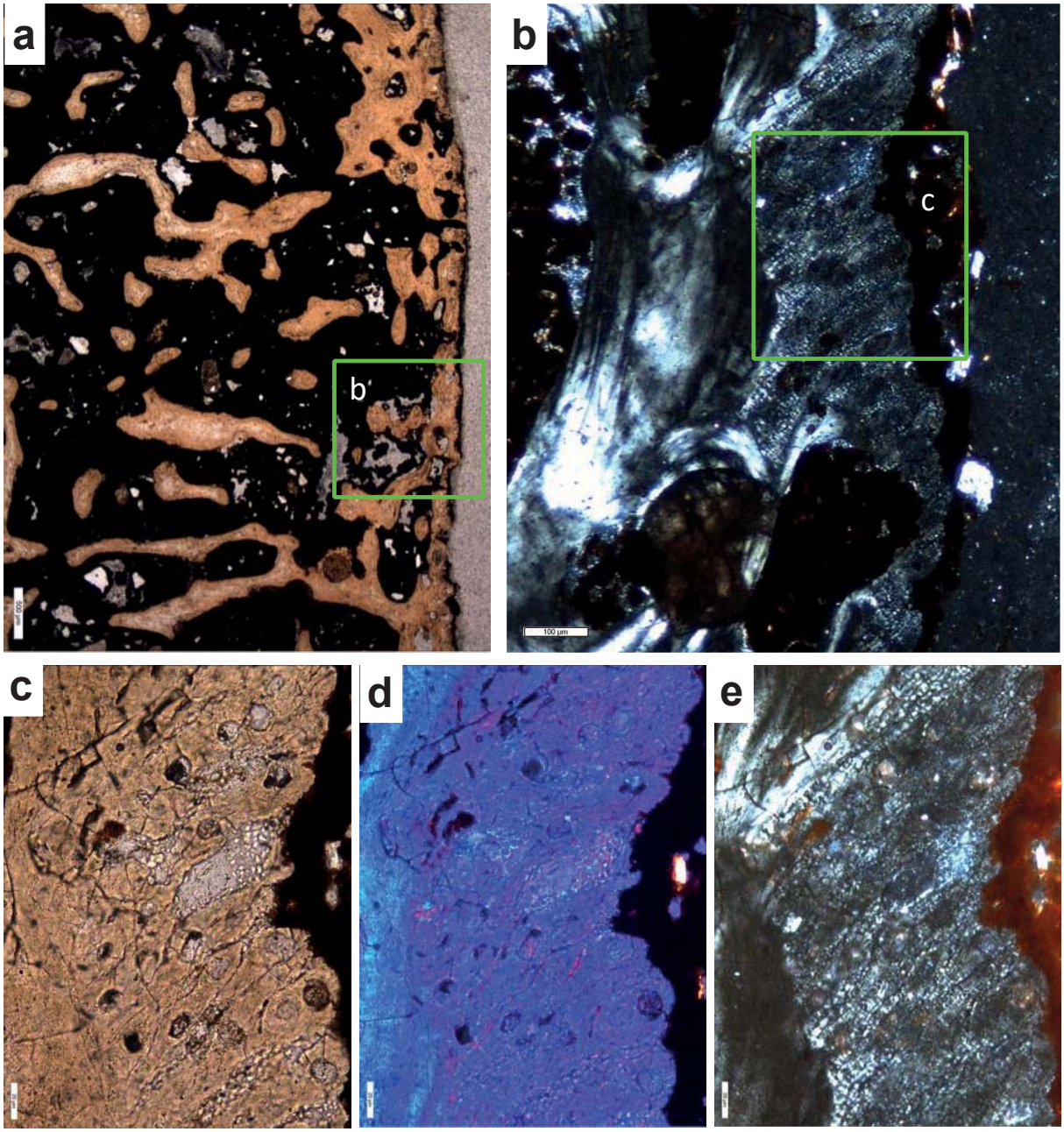

Supplementary Figure S25: Histology of Hadrosauridae indet UACVP 59650, joint with IVD. a Sagittal section of the peripheral part of the articular surface of an isolated vertebral centrum in plane polarised light. **b** Enlargement in cross-polarised light. Note the outwardly inclined mineralised fibers. **c** Close-up showing mineralised fibers and scattered chondrocyte lacunae (large globular bodies). **d** Same in cross-polarised light and lambda filter. **e** Same in in cross-polarised light.

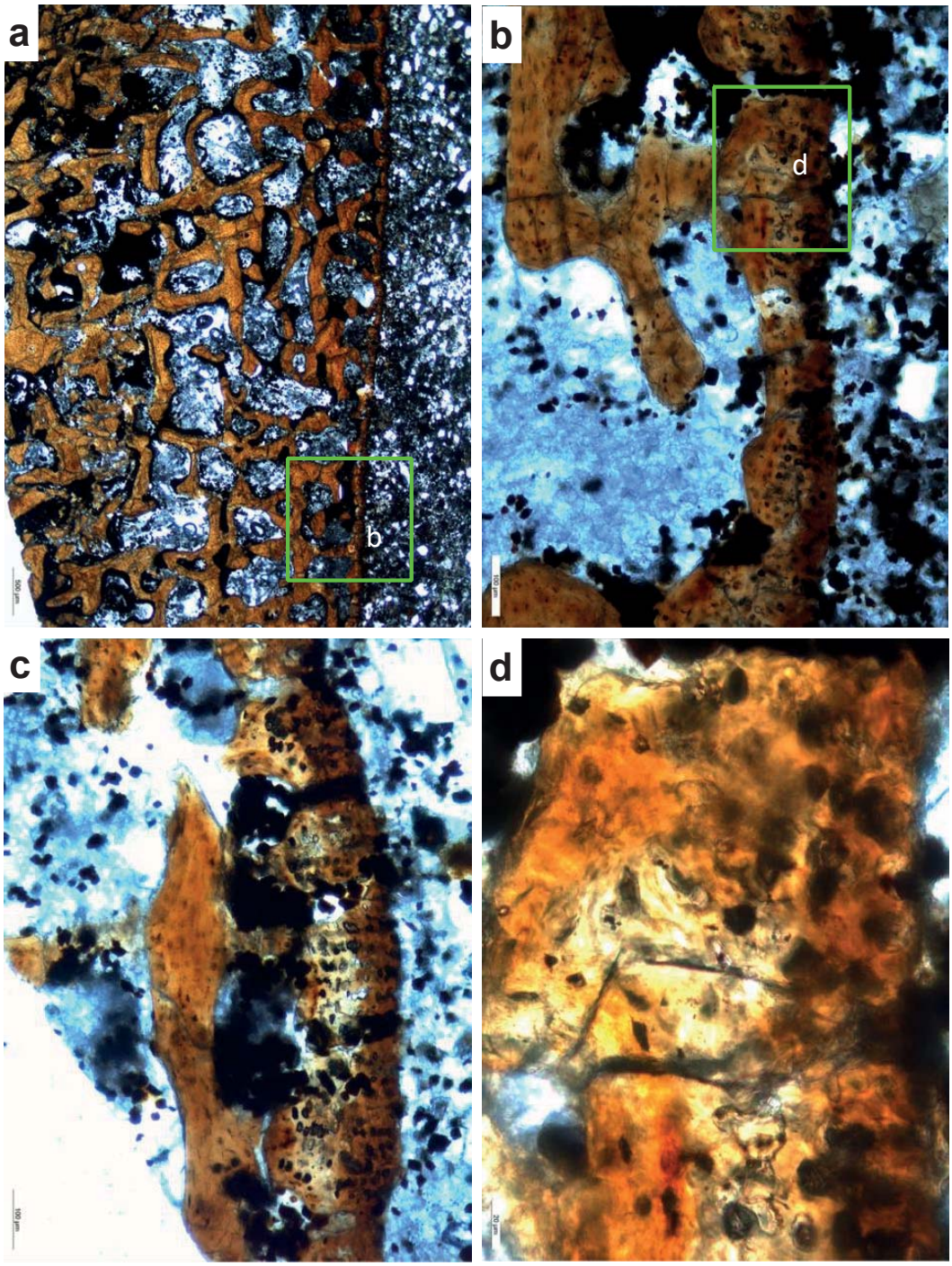

Supplementary Figure S26: Histology of indet. Ornithomimosaur UACVP 59651, joint with IVD. a Sagittal section of the articular surface of an isolated vertebral centrum in cross-polarised light. **b** Enlargement showing transition from zone of irregular chondrocyte lacunae to zone with files of chondrocyte lacunae oriented perpendicular to the articular surface. **c** Other area of files of chondrocyte lacunae oriented perpendicular to the articular surface. **d** Close-up of irregular chondrocyte lacunae in **b**. All images in cross-polarised light.

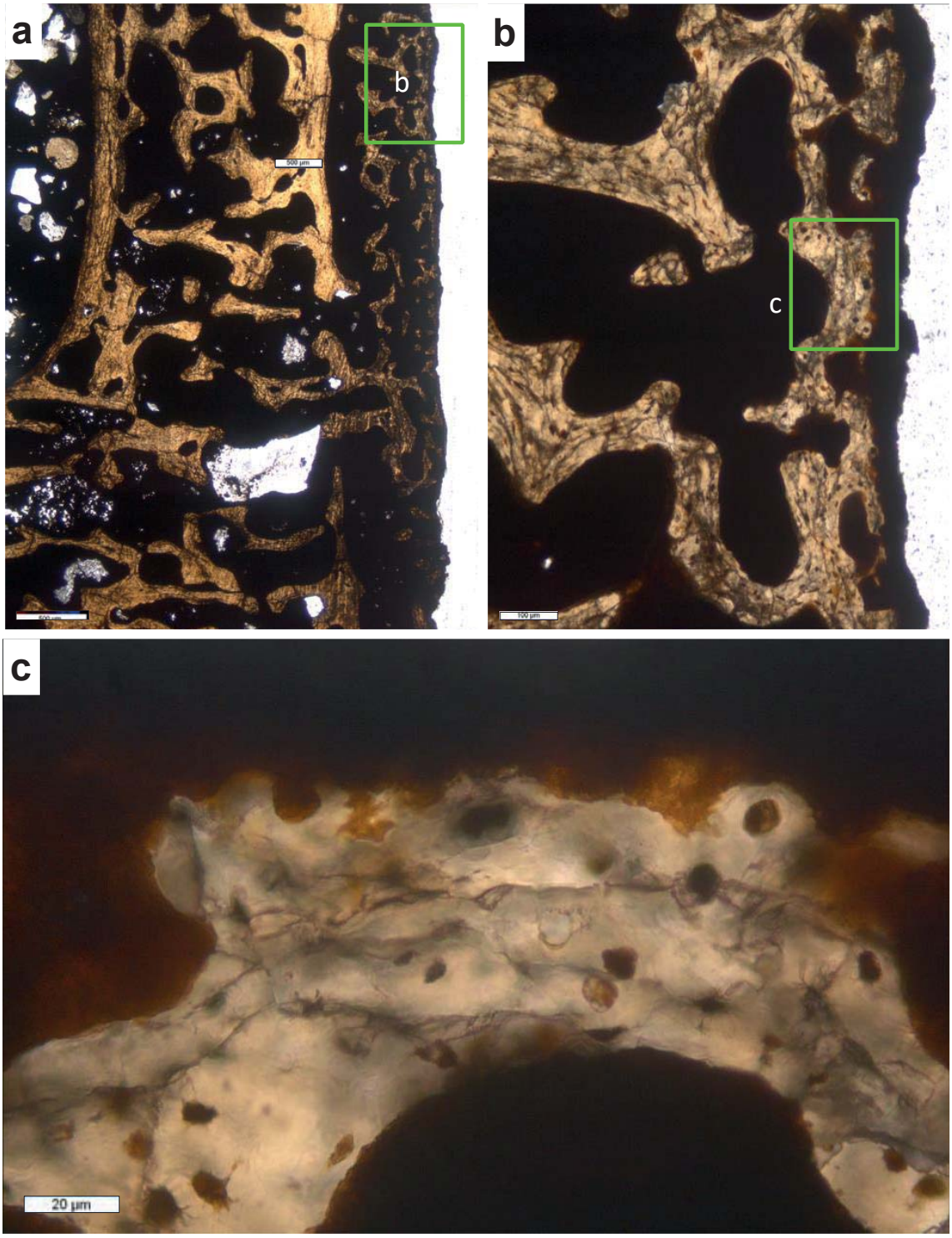

Supplementary Figure S27: Histology of indet. Dromaeosauridae UACVP 56952, fibrous cartilage joint. a Sagittal section of the articular surface of an isolated vertebral centrum. **b** Enlargement of **a**. Note the apparent lack of any cartilage. **c** Closeup of **b**. Note the scattered chondrocyte lacunae and the bony trabeculae with osteocyte lacunae (bottom left). All images in plane polarised light

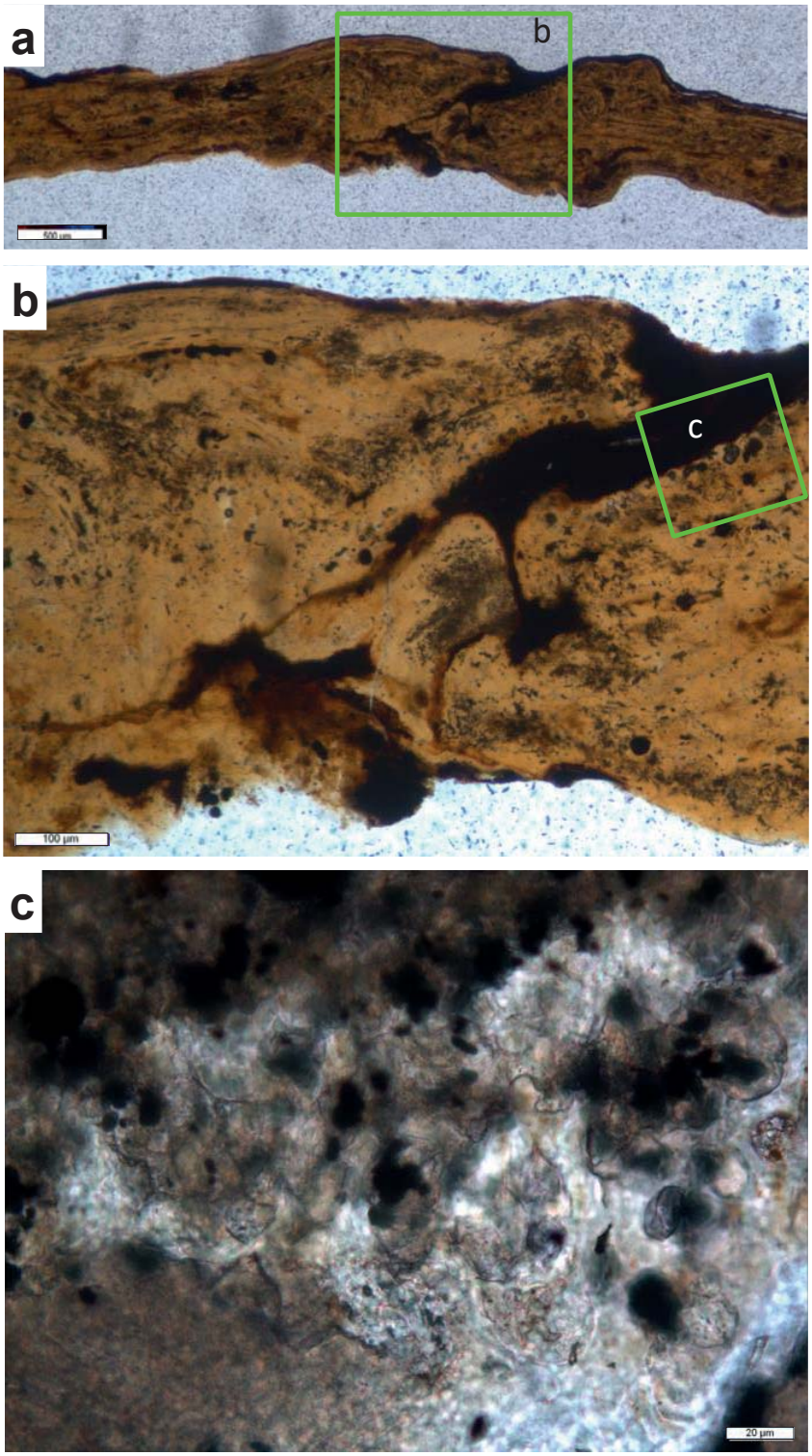

Supplementary Figure S28: Histology of indet. Aves HLMD ME 13019 from Messel, fibrous cartilage joint. a Sagittal section of two articulated vertebral centra. Image in plane polarised light. **b** Enlargement of joint (green box) in plane polarised light. The joint space appears closed over during fossilisation. **c** Close-up of **b**. Note the well scattered chondrocyte lacunae. Image in cross-polarised light

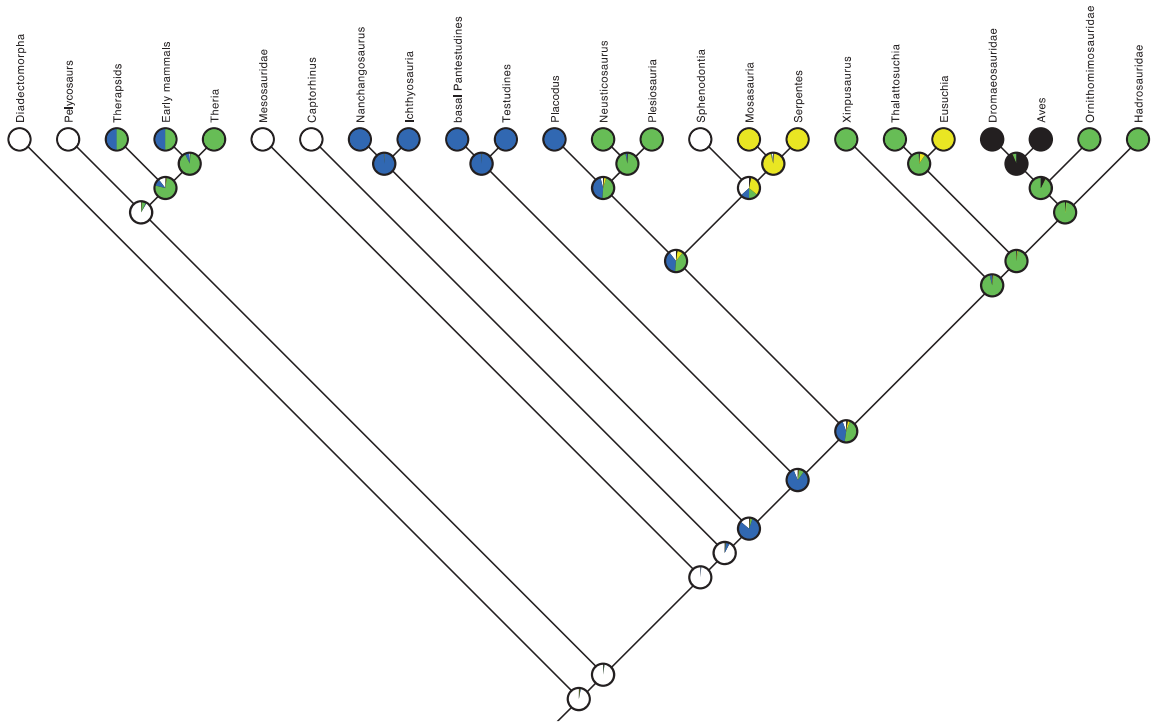

Supplementary Figure S29: Ball-and-stick diagram of ancestral state reconstruction of the intervertebral articulation in amniotes using maximum likelihood as optimality criterium. Colour coding of character states: White, persisting notochord; blue, IVD between amphicoelous centra; green, IVD between platycoelous centra; yellow, synovial joint with hyaline cartilage in between procoelous or opisthocoelous centra; black, fibrous cartilage joint.

Supplementary Tables 1-2

Supplementary Table 1: Phylogenetically organized list of fossil and extant specimens sampled for this study, the higher clade they belong to, the specimen numbers, the region of the spine represented, the kind of section and the type of joint and character state.
Abbreviations for kind of section: GS, ground petrographic section; MS, decalcified and stained microtome section. Abbreviations for kind of specimen: IA, Intervertebral articulation; IV, isolated vertebra. Abbreviations for type of joint: AC, amphicoelous; CN, continuous notochord; PC, platycoelous; IVD, intervertebral disc; SBSJ, synovial joint, ball- and-socket joint; SJS, saddle-shaped; NN, no notochord. Bold indicates observed soft parts. Explanation of character states: 0: CN, AC; 1: IVD, AC; 2: IVD, PC; 3: SBSJ; 4: SJS, AGP. Collections acronyms: HFUT, Hefei University of Technology, Hefei, China; HLMD-ME, Hessisches Landesmuseum Darmstadt, Messel collection, Darmstadt, Germany; NHMW, Naturhistorisches Museum Wien, Vienna, Austria; PIMUZ, Paläontologisches Institut und Museum, Universität Zürich, Zurich, Switzerland; PXD, private collection Xaver Donhauser, Stuttgart, Germany; STIPB, Steinmann Institute Paleontology Collection, University of Bonn, Bonn, Germany; UACVP, University of Alberta Collection of Vertebrate Paleontology, Edmonton, Canada.

Taxon	Higher Clade	Specimen reference	Thin section reference	Kind of section	Region	Joint type, state
Diadectes sideropelicus	Diadectomorpha	STIPB A 169	STIPB A 169	GS, IV	Dorsal vertebra	0: CN, AC
Dimetrodon natalis juvenile	Synapsida	STIPB R 653a	STIPB R 653a	GS, IV	Dorsal vertebra	0: CN, AC
Dimetrodon natalis adult	Synapsida	STIPB R 652a	STIPB R 652b	GS, IV	Dorsal vertebra	0: CN, AC
Dimetrodon natalis	Synapsida	STIPB R 658	STIPB R 658	GS, IA	Sacral vertebrae	0: CN, AC
non- mammalian Therapsida	Synapsida	Romer 1956, Kemp 2006			Dorsal vertebra	1/2: IVD, AC/PC
basal mammals	Synapsida	Kemp 2006			Dorsal vertebra	1/2: IVD, AC/PC
Phoca vitulina	Mammalia, Carnivora	STIPB M 60	STIPB M 60	GS, IV	Anterior dorsal vertebra	2: IVD, PC
Eurohippus sp.	Mammalia, Perissodactyla	HLMD-ME 106	HLMD-ME 106	GS, IA	Lumbar vertebra	2: IVD, PC

Eurohippus sp.	Mammalia, Perissodactyla	HLMD-ME 139	HLMD-ME 139	GS, IA	Lumbar vertebra	2: IVD, PC
Eurohippus sp.	Mammalia, Perissodactyla	HLMD-ME 7835	HLMD-ME 7835	GS, IA	Lumbar vertebra	2: IVD, PC
Stereosternum tumidum	Mesosauria	STIPB R 622	STIPB R 622	GS, IA	Dorsal vertebrae	0: **CN**, AC
Captorhinus sp.	Capthorhinidia	LeBlanc et al. 2018	Fig. 2E, Extended Data Figure 1g	GS, IV	Caudal vertebrae	0: **CN**, AC
Nanchangosaurus suni	Hupehsuchia	HFUT YAN- 10-02	HFUT Uk 1703	GS, IA	Middle dorsal vertebrae	1/2: IVD, AC/PC
Cymbospondylidae new taxon A	Ichthyosauria	LACM DI 158109	LACM DI 158109	GS, IA	Anterior dorsal vertebrae	1: IVD, AC
cf. *Cymbospondylus*	Ichthyosauria	STIPB R 660	STIPB R 661	GS, IA	Posterior dorsal vertebrae	1: IVD, AC
Stenopterygius sp.	Ichthyosauria	STIPB R 661	STIPB R 661	GS, IA	Anterior dorsal vertebrae	1: IVD, AC

Leptopterygius sp.	Ichthyosauria	STIPB R 235	STIPB R 235	GS, IA	Anterior caudal vertebrae	1: IVD, AC
Sphenodon punctatus	Sphenodontia	NHMW 8108:2	NHMW 8108:2	MS, IA	Dorsal and sacral vertebra	0: **CN**, AC
Mosasaurus missouriensis	Mosasauroidea	STIPB Goldfuß 1230 (Type specimen of *M. maximiliani*)	STIPB Goldfuß 1230	GS, IA	Posterior dorsal and anterior caudal vertebrae	3: SBSJ
Python sp.	Ophidia	STIPB R 662	STIPB R 662	MS, IA	Dorsal vertebra	3: SBSJ
Ophidia indet.	Ophidia	HLMD ME 7624b	HLMD ME 7624b	GS, IA	Dorsal vertebra	3: SBSJ
Placodus gigas	Placodontia	STIPB R 86	STIPB R 86	GS, IV	Dorsal vertebra	1: IVD, AC
Neusticosaurus peyeri	Sauropterygia	PIMUZ T 3768	PIMUZ T 3768	GS, IA	Dorsal vertebra	2: IVD, PC
Plesiosaurus dolichodirus	Sauropterygia	STIPB R 88	STIPB R 88	GS, IA	Anterior dorsal vertebrae	2: IVD, PC

Xinpusaurus suni	Thalattosauria	HFUT GL 17003	HFUT GL 17003	GS, IA	Anterior dorsal vertebrae	2: IVD, PC
Xinpusaurus suni	Thalattosauria	HFUT GL 17006	HFUT GL 17006	GS, IA	Posterior dorsal vertebrae	2: IVD, PC
Steneosaurus bollensis	Thalattosuchia	PXD	STIPB R 663	GS, IA	Anterior dorsal vertebrae	2: IVD, PC
Alligator mississippiensis	Eusuchia	Wettstein, 1962			Dorsal vertebra	3: SBSJ
Hadorsauridae indet.	Dinosauria	UACVP 59650	UACVP 59650	GS, IV	Dorsal vertebra	2: IVD, PC
Ornithomimidae indet.	Dinosauria	UACVP 59651	UACVP 59651	GS, IV	Dorsal vertebra	2: IVD, PC
Dromaeosauridae indet.	Dinosauria	UACVP 56952	UACVP 56952	GS, IV	Dorsal vertebra	4: IVD, PC
cf. *Messelornis*	Aves	HLMD-ME 13019	HLMD-ME 13019	GS, IA	Dorsal vertebra	4: SJS

Supplementary Table 2: Summary of results: relationship between vertebral centrum shape, observed tissues (bony tissues, altered cartilaginous tissues, and soft tissues), inferred joint tissue types, inferred joint type, and occurrence in this study.

Centrum shape	Articular surface tissues	Inferred joint tissue types	Joint type	Occurrence in this study
Amphicoelous, **notocordal**	concave area with thin cartilage or bone, convex area with files in longitudinal direction and bone spicules	annulus fibrosus, notochord	plesiomorphic amniote	stem amniotes, basal synapsids, basal reptiles
Amphicoelous, **non-notocordal**	concave area with irregular cartilage, outer area with files in longitudinal direction and bone spicules or diverging files	annulus fibrosus, nucleus pulposus	intervertebral disc	hupehsuchians, ichthyosaurs, placodonts
Platycoelous	central area with irregular cartilage, outer area with diverging cartilage files and bone spicules	annulus fibrosus, nucleus pulposus	intervertebral disc	mammals, eosauropterygians , most archosauromorphs, including most dinosaurs

Centrum shape	Articular surface tissues	Inferred joint tissue types	Joint type	Occurrence in this study
Procoelous /opisthocoelous	hyaline cartilage, unorganized or files normal to surface	hyaline cartilage, joint cavity with synovial fluid	synovial ball-and-socket	squamates, eusuchians
Procoelous /opisthocoelous	irregular, thin cartilage, bone with fiber insertion	fibrocartilage	fibrous, bird-type	dromaeosaurs, birds

Chapter 6

In preparation:

Wintrich, T., Benson, R. B. J., Böhmer, C., Druckenmiller, P., Fischer, V., Neenan, J. M., O´Keefe, R. F., Soul, L., Zverkov, N., Sander, P. M. (in preparation). Biology and evolution of long-necked Plesiosauria.

Author contributions:

Tanja Wintrich wrote the paper with contributions from Roger Benson, Christine Böhmer, Valentin Fischer, James Neenan, Robin O´Keefe, Laura Soul, Nikolay Zverkov and P. Martin Sander.

Biology and Evolution of Long-Necked Plesiosauria

Wintrich, T.[1*], Benson, R. B. J.[2], Böhmer, C.[3], Druckemiller, P.[4], Fischer, V.[5], Neenan, J. M.[6], O´Keefe, R. F.[7], Soul, L.[2], Zverkov, N.[8***], Sander, P. M.[1,9]

[1] Steinmann Institute, University of Bonn, Bonn, Germany. Nussallee 8, 53115 Bonn, Germany *tanja.wintrich@uni-bonn.de

[2] Department of Earth Sciences, University of Oxford, Oxford, United Kingdom

[3] Muséum National d´Histoire Naturelle, Paris, France

[4] Department of geology and Geophysics, University of Alaska Museum of the North, University of Alaska Fairbanks, United States of America

[5] Department of Geology, University of Liège, Liège, Belgium

[6] Oxford University Museum of Natural History, University of Oxford, UK [7] Marshall University, Huntington, United States of America

[7] Marshall University, Huntington, United States of America

[8]*Geological Faculty, Lomonosov Moscow State University, Leninskie Gory 1, Moscow, 119899, Russia
**Geological Institute of the Russian Academy of Sciences, Pyzhevsky Lane 7, Moscow, 119017, Russia
***Borissiak Paleontological Institute of the Russian Academy of Sciences, Profsoyuznaya St. 123, Moscow, 117647, Russia

[9]Dinosaur Institute, National History Museum Los Angeles County, Los Angeles, United States of America

Abstract

Plesiosaurs are an iconic group Mesozoic marine reptiles, instantly recognizable by their long neck, short and broad trunk, short tail, and four large, evenly shaped flippers. In their long evolutionary history (Late Triassic to Late Cretaceous, 205 - 66 million years ago), large-headed and short-necked macropredators ("pliosauromorphs") repeatedly evolved from the long-necked forms ("plesiosauromorphs"). Over 120 genera are known from all continents and latitudes, from the high Arctic (Spitsbergen) to Antarctica. Adult body length ranged from less than 1.5 m to over 14 m, but body mass remains poorly constrained.

Plesiosaurs are of particular interest to evolutionary biologists because they represent an extinct body plan that never evolved convergently again. Understanding their biology thus represents a challenge because of the lack of modern analogs. However, inferences based on diverse evidence from different fields now allow a much improved understanding of plesiosaurs as living animals. Many enigmas remain, especially regarding the evolution and function of the long neck and the locomotion by four-winged underwater flight.

Plesiosaurian bone histology is equally as unique as their body plan. Radial fibrolamellar bone indicates high growth rates, as do cyclical growth marks. Histomorphometrics suggests that plesiosaurian resting metabolic rates were in the range of birds. A pregnant plesiosaur and the histological growth mark record indicate a K-selected reproductive strategy.

Plesiosauromorph plesiosaurians have the relatively longest neck and the highest number of cervical vertebrae (up to 76 in elasmosaurids) of any amniote, whereas the number of trunk vertebrae is within the normal amniote range. We posit that changes in early development related to the segmentation clock allowed the evolutionary increase in and great plasticity of cervical vertebral numbers. Evidence for strong paedomorphosis is also found in the retention of the embryonic intersegmental arteries in adult plesiosaurians.

Osteological observations, analog models, and finite element analysis indicate that the long neck of most plesiosauromorphs was remarkably immobile, with a maximum deflection angle of <180º in all directions, even in elasmosaurids. The long but relatively rigid neck must have served in visual and hydrodynamic camouflage, allowing highly efficient ambush predation on schooling small fish and squid. Long-

necked plesiosaurs thus occupied a unique niche in the Mesozoic oceans, successfully avoiding competition with a plethora of other large-bodied marine reptiles, i.e., short-necked plesiosaurians, ichthyosaurs, and mosasaurs.

Table of Contents

I Introduction

1.1 General introduction

Plesiosaurs have been known for more than 300 years, but many aspect of the biology of this arguably most successful and long-lived marine reptile group (Motani 2009; Kelley & Pyenson 2015) remained unstudied until recently. One of the first fossil reptile skeletons ever reported was a slab containing the articulated posterior half of a plesiosaur skeleton from the Jurassic of Nottinghamshire, England (Stukely 1719). This skeleton did not preserve any parts anterior to the shoulder girdle, but nevertheless showed many of the unusual aspects of the plesiosaur body plan. It was interpreted as the remains of either a crocodilian or dolphin (Stukely 1719). The affinities and unique body design of plesiosaurians became apparent with the discoveries on the Dorset coast of England in the early 19th century (Conybeare 1824) who reported "On the discovery of an almost perfect skeleton of the *Plesiosaurus*".

Since 1822, many more complete or subcomplete skeletons have been described, and much is known about the evolutionary history of plesiosaurians, including variation in their body proportions, particularly the relative length of the neck (O'Keefe 2002; O'Keefe & Carrano 2005; Soul & Benson 2017). Plesiosaurians are instantly recognizable as such because of their uninque body plan and the wide morphological gap that separates them from their closest relatives of the Middle and early Late Triassic (Wintrich et al. 2017). Plesiosaurians are characterized by a short and wide trunk, a short tail, and four large, evenly shaped limbs modified into flippers. Plesiomorphically, plesiosaurians have a small head on a long neck. Several groups of plesiosaurians independently evolved very long necks, including microcleidids, cryptoclidids, and especially elasmosaurids. Elasmosaurids include species with necks almost four times the length of the trunk, and including up to 76 cervical vertebrae, the largest count of all tetrapods (Sachs 2005; Kubo et al. 2012). Equally, several groups independently evolved large heads on shorter necks, commonly referred to as the pliosauromorph body type (Brown 1981; O'Keefe 2002; O'Keefe & Carrano 2005). Among these are macropredators with skulls approaching 3 m in length, which is only surpassed by extant whales and ichthyosaurs. However, the long-necked plesiosaurians represent the greater challenge from the functional, developmental, and evolutionary perspective because of the lack of a modern analog

and are the focus of this review paper.

Many different hypotheses were developed regarding the function of very long necks, particularly in terms of mobility of the cervical vertebral column (e.g., Massare 1988; Storrs 1993; Zammit et al. 2008; Wilkinson and Ruxton 2012; Noé et al. 2017). However, we note that there is quite a range of relative and absolute neck lengths among plesiosaurians, and there may have been differences in mobility and function. Obviously, neck function is closely linked to the mode of feeding in the long-necked forms in particular, and the two need to be considered together. Our review focuses on the biology of plesiosaurians but also provides relevant information on systematics and evolution.

To understand the biology of extinct amniotes, a comparison with recent amniotes is necessary, and in-depth knowledge of anatomy, histology, biomechanics, and development is prerequisite. In the review, we cover all anatomical systems, from the skeleton to what is preserved or can be inferred about the soft parts. We review life history, reproductive biology, and physiology to provide a holistic view of plesiosaurs, particularly the long-necked forms, as living animals, ultimate asking how biology is linked to the evolutionary success of the group.

Plesiosaurians were well adapted to the marine lifestyle (Storrs 1993; Rieppel 2000) as suggested by both their skeleton and their fossil record. Their body plan is strikingly different from all other marine tetrapods, which evolved elongate snake-like and fish-like forms or employed only the forelimbs in propulsion. Plesiosaurian remains are almost exclusively known from marine open-water deposits spanning at least 140 Ma, from the latest Triassic to the latest Cretaceous (Bardet et al. 2014, Wintrich et al. 2017; Fischer et al. 2018). Sauropterygians, the marine reptile clade that plesiosaurians belog to, span nearly the entire Mesozoic. By the Maastrichtian, plesiosaurians had accumulated 185 Ma of marine ancestry, substantially longer than their preceding period of terrestrial ancestry, the last common ancestor of lepidosauromorphs and archosauromorphs that live sometime in the Late Permian.

In the review, we place particular emphasis on arguably the most unique structure of many plesiosaurians, their long neck. The aim is to look at neck function from several points of view, the historical and paleohistological view, neck development, and importance for plesiosaur ecology and lifestyle. The review attempts to bring together several lines of reasoning to formulate a more comprehensive understanding of why and how plesiosaurians evolved the relatively

longest necks (absolutely, sauropod dinosaur have the longest necks) ever seen in the evolutionary history of vertebrates.

To understand the extremely long neck of some plesiosaurians, there must be consideration of the developmental processes of the plesiosaur axial skeleton, and this will be discussed as well. Overviews of the developmental processes in the axial skeleton in different amniote taxa and of different functionalities in the amniote neck are presented. By considering a comparative framework, we can ask different novel questions that cannot be addressed by looking only at a single specimen or a single taxon. An important aspect of the comparative approach is to quantitatively infer the pattern of neck evolution, and this provides relevant information without which many hypotheses remain speculative.

1.2 Plesiosaur phylogeny, diversity, and evolution

Plesiosaurs originated from within Sauropterygia, a group of marine reptiles that first appeared in the Early Triassic, about 3 million years after the end-Permian extinction event. Triassic sauropterygians include several nearshore groups, i.e., Placodontiformes, Pachypleurosauria and Nothosauroidea (Rieppel 1994; 2000; Neenan et al. 2013). Pachypleurosauria and Nothosauroidea form a clade Eosauropterygia, which also includes Pistosauria. Pistosauria includes Plesiosauria and the non-plesiosaurian pistosaurs (Storrs 1991; Rieppel 1994, 2000; Benson et al. 2012). Importanly, pistosaurians are known from deeper-water settings than other sauropterygians from early in their history (Sander et al. 1997; Hagdorn & Rieppel; 1999; Rieppel 2000). Plesiosaurs are known from the Late Triassic to the end of the Cretaceous and are recorded globally from open-water marine deposits (Mulder 2000; Ketchum & Benson 2010; Vincent et al. 2011; Benson et al. 2012; Bardet et al. 2014; Wintrich et al. 2017a). The occurrence of unquestionable plesiosaurians in the Late Triassic has only been established recently with the discovery of *Rhaetiocosaurus mertensi* (Wintrich et al. 2017a). This is despite an earlier putative record of an "elasmosaur" from the Siberian Arctic (Sennikov et al. 2010) and the long history of assignment of plesiosaur-like vertebrae from European Rhaetic bonebeds to the clade (see Storrs 1994; Fischer et al. 2014), suggesting that the clade had crossed the Triassi-Jurassic boundary (Bardet 1992, 1994; Benson et al. 2010; Benson & Butler 2011; Benson et al. 2012; Benson and Druckenmiller 2014; Wintrich et al. 2017a).

The evolutionary origin of plesiosaurians has been discussed repeatedly in the

literature (Dalla Vecchia 2006; Benson et al. 2012; Fabbri et al. 2014; Wintrich et al. 2017). One of the most problematic facts is that the pistosaurian fossil record shows a long temporal gap, spanning the entire Norian, approx. 20 Ma. This geological stage separates the youngest non-plesiosaurian pistosaurs, i.e., *Bobosaurus,* from the Carnian of Italy (Dalla Vecchia 2006, 2017; Fabbri et al. 2014), from the earliest plesiosaurians. However, this is the interval during which most plesiosaurian features evolved, for example, the radial fibrolamellar bone, the increase in growth rate, the large cervical intersegmental artery foramina, the reduction of the tail, as well as the short trunk and the immobile neck (Wintrich et al. 2017; Wintrich in revision; see also discussion on neck mobility below). All of these features are lacking in non-plesiosaurian Pistosauria. The scarcity of relevant Late Triassic fossils prevents us from knowing when and in which order these derived traits of plesiosaurians first evolved. This will be central to understanding the unquestionable evolutionary success of plesiosaurians and their survival of the end-Triassic extinctions.

Plesiosaurs were a highly diverse group with over 120 valid genera known as of 2018 (Fischer et al. 2018). The most recent phylogeny is that of Fischer et al. (2018), with a data matrix of 270 unordered morphological characters and 118 valid taxa, based on the matrix of Benson & Druckenmiller (2014). In the earliest Jurassic (Hettangian of the UK), there were basal Plesiosauroidea (i.e., Microcleidiae, *Plesiosaurus dolicodeirus*), basal Pliosauridae (i.e., *Thalassiodracon*, *Hauffiosaurus*) and the clade Rhomaleosauridae (Benson et al. 2012; Wintrich et al. 2017). Rhomaleosauridae only survived to the end of the Middle Jurassic (Benson et al. 2015) whereas Pliosauridae survived to the Turonian (Brachaucheninae) (Benson and Druckenmiller 2014). Plesiosauroidea also crossed the Jurassic-Cretaceous boundary in the form of the Cryptoclididae and the Xenopsaria (Benson & Druckenmiller 2014), the major Cretaceous clade of plesiosaurians. Xenopsaria contains the extremely long-necked Elasmosauridae and Leptocleidia. Leptocleidia primarily contains the Polycotylidae and some earlier-branching taxa (Fischer et al. 2018). Polycotylidae survived to the Maastrichtian but only Elasmosauridae are known from the latest Maastrichtian. Plesioaurians thus fell victim to the end-Cretaceous mass extinction.

All major lineages of plesiosaurians are represented by fossils from the earliest Jurassic of the UK, and in particular the rhomaleosaurids among these are characterized by a high diversity. The phylogenetic analyses by Benson et al. (2012)

and Wintrich et al. (2017) also suggest that the fossil record in the Late Triassic is poor and infer a greater diversity in the Late Triassic with multiple lineages crossing the Triassic-Jurassic boundary. This statement can be made independently of the uncertainties regarding the phylogenetic position of *Rhaeticosaurus* (Wintrich et al. 2017) and was found already in the analysis by Benson et al. (2012). Hettangian and Sinemurian named plesiosaur taxa are restricted to Europe, tentatively suggesting together with the Triassic records that plesiosaurians originated in Europe. However, from at least the late Early Jurassic onward, plesiosaur remains are found globally (Bardet et al. 2014) in open-water deposits.

II Body plan, functional morphology, and biology of plesiosaurians

2.1 Unique body plan and plesiosauromorph vs. pliosauromorph body plan

The unique body plan of plesiosaurians shows four enlarged limbs modified into flippers, a stiff trunk, short tail, and plesiomorphically an elongated neck (Storrs 1993). Deep plesiosaurian divergences gave rise to three groups during the Late Triassic: Rhomaleosauridae, Pliosauridae, and Plesiosauroidea (Benson et al. 2012; Benson & Druckenmiller 2014; Wintrich et al. 2017). All three groups exhibit a wide range of body proportions, i.e., length of the skull, neck, tail, and flippers relative to the trunk length and trunk width. All three groups have representatives of the plesiosauromorph and the pliosauromorph body plan.

This dichotomy into plesiosauromorphs and pliosauromorphs historically was formalized in the taxonomy of the Plesiosauria as the Plesiosauroidea and Pliosauroidea (Andrews 1910, 1913; Brown 1981). Today, it is generally accepted that short-necked plesiosaurians evolved convergently in different clades (Carpenter 1997; O´Keefe 2001; O´Keefe 2002; O´Keefe & Carrano 2005; Benson & Druckenmiller 2014). However, not only the different neck lengths and head sizes traditionally defined the two groups but also other body proportions. Brown (1981) compiled characters for the plesiosauromorph and pliosauromorph body plan. For the plesiosauromorph body plan, he noted that the ischium is relatively short, whereas the scapula is relatively long, and the forelimb is larger than the hind limb. In the pliosauromorphs, this is the other way around. While the fossil record lacks information on the transition from Pistosauridae into Plesiosauria, as noted above, recent studies show that there is a wide morphospace occupation by the different

plesiosaur lineages already in the Triassic (Benson et al. 2012; Wintrich et al. 2017).

2.1.1 Skull osteology

In general, plesiosaur skull architecture is relatively uniform despite the great size range observed in the clade, from skulls less than 20 cm long (Benson et al. 2012) to some that may have approached 3 m in length, i.e., in the large pliosauromorphs of the Middle Jurassic to Early Cretaceous (Benson et al. 2013, Fischer et al. 2018). Like all sauropterygians, plesiosaur skulls have a single temporal opening, a condition also known as euryapsid. The opening is large and separated from its counterpart by a high and sharp sagittal crest. The external naris is located closer to the anterior border of the orbit than to the tip of the snout. The nasal bone is lacking in all plesiosaurians and in the stem taxa *Pistosaurus* and *Augustasaurus* (Rieppel et al. 2002) which, in fact, show essentially the plesiosaurian skull architecture. The orbit is not particularly large, unlike in ichthyosaurs. Plesiosaurs have a posteriorly open palate, meaning that the braincase is exposed in ventral view in an interpterygoid vacuity. While this is the plesiomorphic condition for amniotes, it probably is secondarily derived in plesiosaurs because more basal sauropterygians have a closed palate (Rieppel 2000). The teeth of plesiosaurs are conical and somewhat recurved, with distinct ridges on the tooth enamel of the crown and sharp carinae forming cutting edges in some pliosaurs (Benson et al. 2013). Different from nothosaurs, the ridges and carinae of plesiosaur teeth are formed entirely by the enamel and not by the dentine (Sander 1999).

Differences in skull proportions appear mainly related to feeding adaptations and are found in particular in the snout. Four general types can be distinguished (although the transitions are gradual): the plesiomorphic type with a snout shorter than the length of the orbital and postorbital region (e.g., *Cryptoclidus*, *Plesiosaurus*, *Stratesaurus*, *Thalassiodracon*; Benson et al. 2012, 2015) carried on a long neck, the pliosauromorph type (e.g., *Pliosaurus*, *Kronosaurus*; Benson et al. 2013) with a massive wedge-shaped rostrum longer than the orbital and postorbital region, carried on a short neck. The rostrum and the lower jaw of this type show an expansion at the tip to house a crown of large fangs. This snout shape evolved convergently in many aquatic macropredators and is also seen in nothosaurs, some crocodiles, spinosaurid dinosaurs, and even archaeocete whales. The third shape, also born on a short neck, is an even more elongate and slender rostrum (e.g., *Luskhan*; Fischer et al. 2017)

resembling ichthyosaurs and other long-snouted piscivores. The fourth type is seen in aristonectine elasmosaurs of the Late Cretaceous that have a broad and flat snout with a vaulted palate that in combination with numerous small and laterally directed teeth may have allowed filter feeding (e.g., *Morturneria*; O'Keefe et al. 2017).

2.1.2 Functional morphology of the postcranial axial skeleton

The postcranial axial skeleton (i.e., the vertebral column and ribs) holds an important position among the unique morphological features in the long-necked plesiosaurian body plan since it is tightly linked to their aquatic lifestyle (Carroll 1985). In particular, this includes aspects of hydrodynamics and buoyancy which have ecological consequences (Braun & Reif 1985; Carroll 1985; Massare 1988)

2.1.3 Neck length and cervical vertebral counts

Since there is considerable variation in the number of cervical vertebrae and therefore in neck length in different plesiosaurian species, estimation of the completeness of the cervical region in taxa with incomplete necks is complicated (Tutin & Butler 2017). However, due to the exceptionally rich fossil record of plesiosaurians (Tutin & Butler 2017) and a number of completely articulated skeletons in excellent preservation (e.g., Frey et al. 2017), there is robust data available on neck length. In general, there is a correlation between neck length and number of cervical vertebrae; i.e., longer-necked plesiosaurians have proportionally higher cervical counts (Soul & Benson 2017). Soul & Benson (2017, fig. 3A) shows the inferred pattern of ancestral body proportions for plesiosaurians. The ancestor of Plesiosauria is inferred to have had a neck only slightly longer than the trunk, which is long compared to many tetrapods and all other marine tetrapods except protorosaurs. A neck longer than 1.5 times the trunk is already seen in the only Triassic plesiosaur, *Rhaeticosaurus*, which has an estimated neck length 1.6 times that of the trunk. The neck (including the length of the gap in the cervical and pectoral column) of *Rhaeticosaurus* is 1028 mm compored to the length of the dorsal column, (553 mm) and sacral column (96 mm) (Wintrich et al. 2017a).

By the definition given above, *Yunguisaurus* (Sato et al. 2014) and all early plesiosaurians have long necks. A long neck thus is plesiomorphic for both, Pistosauria and Plesiosauria. *Yunguisaurus liae* currently is the only pistosaur for which relative neck length and dorsal as well as cervical vertebral counts are known

(contra Soul & Benson 2017). No specimen of *Pistosaurus* preserves the complete neck (Sues 1987), the only specimen of *Augustasaurus* has an incomplete trunk but a complete neck with 38 cervicals (Rieppel et al. 2002), and the only specimen of *Bobosaurus* has an uncertain cervical count because of a gap in the vertebral column (Dalla Vecchia 2006, 2017). *Wangosaurus* (Ma et al. 2015) may not be pistosaurian because of its palatal architecture (Jiang et al. 2018).

In non-plesiosaurian pistosauroids, the maximum number of cervical vertebrae is 49, exceeding the cervical counts of early plesiosaurians (*Yunguisaurus*; Sato et al. 2010; Sato et al. 2014). However, methods of counting cervicals differ between different studies, introducing confusion. Either, all vertebrae anterior to the pectorals can be counted as cervicals or those that bear short ribs and are posterior to the anterior margin of the pectoral girdle, as advocated by Soul & Benson (2017, p. 1167) who only counted 44 cervicals in *Yunguisaurus*. Sato et al. (2014) identified 50–51 cervical vertebrae, including the pectorals. According to this definition, cervicals are all vertebrae in which the rib articular facet is at least partially situated on the centrum. Historically, the determination of the cervical-dorsal boundary has been difficult because of the gradual change in rib morphology and the possible dislocation of the shoulder girdle during fossilization (Sander 1989). It thus is important to always use the same definition in comparative studies. The cervical counts of, e.g., *Attenborosaurus*, *Eoplesiosaurus* and *Plesiosaurus* are lower than those of *Yunguisaurus* (44) and *Augustasaurus* (38), but the neck itself is proportionally longer in the plesiosaurians (Soul & Benson 2017).

A long neck can result from shortening of the trunk relative to other body parts or from lengthening of the neck relative to the trunk. As noted by Sander (1989) and Soul & Benson (2017), neck lengthening either can evolve by increasing the number of segments in the neck (by faster somitogenesis and by homeotic shifts in the position of the cervical/dorsal boundary) or by lengthening of the individual neck segments, i.e., cervical vertebrae (postpatterning differential growth). The former processes appear to be most active in plesiosaurians in particular and eosauropterygians in general (Soul & Benson 2017).

The longest neck of all plesiosaurians can be found in *Albertonectes* (Kubo et al. 2012). It is approximately 7 m long, which equals 67% of total postcranial length, and consists of 76 cervical vertebrae (Kubo et al. 2012) (for comparison: the neck length in the giraffe equals 50% of total postcranial length; Badlangana et al. 2009).

Comparably high cervical counts are found in *Elasmosaurus* with 72 vertebrae (Carpenter 1999) and *Hydrotherosaurus* with 62 vertebrae (Sato 2002). Interestingly, within Elasmosauridae, neck length has been reduced several times during evolution resulting from a reduction in both centrum length and number of cervical vertebrae (Serratos et al. 2013). For instance, a number of 39-42 cervical vertebrae has been described in the elasmosaurid plesiosaur *Nakonanectes bradti* (Serratos et al. 2013).

Among the three groups of plesiosaurians, plesiosauroids include taxa with the longest (in some microcleidids, cryptoclidids and elasmosaurids) and shortest (in some polycotylids) relative neck lengths. Taxa with these end-member morphotypes have been described as 'plesiosauromorphs', with long necks and a small heads, and 'pliosauromorphs', with shorts neck and large heads (O'Keefe 2002; O'Keefe & Carrano 2005). Both terms are intended explicitly polyphyletic, descriptive terms rather than clade names. Likely both morphotypes evolved repeatedly from taxa with intermediate body proportions, and there are plenty of such taxa among cryptoclidids (*Cryptoclidus*, *Tricleidus*), microcleidids (*Seeleyosaurus*), and of course rhomaleosaurids and leptocleidids. The long neck likely was already present in plesiosaurian ancestors because some Triassic pistosaurians such as *Yunguisaurus* (Sato et al 2014) have comparable proportions to early plesiosauroids such as *Eoplesiosaurus* and *Rhaeticosaurus* (Wintrich et al. 2017a).

The morphology of the cervical vertebra in non-plesiosaurian pistosaurs differs from the morphology of the cervical vertebra in plesiosaurians (Storrs 1993; Sato et al. 2010, 2014; Benson et al. 2012; Benson & Druckenmiller 2014; Wintrich et al. 2017a) in the orientation of the zygapophyseal facets, which are medially inclined in plesiosaurs and horizontal in more basal taxa. In addition, plesiosaurians have large paired ventral foramina (intersegmental artery foramina of Wintrich et al. 2017b; see below).

2.1.4 Functional morphology of atlas-axis and cervical vertebral column

Despite debate on the degree of mobility in the cervical vertebral column (e.g., Zammit et al. 2008; Noè et al. 2017) (but refer to section IV for more details), the long neck in plesiosaurians is considered to be an adaptation for feeding and/or breathing (e.g., Andrews 1910; Williston 1914; Brown 1981; Carroll 1981; McHenry et al. 2005; Wilkinson & Ruxton 2012; Noè et al. 2017). It is also very likely that different species used the long neck for feeding in different ways (Wilkinson &

Ruxton 2012). Thus, neck elongation in plesiosaurians appears to be associated with aquatic specialization in this group (refer to section IV, for more details).

Traditionally, the cervical vertebral column was reconstructed as a straight line (e.g., Andrews 1910; Welles 1943). However, it has been argued that forcing the vertebrae into such a posture results in an odd angulation, which would constrict or pinch the spinal cord in the living animals (Carpenter et al. 2010). The rearrangement of the cervical vertebrae so that the centra faces are parallel and the zygapophyses articulated results in a slight sigmoidal curve (Carpenter et al. 2010). Although the reconstruction of the vertebrae in the osteological neutral position (ONP) generally reveals the characteristic curve of the undeflected neck, determining the ONP in extinct animals is necessarily speculative since the cartilage, and thus the intervertebral spacing, is unknown (reviewed by Stevens 2013). Nevertheless, a gently curved neck appears widespread among plesiosaurians, but its hydrodynamic effect is in need of further study (Carpenter et al. 2010).

The first and second cervical vertebrae (atlas-axis complex) form the joint connecting the skull with the vertebral column. This structure arose as an adaptation to permit greater mobility, but also provides surface areas for the attachment of craniocervical muscles and tendons that stabilize the head. The vertebral elements of the atlas-axis complex are either separate (plesiomorphic condition in tetrapods) or fused together, and allow different degrees of flexion, extension and rotation of the head depending on their morphology (Evans 1939). In plesiosaurians, there is a strong tendency for fusion of the entire complex, although the sutures between the individual elements may remain visible (e.g., Owen 1847; Romer 1976; Smith & Vincent 2010). In contrast to mammals, where the dens (odontoid process of the axis) evolved in order to prevent supraphysiological flexion (Lopez et al. 2015), the fusion of the atlas-axis complex may serve a similar function in plesiosaurian restricting motion between the first two vertebrae to rotations. Two divergent types of the atlas-axis complex have been described in plesiosaurians (Romer 1976). In one type (e.g., *Muraenosaurus*) the atlas centrum is large, takes over much of the socket receiving the condyle, and widely separates the neural arch and intercentrum of the atlas (Romer 1976). In a second type this centrum is much reduced, so that the atlas ring is expanded and the intercentra of the two segments meet below it (e.g., *Trinacromerum*) (Romer 1976). Forms such as *Peloneustes* show an intermediate and presumably primitve condition (Romer 1976).

With the marked exception of the plesiosaurians, aquatic forms do not usually possess a highly mobile occipitovertebral joint or a long, flexible neck, for such structures would be a disadvantage in swimming (Evans 1939). For instance, in sirenians and cetaceans the cervical vertebrae are usually compressed and often fused, stabilizing the head and simultaneously limiting its mobility (e.g., Buchholtz 2001; Buchholtz et al. 2007). Despite their external appearance, pinnipeds have a relatively long neck, but it is held in an S curve (Würsig et al. 2008). It has been proposed that this retracted neck posture provides them with a "slingshot potential" for grasping prey (Würsig et al. 2008). In combination with the very long neck, the co-ossification of the first two cervical vertebrae in plesiosaurians may provide stability for their head and mobility between the postaxial vertebrae.

Morphological characteristics (such as strong intervertebral connections, very long neural spines, well-developed zygapophyses, shape of the articular faces of the vertebral centra, and cervical ribs) suggest a rather restricted range of neck movement (reviewed by Noè et al. 2017). However, the neck is envisaged as mobile enough to permit efficient foraging and stiff enough to avoid problems of hydrodynamic destabilization (Noè et al. 2017). In addition to the different hypotheses in terms of neck use in plesiosaurians, there is also a type of specialized foraging behavior that has not been considered yet. When a fish enters the region between head and body of the tentacled snake (*Erpeton tentaculatus*), the reptile moves anterior portions of its body which triggers the escape behavior of its prey (Catania 2009). The movement of the snake's body makes the fish flee towards the striking head instead of to safety (Catania 2009).

2.1.5 Functional morphology of cervicodorsal transition: pectoral vertebrae

Not recognized in extant reptiles (Hoffstetter & Gasc 1969), some authors subdivide the cervicodorsal vertebral column of plesiosaurians into an additional unit, the "pectoral" vertebrae. The term describes vertebrae at the cervicodorsal transition that are morpholgically distinguishable from typical cervical and dorsal vertebrae (Seeley 1874; Andrews 1910). However, the definition of this vertebral region was rather ambiguous (Carpenter 1999) and, thus, not used uniformly in the literature. Sachs and colleagues proposed a standardization of the debated cervicodorsal transition in plesiosaurians and suggested to retain the three-subunit division of the presacral vertebral column (Sachs et al. 2013). They define pectoral vertebrae as

"usually three or more distinctive vertebrae close to the cranial margin of the forelimb girdle that bear a functional rib facet transected by the neurocentral suture, and thus conjointly formed by both the parapophysis on the centrum body and diapophysis from the neural arch" (irrespective of rib length) (Sachs et al. 2013). Consequently, cervical vertebrae bear rib facets exclusively on the centrum, and dorsal vertebrae have rib facets on the neural arch only (Andrews 1910; Brown 1981; Romer 1976).

The development of the pectoral vertebral region may be associated with the evolution of the unique plesiosaur pectoral girdle (e.g., Andrews 1895; Watson 1924; Nicholls & Russell 1991). Muscles that connect the vertebral column with the forelimb originate on the ribs and insert on the humerus (e.g. *musculus serratus*) (Araújo & Correia 2015). Inference of soft tissue anatomy of the pectoral girdle in the extinct marine reptiles suggests that several muscles atrophied in plesiosaurians similar to secondarily aquatic modern analogues (Carpenter et al. 2010; Araújo & Correia 2015).

2.1.6 Functional morphology of the dorsal vertebral column

On the one hand, the dorsal vertebral column provides information on the trunk body shape of the extinct animals. The spinal curvature and orientation of the ribs have a significant impact on thoracic cage morphology, and, thus, impact the hydrodynamic properties of the animal (Maddock et al. 1994; O'Keefe et al. 2011). On the other hand, the skeletal tissue of the axial skeleton may display specific adaptations in order to regulate buoyancy and to manage dramatic changes in pressure as plesiosaurians rose and fell in the water column (Vogel 1994; Rothschild & Storrs 2003; Houssaye 2009).

Many marine animals have modified their external shape in order to increase the hydrodynamic efficiency since friction and pressure drag depend on the body shape (Webb 1984; Carroll 1985; Massare 1988; Hildebrand & Goslow 1998). For plesiosaurians, vertebral profile reconstructions revealed different types of spinal curvature patterns in lateral view, ranging from vertebral columns with little (e.g., *Tatenectes*), to intermediate (e.g., *Cryptoclidus*), and high dorsoventral curvature (e.g., *Muraenosaurus*) (Andrews 1910; Brown 1981; O'Keefe et al. 2011). Although a linear correlation between the maximum curvature and number of functional intervertebral joints has been shown in fish (Brainerd & Patek 1998), the number of vertebrae does not appears to primarily influence the spinal curvature in

plesiosaurians. The curve arises from the rhomboid centrum shape of the dorsal vertebrae (O'Keefe et al. 2011).

We lack knowledge of the intervertebral mobility in the dorsal vertebral column of plesiosaurians, but a strong correlation between vertebral mechanics and aquatic locomotory behavior has been shown in secondarily aquatic pinnipeds (Pierce et al. 2011). Perhaps the differences in spinal curvature patterns in the extinct marine reptiles are also related to different biomechanics in terms of aquatic locomotion (but refer to section 2.2 for more details). Overall, the trunk vertebrae of plesiosaurians appears little suited for rapid manoeuverability in the water since they commonly have high neural spines and relatively narrow arches (Carroll 1981). This morphology may suggest limitations of the degree of sinuous locomotion possible in the vertebral column between the limbs (Carroll 1981). In contrast, low neural spines and broad neural arches appear to be associated with a considerable degree of lateral undulation of the dorsal vertebral column (e.g., in snakes) (Olson 1976; Carroll 1981).

Cross-sectional body shape reconstructions revealed different types of trunk shapes ranging from shallow, dorsoventrally compressed thoracic cages (oblate spheroid body shape) to relatively tall thoracic cages (prolate body shape) (Andrews 1910; Brown 1981; O'Keefe et al. 2011). These differences arise from the morphology of the dorsal vertebrae and ribs, including different vertebral proportions and curvature of the dorsal ribs (Andrews 1910; Brown 1981; O'Keefe et al. 2011). The attachments of the ribs in plesiosaurians are ofted shifted dorsal wards making a widened chest (Gadow 1933). Although the cross-sectional shape changes along the axis of a given vertebrae, and an elliptical model of the animal only approximates its shape (Motani 2001), the thoracic rib cage morphology provides information on the body volume and, consequently, on swimming performance of plesiosaurians. In general, a relatively bulbous body minimizes drag relative to body volume, whereas a more elongate body minimizes acceleration reaction, by demanding that less water be accelerated (Vogel 2008). Furthermore, the body shape may indicate if the animals were adapted for a benthic or pelagic lifestyle. Rather flat-shaped animals can take advantage of a close contact to the ground, whereas streamlined animals are agile swimmers, capable of long distance migration (Webb 1984, 1988; Hildebrand & Goslow 1998).

2.1.7 Functional morphology of the sacral vertebral column

Many secondarily aquatic animals lost their sacral vertebrae in paralogue with the reduction of the pelvic girdle since they do not use their hindlimbs for locomotion (e.g., ichthyosaurs, cetaceans, sirenians) (Romer 1976; Würsig et al. 2008). Plesiosaurs, however, have modified their four limbs into flippers, essentially as in turtles (e.g., Liu et al. 2015). Thus, sacral vertebrae as being a part of the pelvic girdle are well-formed elements. A number of three to four sacral vertebrae is typical for plesiosaurians (Williston 1914; Brown 1981; Vincent 2010; Berezin 2011). The sacral ribs are short and stout structures that converge distally (Romer 1976). Interestingly, they usually remained free, and the joint between the sacral ribs and the ilium appears to have been relatively mobile with respect to the vertebrae (Romer 1976; Brown 1981). An important function of the sacral vertebral region is to transmit the forces generated by the hindlimbs to the vertebral column and, thus, a firm sacroiliac joint would have been advantageous in plesiosaurians (Cheng et al. 2004). However, the absence of a strong articulation between sacral ribs and ilium may indicate that plesiosaurians have been committed to viviparity since it would have eased labour, allowing the live young to pass throught the birth canal as quickly as possible (Cheng et al. 2004) (refer to section 2.9 for more details on viviparity).

2.1.8 Functional morphology of the caudal vertebral column

A number of about 30 to 40 caudal vertebrae are typical for plesiosaurians (Romer 1976; Smith 2013, 2015; Wintrich 2017a). However, using the caudal count as a phylogenetic character (Benson & Druckenmiller 2014) reveals a progressive reduction of caudal count during evolutionary history. Some of the older taxa have quite long tails. Younger taxa have fewer vertebrae, and they are individually short and end in a ‘pygostyle’. In general, the caudal vertebral region is reconstructed as a rather short, tapering tail that was of relatively little functional importance (Romer 1976). This may be comparable with the essentially functionless and much reduced caudal vertebral column in most turtles, but is in contrast to other marine animals that use their powerful swimming tail for propulsion (Romer 1976).

However, the morphology of the caudal vertebral region in some plesiosaurians indicates that it may have played a role in locomotion (Wilhelm & O’Keefe 2010). For one, convex articular centrum facets of the caudal vertebrae suggest some lateral mobility in the proximal tail (Wilhelm & O’Keefe 2010). Also, the fusion of several

caudal vertebrae forming a pygostyle-like structure (Kear et al. 2006; Wilhelm 2010; Kubo et al. 2012) in some plesiosaurians has been been interpreted to indicate the presence of a tail fin (Welles 1943; Otero et al. 2014).

Two types of osteological features in the terminal caudals of plesiosaurs have been cited as evidence for a tail fin. The first of these is a distinct node consisting of two relatively anteroposteriorly shortened vertebrae that is regarded as the point of origin for a skin lobe. This, however, may be a pathology in a single specimen of *Rhomaleosaurus*. Second, lateral compression of the terminal caudal centra has been interpreted as evidence for a laterally compressed dermal tail fin (Dames 1895; Smith 2013), but a critical evaluation of the evidence is clearly in order.

2.1.9 Appendicular skeleton

2.1.9.1 Girdle skeleton

Plesiosaurians have a highly modified girdle skeleton (Ketchum & Benson 2010). While the ventral parts of the pectoral girdle (coracoid, glenoid portion of the scapula, clavicle, interclavicle) and the pelvic girdle (pubis and ischium) are flattened and expanded, the dorsally directed parts (scapular blade and ilium) are small and weak. In particular the coracoid and the pubis form large plates that are linked by the well-developed and densely packed gastralia. The great ventral expansion of the girdle bones would suggest that muscles adducting (or depressing) the limbs are much better developed than those abducting (or lifting) the limb. The ilium connects to two to four sacral vertebrae in derived plesiosaurians, while basal ones retain a higher number typical of more basal sauropterygians (Benson et al. 2012; Wintrich et al. 2017a).

2.1.9.2 Limb skeleton

Plesiosaur limbs are perfect, hydrodynamically shaped flippers that are uniquely similar in anatomy between the forelimb and the hindlimb, to the extent that isolated flippers or even isolated propodials (humerus and femur) are difficult to identify as coming from the front or the rear (Romer 1976). However, plesiosaurian limbs are not as highly modified from the terrestrial condition as ichthyosaurian limbs, and the identity of the limb bone generally remains apparent. Propodial and zeugopodial bones are dorsoventrally flattened and have a greatly simplified morphology compared to more basal pistosaurians and the terrestrial condition. The propodials

have a straight shaft and are distally expanded. The small long bones of the limbs (metacarpals, metatarsals, phalanges) also retain a complete shaft, again unlike in ichthyosaurs (Caldwell 1997a; Caldwell 1997b). This is not the case for the zeugopodial elements that even in the most basal taxa are dorsoventrally flattened, with at least some opening up of the periosteal ossification in the shaft region (Benson et al. 2012; Wintrich et al. 2017a).

The most striking feature of the plesiosaurian limb from a developmental perspective, however, may be the extreme shortening of the zeugopodial elements compared to more basal pistosaurians and the terrestrial condition. Thus, the zeugopodial bones are between one-third and one-fourth of the length of the corresponding propodial bones (Wintrich et al. 2017a), distinctly different from non-plesiosaurian pistosaurs. As in most highly aquatic amniotes, there is hyperphalangy. The distal expansion of the propodials, shortening of the zeugopodium, and the long, tapering digits result in a pointed, elongate shape of the flipper, as is typical for hydrofoils, e.g., in sea turtles and penguins. Obviously, strong paedomorphosis was involved in the evolution of the plesiosaurian limb. This is evident from the simplification of the propodials and the foreshortening of the zeugopodials since the embryonic limb develops from proximal to distal (Hall 2015).

2.2 Locomotion and foraging

Plesiosaurs were well adapted to aquatic lifestyles. This includes a locomotion style which is known as four-winged underwater flight. Underwater flight as a lift-based propulsive mode can be seen also in recent secondarily aquatic tetrapods (i.e., birds, seat turtles, and probably pinnipeds). Nevertheless, the underwater flight in plesiosaurians employed a unique technique, because plesiosaurians used four equally formed flippers for their locomotion (Carpenter et al. 2010; Liu et al. 2015; Araujo et al. 2016). Even though sea turtles use their sometimes rather large hind flippers in locomotion as well (Roger Beonson pers obs.), there are great shape difference in between fore and hind flippers, and it is generally agreed that the hind flippers do not produce lift-based propulsion (Davenport et al. 1984; Rivera et al. 2011; Rivera et al. 2013).

Currently, there are several hypotheses of how underwater flight was performed in plesiosaurians (Robinson 1975; Massare 1988; Halstead 1989; Riess & Frey 1991; Massare 1994; Carpenter et al. 2010; Liu et al. 2015), and in recent publications more

and more computer-based models (e.g., Liu et al. 2015) and morphometric approaches (e.g., Araujo et al. 2016) are seen. Furthermore, there are attempts at estimating speed using hydrodynamic models and comparisons with extant aquatic vertebrates (Motani 2002). However, although it is widely accepted that plesiosaurians used underwater flight as a locomotion style, differences between plesiosauromorph and pliosauromorph plesiosaurians have been hypothesized (Massare 1988). The pliosauromorph plesiosaurians had a more massive body than the compact bodies of the plesiosauromorph type and therefore a difference in hydrodynamics can be assumed (Massare1988). It appears likely that large limbs, although they moved slowly, were more efficient than small limbs with a more rapid motion (Massare 1988); thus, pliosauromorph plesiosaurians were more efficient swimmers than plesiosauromorph plesiosaurians. Muscle reconstructions (e.g., Araujo et al. 2016) may allow testing of competing hypotheses of different styles of underwater flight, but this has not been done explicitly.

The difference in swimming speed between plesiosauromorphs and pliosauromorphs would also represent an adaptation to the different hunting styles in these two types. As pursuit predators, pliosauromorph plesiosaurians are assumed to have hunted larger prey, whereas for plesiosauromorph plesiosaurians an ambush predator style with a camouflage strategy hunting in schools of fish seems to be most likely (Massare 1988; Wintrich et al. in revision). The issue of food preferences and prey items are discussed further in the section on the digestive system (section 2.5).

Albeit short and stout, the tail may have been used as a rudder, aiding in stabilization and directional control and would have been even more effective in combination with a dermal fin (Robinson 1975; Taylor 1981; Massare 1988; Wilhelm & O'Keefe 2010).

However, the presence of a tail fin is not well established (see section on integument).

2.3 Integument and other soft tissues

Soft tissue, such as ligaments, tendons, muscles and cartilages are largely destroyed during fossilization. Nevertheless these structures are very important when we want to understand the biology of extinct vertebrates. In some localities, the potential for soft part preservation is higher than in others. Most examples have been described from conservation deposits (Seilacher 1970) such as for example the famous Holzmaden locality (Toarcian Posidonien-Schiefer Formation) in Germany (Reitner & Urlichs 1983). However, not only soft part preservation gives insights into

soft tissues, but also histological samples (Petermann & Sander 2013) and morphology (Wintrich et al. 2017b), combined with comparative anatomy of recent amniotes.

Very limited evidence exists for the structure of the integument and other soft parts in plesiosaurians. Carbonized skin and other soft tissue remains in a polycotylid plesiosaur from the Late Cretaceous of Mexico (Frey et al. 2017) have offered the most extensive information. The specimen preserves evidence of regular epidermal squamation with vaulted squamae, orientated transversely across the entire belly (Frey et al. 2017), as well as squamation for stabilization of the dorsal side of the flippers and a skin flap on the trailing edge of the flippers. Further areas of this specimen show a smooth surface with no squamation (Frey et al. 2017). The body outline was drop-shaped with a basically immobile fat tail that formed a functional unit with the trunk (Frey et al. 2017).

Soft tissue preservation was also seen in the holotype of *Seeleyosaurus guilelmiilmperatoris* from the Toarcien Posidonien-Schiefer Formation well known for skin preservation in ichthyosaurs. Specifically, Dames (1895) reported in the tail region a vertical fin, but this was covered with paint after remounting of the specimen after war damage, so this evidence cannot currently be verified (Smith 2012).

The tail region has been considered from osteological aspects that it might have had a soft tissue fin (Smith 2012; Otero et al. 2018), and a vertically oriented fin on the end of the tail was portrayed several times (Dames 1895; Woodward 1896; Zarnik 1925; Newman & Tarlo 1967; Smith 2012). An osteological structure of fused caudal vertebrae, resulting in a pygostyle-like structure, has been described in several plesiosaur lineages and may be evidence of a proper horizontal tail fin (O´Keefe et al. 2011; Wilhelm 2012; Otero et al. 2018). However, the presence of a proper tail fin must await discovery of conclusive soft part preservation. We also note that the interpretation of the pygostyle as evidence for a tail fin (see section on caudal vertebrae) is not grounded in comparative observations because pygostyles are not correlated with tail fins in extant animals. Furthermore, the preserved tail fin in *Seeleyosaurus* (Dames 1895) also weakens this interpretation because this taxon lacks a pygostyle.

2.4 Respiratory system

Plesiosaurs clearly were aquatic air breathers. However, the respiratory system remains poorly studied. One of the major questions regarding plesiosauromorph plesiosaurians is how an amniote with such an extremely long neck was able to breathe. The lifestyle of plesiosaurians required feeding and locomotion below the water surface, while respiration requires ascent to the surface (Cowen 1996). Some aquatic air breathers have evolved special adaptations to optimize respiratory performance during lengthy dives by using stored oxygen. Recent whales and possibly extinct marine crocodiles (Thalattosuchians), for example, evolved different adaptations to store oxygen or tolerate a low oxygen level in their blood system (Bennett et al. 1985; Croll et al. 2001). Deep-diving whales avoid decompression syndrome by storing extra oxygen in an extensive vascular network (Young 1950) or by compression of pulmonary gas into non-exchanging areas in the lung or trachea (Seymour 1982). Adaptations for oxygen storage or tolerating a low oxygen level in the blood system cannot be ruled out for plesiosaurians at all.

Nevertheless, we might have to consider different problems related to respiration that had to be solved by plesiosaurians. First, plesiosaurians appear to have had a massive dead space problem in their respiratory system because of the extremely long neck as well as a very short and compact trunk with limited space for lung volume. Furthermore, if we assume that plesiosaurians were adapted for deep diving, the lung must have been compressible to protect the animal from decompression syndrome. A compression of the lung through collapse of the rib cage, like in dolphins and whales, cannot be assumed for plesiosaurians, because of the massive flat shoulder girdle elements. Therefore a mechanism known from sea turtles which compress their lung with specialized muscles during dives appears more likely.

However, decompression syndrome is believed to have been frequent in plesiosaurians based on the freqent occurrence of avascular necrosis (see below) in plesiosaurian limb bones (Rothschild 1982; Rothschild & Storrs 2003) and even in stem pistosaurians (Surmik et al. 2017). However, avascular necrosis can only be seen in the long bones of plesiosaurians but not in the vertebrae. This is maybe linked to the retention of the embryonic intersegmental arteries in plesiosaur vertebrae (Wintrich et al. 2017b) that could have supplied sufficent blood so that bone nutrition was not compromised (Rothschild & Storrs 2003; Wintrich et al. 2017b). However, although avascular necrosis would suggest decompression syndrome, this does not

mean that plesiosaurians were not adapted to deep diving. Even sea turtles, like *Caretta caretta*, can suffer from the decompression syndrome although these species are highly adapted to deep diving (Gracia-Parraga et al. 2014). Furthermore, osteonecrosis has been described for the sperm whale (*Physeter macrocephalus*), the second deepest diving mammal, possibly indicating a maladaptation to deep diving (Rolvien et al. 2017).

Further evidence on plesiosaur diving adaptations comes from red blood cell size. The characteristic of red blood cells as oxygen storing cells makes them relevant to the diving problem. The trend of increased red blood cell size in secondarily aquatic tetrapods compared to their terrestrial relatives is a common phenomenon in amniotes. In fewer but larger cells, comparatively more oxygen can be stored and kept, making it an adaptive trait for diving species. Red blood cell volume has been estimated in plesiosaurians and in basal sauropterygians, the latter inhabiting shallow coastal waters. Plesiosaurs have 238% larger cells than basal sauropterygians, suggesting pronounced diving behavior in plesiosaurians (Fleischle et al. unpublished data). Thus, although there is currently no hard evidence for special diving adaptations in plesiosaurians, living as fully aquatic vertebrate indicates that plesiosaurians probably had such special lung adaptations. However, it will be difficult to obtain the evidences from the fossil record.

2.5 Dentition and digestive system

Based on cranial evidence, plesiosaurians are mostly presumed to have been piscivorous (Massare 1987) in their feeding habit, whereas pliosauromorph plesiosaurians were mostly presumed to have been carnivorous. Despite the great taxonomic diversity of plesiosaurians, their teeth display a limited variety of morphologies (Massare 1987) and generally consisting of fairly simple conical, pointed teeth with sharp longitudinal ridges that are formed by the enamel (Sander 1999; Wintrich et al. 2017a).

There are several instance of preserved stomach content of plesiosaurians, showing fish remains as well as cephalopod jaw elements and hooklets (Cope 1871; Brown 1904; Storrs 1995; Tarlo 1959; Sato and Tanabe 1998), and stones (gastroliths) (McHenry et al 2005). These stomach contents raise some questions, especially regarding the gastroliths. As noted, plesiosauromorph plesiosaurians have been understood as ambush predators capturing free-swimming prey (Massare 1987).

The gastrolith content may be interpreted as deliberate ingestion (Brown 1904), which is seen in some crocodilians (Darby & Ojakangas 1980; McHenry et al. 2005). In crocodilians, the gastroliths are related to buoyancy control and digestion (Taylor 1993; Cicimurri & Everhart 2001; Wings 2007). In addition, stomach content evidence suggests that dietary preferences varied with ontogeny, shifting from nektonic cephalopods to teleosts (McHenry et al. 2005; Wiffen et al. 1995).

Gastroliths are more common in elasmosaurid plesiosaurians and are always found in association with styxosaurinae skeletons, including massive pebbles (e.g. Williston 1843; Everhart 2000, 2005a; O'Gorman et al 2012a, b, 2013). Gastroliths are less common in polycotylids (Schmeisser & Gilette 2009) and unknown in pliosaurids. The reasons for these differences in distribution of gastroliths are unclear.

2.6 Circulatory system

The reconstruction of the circulatory system in fossils is one of the most difficult soft part anatomical reconstruction. Whereas, for example, muscles and ligament can be inferred from the morphology and histology of the bone material, the visceral system and the circular system leave fewer traces. Usually blood vessels do not have contact with the bone and therefore the fossilization of the circular system does not take place. However, in plesiosaur vertebrae (especially in the cervical region), a special character is visible which is linked to the circulatory system. All cervical vertebral centra exhibit highly symmetrical, paired canals, crossing the whole centrum from the ventral to the dorsal side. The expressions of these canals are paired ventral and dorsal foramina. The anatomical interpretation of the foramina was for a long time as nutrient foramina for the nutrient blood vessel which goes into the primordium of the cervical vertebra (Storrs 1991; Noé et al. 2017). Recent, detailed studies show that these foramina developed from an early ontogenetic stage (Wintrich et al. 2017b) and that the canals represent a persistent embryonic vascular feature, intersegmental arteries. The persistence of the intersegmental arteries may be correlated to, and presumably linked with, the uniquely high number of cervical vertebrae, stiffening of the neck, and increased pelagic adaption in plesiosaurians. It also could be a possible adaptation for deep diving and thermoregulation (Wintrich et al. 2017b).

2.7 Nervous system and sense organs

It has to be assumed that secondarily aquatic vertebrates exercise strong buoyancy control that allows movement in a three-dimensional environment. Therefore, special characters in the sensory system evolved (Motani 2005; Kelly & Pyenson 2015; Neenan et al. 2017). Regarding the osseous labyrinth, which contains the sense organ of orientation and plays an important role in head stabilisation (Neenan et al. 2017), different relative labyrinth morphologies and sizes can be seen among sauropterygians, which correspond to different habitats and locomotion styles. In comparison to living amniotes, plesiosaurians show as similar morphology to that seen in sea turtles (Neenan et al. 2017). Specifically, plesiosaurians and sea turtles share the condition of shorter semicircular canals with wider cross-sectional diameters and anterior and posterior canals that are roughly equal in height (Neenan et al. 2017; Walsh et al. 2009). This similarity may result from the nearly identical locomotion of plesiosaurians and sea turtles, i.e., underwater flight. Neenan et al. (2017) also reported that short-necked pliosauromorph plesiosaurians with cetacean-like bauplans had reduced labyrinths in relation to head size, a feature also observed in extant whales. This apparent convergence between plesiosaurians and extant taxa demonstrates a functional signal in labyrinth morphology, indicating that swimming style and/or body shape strongly influence this structure in aquatic amniotes.

Furthermore, beyond the buoyancy control, plesiosaurians (especially pliosauromorph plesiosaurians) exhibit a strong snout ornamentation and a complex neurovascular system inside the rostrum (Buchy et al 2006; Ketchum & Benson 2011; Foffa et al. 2014), i.e., in the premaxillae and maxillae. These features could be correlates of a pressure sensing system as in extant crocodiles or have functioned in electroreception (Foffa et al. 2014) or some other sense organ. Although it has been suggested that plesiosaurians (especially pliosauromorph plesiosaurians) were mainly visual predators (Taylor 1992), it is unlikely that an aquatic predator would rely only on one (the visual) stimulus (Foffa et al. 2014).

2.8 Unique bone histology: implications for physiology and aquatic adaptation

Bone histology (tissue level) and microanatomy (tissue distribution level) inform on diverse aspects of paleobiology relevant to plesiosaurians: life history, aquatic adaptation, physiology and metabolic rate. Thus, given the two centuries of research on plesiosaurs and their many peculiarities, their bone histology has

remained remarkably litte studied and remains incompletely understood, in contrast to that of basal sauropterygians. Nevertheless, it is clear that the histology of plesiosaurians is strikingly uniform and that it differs strongly from that of the other Eosauropterygia (Wintrich et al. 2017a) as well as that of any other marine reptile. Published accounts primarily deal with long bones, vertebrae, and ribs (Kiprijanoff 1881-1883; Wiffen et al. 1995; Fostowicz-Frelik & Gazdzicki 2001; Salgado, Fernandez & Talevi 2007; Street & O'Keefe 2010; Liebe & Hurum 2012; Krahl et al. 2013; Araujo et al. 2015; Ossa-Fuentes et al. 2017; Wintrich et al. 2017a; O'Gorman et al. 2017; O'Keefe et al. 2018), with sample coverage being best for propodials. A synthesis of these studies is lacking, although Houssaye et al. (2016) provide some comparative data. An important gap in our knowledge of plesiosaur histology is ontogenetic change because no plesiosaur taxon has been sampled from a proper growth series containing several size classes. A partial growth series (fetus, neonate, old adult) is represented by the polycotylid material studied by O'Keefe et al. (2018) but it is too incomplete to derived a standard for histological ontogenetic change.

All previously sampled taxa of plesiosaurian propodials show a similar cortical histology (independently of ontogenetic stage) in which the primary cortex of periosteal origin consists of dense and strictly radially orientated primary osteons set in woven bone matrix (Wintrich et al. 2017a; O'Keefe et al. in press), thus forming highly vascularized radial fibrolamellar bone tissue (FLB). Furthermore, this tissue shows dense, large, and plump osteocyte lacunae, already illustrated by Kiprijanoff (1881-1883), derived from static osteocytes (Wintrich et al. 2017a). FLB tissue with radial canals suggests very rapid bone apposition (Francillion-Vieillot et al. 1990; Cubo et al. 2012; Stein and Prondvai 2014). There are distinctive growth marks consisting of a sudden change in orientation of the vascular canals (Wintrich et al. 2017), but these growth marks do not incorporate a line of arrested growth (LAG). LAGs are laid down upon the attainment of skeletal maturity in an external fundamental system, however (Krahl et al. 2013; Wintrich et al. 2017). The implications of this bone tissue and the growth marks will be explored below.

The endochondral bone formed below the articular surfaces of the long bones and vertebral centra is less unusual than the cortical bone. It consists of primary trabecular bone, usually without cartilage retention in adults, which is transformed into secondary cancellous bone by processes of erosion and redeposition (remodeling). In long bones, large vascular canals extend from the articular surface

into the interior of the bone, similar to what is seen in some ichthyosaurs and marine turtles (Rhodin et al. 1981, 1985). Juveniles show the retention of cartilage in the endochondral domain (e.g., Wiffen et al. 1995; Araujo et al. 2015; O'Gorman et al. 2017; Ossa-Fuentes et al. 2017).

Plesiosaur propodials and zeugopodials are very stout, meaning that they have a very short shaft and a low length-to-circumference ratio. The spatial relationship of the endochondral domain and the periosteal domain is controlled by this stout shape of the bone. The endochondral domain takes on the shape of two blunt cones, the tips of which meet in the embryonic center of ossification. The periosteal domain then forms a mantle, the cortex, surrounding these two cones, and the thickness of the cortex decreases rapidly towards either end of the bone. Cortical resorption from the medullary region is very limited in plesiosaurs, and there is no or only a very small medullary cavity. As a result, in longitudinal section plesiosaur long bone microanatomy reveals an hour-glass shape (Liebe & Hurum 2012; Wintrich et al. 2017 Fig. S8E), similar to that of the microanatomy of a vertebral centrum. The long bones thus appear rather compact and osteosclerotic because of the inhibition of cortical resorption (Ricqlès et al. 2001), resulting in bone mass increase (Houssaye 2013). Plesiosaurian long bones do not show the second type of bone mass increase, pachyostosis, however. Pachyostosis has been reported for ribs and gastralia of some plesiosaurians (Wiffen et al. 1995; Street & O'Keefe 2010), however.

Surprisingly, the unusual nature of plesiosaur primary and secondary cortical bone tissue was not recognized until recently (Wintrich et al. 2017a) although it is clearly apparent from descriptions and figures in published accounts from Kiprijanoff to the papers published as late as 2017. There are probably two explanations for this lack of recognition: the relationship of the different bone-forming domains in the long bones as explained above and the fast remodeling front (Mitchell & Sander 2014). The microanatomy described above means that the plane of any transverse section aiming at a maximum growth record has to be chosen carefully and needs to be located exactly in the neutral zone, i.e., the zone where ossification started in the embryo (Francillion-Vieillot et al. 1990). The neutral zone is demarkated by the nutrient canal which connects the center of ossificiation with the surface. Failure to intersect the neutral zone means that only a limited part of the cortical growth record will be accessed. The problem is exacerbated by the neutral zone often being shifted well proximally from the middle of the shaft because plesiosaur propodials grew

faster in distal than in proximal direction. CT scanning before sectioning thus is essential to determine the proper plane of section. If the proper plane of section is missed, the result is great underestimation of cortical thickness and misinterpretation of other features of histology, as seen, e.g., in the studies by Wiffen et al. (1995), Araujo et al. (2015), O'Gorman et al. (2017), and Ossa-Fuentes et al. (2017). For example, the primary vascular canals in the cortex are only stricly radial in the ideal plane of section but diverge increasingly away from the neutral zone.

The second explanation, the fast remodelling front, means that in many adult plesiosaurian, the primary periosteal bone is completely replaced by secondary osteons (e.g., Wintrich et al. 2017a). While this secondary cortical bone also shows some peculiarities, i.e., the irregular shape and orientation of the secondary osteons (Krahl et al. 2013), it masks the unique nature of the primary bone. These considerations apply to vertebral centra as well, but vertebrae have been less studied in the past.

The strong morphological adaptations of plesiosaurians to a fully aquatic lifestyle suggest similar adaptations at the microanatomical level. Indeed, there is bone mass increase in the propodials and ribs and gastralia in some taxa, but also a redistribution of trabecular architecture in the vertebral centra of the kind seen in other highly aquatic taxa (Houssaye 2013; Houssaye et al. 2016). There is thus a somewhat conflicting signal because bone mass increase appears inconsistent with the multiple lines of evidence suggesting a highly aquatic lifestyle (Houssaye et al. 2016).

An increase in bone density (bone mass increase) can be achieved by two different mechanisms (pachyostosis, osteosclerosis) which may act together (pachyosteosclerosis). Bone mass increase is typical for animals employing passive buoyancy control, and denser bones allow animals living in shallow water to stabilize their body since they act as a form of ballast to weigh down the body (e.g., Würsig et al. 2008) whereas lightening of the skeleton is typical for active swimmers such as ichthyosaurs and cetaceans (Ricqlès 1989; Wall 1983; O'Keefe et al. 2011; Houssaye 2013). Less dense bones are advantageous in deep-diving or pelagic animals since a reduction in bone density allows faster acceleration and increased maneuverability (e.g., Würsig et al. 2008). Such an osteoporotic-like state of the skeleton was described the vertebrae of adult plesiosaurians (reviewed by Houssaye 2013). Possibly, there are other factors than aquatic adaptation, such as axial muscular loading, explaining the dense bone of the propodials. Wiffen et al. (1995) proposed

that the inner bone architecture changes throughout ontogeny. This may indicate an ontogenetic shift in lifestyle from benthic to pelagic (Wiffen et al. 1995; Ossa-Fuentes et al. 2017). However, the hypothesis of ontogenetic shift from dense to light bone requires further testing based on unequivocal growth series and well constrained samples.

In the evolution of pistosauroids, there is an increase in growth rate from pistosaurians to plesiosaurians (Krahl et al. 2013; Wintrich et al. 2017a). The distinctive growth marks in long bone histology suggest that plesiosaurians reached over 60% of their linear size by the end of their first year and their final body size within a few years (Wintrich et al. 2017a; O'Keefe et al. in press). However, the histology of skeletally mature older individuals shows that the primary bone tissue was replaced by dense Haversian bone tissue (Kiprijanoff 1881-1883; Wiffen et al. 1995; Krahl et al. 2013; Wintrich et al. 2017a; O'Keefe et al. 2018), thus destroying the cortical growth mark record.No growth curves have been fitted to plesioaur growth records, and fitting may not be successful because of the low number of marks.

Bone histology also provides insights into plesiosaur metabolism and therefore thermoregulation. For active and pelagic vertebrates, like plesiosaurians, a high metabolic rate appears likely (Druckenmiller & Russell 2008) and is supported by stable isotope thermometry (Bernard et al. 2010). Qualitative features such as a dominance of radial canals and FLB as well as the low number of growth marks are clear indicators of rapid growth in plesiosaurians and suggest a high metabolic rate. Recently, plesiosaur resting metabolic rates were modeled from histomorphometric data in a phylogenetic framework and yielded values in the range of birds, clearly indicating endothermy (Fleischle et al. 2018).

2.9 Reproduction and K-strategy

Until the end of the twentieth century, it had been considered possible that early plesiosaurians (like *Thalassiodracon hawkinsi*) may have crawled up onto the beach to lay eggs, as seen in modern sea turtles. This suggestion came up because reptiles are in general known for their oviparous reproduction. However, currently the evidence is in favor of plesiosaurians having had a viviparous life-style with a strong K-strategy in reproduction (O´Keefe and Chiappe 2011; Wintrich et al. 2017a). The best, and unfortunately only, fossil of a pregnant plesiosaur is an individual of

Polycotylus latipinnis. This fossil consists of a largely articulated skeleton of a pregnant pliosauromorph plesiosaur which was discovered in 1987 in Kansas (USA) (O´Keefe & Chiappe 2011). It is seen that the fetus is notably large in comparison to its ontogenetic stage which is an indicator for large birth size. Furthermore, the fossil represents only a single offspring, which can be understood as a strong indicator for parental care and therefore for a K-selected life history (O´Keefe & Chiappe 2011). Support for these hypotheses comes from the frequent discovery of early ontogenetic stages of in particular Cretaceous plesiosaurs (Moodie 1916; Wiffen at el. 1995; O'Keefe and Byrd 2012; Araujo et al. 2015; O'Gorman et al. 2017; Ossa-Fuentes et al. 2017, O'Keefe et al. 2018) that are both relatively large and lived in the open sea. Although basal eosauropterygians show vivipary (Cheng et al. 2004; Sander 2012), it is unknown when plesiosaur ancestors became viviparous. It appears likely that the oldest plesiosaur already had a viviparous lifestyle (Wintrich et al. 2017a), because it already shares the unique body plan and bone histology with later plesiosaurians.

2.10 Ontogeny and life history

Ontogenetic changes in fossils can help us understand developmental processes in extinct animals (e.g., Hall 2002). In plesiosaurians, there is a considerable record of juvenile specimens and observed ontogenetic variation (e.g., Andrews 1910, 1913; Brown 1981; Storrs 1993; Cruickshank 1994; Wiffen et al. 1995; Caldwell 1997a, b; Kear 2007; Krahl et al. 2013; O'Gorman et al. 2013; Vincent 2010; Frey et al. 2017). There is even a fossil that preserves an *in situ* fetus (O'Keefe & Chiappe 2011) (see previous section). Compared with stem-group sauropterygians, plesiosaurians display a broad trend of delayed and reduced ossification (Storrs 1991; O'Keefe 2006). Many secondarily aquatic tetrapods retain much cartilage in their limb and girdle skeletons, and this trend has been linked to the acquisition of a truly pelagic lifestyle (Romer 1976).

The general criteria for determining whether an individual represents an early ontogenetic stage include size and, most importantly, ossification state of the skeleton (i.e., incomplete fusion of bony elements, absence of elements, incomplete ossification of joint surfaces). In plesiosaurians, vertebral morphology that has been traditionally associated with the juvenile stage includes open neurocentral sutures and extremely short vertebral centra, including a short atlas-axis complex (Brown 1981; Gasparini et al. 2003a; O'Keefe & Hill 2006). A high ratio between vertebral centrum

width and length also is characteristic for juvenile plesiosaurians (e.g., Gasparini et al. 2003b). The bony part of the neural spine is assumed to be proportionally shorter in juveniles since the juvenile spines were terminated in cartilage (Brown 1981). However, vertebral indices change ontogenetically, and low neural spines as well as short vertebral centra do not necessarily indicate a juvenile condition (Gasparini et al. 2003b). Therefore, the whole skeleton has to be considered for the estimation of the ontogenetic stage.

Complete ontogenetic series of plesiosaurians are very scarce (Carpenter 1999) and, thus, the ontogenetic development of plesiosaurians remains poorly known. Nevertheless, there are specimens that provide insights into the ossification sequence of the extinct reptiles. Vincent (2010) described a subcomplete plesiosaur skeleton from the Posidonien-Schiefer Formation (Germany). It represents one of the most complete and ontogenetically youngest plesiosaurians known from the Lower Jurassic. As in other reptiles, the neurocentral suture remained open during postembryonic development (Rieppel 1992; Brochu 1996). In squamates, the sequence of closure follows a craniocaudal pattern as opposed to crocodilians in which a caudocranial pattern has been observed (Rieppel 1992; Brochu 1996), but the pattern of suture closure is unknown in plesiosaurians.

However, care has to be taken in the interpretation of seemingly immature specimens, and histological evidence has to be considered. A possible example of the retention of juvenile traits (paedomorphism) was recently described by Araújo et al. (2015). The fossils display an osteologically immature external morphology (small size, unfaceted distal propodials, flat articular facets of the vertebrae, non-fusion of the neural arches with the vertebral centra, near-absence of the posterior cornua of the coracoids, absence of the pectoral bar), but bone histology– that is the presence of three LAGs - suggested an adult condition to the authors (Araújo et al. 2015). However, the histological evidence for maturity is inconclusive in the light of our current understanding of plesiosaur bone histology (see histology section).

An Early Cretaceous assemblage from Australia suggests that juvenile plesiosaur remains are particularly common in inshore marine/estuarine freswater depositional environments (Kear 2007). This may be interpreted as ontogeny-related habitat partioning (Wiffen et al. 1995; Kear 2007; Ossa-Fuentes et al. 2017). However, the generality of this pattern can not be proven because of the lack of suitable fossil occurrences and research. The pattern would be also consistent with the

observed higher bone density in juvenile plesiosaurians (Wiffen et al. 1995). Ossa-Fuentes et al. (2017) reported on a specimen displaying histological features confirming the presence of osteosclerosis and the absence of any sign of growth zones or annuli/ lines of arrested growth (LAGs). However, both of these histological studies are not conclusive because of poor control on location of the plane of section (see histology section).

2.11 Paleopathology

Plesiosaurians have received considerable interest from the perspective of paleopathology. Trauma-induced pathology of the forelimb in a *Cryptoclidus* individual (Rothschild et al. 2018) resulted from healing of a bite by a predator, possibly a pliosauromorph plesiosaur. The pathology showed that the individual not only survived the attack but was able to compensate for the loss of mobility in one forelimb. The animal must have shifted to hind-limb propulsion with the forelimbs compromised, supporting the general importance of the hind limbs in plesiosaur locomotion.

Pathologies of the axial skeleton have only been documented once in plesiosaurs, in the form of Schmorl's node resulting from a hearniad nucleus pulposus of the intervertebral disk (Hopley 2001). The pathology is found on the anterior articular surface of most vertebrae of a partial skeleton of a long-necked plesiosaur preserving cervical and pectoral vertebrae. While the cause of the pathology awaits an explanation, the find is of relevance because it strongly suggests that there were intervertebral disks in the neck of plesiosaurs. This recently has been confirmed based on histological evidence (Wintrich et al. in revision b).

In particular, avascular necrosis as diagnostic evidence for decompression syndrome (see above) has been in the focus of paleopathological research (Rothschild & Storrs 2003; Farke 2007; Surmik et al. 2017). Avascular necrosis is local death of bone tissue underlying the joint surfaces of plesiosaur propodials. The diagnosis was made based on surface features in comparison with extant animals (Rothschild & Storrs 2003). However, the structures identified by Rothschild & Storrs (2003) as lesions potentially could be expressions of the non-pathologic large vascular canals extending from the articular surface into the endochondral domain. While the diagnosis of avascular necrosis in plesiosaurs potenially could be made on the basis of bone histology as well, this has not been done so far but would allow easy distinction

between non-pathologic vascular canals and lesions.

Rothschild & Storrs (2003) noted that avascular necrosis was statistically less frequent in cryptoclidid plesiosaurs than in other plesiosaurs, possibly suggesting less diving activity in the former. However, Farke (2007) reanalyzed the data set of Rothschild & Storrs (2003) using more appropriate statistical test and did not find significant differences between the groups.

III Evolution, function and development of long necks

The vital importance of the vertebrae column for vertebrate life is clear because its key functions, protection of the spinal chord and providing a balance between stability and mobility, have remained the same in a huge variety of vertebrate taxa (Gadow 1933; Hildebrand & Goslow 1998). However, vertebrae show considerable variation in number and shape within the column, resulting in varying degrees of regionalization (e.g., Ward & Mehta 2014). The axial skeleton of teleost fish is relatively uniform, including only two morphological regions (precaudal and caudal). By contrast, the vertebral column of tetrapods is usually divided into cervical (neck), dorsal (trunk), sacral (pelvis) and caudal (tail) units (Gadow 1933), reflecting distinct functional demands acting along the body axis. The evolution of the tetrapod axial skeleton into specialized regions thus was important for their functional diversity and adaptation (Burke et al. 1995). The specialized regions of the axial skeleton made the adaptation to different environments and the advancement from fish to tetrapods possible and therefore the transition from the aquatic environment to the terrestrial environment. Usually, one finds the notion in the literature that the most important step during terrestrialization was the development of fins into limbs. But the neck is a highly important step during the evolution of the vertebrates as well. It allows the animal to have more degrees of freedom of the head and therefore have greater perception, in particular by vision, of the surrounding environment.

Surrounding the neck vertebrae are several soft tissue structures which need to be considered. Muscles, ligaments, intervertebral tissue, trachea, and oesophagus play an important roles in the discussion of neck function and evolutionary trends. Without muscles, ligaments, and intervertebral tissue, the neck would not be moveable, and without the trachea and the oesophagus, the organism would not have been able to live. These structures have to be equally examined for understanding of the function

of the vertebrate neck. When we go from recent vertebrates into fossil vertebrates, this gets more difficult. With anatomical comparison from living vertebrates to fossil vertebrates, we are able to get a better understanding. But even with comparative anatomy, discussing the biology of plesiosaur necks gets difficult because of the unique and enigmatic body plan of plesiosaurians.

In general, the cervical vertebrae form part of the head-neck system and therefore are critical in terms of feeding adaptations. They provide the skull with movement and control the position and orientation of the neck (Berthoz et al. 1992). The head also carries most of the sensory systems that allow orientation in a three-dimensional habitat. Consequently, the evolution of a functionally distinct neck is also closely linked to locomotor adaptations since it allowed the independence of (almost) all senses of perception (Berthoz et al. 1992). In concert with the modification of fins to limbs (e.g., Caldwell 2002), this was a critical step during the evolutionary transition from a life in water to a life on land (Laurin 2010). The re-invasion of the marine environment by different terrestrial vertebrate lineages resulted in a suite of adaptations for an aquatic lifestyle, which commonly included a reduction of neck length, except in the case of pistosaurians and protorosaurs that evolved necks that are longer than the trunk.

Long necks have evolved independently in a wide range of extant and extinct taxa, and a common selective factor in the evolution of long necks appears to be foraging (reviewed by Wilkinson & Ruxton 2012). Alternative explanations for long necks include thermoregulation, predation pressure, and sexual selection (Wilkinson & Ruxton 2012). Although it has been proposed that an elongate neck is a sexually selected trait (e.g., in giraffes) (Simmons & Scheepers 1996), there is evidence that sexual selection is not the origin of a long neck, at least in giraffes (Mitchell et al. 2009).

As noted, a long neck can evolve by an increase of the number of cervical vertebrae (e.g., birds, plesiosaurians) and/or by an increase of the length of the individual vertebrae (e.g., sauropodomorph dinosaurs, mammals, protorosaurs) (e.g., Müller et al. 2010; Solounias 1999; Arnold et al. 2017; Soul & Benson 2017). Although it is not completely understood why different amniote clades, in particular mammals, are highly constrained in their cervical counts, it is assumed that a change in the number of cervical vertebrae may be associated with negative pleiotropic

effects or other developmental constraints (Galis 1999; Narita & Kuratani 2005; Buchholtz et al. 2012; Szczygielski 2017).

IV Neck elongation and mobility in plesiosaurians

4.1 Introduction

As noted, plesiosaurians have the relatively longest neck (absolutely, only sauropod dinosaurs had longer necks), built up by the highest number of cervical vertebrae in any tetrapod. Thus, the focus of this section is on the plesiosauromorph body plan with its long neck, exceeding trunk length by the factor of 1.5. The pliosauromorph body plan does not represent a challenge to our understanding of neck function. As in other extinct and extant macropredators, the short pliosauromorph neck mainly served in supporting and orienting the large skull.

The function of the long neck in plesiosauromorph plesiosaurians is controversially discussed in the literature (Everhart 2005; Zammit et al. 2008; Wilkinson et al. 2012; Noé et al. 2017; Wintrich et al. 2017a; Nagesan et al. 2018; Wintrich et al in revision a), and there are several hypotheses as to why plesiosaurians evolved the long neck. However, not much attention has been paid to the fact that the long plesiosaurian neck was inherited from Triassic non-plesiosaurian pistosaurs and thus evolved under selective pressures particular to these animals. In these, neck undulation as part of locomotion was retained, whereas plesiosaurians show underwater flight. Undulation with a long neck is only possible when the neck allows a high lateral mobility. In plesiosaurs, the neck lost this function because it does not play an important role in underwater flight.

The neck is a complex structure with several different muscles and ligaments, different intervertebral tissues in the intervertebral spaces, different vertebral numbers and a complex development. While some aspects of neck mobility can be observed and studied directly in living tetrapods, the question of neck mobility in extinct ones such as plesiosaurians has to rely on observations on fossil material. Inferences on neck mobility and function can draw on evidence from functional morphology, biomechanics and taphonomy.

Any discussion of the flexibility of the plesiosauromorph neck requires reliable estimates of the range of motion for the cervical segments, usually called Junghans segment of motion (JSM) or motion segment in functional anatomy. Highly disparate

estimates of neck mobility in plesiosauromorphs can be found in the literature (reviewed below). While this disparity may be mainly due to different methods and different assumptions employed, variation in neck osteology among plesiosauromorphs suggests differences in mobility. In addition, taphonomy may offer clues as well (see below).

4.2 The camouflage hypothesis

One of the first and even today most comprehensive studies of marine body plan morphologies was done by Massare (1988) in which she focused on the swimming style in different marine reptiles. Massare (1988) also briefly formulated an important hypothesis (see also Everhart 2005) explaining the function of the long-necked plesiosauromorph body plan in feeding. This hypothesis involves preying on schools of fish and squid. Catching prey in the aquatic environment is in some ways more challenging than on land. For one, fish in the Mesozoic must have been able to detect hydrodynamic disturbances with their current sense organs just like today's fish. Such disturbances are caused by any swimming animal, including a hunting plesiosaurian. The magnitude and distribution of the hydrodynamic disturbance would have depended on the size, shape, and speed of the hunter. In addition, a large body would have been highly visible to the prey species and would have betrayed the plesiosaur. However, if the head was at a distance in front of the massive body, supported by a long neck, the prey would not be able to recognize the true bulk of an approaching plesiosaur. Therefore the long neck can be understood as camouflage of an ambush predator, both visually (Massare 1988; Everhart 2005) and hydrodynamically. In fact, a similar hydrodynamic camouflage effect has been hypothesized for the ubiqitous Triassic predatory fish *Saurichthys* (Kogan et al. 2015).

4.3 Sea snakes as plesiosauromorph analogs?

Although they do not have a long neck, sea snakes are the only extant secondarily aquatic vertebrates that exhibit an elongate body form (e.g., Brischoux & Shine 2011) which may provide hints on the biology of plesiosaurians. For instance, piscivore snakes evolved different strategies to capture prey. There are species that almost always strike from beneath the prey, whereas others launch attacks from above as well (Brischoux & Shine 2011). Furthermore, snakes use mostly one of two types of capture behaviour: frontally or laterally directed strikes (Herrel et al. 2008).

However, sea snakes have rather different intervertebral joints compared to plesiosaurs in possessing synovial ball-and-socket joints and complex facets joints. In addition, there is the distinction between moving the whole, elongate animal using the vertebral column (as in a snake) and moving the body using flippers. Sea snake functional morphology thus probably does not provide a good analog to inform on plesiosauromorph neck function.

4.4 Studies supporting a mobile neck

In the decades after their discovery, plesiosaurs were generally depicted as having a highly flexible, and often swan-like, neck (Everhart 2005). This view persisted even into the 21st century. Thus, Wilkinson & Ruxton (2012) implicitly assumed flexible plesiosaur necks, and without supporting anatomical discussion, hypothesize the use of the neck "for rapid acceleration of the head".

Based on a review of the osteological evidence, Noé et al. (2017) offer a functional interpretation of the plesiosauromorph neck based on the Middle Jurassic cryptoclidid plesiosauroids *Muraenosaurus* and *Cryptoclidus*. To determine flexibility, they provide a detailed osteological description of the skull and cervical vertebrae, reaching the conclusion that the flexibility of the neck is limited in lateral and dorsal direction but less so in ventral direction. Accordingly, they infer a new feeding strategy which would be feeding on benthic organisms and gliding over the seafloor to catch prey. The conclusions of Noé et al. (2017) were based on the premiss that the long plesiosaur neck would not have evolved towards limited mobility from a mobile ancestor.

A more stringent osteological approach was taken by Nagesan et al. (2018), based on the digital manipulation of the virtual vertebral column of the leptoclidid *Nichollssaura* from the Early Cretaceous of Canada. The virtual vertebral column consisted of surface models of the individual cervicals obtained from CT data.

Nagesan et al. (2018) found high mobility in the *Nichollssaura* neck in lateral direction (nearly 360º) but less so in dorsal direction (ca. 90º) and ventral direction (ca. 120º). *Nichollssaura* differs from other small-headed plesiosaurs in the low cervical number (24) despite having a long neck. The great lateral flexibility observed in this taxon thus may not be representative for long-necked plesiosaurs in general.

4.5 Studies supporting a rigid neck

Everhardt (2005) summarized the older literature and concluded that the long neck of in particular elasmosaurs was not very flexible and also pointed out the close spacing of the cervical vertebral centra (<< 5 mm) that would have greatly limited flexibility. This hypothesis was tested by Zammit et al. (2008) who used a life-sized 2-D models of individual vertebrae in dorsal and lateral view of an Australian elasmosaurid. For intervertebral spacing, Zammit et al. (2008) used values of between 1 and 3 mm of intervertebral cartilage thickness. The cardboard model elasmosaurid vertebrae were then articulated and manipulated on a flat surface for each thickness to reconstruct the mobility in each joint of the neck. Zammit et al. (2008) concluded that the range of motion in the elasmosaurid was approximately 75-177° in ventral direction, 87-155° in dorsal direction, and 94-177° in lateral direction, depending on cartilage thickness.

Wintrich et al. (2017a) echo the conclusion of Everhart (2005) in noting the close intervertebral spacing and steeply inclined zygapophyses already present in the oldest (albeit not basal-most) plesiosaur, *Rhaeticosaurus*. They note that a rigid neck is a plesiosaurian feature because all more basal pistosaurians have horizontal zygapophyses (Wintrich et al. 2017a), permitting great lateral neck flexibility, correlated with swimming by lateral undulation.

Using an approach from human biomechanics, Wintrich et al. (in revision a) estimated neck mobility based on finite element modeling of a single motion segment of *Cryptoclidus*. The model employed material properties of human bone and connective tissues (articular cartilage, annulus fibrosus and nucleus pulposus of the IVD) and also different values for intervertebral spacing. Different from Zammit et al. (2008), not the entire neck was modeled but the values obtained from the FE model for the single motion segment were multiplied by the number of cervical vertebrae. The results are generally similar to those of Zammit et al. (2008), also indicating a maximum neck mobility of <180º in each direction.

4.6 Taphonomic evidence for mobility

Taphonomic evidence for limited neck mobility also needs to be considered. Fortunately, pistosaurians including plesiosauromorph plesiosaurians are often preserved as articulated skeletons in conservation deposits such as black shales and laminated limestones, representing a temporal range from the Anisian (early Middle

Triassic) to the latest Cretaceous. Articulated skeletons of plesiosauromorph plesiosaurians typically show fairly straight or gently curved necks (Rieppel et al. 2002; Benson et al. 2012; Sato et al. 2014; Wintrich et al. 2017a) This is different from fossil snakes that are often highly coiled. Coiling has not been observed in any articulated plesiosaurian skeleton. While decay of the neck musculature and connective tissue may have led to a relaxation and straightening of the neck, postmortem forces such as bottom currents and scavengers could not have bent the neck beyond what was osteologically possible without disarticulating it.

4.7 Conclusions on neck mobility

As will have become clear from the previous sections, studies employing stringent methodology generally conclude that long-necked plesiosaurs had remarkably immobile necks, the apparent exception being *Nichollssaura* (Nagesan et al. 2018). Most long-necked plesiosaurs thus appear to have been unable to even bend their neck into a semicircle, and probably excursion was much less. This begs the question of the function and selective advantages of such an extremely long but immobile neck. The camouflage hypothesis appears to offer the best answer for neck elongation, although the question remains as to why the neck needed to be immobile. Possibly, stiffening of the neck was necessary to passively withstand hydrodynamic forces generated during foraging, in particular during rapid acceleration of the whole animal during an ambush attack. Also, an immobile neck may have been more compatible with underwater flight than a mobile one (Everhart 2005).

V Discussion

5.1 Evolution and diversity

Just as for many other Mesozoic vertebrate groups, the last decades have witnessed numerous new discoveries and new taxa of pistosaurians, in particular plesiosaurians, and there is no sign of the rate of discovery slowing down. Phylogenetic hypotheses have kept pace with these discoveries, and a consensus appears to be emerging, centering around the hypothesis of Benson & Druckenmiller (2014).

However, the Late Triassic record of plesiosaurians remains extremely scanty, considering that this time period lasted at least 35 million years (Cohen et al. 2018). This is particularly problematic considering that the origin of the unique and peculiar plesiosaurian body plan falls within this period (Dalla Vecchia 2006; Benson et al. 2012; Wintrich et al. 2017a). Targeting in particular the Norian stage for fieldwork aimed at discovering pistosaurians thus should offer considerable scientific rewards. Understanding Late Triassic plesiosaurians is also crucial for constraining the nature and magnitude of the end-Triassic extinction which appears to have severely affected some marine reptiles clades such as ichthyosaurs and non-plesiosaurian sauropterygians (Wintrich et al. 2017a; Lomax et al. 2018) but left plesiosaurians relatively unscathed.

5.2 Biology

Several aspects of plesiosaurian biology are at the center of current research, leading to an improved understanding. These include locomotion, reproduction, and physiology. Others, such as ecology and behaviour, have received less attention but also may be less amenable to paleobiological research. While there appears to be a consensus that plesiosaurians were four-winged underwater flyers, i.e., employed lift-based propulsion, there is less agreement on the exact movements and possible variation between taxa.

Our understanding of plesiosaurian reproductive biology is slowly solidifying by a combination of new informative finds, reevaluation of historic finds, and the application of bone histology. Bone histological work clearly holds great potential but currently suffers from poorly constrained samples and misinterpretations. However, cortical bone uneqivocally records very high growth rates in plesiosaurians and supports hypotheses of reproductive K strategy and high metabolic rates, consistent with evidence from functional morphology (adaptations to cruising) and habitat preference (open marine).

5.3 Neck function and evolutionary success in long-necked plesiosaurians

Our review of the evidence and hypotheses leads to the recognition that the extremely long neck in plesiosauromorph plesiosaurians was made possible by a unique combination of selection, embryogenesis, and evolutionary innovations. The extremely long neck must have been a key adaptation for the aquatic lifestyle. With

their elongated neck, plesiosauromorph plesiosaurians were successful in the niche of the ambush predator. In the Mesozoic, several other secondarily marine tetrapods were well adapted to the aquatic lifestyle but occupied other niches. Ichthyosauria, Thalattosuchia and Mosasauria were the most prominent among these marine reptiles. Therefore, the special hunting strategy evolved by the plesiosauromorph plesiosaurians may have avoided competition with the more conventional feeding style of the other marine reptils and can be assumed to have been more efficient for hunting in schools of fish than the long rostra of the other piscivores, ichthyosaurs and thalattosuchians. The long neck may have allowed hunting with a camouflages advantage not enjoyed by ichthyosaurs and thalattosuchians. Camouflage would have significantly increased hunting success and decreased the energetic cost of feeding. Furthermore, the evolution of the long neck was biomechanically possible in plesiosaurians because of the small head which was sufficient for fish catching. Interestingly, predation on schooling fish is constistent with a pelagic lifestyle for plesiosaurians, because it is open-water fish that show the most pronounced schooling behavior. In addition, in the aquatic environment, the gravitational force can be disregarded as opposed to terrestrial long-necked amniotes such as sauropod dinosaurs. These considerations also may apply to the enigmatic long-necked protorosaurs of the Triassic such as *Tanystropheus* (Tschanz 1988; Nosotti 2007) and *Dinocephalosaurus* (Li et al. 2004) which similarly may have evolved their long necks as camouflage for ambush predation.

VI Conclusions

1. Plesisaurians were the most diverse and long-lived clade of globally distributed marine reptiles.

2. Plesiosaurians have a unique body plan that still holds many challenges.

3. Plesiosaurians have unique bone histology that suggests endothermy.

4. Plesiosaurians were K strategists.

5. The uniquely high and plastic number of cervical vertebrae in pistosaurians evolved through changes in embryonic development.

6. Traces of these changes are seen in the intervertebral artery foramina of plesiosaurians.

7. The long neck of most plesiosauromorph plesiosaurians was surprisingly rigid with low intersegmental mobility.

8. The long neck of plesiosauromorph plesiosaurians evolved for visual and hydrodynamic camouflage in the context of ambush predation.

9. Plesiosauromorph plesiosaurian success was linked to this feeding style.

References

Andrews, C. W. (1895). XLII. — On the development of the shoulder-girdle of a plesiosaur (*Cryptoclidus oxoniensis*, Phillips, sp.) from the Oxford Clay. *Annals and Magazine of Natural History*, 15(88), 333-346.

Andrews, C. W. (1910). *A Catalogue of the Marine Reptiles of the Oxford Clay: based on the leeds collection in the British Museum (Natural History) Library, London* (Vol. 1). London: Trustees of the British Museum (Natural History).

Andrews, C. W. (1913). *A Descriptive Catalogue of the Marine Reptiles of the Oxford Clay: based on the leeds collection in the British Museum (Natural History) Library, London* (Vol. 2). London: Trustees of the British Museum (Natural History).

Araújo, R. & Correia, F. (2015). Soft-tissue anatomy of the plesiosaur pectoral girdle inferred from basal Eosauropterygia taxa and the extant phylogenetic bracket. *Palaeontologia Electronica*, 18, 1-32.

Araújo, R. & Correia, F. (2016). Soft-tissue anatomy of the Plesiosaur pectoral girdle inferred from basal Eosauropterygia taxa and the extant phylogenetic bracket. *Palaeontologica Electronica*, 18.1.8A.

Araújo, R., Polcyn, M. J., Lindgren, J., Jacobs, L. L., Schulp, A. S., Mateus, O. & Morais, M.-L. (2015). New aristonectine elasmosaurid plesiosaur specimens from the Early Maastrichtian of Angola and comments on paedomorphism in plesiosaurians. *Netherlands Journal of Geosciences*, 94(1), 93-108.

Arnold P., Amson E. & Fischer M. S. (2017). Differential scaling patterns of vertebrae and the evolution of neck length in mammals. *Evolution,* 71, 1587-1599.

Badlangana N. L., Adams J. W. & Manger P. R. (2009). The giraffe (*Giraffa camelopardalis*) cervical vertebral column: a heuristic example in understanding evolutionary processes? *Zoological Journal of the Linnean Society*, 155, 736-757.

Bardet, N. (1994). Extinction events among Mesozoic marine reptiles. *Historical Biology*, 7, 313–324.

Bardet, N. (1992). Stratigraphic evidence for the extinction of the ichthyosaurs. *Terra Nova*, 4, 649–656.

Bardet, N., Falconnet, J., Fischer, V., Houssaye, A., Jouve, S., Suberbiola, X. P., Pérez-García, A., Rage, J.-C. & Vincent, P. (2014). Mesozoic marine reptile palaeobiogeography in response to drifting plates. *Gondwana Research*, 26, 869–887.

Bennett, A., Seymour, R. & Bradford, D. (1985). Mass-dependence of anaerobic metabolism and acid-base disturbance during activity in the salt-water crocodile, *Crocodylus porosus*. *Journal of Experimental Biology*, 118, 161-171.

Benson, R. B. J. & Butler, R. J. (2011). Uncovering the diversification history of marine tetrapods: ecology influences the effect of geological sampling biases. In *Comparing the Geological and Fossil Records: Implications for Biodiversity Studies. Geological Society, London, Special Publications* (ed. A. J. McGowan & A. S. Smith), pp. 191–208.

Benson, R. B. J., Butler, R. J., Lindgren, J. & Smith, A. S. (2010). Mesozoic marine tetrapod diversity: mass extinctions and temporal heterogeneity in geological megabiases affecting vertebrates. *Proceedings of the Royal Society B* 277, 829-834.

Benson, R. B. J., Evans, M. & Druckenmiller, P. S. (2012). High diversity, low disparity and small body size in plesiosaurians (Reptilia, Sauropterygia) from the Triassic–Jurassic boundary. *PLoS One*, *7*(3), e31838.

Benson, R. B. J., Evans, M., Smith, A. S., Sassoon, J., Moore-Faye, S., Ketchum, H. F. & Forrest, R. (2013). A giant pliosaurid skull from the Late Jurassic of England. *PLOS ONE*, 8, e65989.

Benson, R. B. J., Zverkov, N. G. & Arkhangelsky, M. S. (2015). Youngest occurrences of rhomaleosaurid plesiosaurians indicate survival of an archaic marine reptile clade at high palaeolatitudes. *Acta Palaeontologica Polonica*, 60(4), 769-780.

Benson, R. B. J. & Druckenmiller, P. S. (2014). Faunal turnover of marine tetrapods during the Jurassic–Cretaceous transition. *Biological Reviews*, 89(1), 1-23.

Berezin, A. Y. (2011). A new plesiosaur of the family Aristonectidae from the Early Cretaceous of the center of the Russian platform. *Paleontological Journal*, 45**,** 648-660.

Bernard, A. L., Lécuyer, C., Vincent, P., Amiot, R., Buffetaut, E., Bardet, N., Simon, L., Prieur, A., Fourel, F. O. & Martineau, F. O. (2010). Regulation of body temperature by some Mesozoic marine reptiles. *Science*, 328, 1379-1382

Berthoz, A., Vidal, P. P. & Graf, W. Eds (1992). *The Head-Neck Sensory Motor System.* Oxford: Oxford University Press, 784 pp.

Brainerd E. L. & Patek S. N. (1998). Vertebral column morphology, C-start curvature, and the evolution of mechanical defenses in tetraodontiform fishes. *Copeia*, 4, 971-984.

Braun, J. & Reif, W. E. (1985). A survey of aquatic locomotion in fishes and tetrapods. *Neues Jahrbuch für Geologie und Paläontologie Abhandlungen*, 169, 307-332.

Brischoux, F. & Shine, R. (2011). Morphological adaptations to marine life in snakes. *Journal of Morphology*, 272**,** 566-572.

Brochu, C. A. (1996). Closure of neurocentral suture during crocodilian ontogeny: implications for maturity assessment in fossil archosaurs. *Journal of Vertebrate Paleontology*, 16, 49-62.

Brown, B. (1904). Stomach stones and food of plesiosaurians. *Science*, 20(501), 184-185.

Brown, D. S. (1981). The English Upper Jurassic Plesiosauroidea (Reptilia) and a review of the phylogeny and classification of the Plesiosauria. *Bulletin of the British Museum (Natural History)*, 35, 253–347.

Buchholtz, E. A., Booth, A. C. & Webbink, K. E. (2007). Vertebral anatomy in the Florida manatee, *Trichechus manatus latirostris*: a developmental and evolutionary analysis. *The Anatomical Record*, 290(6), 624-637.

Buchholtz E. A., Bailin H. G., Laves S. A., Yang J. T., Chan M. Y. & Drozd L. E. (2012). Fixed cervical count and the origin of the mammalian diaphragm. *Evolution & Development*, 14, 399-411.

Burke, A. C., Nelson, C. E., Morgan, B. A. & Tabin, C. (1995). Hox genes and the evolution of vertebrate axial morphology. *Development*, 121(2), 333-346.

Buchy, M. C., Frey, E. & Salisbury, S. W. (2006). The internal cranial anatomy of the Plesiosauria (Reptilia, Sauropterygia): evidence for a functional secondary palate. *Lethaia*, 39(4), 289-303.

Caldwell, M. W. (1997a). Limb osteology and ossification patterns in *Cryptoclidus* (Reptilia: Plesiosauroidea) with a review of sauropterygian limbs. *Journal of Vertebrate Paleontology*, 17(2), 295-307.

Caldwell, M. W. (1997b). Modified perichondral ossification and the evolution of paddle-like limbs in ichthyosaurs and plesiosaurians. *Journal of Vertebrate Paleontology*, 17(3), 534-547.

Caldwell, M. W. (2002). From fins to limbs to fins: limb evolution in fossil marine reptiles. *American Journal of Medical Genetics*, 112(3), 236-249.

Carpenter, K. (1997). Comparative cranial anatomy of two North American Cretaceous plesiosaurians. in *Ancient Marine Reptiles* (Ed. Callaway, J. M. & Nicholls, E. L.) San Diego: Academic Press, pp. 191-216.

Carpenter K. (1999). Revision of North American elasmosaurs from the Cretaceous of the Western Interior. *Paludicola*, 2, 148-173.

Carpenter, K., Sanders, F., Reed, B., Reed, J. & Larson, P. (2010). Plesiosaur swimming as interpreted from skeletal analysis and experimental results. *Transactions of the Kansas Academy of Science*, 113(1/2), 1-34.

Carroll, R. L. (1981). Plesiosaur ancestors from the Upper Permian of Madagascar. *Philosophical Transactions of the Royal Society of London*, *Series B, Biological Sciences,* 293, 315-383.

Carroll, R. L. (1985). Evolutionary constraints in aquatic diapsid reptiles. *Special Papers in Palaeontology,* 33, 145-155.

Catania, K. C. (2009). Tentacled snakes turn C-starts to their advantage and predict future prey behavior. *Proceedings of the National Academy of Sciences USA*, 106**,** 11183-11187.

Cheng, Y. N., Wu, X. C. & Ji, Q. (2004). Triassic marine reptiles gave birth to live young. *Nature*, 432(7015), 383-386.

Cicimurri, D. J. & Everhart, M. J. (2001). An elasmosaur with stomach contents and gastroliths from the Pierre Shale (Late Cretaceous) of Kansas. *Transactions of the Kansas Academy of Science*, 104(3), 129-143.

Cohen, K. M., Finney, S. C., Gibbard, P. L. & Fan, J.-X. (2018). The ICS International Chronostratigraphic Chart. *Episodes*, 36, 199-204.

Conybeare, W. D. (1824). XXI.—On the discovery of an almost perfect skeleton of the *Plesiosaurus*. *Transactions of the Geological Society of London*, S2-1, 381-389.

Cope, E. D. (1871). Synopsis of the extinct Batrachia and Reptilia of North America. *Proceedings of the American Philosophical Society*, 12(86), 41-52.

Cowen, R. (1996). *Locomotion and respiration in aquatic air-breathing vertebrates.* In *Evolutionary Paleobiology* (ED. James Valentine) Chicago Press, pp. 337-354.

Croll, D. A., Acevedo-Gutiérrez, A., Tershy, B. R. & Urbán-Ramírez, J. (2001). The diving behavior of blue and fin whales: is dive duration shorter than expected based on oxygen stores? *Comparative Biochemistry and Physiology Part A: Molecular & Integrative Physiology*, 129(4), 797-809.

Cruickshank, A. R. I. (1994). A juvenile plesiosaur (Plesiosauria: Reptilia) from the Lower Lias (Hettangian: Lower Jurassic) of Lyme Regis, England: a pliosauroid-plesiosauroid intermediate? *Zoological Journal of the Linnean Society*, 112, 151-178.

Cubo, J., Le Roy, N., Martinez-Maza, C. & Montes, L. P. (2012). Paleohistological estimation of bone growth rate in extinct archosaurs. *Paleobiology*, 38, 335-349.

Dalla Vecchia, F. M. (2006). A new sauropterygian reptile with plesiosaurian affinity from the Late Triassic of Italy. *Rivista Italiana di Paleontologia e Stratigrafia*, 112, 207-225.

Dalla Vecchia, F. M. (2017). Comments on the skeletal anatomy of the Triassic reptile *Bobosaurus forojuliensis* (Sauropterygia, Pistosauroidea). *Gortania*, 38, 39-75.

Dames, W. (1985). Die Plesiosaurier der süddeutschen Liasformation. *Abhandlungen der Königlichen Preussischen Akademie der Wissenschaften zu Berlin*, 2, 1-83

Darby, D. G., & Ojakangas, R. W. (1980). Gastroliths from an Upper Cretaceous plesiosaur. *Journal of Paleontology*, 54 548-556.

Davenport, J., Monks, S. A. & Oxford, P. J. (1984). A comparison of the swimming in marine and freshwater turtles. *Proceedings of the Royal Society of London B*, 220, 447–475.

Druckenmiller, P. S., & Russell, A. P. (2008). Skeletal anatomy of an exceptionally complete specimen of a new genus of plesiosaur from the Early Cretaceous (Early Albian) of northeastern Alberta, Canada. *Palaeontographica Abteilung A*, 283 1-33.

Evans, F. G. (1939). The morphology and functional evolution of the atlas-axis complex from fish to mammals. *Annals of the New York Academy of Sciences*, 39, 29-104.

Everhart, M. J. (2005). Probable plesiosaur gastroliths from the basal Kiowa Shale (Early Cretaceous) of Kiowa County, Kansas. *Kansas Academy of Science, Transactions*, 108, 109-115.

Everhart, M. J. (2005). *Oceans of Kansas - A Natural History of the Western Interior Sea*. Bloomington: Indiana University Press, 320 pp.

Everhart, M. J. (2000). Gastroliths associated with plesiosaur remains in the Sharon Springs Member (Late Cretaceous) of the Pierre Shale, western Kansas. *Kansas Academy of Science, Transactions*, 103, 58-69.

Fabbri, M., Dalla Vecchia, F. M. & Cau, A. (2014). New information on *Bobosaurus forojuliensis* (Reptilia: Sauropterygia): implications for plesiosaurian evolution. *Historical Biology*, 26, 661-669.

Farke, A. A. (2007). Reexamination of paleopathology in plesiosaurs and implications for behavioral interpretations. *Journal of Vertebrate Paleontology*, 27, 724-726.

Fischer, V., Cappetta, H., Vincent, P., Garcia, G. R., Goolaerts, S., Martin, J. E., Roggero, D. & Valentin, X. (2014). Ichthyosaurs from the French Rhaetian indicate a severe turnover across the Triassic–Jurassic boundary. *Naturwissenschaften*, 101**,** 1027–1040.

Fischer, V., Benson, R. B. J., Druckenmiller, P. S., Ketchum, H. F. & Bardet, N. (2018). The evolutionary history of polycotylid plesiosaurians. *Royal Societey Open Science*, 5(3), 172177.

Foffa, D., Sassoon, J., Cuff, A. R., Mavrogordato, M. N. & Benton, M. J. (2014). Complex rostral neurovascular system in a giant pliosaur. *Naturwissenschaften*, 101(5), 453-456.

Fostowicz-Frelik, L. & Gazdzicki, A. (2001). Anatomy and histology of plesiosaur bones from the Late Cretaceous of Seymour Island, Antarctic Peninsula. *Palaeontologia Polonica*, 60, 7-32.

Francillon-Vieillot, H., Buffrénil, V. de, Castanet, J., Géraudie, J., Meunier, F. J., Sire, J. Y., Zylberberg, L. & Ricqlès, A. de (1990). Microstructure and mineralization of vertebrate skeletal tissues. In *Skeletal Biomineralization: Patterns, Processes and Evolutionary Trends. Vol. 1* (ed. J. G. Carter), New York: Van Nostrand Reinhold, pp. 471530.

Frey, E., Mulder, E. W., Stinnesbeck, W., Rivera-Sylva, H. E., Padilla-Gutiérrez, J. M. & González-González, A. H. (2017). A new polycotylid plesiosaur with extensive soft tissue preservation from the early Late Cretaceous of northeast Mexico. *Boletín de la Sociedad Geológica Mexicana*, 69(1), 87-134.

Gadow H. F. (1933). *The Evolution of the Vertebral Column. A Contribution to the Study of Vertebrate Phylogeny.* Cambridge: Cambridge University Press, 356 pp.

Galis F. (1999). Why do almost all mammals have seven cervical vertebrae? Developmental constraints, Hox genes, and cancer. *Journal of Experimental Zoology Part B, Molecular and Developmental Evolution,* 285, 19-26.

Gasparini, Z., Bardet, N., Martin, J. E. & Fernandez, M. (2003a). The elasmosaurid plesiosaur *Aristonectes cabrera* from the latest Cretaceous of South America and Antarctica. *Journal of Vertebrate Paleontology*, 23(1), 104-115.

Gasparini, Z., Salgado, L. & Casadío, S. (2003b). Maastrichtian plesiosaurians from northern Patagonia. *Cretaceous Research*, 24, 157-170.

Garcia-Parraga, D., Crespo-Picazo J. L., de Quirós Y. B., Cervera V., Martí-Bonmati L., Díaz-Delgado J., Arbelo M., Moore M. J., Jepson P. D., Fernández A. (2014). Decompression sickness (‘the bends’) in sea turtles. *Diseases of Aquatic Organisms*, 111(1), 191-205.

Hall, B. K. (2002). Palaeontology and evolutionary developmental biology: a science of the nineteenth and twenty-first centuries. *Palaeontology*, 45(4), 647-669.

Hall, B. K. (2015). *Bones and Cartilage. 2nd Edition. Developmental and Evolutionary Skeletal Biology*. San Diego: Academic Press.

Hagdorn, H. & Rieppel, O. (1999). Stratigraphy of marine reptiles in the Triassic of Central Europe. *Zentralblatt für Geologie und Paläontologie Teil I*, 1998, 651-678.

Halstead, L. B. (1989). Plesiosaur locomotion. *Journal of the Geological Society*, 146(1), 37-40.

Herrel, A., Vincent, S. E., Alfaro, M. E., Van Wassenbergh, S. & Irschick, D. J. (2008). Morphological convergence as a consequence of extreme functional demands: examples from the feeding system of natricine snakes. *Journal of Evolutionary Biology*, 21(5), 1438-1448.

Hildebrand M. & Goslow G. E., (1998). *Analysis of Vertebrate Structure, 5th Edition*. New York: John Wiley, 660 pp.

Hoffstetter R. & Gasc J.-P. (1969). Vertebrae and ribs of modern reptiles. In *Biology of the Reptilia.* (ED.Chris Gans)San Diego: Academic Press, p. 201-310.

Hopley, P. J. (2001). Plesiosaur spinal pathology: the first fossil occurrence of Schmorl's nodes. *Journal of Vertebrate Paleontology*, 21, 253-260.

Houssaye A. (2009). "Pachyostosis" in aquatic amniotes: a review. *Integrative Zoology* 4, 325-340.

Houssaye, A. (2013). Bone histology of aquatic reptiles: what does it tell us about secondary adaptation to an aquatic life? *Biological Journal of the Linnean Society*, 108, 3–21.

Houssaye, A., Sander, P. M. & Klein, N. (2016). Adaptive patterns in aquatic amniote bone microanatomy - More complex than previously thought. *Integrative and Comparative Biology*, 56(6) 1349-1369.

Jiang, D.-J., Motani, R., Tintori, A., Rieppel, O., Zhou, M. & Lu, H. (2018). Palatal view of *Wangosaurus brevirostirs*, a basal pistosaur sauropterygian from the late

Middle Triassic (Ladinian) of Xingji of southwestern China. *Society of Vertebrate Paleontology, Abstract of Papers, 78th Annual Meeting*, 155.

Kear, B. P., Schroeder, N. I. & Lee, M. S. (2006). An archaic crested plesiosaur in opal from the Lower Cretaceous high-latitude deposits of Australia. *Biology Letters*, 2(4), 615-619.

Kear, B. P. (2007). A juvenile pliosauroid plesiosaur (Reptilia: Sauropterygia) from the Lower Cretaceous of South Australia. *Journal of Paleontology*, 81(1), 154-162.

Kelley, N. P. & Pyenson, N. D. (2015). Evolutionary innovation and ecology in marine tetrapods from the Triassic to the Anthropocene. *Science*, 348(6232), aaa3716.

Ketchum, H. F. & Benson, R. B. J. (2010). Global interrelationships of Plesiosauria (Reptilia, Sauropterygia) and the pivotal role of taxon sampling in determining the outcome of phylogenetic analyses. *Biological Reviews*, 85(2), 361-392.

Ketchum, H. F. & Benson, R. B. J. (2011). A new pliosaurid (Sauropterygia, Plesiosauria) from the Oxford Clay Formation (Middle Jurassic, Callovian) of England: evidence for a gracile, longirostrine grade of Early-Middle Jurassic pliosaurids. *Special Papers in Palaeontology*, 86, 109-129.

Kiprijanoff, A. V. (1881-1883). Studien über die fossilen Reptilien Russlands. *Mémoires de l'Académie Impériale des Sciences de St. Petersbourg*, 7, 1–144.

Kogan, I., Pacholak, S., Licht, M., Schneider, J. W., Brücker, C. & Brandt, S. (2015). The invisible fish: hydrodynamic constraints for predator-prey interaction in fossil fish *Saurichthys* compared to recent actinopterygians. *Biology Open*, bio.014720.

Krahl, A., Klein, N. & Sander, P. M. (2013). Evolutionary implications of the divergent long bone histologies of *Nothosaurus* and *Pistosaurus* (Sauropterygia, Triassic). *BMC Evolutionary Biology*, 13(1), 123.

Kubo T., Mitchell M. T. & Henderson D. M. (2012). *Albertonectes vanderveldei*, a new elasmosaur (Reptilia, Sauopterygia) from the Upper Creteaceous of Alberta. *Journal of Vertebrate Paleontology* 32, 557-572.

Laurin, M. (2010). *How Vertebrates Left The Water*. Berkeley: University of California Press, 224 p.

Li, C., Rieppel, O. & LaBarbera, M. C. (2004). A Triassic aquatic protorosaur with an extremely long neck. *Science*, 305 (5692), 1931.

Liebe, L. & Hurum, J. H. (2012). Gross internal structure and microstructure of plesiosaur limb bones from the Late Jurassic, central Spitsbergen. *Norwegian Journal of Geology*, 92, 285-309.

Liu, S., Smith, A. S., Gu, Y., Tan, J., Liu, C. K. & Turk, G. (2015). Computer simulations imply forelimb-dominated underwater flight in plesiosaurians. *PLoS Computational Biology*, 11(12), e1004605.

Lomax, D., De La Salle, P., Massare, J. & Gallois, R. (2018). A giant Late Triassic ichthyosaur from the UK and a reinterpretation of the Aust Cliff 'dinosaurian' bones. *PLoS ONE*, 13, e0194742.

Lopez, A. J., Scheer, J. K., Leibl, K. E., Smith, Z. A., Dlouhy, B. J. & Dahdaleh, N. S. (2015). Anatomy and biomechanics of the craniovertebral junction. *Neurosurgical Focus*, 38(4) E2.

Ma, L.-T., Jiang, D.-Y., Rieppel, O., Motani, R. & Tintori, A. (2015). A new pistosauroid (Reptilia, Sauropterygia) from the late Ladinian Xingyi marine reptile level, southwestern China. *Journal of Vertebrate Paleontology*, 35, e881832.

Maddock, L., Bone, Q. & Rayner, J. M. V. (1994). *The Mechanics and Physiology of Animal Swimming*. Cambridge: Cambridge University Press. 250 p.

Massare, J. A. (1987). Tooth morphology and prey preference of Mesozoic marine reptiles. *Journal of Vertebrate Paleontology*, 7(2), 121-137.

Massare, J. A. (1988). Swimming capabilities of Mesozoic marine reptiles: implications for method of predation. *Paleobiology*, *14*(2), 187-205.

Massare, J. A. (1994). Swimming capabilities of Mesozoic marine reptiles: a review. In *Mechanics and Physiology of Animal Swimming* (ed. L. Maddock, Q. Bone and J. M. V. Rayner). Cambridge: Cambridge University Press, pp. 133-149. .

McHenry, C. R., Cook, A. G. & Wroe, S. (2005). Bottom-feeding plesiosaurians. *Science*, 310(5745), 75.

Mitchell, G., Van Sittert, S. J. & Skinner, J. D. (2009). Sexual selection is not the origin of long necks in giraffes. *Journal of Zoology*, 278, 281-286.

Mitchell, J. & Sander, P. M. (2014). The three-front model: a developmental explanation of long bone diaphyseal histology of Sauropoda. *Biological Journal of the Linnean Society, London*, 112, 765–781.

Moodie, R. L. (1916). The structure and growth of the plesiosaurian propodial. *Journal of Morphology*, 27, 401-411.

Motani R. (2001). Estimating body mass from silhouettes: testing the assumption of elliptical body cross-sections. *Paleobiology,* 27, 735-750.

Motani, R. (2002). Swimming speed estimation of extinct marine reptiles: energetic approach revisited. *Paleobiology*, 28(2), 251-262.

Motani, R. (2005). Evolution of fish-shaped reptiles (Reptilia: Ichthyopterygia) in their physical environments and constraints. *Annual Review of Earth and Planetary Sciences*, 33, 395-420.

Motani, R. (2009). The evolution of marine reptiles. *Evolution: Education and Outreach*, *2*(2), 224-235.

Mulder, E. W. A., Bardet, N., Godefroit, P. & Jagt, J. W. M. (2000). Elasmosaur remains from the Maastrichtian type area, and a review of latest Cretaceous elasmosaurs (Reptilia, Plesiosauroidea). *Bulletin de l'Institut royal des Sciences naturelles de Belgique, Sciences de la Terre*, 70, 161-178.

Müller, J., Scheyer, T. M., Head, J. J., Barrett, P. M., Werneburg, I., Ericson, P. G. P., Pol, D. & Sánchez-Villagra, M. R. (2010). Homeotic effects, somitogenesis and the evolution of vertebral numbers in recent and fossil amniotes. *Proceedings of the National Academy of Sciences USA*, 107, 2118-2123.

Nagesan, R. S., Henderson, D. M., Anderson, J. S. (2018). A method for deducing neck mobility in plesiosaurs, using the exceptionally preserved *Nichollssaura borealis*. *Royal Society Open Science*, 5(8) 172307.

Narita, Y. & Kuratani, S. (2005). Evolution of the vertebral formulae in mammals: a perspective on developmental constraints. *Journal of Experimental Zoology Part B Molecular and Developmental Evolution*, 304, 91-106.

Neenan, J. M., Klein, N. & Scheyer, T. M. (2013). European origin of placodont marine reptiles and the evolution of crushing dentition in Placodontia. *Nature Communications*, 4, 1621.

Neenan, J. M., Reich, T., Evers, S. W., Druckenmiller, P. S., Voeten, D. F. A. E., Choiniere, J. N., Barrett, P. M., Pierce, S. E, Benson, R. B. J. (2017). Evolution of the sauropterygian labyrinth with increasingly pelagic lifestyles. *Current Biology*, 27(24), 3852-3858.

Newman, B. & Tarlo, L. H. (1967). A giant marine reptile from Bedfordshire. *Animals*, 10(2), 61-63.

Nicholls, E. L. & Russell, A. P. (1991). The plesiosaur pectoral girdle: the case for a sternum. *Neues Jahrbuch für Geologie und Paläontologie, Abhandlungen*, 182(2), 161-185.

Noè, L. F., Taylor, M. A. & Gómez-Pérez, M. (2017). An integrated approach to understanding the role of the long neck in plesiosaurians. *Acta Palaeontologica Polonica*, *62*(1), 137-162.

Nossotti, S. (2007). *Tanystropheus longobardicus* (Reptilia Protorosauria): Re-interpretations of the anatomy based on new specimens from the Middle Triassic of Besano (Lombardy, northern Italy). *Memoire della Societa Italiana di Scienze Naturali e del Museo Civico di Storia Naturale di Milano*, 35(3), 1-88.

O'Gorman, J. P., Gasparini, Z. & Salgado, L. (2013). Postcranial morphology of *Aristonectes* (Plesiosauria, Elasmosauridae) from the Upper Cretaceous of Patagonia and Antarctica. *Antarctic Science*, 25(1), 71-82.

O'Gorman, J. P., Talevi, M. & Fernández, M. S. (2017). Osteology of a perinatal aristonectine (Plesiosauria; Elasmosauridae). *Antarctic Science*, 29, 61-72.

O'Keefe, F. R. (2001). A cladistic analysis and taxonomic revision of the Plesiosauria (Reptilia: Sauropterygia). *Acta Zoologica Fennica*, 213**,** 1–63.

O'Keefe, F. R. (2002). The evolution of plesiosaur and pliosaur morphotypes in the Plesiosauria (Reptilia: Sauropterygia). *Paleobiology*, 28(1), 101-112.

O'Keefe, F. R. (2006). Neoteny and the plesiomorphic condition of the plesiosaur basicranium. In *Amniote Paleobiology, Perspectives on the Evolution of Mammals, Birds, and Reptiles* (ed. M. T. Carrano, T. J. Gaudin, R. W. Blob and J. R. Wible), Chicago: University of Chicago Press, pp. 391–409.

O'Keefe, F. R. & Carrano, M. T. (2005). Correlated trends in the evolution of the plesiosaur locomotor system. *Paleobiology*, 31(4), 656-675.

O'Keefe, F. R. & Hiller, N. (2006). Morphologic and ontogenetic patterns in elasmosaur neck length, with comments on the taxonomic utility of neck length variables. *Paludicola*, 5, 206-229.

O'Keefe, F. R. & Chiappe, L. M. (2011). Viviparity and K-selected life history in a Mesozoic marine plesiosaur (Reptilia, Sauropterygia). *Science*, 333(6044), 870-873.

O'Keefe F. R., Street H. P., Wilhelm B. C., Richards C. D. & Zhu H. (2011). A new skeleton of the cryptoclidid plesiosaur *Tatenectes laramiensis* reveals a novel body shape among plesiosaurians. *Journal of Vertebrate Paleontology*, 31, 330-339.

O'Keefe, F. R., Sander, P. M., Wintrich, T. & Werning, S. (in press). Ontogeny of polycotylid long bone microanatomy and histology. *Integrative Organismal Biology*.

Olson, E. C. (1976). The exploitation of land by early tetrapods. in *Morphology and Biology of Reptiles*. (Bellairs, A. & Cox, C. D. eds.) San Diego: Academic Press, p. 1-30.

Ossa-Fuentes, L., Otero, R. A. & Rubilar-Rogers, D. (2017). Microanatomy and osteohistology of a juvenile elasmosaurid plesiosaur from the Upper Maastrichtian of Marambio (Seymour) island, Antarctica. *Boletín del Museo Nacional de Historia Natural, Chile*, 66(2), 149-160.

Otero, R. A., Soto-Acuña, S., Vargas, A. O. & Rubilar-Rogers, D. (2014). A new postcranial skeleton of an elasmosaurid plesiosaur from the Upper Cretaceous of central Chile and reassessment of *Cimoliasaurus andium* Deecke. *Cretaceous Research*, 50, 318-331.

Owen, F. R. S. (1847). Description of the atlas, axis, and suvertebral wedge bones in the *Plesiosaurus*, with remarks on the homologies of those bones. *Annals and Magazine of Natural History*, 20, 217-225.

Petermann, H. & Sander, P. M. (2013). Histological evidence for muscle insertion in extant amniote femora: implications for muscle reconstruction in fossils. *Journal of Anatomy*, 222(4), 419-436.

Pierce S. E., Clack J. A. & Hutchinson J. R. (2011). Comparative axial morphology in pinnipeds and its correlation with aquatic locomotory behaviour. *Journal of Anatomy*, 219, 502-514.

Reitner, J. & Urlichs, M. (1983). Echte Weichteilbelemniten aus dem Untertoarcium (Posidonienschiefer) Südwestdeutschlands. *Neues Jahrbuch für Geologie und Paläontologie, Abhandlungen*, 165, 450–465.

Rhodin, A. G. J. (1985). Chondro-osseous development and growth of marine turtles. *Copeia*, 1985, 752-771.

Rhodin, A. G. J., Ogden, J. G. & Conlogue, G. J. (1981). Chondro-osseous morphology of *Dermochelys choriacea*, a marine reptile with mammalian skeletal features. *Nature*, 290, 244-246.

Ricqlès, A. de (1989). Les mécanismes hétérochroniques dans le retour des tétrapodes au milieu aquatique. *Geobios*, 12, 337-348.

Ricqlès, A. de & Buffrénil, V. de (2001). Bone histology, heterochronies and the return of tetrapods to life in water: Where are we? In *Secondary Adaptation of Tetrapods to Life in Water* (ed. J.-M. Mazin and V. de Buffrénil), pp. 289-310. Munich: Verlag Dr. Friedrich Pfeil.

Rieppel, O. (1992). Studies on skeleton formation in reptiles. III. Patterns of ossification in the skeleton of *Lacerta vivipara* Jacquin (Reptilia, Squamata). *Fieldiana Zoology*, 68, 1-25.

Rieppel, O. (1994). Osteology of *Simosaurus gaillardoti* and the relationships of stem-group Sauropterygia. *Fieldiana Geology, New Series*, 28, 1-85.

Rieppel, O. (2000). *Handbuch der Paläoherpetologie*, *Teil 12A. Sauropterygia I. Placodontia, Pachypleurosauria, Nothosauroidea, Pistosauria*. Munich: Verlag Dr. Friedrich Pfeil.

Rieppel, O., Sander, P. M. & Storrs, G. W. (2002). The skull of the pistosaur *Augustasaurus* from the Middle Triassic of northwestern Nevada. *Journal of Vertebrate Paleontology*, 22, 577-592.

Riess, J. & Frey, E. (1991). The evolution of underwater flight and the locomotion of plesiosaurians. *Biomechanics in Evolution*. Rayner, J. M. V. and Wootton, R. J., Eds. Cambridge: Cambridge University Press. p, 131-144.

Rivera, A. R., Rivera, G. & Blob, R. W. (2013). Forelimb kinematics during swimming in the pig-nosed turtle, *Carettochelys insculpta*, compared with other turtle taxa: rowing versus flapping, convergence versus intermediacy. *Journal of Experimental Biology*, 216**,** 668-680.

Rivera, A. R., Wyneken, J. & Blob, R. W. (2011). Forelimb kinematics and motor patterns of swimming loggerhead sea turtles (*Caretta caretta*): are motor patterns conserved in the evolution of new locomotor strategies? *Journal of Experimental Biology*, 214**,** 3314-3323.

Robinson, J. A. (1975). The locomotion of plesiosaurs. *Neues Jahrbuch für Geologie und Paläontologie, Abhandlungen*, 149, 286-332.

Rolvien, T., Hahn, M., Siebert, U., Püschel, K., Wilke, H.-J., Busse, B., Amling, M. & Oheim, R. (2017). Vertebral bone microarchitecture and osteocyte characteristics of three toothed whale species with varying diving behaviour. *Scientific Reports*, 7**,** 1604.

Romer, A. S. (1976). *Osteology of the Reptiles*. Chicago: University of Chicago Press, 772 p.

Rothschild, B. M. (1982). *Rheumatology: a Primary Care Approach*. Oxford: Butterworth-Heinemann.

Rothschild, B. M. & Storrs, G. W. (2003). Decompression syndrome in plesiosaurians (Sauropterygia: Reptilia). *Journal of Vertebrate Paleontology*, 23(2), 324-328.

Rothschild, B. M., Clark, N. D. L. & Clark, C. (2018). Evidence for survival in a Middle Jurassic plesiosaur with a humeral pathology: What can we infer of plesiosaur behaviour? *Palaeontologia Electronica*, 21.1.13A 1-11.

Sachs S. (2005). Redescription of *Elasmosaurus platyurus* Cope 1868 (Plesiosauria: Elasmosauridae) from the Upper Cretaceous (lower Campanian) of Kansas, U.S.A. *Paludicola* 5, 92-106.

Sachs, S., Kear, B. P. & Everhart, M. J. (2013). Revised vertebral count in the "longest-necked vertebrate" *Elasmosaurus platyurus* Cope 1868, and clarification of the cervical-dorsal transition in Plesiosauria. *PLOS ONE*, 8, e70877.

Salgado, L., Fernandez, M. & Talevi, M. (2007). Observaciones histologicas en reptiles marinos (Elasmosauridae y Mosasauridae) del Cretacico Tardio de Patagonia y Antartida. *Ameghiniana*, 44, 513–523.

Sander, P. M. (1989). The pachypleurosaurids (Reptilia: Nothosauria) from the Middle Triassic of Monte San Giorgio (Switzerland) with the description of a new species. *Philosophical Transactions of the Royal Society of London*, B 325, 561-670.

Sander, P. M. (1999). The microstructure of reptilian tooth enamel: terminology, function, and phylogeny. *Münchner geowissenschaftliche Abhandlungen*, 38, 1-102.

Sander, P. M. (2012). Reproduction in early amniotes. *Science*, 337, 806-808.

Sander, P. M., Rieppel, O. C. & Bucher, H. (1997). A new pistosaurid (Reptilia: Sauropterygia) from the Middle Triassic of Nevada and its implications for the origin of plesiosaurs. *Journal of Vertebrate Paleontology*, 17, 526-533.

Sato, T. (2002). *Description of Plesiosaurs (Reptilia: Sauropterygia) from the Bearpaw Formation (Campanian – Maastrichtian) and a Phylogenetic Analysis of the Elasmosauridae. PhD thesis, University of Calgary*. Calgary: University of Calgary.

Sato, T. & Tanabe, K. (1998). Cretaceous plesiosaurians ate ammonites. *Nature*, 394(6694), 629.

Sato, T., Cheng, Y. N., Wu, X. C. & Li, C. (2010). Osteology of *Yunguisaurus* (Reptilia; Sauropterygia), a Triassic pistosauroid from China. *Paleontological Research*, 14(3), 179-195.

Sato, T., Zhao, L. J., Wu, X. C. & Li, C. (2014). A new specimen of the Triassic pistosauroid *Yunguisaurus*, with implications for the origin of Plesiosauria (Reptilia, Sauropterygia). *Palaeontology*, 57(1), 55-76.

Schmeisser, R. & Gillette, D. (2009). Unusual occurrence of gastroliths in a polycotylid plesiosaur from the Upper Cretaceous Tropic Shale, southern Utah. *Palaios*, 24**,** 453-459.

Seeley H. G. (1874). On *Muraenosaurus leedsii*, a plesiosaurian from the Oxford Clay. Part I. *Quaterly Journal of the Geological Society*, 30, 197-208.

Seilacher, A. (1970). Begriff und Bedeutung der Fossil-Lagerstätten. *Neues Jahrbuch für Geologie und Paläontologie, Abhandlungen*, 1970, 34–39.

Sennikov, A. G. & Arkhangelsky, M. S. (2010). On a typical Jurassic sauropterygian from the Upper Triassic of Wilczek Land (Franz Josef Land, Arctic Russia). *Paleontological Journal*, 44, 567–572.

Serratos, D. J., Druckenmiller, P. & Benson, R. B. J. (2017). A new elasmosaurid (Sauropterygia, Plesiosauria) from the Bearpaw Shale (Late Cretaceous, Maastrichtian) of Montana demonstrates multiple evolutionary reductions of neck length within Elasmosauridae. *Journal of Vertebrate Paleontology*, 37(2) 1278608.

Seymour, R. S. (1982). Physiological adaptatixons to aquatic life. In *Biology of the Reptilia*, Vol. 13, (Ed. Chris Gans). San Diego:Academic Press, pp. 1-51.

Simmons, R. E. & Scheepers, L. (1996). Winning by a neck: sexual selection in the evolution of giraffe. *The American Naturalist*, 148(5), 771-786.

Smith, A. S. (2013). Morphology of the caudal vertebrae in *Rhomaleosaurus zetlandicus* and a review of the evidence for a tail fin in Plesiosauria. *Paludicola*, 9(3), 144-158.

Smith, A. S. (2015). Reassessment of '*Plesiosaurus*' *megacephalus* (Sauropterygia: Plesiosauria) from the Triassic-Jurassic boundary, UK. *Palaeontologia Electronica*, 18.1.20A, 1-19.

Smith, A. S. & Vincent, P. (2010). A new genus of pliosaur (Reptilia: Sauropterygia) from the Lower Jurassic of Holzmaden, Germany. *Palaeontology*, 53, 1049-1063.

Soul, L. C. & Benson, R. B. J. (2017). Developmental mechanisms of macroevolutionary change in the tetrapod axis: A case study of Sauropterygia. *Evolution*, 71, 1164-1177.

Solounias, N. (1999). The remarkable anatomy of the giraffe's neck. *Journal of Zoology*, 247(2), 257-268.

Stein, K. & Prondvai, E. (2014). Rethinking the nature of fibrolamellar bone: an integrative biological revision of sauropod plexiform bone formation. *Biological Reviews*, 89(1), 24-47.

Street, H. P. & O'Keefe, F. R. (2010). Evidence of pachyostosis in the cryptocleidoid plesiosaur *Tatenectes laramiensis* from the Sundance Formation of Wyoming. *Journal of Vertebrate Paleontology*, 30, 1279-1282.

Stevens, K. A. (2013). The articulation of sauropod necks: methodology and mythology. *PLoS One*, 8(10), e78572.

Storrs, G. W. (1991). Anatomy and relationships of *Corosaurus alcovensis* (Diapsida: Sauropterygia) and the Triassic Alcova Limestone of Wyoming. *Bulletin of the Peabody Museum of Natural History*, 44, 1–151.

Storrs, G. W. (1993). Function and phylogeny in sauropterygian (Diapsida) evolution. *American Journal of Science*, 293(A), 63-90.

Storrs, G. W. (1994). Fossil vertebrate faunas of the British Rhaetian. *Zoological Journal of the Linnean Society*, 112, 217-259.

Storrs, G. W. (1995). A juvenile specimen of *Plesiosaurus* sp. from the Lias (Lower Jurassic, Pliensbachian) near Charmouth, Dorset, England. *Proceedings of the Dorset Natural History and Archaeological Society*, 116, 71-76.

Stukely, W. (1719). III. An Account of the impression of the almost entire sceleton of a large animal in a very hard stone, lately presented the Royal Society, from Nottinghamshire. *Philosophical Transactions of the Royal Society of London*, 30(360), 963-968.

Sues, H.-D. (1987). Postcranial skeleton of *Pistosaurus* and interrelationships of the Sauropterygia (Diapsida). *Zoological Journal of the Linnean Society*, 90, 109-131.

Surmik, D., Rothschild, B., Dulski, M. & Janiszewska, K. (2017). Two types of bone necrosis in the Middle Triassic *Pistosaurus longaevus* bones: the results of integrated studies. *Royal Society Open Science*, 4, 170204.

Szczygielski T. (2017). Homeotic shift at the dawn of the turtle evolution. *Royal Society Open Science*, 4, 160933.

Tarlo, L. B. (1959). *Pliosaurus brachyspondylus* (Owen) from the Kimmeridge Clay. *Palaeontology*, 1(4), 283-291.

Taylor, M. A. (1981). Plesiosaurs - rigging and ballasting. *Nature*, 290, 628-629.

Taylor, M. A. (1992). Functional anatomy of the head of the large aquatic predator *Rhomaleosaurus zetlandicus* (Plesiosauria, Reptilia) from the Toarcian (Lower Jurassic) of Yorkshire, England. *Philosophical Transactions of the Royal Society B*, 335(1274), 247-280.

Taylor, M. A. (1993). Stomach stones for feeding or buoyancy? The occurrence and function of gastroliths in marine tetrapods. *Philosophical Transactions of the Royal Society B*, 341(1296), 163-175.

Tschanz, K. (1988). Allometry and heterochrony in the growth of the neck of Triassic prolacertiform reptiles. *Paleontology*, 31:997–1011.

Tutin, S. L. & Butler, R. J. (2017). The completeness of the fossil record of plesiosaurians, marine reptiles from the Mesozoic. *Acta Palaeontologica Polonica* 62, 563-573.

Vincent, P. (2010). A juvenile plesiosaur specimen from the Lower Jurassic of Holzmaden, Germany. *Palaeontographica Abt. A*, 291, 45-61.

Vincent, P., Bardet, N., Pereda Suberbiola, X., Bouya, B., Amaghzaz, M. B. & Meslouh, S. (2011). *Zarafasaura oceanis*, a new elasmosaurid (Reptilia: Sauropterygia) from the Maastrichtian phosphates of Morocco and the palaeobiogeography of latest Cretaceous plesiosaurs. *Gondwana Research*, 19, 1062-1073.

Vogel S. (1994). *Life in Moving Fluids*. Princeton: Princeton University Press.

Vogel S. (2008). Modes and scaling in aquatic locomotion. *Integrative & Comparative Biology*, 48, 702-712.

Wall, W. P. (1983). The correlation between high limb-bone density and aquatic habits in recent mammals. *Journal of Paleontology*, 57, 197-207.

Walsh, S. A., Barrett, P. M., Milner, A. C., Manley, G., & Witmer, L. M. (2009). Inner ear anatomy is a proxy for deducing auditory capability and behaviour in reptiles and birds. *Proceedings of the Royal Society of London B: Biological Sciences*, 276(1660), 1355-1360.

Ward, A. B. & Mehta, R. S. (2014). Differential occupation of axial morphospace. *Zoology*, 117, 70-76.

Watson, D. M. S. (1924). The elasmosaurid shoulder-girdle and fore-limb. *Proceedings of the Zoological Society of London*, 94, 885-917.

Webb, P. W. (1984). Body form, locomotion and foraging in aquatic vertebrates. *American Zoologist*, 24, 107-120.

Webb, P. W. (1988). Simple physical principles and vertebrate aquatic locomotion. *American Zoologist*, 28, 709-725.

Welles, S. P. (1943). Elasmosaurid plesiosaurians with description of new material from California and Colorado. *Memoirs of the University of California*, 13, 125-254.

Wiffen, J., Buffrénil, V. de, Ricqlès, A. de & Mazin, J. M. (1995). Ontogenetic evolution of bone structure in Late Cretaceous Plesiosauria from New Zealand. *Geobios*, 28(5), 625-640.

Wilhelm, B. C. & O'Keefe, F. R. (2010). A new partial skeleton of a cryptocleidoid plesiosaur from the Upper Jurassic Sundance Formation of Wyoming. *Journal of Vertebrate Paleontology*, 30, 1736-1742.

Wilkinson, D. M. & Ruxton, G. D. (2012). Understanding selection for long necks in different taxa. *Biological Reviews*, 87(3), 616-630.

Williston, S. W. (1914). *Water Reptiles of the Past and Present*. Chicago: University of Chicago Press.

Wintrich, T., Hayashi, S., Houssaye, A., Nakajima, Y. & Sander, P. M. (2017a). A Triassic plesiosaurian skeleton and bone histology inform on evolution of a unique body plan. *Science Advances*, *3*(12), e1701144.

Wintrich, T., Scaal, M. & Sander, P. M. (2017b). Foramina in plesiosaur cervical centra indicate a specialized vascular system. *Fossil Record*, *20*(2), 279.

Wintrich, T., Jonas, R., Wilke, H.-J. & Sander, P. M. (in revision a). Neck mobility in the Jurassic plesiosaur *Cryptoclidus eurymerus* – a new approach to understanding the axial skeleton in fossil vertebrates using finite element analysis. *PeerJ*.

Wintrich, T., Scaal, M., Böhmer, C., Schellhorn, R., Kogan, I., Van Der Reest, A. & Sander, P. M. (in revision b). Fossil soft-tissues indicate convergent evolution of the intervertebral disc in non-mammalian amniotes. *Nature*.

Wings, O. (2007). A review of gastrolith function with implications for fossil vertebrates and a revised classification. *Acta Palaeontologica Polonica*, 52, 1–16.

Woodward, H. (1896). *A Guide to the Fossil Reptiles and Fishes in the Department of Geology and Palaeontology*. London: Trustees of the British Museum Natural History.

Würsig, B., Perrin, W. & Thewissen, J. G. M. (Eds.). (2008). *Encyclopedia of Marine Mammals*. San Diego: Academic Press.

Young, J. Z. (1950). *The Life of Vertebrates*. Oxford: Oxford University Press.

Zammit, M., Daniels, C. B. & Kear, B. P. (2008). Elasmosaur (Reptilia: Sauropterygia) neck flexibility: Implications for feeding strategies. *Comparative Biochemistry and Physiology Part A: Molecular & Integrative Physiology*, 150(2), 124-130.

Zarnik, B. (1925). On the ethology of plesiosaurians, with contributions to the mechanism of the cervical vertebrae of recent sauropsids. *Royal Morphological Biological Institute, Zagreb*, 1–26.

List of Publications

Peer-reviewed Publications

Wintrich, T., Scaal, M., & Sander, P. M. (2017). Foramina in plesiosaur cervical centra indicate a specialized vascular system. *Fossil Record*, 20(2), 279-290.

Wintrich, T., Hayashi, S., Houssaye, A., Nakajima, Y., & Sander, P. M. (2017). A Triassic plesiosaurian skeleton and bone histology inform on evolution of a unique body plan. *Science Advances*, 3(12), e1701144.